

The Institute of Plant Nutrition and Soil Science
of the Christian-Albrechts-Universität Kiel

**Gaseous emissions from biogas-digestate management and from fertilized soils:
A study with special reference to nitrous oxide determination
by stable isotope and isotopomer techniques**

Dissertation
submitted for the Doctoral Degree
awarded by the Faculty of Agricultural and Nutritional Sciences
of the Christian-Albrechts-Universität Kiel

submitted by
M.Sc. Jan Reent Köster
born in Achim

Kiel, 2014

Dean: Prof. Dr. Dr. h. c. Rainer Horn

1. Examiner: Prof. Dr. Karl-Hermann Mühling

2. Examiner: Prof. Dr. Klaus Dittert

Date of Oral Examination: 02.07.2014

Contents

| | | |
|----------|---|-----------|
| 1 | General Introduction | 1 |
| | 1.1 <i>Impact of anthropogenic greenhouse gas emissions on the global climate</i> | 2 |
| | 1.2 <i>Biogas energy production and related trace gas emissions</i> | 2 |
| | 1.3 <i>Utilization of anaerobic digestates as fertilizers and related NH₃ emissions</i> | 3 |
| | 1.4 <i>Advantages of optical remote sensing approaches for measuring trace gas emissions</i> | 4 |
| | 1.5 <i>Impact of organic fertilizers on N₂O emissions from agricultural soils</i> | 5 |
| | 1.6 <i>N₂O isotopomers and their potential use for N₂O source identification</i> | 6 |
| | 1.7 <i>Recent developments in laser spectroscopic techniques for N₂O isotope analysis</i> | 6 |
| | 1.8 <i>Objectives</i> | 7 |
| | 1.9 <i>References</i> | 9 |
| | | |
| 2 | Open-Path quantification of ammonia, methane, and nitrous oxide emissions from co-fermented anaerobic digestates stored in lagoons | 17 |
| | <i>Abstract</i> | 19 |
| | <i>Introduction</i> | 20 |
| | <i>Materials and methods</i> | 22 |
| | <i>Results and discussion</i> | 26 |
| | <i>Acknowledgements</i> | 33 |
| | <i>References</i> | 34 |
| | | |
| 3 | Cold season ammonia emissions from land spreading with anaerobic digestates from biogas production | 39 |
| | <i>Abstract</i> | 40 |
| | <i>Introduction</i> | 40 |
| | <i>Materials and methods</i> | 41 |
| | <i>Results and discussion</i> | 41 |
| | <i>Conclusions</i> | 42 |
| | <i>Acknowledgements</i> | 43 |
| | <i>References</i> | 43 |

| | | |
|------------|---|-----------|
| 3.1 | Corrigendum: Cold season ammonia emissions from land spreading with anaerobic digestates from biogas production | 45 |
| | <i>Results</i> | 46 |
| | <i>References</i> | 46 |
| 4 | Anaerobic digestates lower N₂O emissions compared to cattle slurry by affecting rate and product stoichiometry of denitrification - an N₂O isotopomer case study | 47 |
| | <i>Abstract</i> | 48 |
| | <i>Introduction</i> | 49 |
| | <i>Materials and methods</i> | 49 |
| | <i>Results and discussion</i> | 52 |
| | <i>Acknowledgements</i> | 56 |
| | <i>References</i> | 57 |
| 5 | Soil denitrification potential and its influence on N₂O reduction and N₂O isotopomer ratios | 59 |
| | <i>Abstract</i> | 60 |
| | <i>Introduction</i> | 60 |
| | <i>Experimental</i> | 61 |
| | <i>Results and discussion</i> | 62 |
| | <i>Conclusions</i> | 68 |
| | <i>Acknowledgements</i> | 69 |
| | <i>References</i> | 69 |
| 6 | Experimental determinations of isotopic fractionation factors associated with N₂O production and reduction during denitrification in soils | 71 |
| | <i>Abstract</i> | 72 |
| | <i>Introduction</i> | 73 |
| | <i>Methods</i> | 74 |
| | <i>Results</i> | 77 |
| | <i>Discussion</i> | 81 |
| | <i>Summary</i> | 88 |
| | <i>Acknowledgements</i> | 88 |
| | <i>References</i> | 88 |

| | | |
|-----------|---|------------|
| 7 | Novel laser spectroscopic technique for continuous analysis of N₂O isotopomers – application and intercomparison with isotope ratio mass spectrometry | 91 |
| | <i>Abstract</i> | 92 |
| | <i>Introduction</i> | 92 |
| | <i>Experimental</i> | 93 |
| | <i>Results and discussion</i> | 94 |
| | <i>Conclusions</i> | 96 |
| | <i>Acknowledgements</i> | 97 |
| | <i>References</i> | 97 |
| 8 | General Discussion | 99 |
| | <i>8.1 Emission measurements from open digestate lagoons by OP FTIR</i> | 100 |
| | <i>8.2 NH₃ emissions during AD land spreading during the winter season</i> | 103 |
| | <i>8.3 N₂O and N₂ emissions from agricultural soil amended with AD and cattle slurry</i> | 104 |
| | <i>8.4 N₂O reduction via denitrification in different soils and associated isotope fractionation</i> | 106 |
| | <i>8.5 Isotopic fractionation factors of N₂O production and reduction during denitrification</i> | 107 |
| | <i>8.6 Are new laser spectroscopic techniques an alternative to IRMS for isotopic N₂O analysis?</i> | 110 |
| | <i>8.7 References</i> | 111 |
| 9 | Summary | 119 |
| 10 | Zusammenfassung | 121 |
| 11 | Acknowledgements | 123 |
| 12 | Curriculum vitae | 127 |

Chapter 1

General introduction

1 General Introduction

1.1 Impact of anthropogenic greenhouse gas emissions on the global climate

During the last decades it became more and more evident that the global climate is changing, and the rising global temperature is of particular concern to many scientists and governments, because it causes, amongst others, rising sea levels, melting sea ice in the Arctic Ocean and ice sheets in Antarctica and Greenland, desertification in subtropical climate zones, and increase the number and intensity of extreme weather and climate events (Stocker et al., 2013). There is clear evidence that this global warming is primarily caused by rising atmospheric concentrations of so-called greenhouse gases (GHGs). The major atmospheric GHGs are water vapor (H_2O), carbon dioxide (CO_2), methane (CH_4), nitrous oxide (N_2O), and halocarbons. These GHGs absorb and therefore reduce the terrestrial emission of infrared radiation, and this naturally occurring greenhouse effect amounts to about 33°K (Schmidt et al., 2010) and is therefore essential for life on earth in the present form. However, human activities significantly increased the atmospheric concentrations of CO_2 , CH_4 , N_2O , and different halocarbons since the preindustrial era (i.e. since 1750), which causes positive radiative forcing, i.e. a net energy uptake of the global climate system (Stocker et al., 2013). So far, anthropogenic GHG emissions caused an increase of the global average surface temperature of about 0.85°C ($0.65 - 1.06^\circ\text{C}$) during the period from 1880 to 2012 (Stocker et al., 2013). CH_4 and N_2O , for example, have a global warming potential (GWP) about 34 or 298, respectively, times higher compared to CO_2 , and their atmospheric concentrations increased by a factor of 2.5 and 1.2, respectively, compared to preindustrial levels (Stocker et al., 2013). Besides its impact on the global energy budget, N_2O is also considered the most important ozone depleting substance affecting the stratospheric ozone layer during the 21st century (Ravishankara et al., 2009). Especially burning fossil carbon (C) for energy generation reintroduces huge amounts of CO_2 into the global C cycle, but also land use change, most notably deforestation, is a large CO_2 source. Agricultural activities also contribute largely to the increasing atmospheric GHG concentrations and is the main source of anthropogenic CH_4 and N_2O emissions (Stocker et al., 2013). Here, CH_4 derives mainly from enteric fermentation of ruminants and cultivation of paddy rice, while the main N_2O source are agricultural soils (Stocker et al., 2013), where N_2O is produced by microbial N transformations (Butterbach-Bahl et al., 2013). The invention of the Haber-Bosch process in the early 20th century established the basis for high N fertilizer production to increase agricultural productivity drastically, and thus resulted in doubling the annual input of reactive N species into the global N cycle (Galloway et al., 2004). This led to high N_2O emissions from soils, as these are directly related to N input (Mosier et al., 1998; Galloway et al., 2004; Davidson, 2009). However, trace gas emissions from agricultural activities can be significantly reduced by advancing management and mitigation strategies (Johnson et al., 2007), but these rely on improving the understanding of involved processes and controlling factors.

1.2 Biogas energy production and related trace gas emissions

In several European countries regenerative energy sources like biomass energy are explicitly promoted to replace fossil fuels and thus to reduce GHG emissions. Here, electricity generation from biogas became one of the major technologies (e.g. Herrmann and Rath, 2012). Biogas is produced by anaerobic fermentation of energy crops and organic agricultural wastes like animal slurries and forage waste, but other organic residues, e.g. wastes from food industries, may be included. While the

produced biogas is used for generating electricity and heat, the anaerobic digestates (AD) as the by-products of the biogas fermentation process are usually applied to agricultural land as organic fertilizers to return nutrients into the production cycle. However, also during different steps of the biogas production chain significant GHG and ammonia (NH_3) emissions occur, for example during fertilizer production, transportation of fertilizers, substrate, and AD, CH_4 leakage, AD storage, AD land spreading, exhaust from agricultural machinery, etc. (Claus et al., 2013; Liebetrau et al., 2013).

AD are often stored for several months prior to field application to meet with plants nutrient demands. A high percentage of the AD storage facilities are uncovered or are equipped with non-gastight covers (Daniel-Gromke et al., 2013). Under these conditions, different trace gases such as NH_3 , CH_4 , and N_2O can freely escape to the atmosphere. Only very few data on trace gas emissions from AD storage are available, mainly due to the methodologically challenging measurements; however, open AD storage has been suggested to be the production step with the highest trace gas emission potential, and thus to reduce the GHG savings of biogas energy the most during the whole biogas production process (Meyer-Aurich et al., 2012; Claus et al., 2013).

These AD often have similar characteristics like animal slurries, but are usually characterized by higher ammonium content and pH value due to the fermentation process (Gutser et al., 2005; Tambone et al., 2009), which implies a higher risk of NH_3 volatilization (Wulf et al., 2002); however, reported observations are inconsistent (Novak and Fiorelli, 2010). Organic substrates passing the digester undecomposed may hold substantial residual CH_4 production potential, which can lead to significant CH_4 emissions (FNR, 2009; Gioelli et al., 2011). Anaerobic digestion has been proposed as a measure for reducing CH_4 emissions from animal slurries during storage by breaking down easily degradable organic matter during the fermentation process, though CH_4 emissions may still be significant (Amon et al., 2006; Marañón et al., 2011; Massé et al., 2011). Trace gas emissions during AD storage in uncovered storage facilities are also influenced by other factors. Weather conditions, for example, have been shown to be an important factor controlling emissions from stored animal slurries. In particular, high temperatures promote emissions of CH_4 , NH_3 , and N_2O (Novak and Fiorelli, 2010; Flesch et al., 2013); though, for NH_3 volatilization wind speed is an even stronger controlling factor (Harper et al., 2006). A naturally occurring surface crust can effectively reduce NH_3 emissions as a physical barrier (Sommer et al., 1993; Misselbrook et al., 2005; Smith et al., 2007), and may possibly also reduce CH_4 release due to microbial CH_4 oxidation within the crust (Nielsen et al., 2013). In contrast, it has been shown that significant N_2O production occurs in surface crusts by microbial NH_3 oxidation (nitrification) in oxic zones and subsequent denitrification processes in anoxic zones (Sommer et al., 2000; Berg et al., 2006). Thus, AD pose a source of potentially high GHG and NH_3 emissions when stored in uncovered tanks or lagoons.

1.3 Utilization of anaerobic digestates as fertilizers and related NH_3 emissions

During land spreading of AD as organic fertilizer significant trace gas emissions can occur, which are dominated by NH_3 volatilization, and thus large amounts of NH_3 can be lost to the atmosphere (e.g. Amon et al., 2006; Quakernack et al., 2012). These emissions do not only pose a loss of fertilizer N, but also environmental threads. A large proportion of NH_3 is deposited locally and affects natural ecosystems (Sutton et al., 1998; Sutton et al., 2011; Hertel et al., 2013). Furthermore, it may be assumed that about 1% of NH_3 deposited to soils is converted by microbial processes to N_2O (Mosier

et al., 1998). As there exists substantial emission potential in AD management (Amon et al., 2006), these emissions could significantly reduce GHG savings of biogas energy.

Most studies on NH₃ emissions during AD management including field application only cover the growing season, i.e. the period between spring and early autumn. So far, no data on NH₃ emissions from AD land spreading under cold winter conditions has been published, but results by Sommer et al. (1991) from wind tunnel experiments with cattle slurry indicate that application on frozen soil can lead to high NH₃ emissions, because infiltration into the soil is hampered. The lack of data on NH₃ emissions during winter application is in contrast to the common practice in Germany to apply AD and slurry after snow melt but on still frozen soil. This is due to a better trafficability, assumed low NH₃ emissions because of low temperatures, and limitations in storage capacities. Later in spring the application of organic fertilizers may be hampered by moist soil conditions, and crop damage may be higher. A profound data base about these NH₃ emissions is essential for consulting on good practice in AD and slurry management.

1.4 Advantages of optical remote sensing approaches for measuring trace gas emissions

A well founded data basis about emissions of climate relevant trace gases during all steps of the biogas production chain is crucial to fully evaluate GHG savings from biogas energy production systems and for national greenhouse gas inventories. However, reliable data about emissions during AD storage is particularly scarce, because emission measurements from large open AD lagoons and tanks comprise methodical challenges and difficulties. Few studies were focusing on GHG and NH₃ emissions from anaerobically digested cattle slurry during storage in pilot scale slurry tanks deploying a dynamic chamber technique (Amon et al., 2006; Clemens et al., 2006). In a recent study investigating trace gas emissions from a number of different open AD storage tanks on farm scale biogas plants, an approach with a floating chamber for CH₄ and NH₃ emission measurements was deployed (Liebetrau et al., 2013). However, in an earlier study using floating open chambers to determine CH₄ emissions from a slurry tank Husted (1993) showed large spatial variations in CH₄ emissions of up to two orders of magnitude, which puts such chamber approaches into question. Similar observations were reported by Park et al. (2010) in a study comparing floating chambers with a micrometeorological mass balance technique for measuring CH₄ emissions from slurry tanks. Here, high spatial and temporal variability as well as flux overestimation were observed with the chamber method, which was mainly attributed to chamber placement on the slurry surface (e.g. close to slurry inlet) and chamber disturbance (e.g. chamber aeration fan, chamber movement by wind driven surface perturbation). Wood et al. (2013) reported that the occurrence of a surface crust on animal slurries can lead to less predictable but rather episodic and irregular CH₄ flux events, which implies a risk of high uncertainties of fluxes derived from non-continuous chamber measurements. In addition to the mentioned shortcomings of the chamber approach, NH₃ emissions depend largely on wind speed (Olesen and Sommer, 1993); therefore, chamber measurements of NH₃ emissions are particularly susceptible and may under certain circumstances be out by one order of magnitude as discussed by Parker et al. (2013).

The application of micrometeorological approaches like mass balance methods, flux-gradient techniques, eddy covariance, or micrometeorological dispersion models for trace gas flux measurements poses numerous advantages compared to chamber techniques. These techniques are less susceptible to spatial and temporal heterogeneity of the emission source and capable of noninvasive and continuous flux measurements integrating over large emission source areas

(Denmead, 2008; Park et al., 2010). Compared to other micrometeorological techniques (e.g. “forward” Lagrangian Stochastic models or mass balance methods), the backward Lagrangian Stochastic dispersion technique (bLS; Flesch et al., 1995; Flesch et al., 2004) has the advantages of more flexible calculation of short-range dispersion from area sources, and that wind and concentration measurements at one height only are sufficient to estimate trace gas fluxes from (or to) surface areas of any shape (Flesch et al., 2004; Denmead, 2008). In studies with artificial CH₄ emissions from area sources under undisturbed conditions very good recovery rates with inaccuracies of often less than 2% have been documented, while in field trials with wind disturbance the accuracy of this technique has been shown to be lower, but still in most cases satisfying results could be achieved (Flesch et al., 2005). Ro et al. (2013) evaluated the applicability of the bLS technique for determining trace gas fluxes from waste lagoons and ponds, and recovered between 81 and 93% of artificially released CH₄. Ideally, the bLS technique is combined with one or more open-path line-average concentration sensors like open-path Tunable Diode Laser Absorption Spectroscopy (TDLAS) or open-path Fourier Transform infrared (OP FTIR) spectroscopy, where OP FTIR has the advantage of measuring a variety of trace gases simultaneously including NH₃, CH₄, N₂O, CO₂, and H₂O (Denmead, 2008).

1.5 Impact of organic fertilizers on N₂O emissions from agricultural soils

Application of mineral and organic N fertilizers to agricultural soils has been shown to not only be a source for instantaneous NH₃ volatilization, but also to cause significant N₂O emissions from soils (e.g. Galloway et al., 2004). These emissions usually do not appear immediately after fertilizer application, but are rather staggered over longer time intervals, because they derive from microbial N turnover processes in the soil, namely by nitrification, the oxidation of ammonium to nitrate, and by denitrification, the successive reduction of oxidized N (i.e. nitrate and nitrite) via the gaseous intermediates NO and N₂O to N₂; but also several other biological pathways can contribute significant amounts of N₂O (Wrage et al., 2001; Butterbach-Bahl et al., 2013). These N₂O emissions are the main source of anthropogenic N₂O released to the atmosphere, and N₂O production in agricultural soils is directly related to N fertilizer input (Mosier et al., 1998; Galloway et al., 2004), as it has been shown that between 2 and 2.5% of all applied fertilizer N is eventually converted to N₂O and escapes to the atmosphere (Davidson, 2009). However, N₂O emission factors can differ widely, as they depend on various factors, amongst others on fertilizer type, application rate and technique, physicochemical soil properties, climate, and crop type (Snyder et al., 2009).

Denitrification is usually the main N₂O source pathway (Saggar et al., 2013), but also nitrification can contribute significant amounts of N₂O (Bateman and Baggs, 2005). Especially organic fertilizers like AD and animal slurries can promote N₂O emissions (e.g. Jones et al., 2007; Senbayram et al., 2009), because their easily degradable organic C content fosters heterotrophic denitrification processes (Weier et al., 1993; Senbayram et al., 2012; Saggar et al., 2013). Therefore, anaerobic digestion of organic fertilizers like animal slurries prior to land spreading may not only reduce CH₄ production during slurry management (Amon et al., 2006; Marañón et al., 2011), but possibly also lower N₂O production by denitrification after land spreading under certain conditions by reducing the labile carbon content. N₂O reduction to N₂ via denitrification depends largely on the ratio of available organic C as electron donor and nitrate as electron acceptor, but also on other soil properties (Saggar et al., 2013). High nitrate concentrations inhibit N₂O reduction, while low nitrate availability together with high demand for electron acceptors leads to high N₂O reduction to N₂, and thus to lower N₂O/(N₂O+N₂) product ratios (Weier et al., 1993; Senbayram et al., 2012; Saggar et al., 2013).

1.6 N₂O isotopomers and their potential use for N₂O source identification

Several different microbial pathways contribute to N₂O production and consumption in soils (Butterbach-Bahl et al., 2013). Better understanding of factors and drivers controlling these turnover processes is crucial for implementing N₂O reducing management practice. However, determination of N₂ production and thus the N₂O/(N₂O+N₂) product ratio of denitrification is difficult because of the high atmospheric N₂ background (Groffman et al., 2006). N₂O source apportioning to its different production pathways is even more challenging, but of particular significance for process understanding. Different stable isotope approaches have been deployed for this purpose as summarized by Baggs (2008). Only recently, the use of the so-called ‘site preference’ (SP), i.e. the intramolecular ¹⁵N distribution in the linear asymmetric N₂O molecule, has been introduced (Toyoda and Yoshida, 1999; Yoshida and Toyoda, 2000). This approach relies on specific isotopic signatures linked to certain N₂O source processes, which were obtained in pure culture studies (Sutka et al., 2003, 2004; Toyoda et al., 2005; Sutka et al., 2006; Sutka et al., 2008), and is considered to be independent of the isotopic signature of the precursor species (Toyoda et al., 2002). Additional information is obtained from the N₂O δ¹⁵N^{bulk} and δ¹⁸O values (Jinuntuya-Nortman et al., 2008; Snider et al., 2009; Well and Flessa, 2009).

However, this technique is still complicated by some overlap for example of the isotopic signatures of autotrophic nitrification and fungal denitrification (Sutka et al., 2006; Sutka et al., 2008), and for several N₂O producing pathways, e.g. archaeal nitrification and denitrification, anammox, and DNRA, characteristic isotopic signatures have not been determined yet (Ostrom and Ostrom, 2012). Furthermore, N₂O reduction to N₂ has been found to alter the SP by enriching ¹⁵N at the central position of the N₂O molecules (Ostrom et al., 2007; Jinuntuya-Nortman et al., 2008; Well and Flessa, 2009). However, a linear relationship between N₂O SP and δ¹⁸O values may be indicative for N₂O significantly affected by reduction (Jinuntuya-Nortman et al., 2008; Well and Flessa, 2009).

First attempts applying isotopomer signatures of soil-emitted N₂O to distinguish production pathways under natural conditions have been published recently (Opdyke et al., 2009; Park et al., 2011; Toyoda et al., 2011). This approach requires good understanding of isotopic fractionation of involved processes, but fractionation factors of N₂O production and reduction via denitrification are not yet very precisely investigated under complex and variable soil conditions, and published values cover wide ranges (e.g. Baggs, 2008). Thus, better understanding of isotope effects during N₂O production and reduction via denitrification, in addition to isotope signals of N₂O production via different pathways, is crucial to facilitate more precise N₂O source apportioning in studies on whole soil.

1.7 Recent developments in laser spectroscopic techniques for N₂O isotope analysis

Until recently, most studies analyzing N₂O isotopomers were based on the mass determination of molecular (N₂O⁺) and fragment (NO⁺) ions of N₂O by isotope ratio mass spectrometry (IRMS), allowing the calculation of δ¹⁵N^{bulk}, δ¹⁸O, and SP values (Brenninkmeijer and Röckmann, 1999; Toyoda and Yoshida, 1999). In contrast, novel spectroscopic techniques like Fourier transform infrared (FTIR) spectroscopy (Griffith et al., 2009), or quantum cascade laser absorption spectroscopy (QCLAS; Wächter et al., 2008; Mohn et al., 2010; Mohn et al., 2012) enable the direct quantification of individual N₂O isotopomers based on their characteristic rotational-vibrational absorption spectra. Especially QCLAS may hold several advantages compared to IRMS in terms of precision, throughput, and

real-time analysis. Even though real-time analysis of N₂O isotope signatures at ambient concentration levels without pre-concentration is still not possible with the current instrument generation (Mohn et al., 2010), real-time monitoring of N₂O isotopomers in laboratory studies on soil-derived N₂O at elevated concentrations may be technically feasible.

1.8 Objectives

1.8.1 Open-Path quantification of ammonia, methane, and nitrous oxide emissions from co-fermented anaerobic digestates stored in lagoons – Chapter 2

AD pose a significant source of trace gas emissions during storage when storage facilities are not covered gas tight, because they are usually characterized by relative high pH values, high ammonium concentrations, and substantial residual CH₄ production potential. The resulting trace gas emissions may significantly reduce the GHG balance and affect the environmental impact of biogas energy. It may be hypothesized that relevant trace gas emissions occur from open AD storage lagoons to an extent that GHG savings from biogas energy production systems are considerably reduced and that these emissions are dominated by CH₄ and NH₃. A naturally occurring surface crust may significantly reduce NH₃ losses during storage, but promote N₂O formation. Therefore, Chapter 2 addresses these emissions and the effect of a surface crust in a study deploying OP FTIR as a non-invasive remote sensing technique for measuring NH₃, CH₄, and N₂O concentrations along the downwind edge of two AD storage lagoons. Trace gas fluxes were estimated using the bLS technique and GWP weighted emissions were related to energy production of the biogas plants. To evaluate the applicability of this methodical approach for given local conditions with wind disturbance by the elevated lagoons and nearby farm buildings, several trace gas release experiments were carried out and the trace gas recovery by the bLS model was determined.

1.8.2 Cold season ammonia emissions from land spreading with anaerobic digestates from biogas production – Chapter 3

AD application to agricultural land as organic fertilizer often occurs very early in the year, when soils are still partly frozen. This has practical advantages, e.g. better trafficability and reduced crop damage. It was often assumed that under cold weather conditions the NH₃ volatilization is considerably low. However, it was hypothesized, that frozen soil conditions hamper AD infiltration into the soil, which may, together with low canopy coverage and relatively high wind speeds, still result in substantial NH₃ emissions despite of low temperatures. OP FTIR as an optical remote sensing technique integrating over large emission source areas in combination with a micrometeorological dispersion model is less susceptible to spatiotemporal heterogenic emissions and thus provides advantages compared to other techniques for emission measurements in large agricultural fields.

The objective of Chapter 3 was to determine NH₃ emissions during and after AD land spreading using OP FTIR and the bLS technique during a field trial in late February under winter conditions.

1.8.3 Anaerobic digestates lower N₂O emissions compared to cattle slurry by affecting rate and product stoichiometry of denitrification – an N₂O isotopomer case study – Chapter 4

Application of AD or animal slurries to agricultural soils as organic fertilizers may contribute to N₂O production via denitrification, but also foster N₂O consumption by N₂O reduction to N₂ by denitrifiers. However, factors controlling the resulting N₂O/(N₂O+N₂) product ratio are poorly understood.

A soil incubation experiment was carried out with the objective to study the effects of different organic fertilizers (cattle slurry and digestate from anaerobic food waste digestion) on total N₂O and N₂ losses by denitrification and their influence on the N₂O/(N₂O+N₂) product ratio under conditions favoring denitrification. An N₂-free helium oxygen incubation atmosphere allowed direct determination of N₂ in addition to N₂O, CO₂, and CH₄. Gas samples were taken at frequent intervals and the major N₂O isotopomers were determined by IRMS. The intramolecular ¹⁵N distribution of emitted N₂O was used for estimating the relative contribution of denitrification and nitrification to N₂O production.

High N₂O production as well as high N₂O reduction by denitrification were expected, but also significant N₂O release from nitrification due to the addition of the ammonium based organic fertilizers. Anaerobic digestate was expected to result in lower denitrification rates due to its lower organic carbon content, while it was hypothesized that cattle slurry with higher organic C content will lead to a lower N₂O/(N₂O+N₂) product ratio due to increased N₂O reduction.

1.8.4 Soil denitrification potential and its influence on N₂O reduction and N₂O isotopomer ratios – Chapter 5

The usage of isotopomer ratios for N₂O source apportioning requires much better understanding of isotope effects during N₂O reduction, alongside of the isotope signals of N₂O production via different other microbial pathways. Chapter 5 is focused on N₂O reduction, described by the N₂O/(N₂O+N₂) product ratio, during denitrification in different soils and the associated isotope signals. Two laboratory incubation experiments with three typical but contrasting soils from Northern Germany were set up to compare the denitrification potential and N₂O/(N₂O+N₂) product ratio of denitrification of these soils, and to investigate the effect of N₂O reduction on the intramolecular ¹⁵N distribution and on δ¹⁸O values of emitted N₂O.

It was hypothesized that N₂O reduction is not solely controlled by the ratio of nitrate and easily degradable C sources, and that thus excess nitrate supply will not necessarily result in identical N₂O/(N₂O+N₂) product ratios in different soils. The observed isotope effects of during N₂O reduction might vary with the experimental setup (e.g. N₂O added to the headspace vs. N₂O production within soil microorganisms); therefore, an approach was chosen contrasting recently published studies and the resulting isotope effects during N₂O reduction were compared to the literature.

1.8.5 Experimental determinations of isotopic fractionation factors associated with N₂O production and reduction during denitrification in soils – Chapter 6

Quantifying denitrification in arable soils is crucial for predicting nitrogen fertilizer losses and N₂O emissions. Stable isotopologue analyses of emitted N₂O (δ¹⁵N, δ¹⁸O, and SP) may help to distinguish

production pathways and to quantify N₂O reduction to N₂. However, interpretation of experimental data is often ambiguous due to insufficient knowledge on isotopic fractionation mechanisms.

The objective of the study presented in Chapter 6 was to determine fractionation factors associated with N₂O production and reduction during heterotrophic denitrification in soil. Furthermore, it is aiming to elucidate factors controlling the magnitude of the apparent isotope effects. In a complex experimental approach based on three laboratory experiments differing in their experimental set-up and soil properties, the net fractionation factors (η) associated with denitrification were determined. All available methods for independent determination of N₂O reduction were used, i.e. soil incubation in N₂-free atmosphere, the acetylene inhibition technique, and the ¹⁵N gas-flux method.

1.8.6 Novel laser spectroscopic technique for continuous analysis of N₂O isotopomers – application and intercomparison with isotope ratio mass spectrometry – Chapter 7

Most reported studies analyzing N₂O isotopomers are based on mass spectrometric determination of N₂O $\delta^{15}\text{N}^{\text{bulk}}$, $\delta^{18}\text{O}$, and SP signatures, but QCLAS as a novel laser spectroscopic technique may provide several advantages in terms of precision, throughput, and real-time monitoring. Therefore, a laboratory based setup involving a QCL spectrometer and two FTIR spectrometers was established, in which a soil was incubated over several days and the isotopic signatures of evolving N₂O were monitored continuously.

The objective of this study presented in Chapter 7 was to test and demonstrate the feasibility of continuous N₂O isotopomer analysis of soil-derived N₂O by QCLAS and its validation by inter-comparison to IRMS as state of the art technique.

1.9 References

- Amon, B., Kryvoruchko, V., Amon, T., Zechmeister-Boltenstern, S., 2006. Methane, nitrous oxide and ammonia emissions during storage and after application of dairy cattle slurry and influence of slurry treatment. *Agriculture Ecosystems & Environment* 112, 153-162.
- Baggs, E.M., 2008. A review of stable isotope techniques for N₂O source partitioning in soils: recent progress, remaining challenges and future considerations. *Rapid Communications in Mass Spectrometry* 22, 1664-1672.
- Bateman, E.J., Baggs, E.M., 2005. Contributions of nitrification and denitrification to N₂O emissions from soils at different water-filled pore space. *Biology and Fertility of Soils* 41, 379-388.
- Berg, W., Brunsch, R., Pazsiczki, I., 2006. Greenhouse gas emissions from covered slurry compared with uncovered during storage. *Agriculture Ecosystems & Environment* 112, 129-134.
- Brenninkmeijer, C.A.M., Röckmann, T., 1999. Mass spectrometry of the intramolecular nitrogen isotope distribution of environmental nitrous oxide using fragment-ion analysis. *Rapid Communications in Mass Spectrometry* 13, 2028-2033.

- Butterbach-Bahl, K., Baggs, E.M., Dannenmann, M., Kiese, R., Zechmeister-Boltenstern, S., 2013. Nitrous oxide emissions from soils: how well do we understand the processes and their controls? *Philosophical Transactions of the Royal Society B-Biological Sciences* 368.
- Claus, S., Taube, F., Wienforth, B., Svoboda, N., Sieling, K., Kage, H., Senbayram, M., Dittert, K., Gericke, D., Pacholski, A., Herrmann, A., 2013. Life-cycle assessment of biogas production under the environmental conditions of northern Germany: greenhouse gas balance. *Journal of Agricultural Science FirstView*, 1-10.
- Clemens, J., Trimborn, M., Weiland, P., Amon, B., 2006. Mitigation of greenhouse gas emissions by anaerobic digestion of cattle slurry. *Agriculture, Ecosystems & Environment* 112, 171-177.
- Daniel-Gromke, J., Denysenko, V., Sauter, P., Naumann, K., Scheftelowitz, M., Krautz, A., Beil, M., Beyrich, w., Peters, W., Schicketanz, S., Schultze, C., Deumelandt, P., Reinicke, F., 2013. *Stromerzeugung aus Biomasse*; In: Deutsches Biomasseforschungszentrum (DBFZ); Leipzig, Germany; pp 47-48. URL: https://www.dbfz.de/web/fileadmin/user_upload/Referenzen/Berichte/biomassemonitoring_zwischenbericht_bf.pdf; accessed: 24.01.2014.
- Davidson, E.A., 2009. The contribution of manure and fertilizer nitrogen to atmospheric nitrous oxide since 1860. *Nature Geoscience* 2, 659-662.
- Denmead, O.T., 2008. Approaches to measuring fluxes of methane and nitrous oxide between landscapes and the atmosphere. *Plant and Soil* 309, 5-24.
- Flesch, T.K., Wilson, J.D., Yee, E., 1995. Backward-time Lagrangian stochastic dispersion models and their application to estimate gaseous emissions. *Journal of Applied Meteorology* 34, 1320-1332.
- Flesch, T.K., Wilson, J.D., Harper, L.A., Crenna, B.P., Sharpe, R.R., 2004. Deducing ground-to-air emissions from observed trace gas concentrations: A field trial. *Journal of Applied Meteorology* 43, 487-502.
- Flesch, T.K., Wilson, J.D., Harper, L.A., 2005. Deducing ground-to-air emissions from observed trace gas concentrations: A field trial with wind disturbance. *Journal of Applied Meteorology* 44, 475-484.
- Flesch, T.K., Verge, X.P.C., Desjardins, R.L., Worth, D., 2013. Methane emissions from a swine manure tank in western Canada. *Canadian Journal of Animal Science* 93, 159-169.
- FNR, 2009. Biogas-Messprogramm II - 61 Biogasanlagen im Vergleich. Fachagentur Nachwachsende Rohstoffe e.V. (FNR), Gülzow, Germany. URL: http://www.fnr-server.de/ftp/pdf/literatur/pdf_385messdaten_biogasmessprogramm_ii.pdf; accessed: 01.09.2013.
- Galloway, J.N., Dentener, F.J., Capone, D.G., Boyer, E.W., Howarth, R.W., Seitzinger, S.P., Asner, G.P., Cleveland, C.C., Green, P.A., Holland, E.A., Karl, D.M., Michaels, A.F., Porter, J.H., Townsend, A.R., Vorosmarty, C.J., 2004. Nitrogen cycles: past, present, and future. *Biogeochemistry* 70, 153-226.
- Gioelli, F., Dinuccio, E., Balsari, P., 2011. Residual biogas potential from the storage tanks of non-separated digestate and digested liquid fraction. *Bioresource Technology* 102, 10248-10251.

- Griffith, D.W.T., Parkes, S.D., Haverd, V., Paton-Walsh, C., Wilson, S.R., 2009. Absolute Calibration of the Intramolecular Site Preference of ¹⁵N Fractionation in Tropospheric N₂O by FT-IR Spectroscopy. *Analytical Chemistry* 81, 2227-2234.
- Groffman, P.M., Altabet, M.A., Bohlke, J.K., Butterbach-Bahl, K., David, M.B., Firestone, M.K., Giblin, A.E., Kana, T.M., Nielsen, L.P., Voytek, M.A., 2006. Methods for measuring denitrification: Diverse approaches to a difficult problem. *Ecological Applications* 16, 2091-2122.
- Gutser, R., Ebertseder, T., Weber, A., Schraml, M., Schmidhalter, U., 2005. Short-term and residual availability of nitrogen after long-term application of organic fertilizers on arable land. *Journal of Plant Nutrition and Soil Science-Zeitschrift Fur Pflanzenernahrung Und Bodenkunde* 168, 439-446.
- Harper, L.A., Weaver, K.H., Dotson, R.A., 2006. Ammonia emissions from swine waste lagoons in the Utah Great Basin. *Journal of Environmental Quality* 35, 224-230.
- Herrmann, A., Rath, J., 2012. Biogas Production from Maize: Current State, Challenges, and Prospects. 1. Methane Yield Potential. *Bioenergy Research* 5, 1027-1042.
- Hertel, O., Geels, C., Frohn, L.M., Ellermann, T., Skjoth, C.A., Lostrom, P., Christensen, J.H., Andersen, H.V., Peel, R.G., 2013. Assessing atmospheric nitrogen deposition to natural and semi-natural ecosystems - Experience from Danish studies using the DAMOS. *Atmospheric Environment* 66, 151-160.
- Husted, S., 1993. An open chamber technique for determination of methane emission from stored livestock manure. *Atmospheric Environment Part a-General Topics* 27, 1635-1642.
- Jinuntuya-Nortman, M., Sutka, R.L., Ostrom, P.H., Gandhi, H., Ostrom, N.E., 2008. Isotopologue fractionation during microbial reduction of N₂O within soil mesocosms as a function of water-filled pore space. *Soil Biology & Biochemistry* 40, 2273-2280.
- Johnson, J.M.F., Franzluebbers, A.J., Weyers, S.L., Reicosky, D.C., 2007. Agricultural opportunities to mitigate greenhouse gas emissions. *Environmental Pollution* 150, 107-124.
- Jones, S.K., Rees, R.M., Skiba, U.M., Ball, B.C., 2007. Influence of organic and mineral N fertiliser on N₂O fluxes from a temperate grassland. *Agriculture Ecosystems & Environment* 121, 74-83.
- Liebetrau, J., Reinelt, T., Clemens, J., Hafermann, C., Friehe, J., Weiland, P., 2013. Analysis of greenhouse gas emissions from 10 biogas plants within the agricultural sector. *Water Science and Technology* 67, 1370-1379.
- Marañón, E., Salter, A.M., Castrillón, L., Heaven, S., Fernández-Nava, Y., 2011. Reducing the environmental impact of methane emissions from dairy farms by anaerobic digestion of cattle waste. *Waste Management* 31, 1745-1751.
- Massé, D.I., Talbot, G., Gilbert, Y., 2011. On farm biogas production: A method to reduce GHG emissions and develop more sustainable livestock operations. *Animal Feed Science and Technology* 166-67, 436-445.
- Meyer-Aurich, A., Schattauer, A., Hellebrand, H.J., Klaus, H., Plochl, M., Berg, W., 2012. Impact of uncertainties on greenhouse gas mitigation potential of biogas production from agricultural resources. *Renewable Energy* 37, 277-284.

- Misselbrook, T.H., Brookman, S.K.E., Smith, K.A., Cumby, T., Williams, A.G., McCrory, D.F., 2005. Crusting of stored dairy slurry to abate ammonia emissions: Pilot-scale studies. *Journal of Environmental Quality* 34, 411-419.
- Mohn, J., Guggenheim, C., Tuzson, B., Vollmer, M.K., Toyoda, S., Yoshida, N., Emmenegger, L., 2010. A liquid nitrogen-free preconcentration unit for measurements of ambient N₂O isotopomers by QCLAS. *Atmospheric Measurement Techniques* 3, 609-618.
- Mohn, J., Tuzson, B., Manninen, A., Yoshida, N., Toyoda, S., Brand, W.A., Emmenegger, L., 2012. Site selective real-time measurements of atmospheric N₂O isotopomers by laser spectroscopy. *Atmospheric Measurement Techniques* 5, 1601-1609.
- Mosier, A., Kroeze, C., Nevison, C., Oenema, O., Seitzinger, S., van Cleemput, O., 1998. Closing the global N₂O budget: nitrous oxide emissions through the agricultural nitrogen cycle. *Nutrient Cycling in Agroecosystems* 52, 225-248.
- Nielsen, D.A., Schramm, A., Nielsen, L.P., Revsbech, N.P., 2013. Seasonal Methane Oxidation Potential in Manure Crusts. *Applied and Environmental Microbiology* 79, 407-410.
- Novak, S.M., Fiorelli, J.L., 2010. Greenhouse gases and ammonia emissions from organic mixed crop-dairy systems: a critical review of mitigation options. *Agronomy for Sustainable Development* 30, 215-236.
- Olesen, J.E., Sommer, S.G., 1993. Modelling effects of wind speed and surface cover on ammonia volatilization from stored pig slurry. *Atmospheric Environment Part a-General Topics* 27, 2567-2574.
- Opdyke, M.R., Ostrom, N.E., Ostrom, P.H., 2009. Evidence for the predominance of denitrification as a source of N₂O in temperate agricultural soils based on isotopologue measurements. *Global Biogeochemical Cycles* 23. DOI: 10.1029/2009GB003523.
- Ostrom, N.E., Pitt, A., Sutka, R., Ostrom, P.H., Grandy, A.S., Huizinga, K.M., Robertson, G.P., 2007. Isotopologue effects during N₂O reduction in soils and in pure cultures of denitrifiers. *Journal of Geophysical Research-Biogeosciences* 112. DOI: 10.1029/2006JG000287.
- Ostrom, N.E., Ostrom, P.H., 2012. The Isotopomers of Nitrous Oxide: Analytical Considerations and Application to Resolution of Microbial Production Pathways. In: Baskaran, M. (Ed.), *Handbook of Environmental Isotope Geochemistry*. Springer Berlin Heidelberg, Berlin, pp. 453-476.
- Park, K.H., Wagner-Riddle, C., Gordon, R.J., 2010. Comparing methane fluxes from stored liquid manure using micrometeorological mass balance and floating chamber methods. *Agricultural and Forest Meteorology* 150, 175-181.
- Park, S., Pérez, T., Boering, K.A., Trumbore, S.E., Gil, J., Marquina, S., Tyler, S.C., 2011. Can N₂O stable isotopes and isotopomers be useful tools to characterize sources and microbial pathways of N₂O production and consumption in tropical soils? *Global Biogeochemical Cycles* 25. DOI: 10.1029/2009gb003615.
- Parker, D., Ham, J., Woodbury, B., Cai, L., Spiehs, M., Rhoades, M., Trabue, S., Casey, K., Todd, R., Cole, A., 2013. Standardization of flux chamber and wind tunnel flux measurements for quantifying volatile organic compound and ammonia emissions from area sources at animal feeding operations. *Atmospheric Environment* 66, 72-83.

- Quakernack, R., Pacholski, A., Techow, A., Herrmann, A., Taube, F., Kage, H., 2012. Ammonia volatilization and yield response of energy crops after fertilization with biogas residues in a coastal marsh of Northern Germany. *Agriculture Ecosystems & Environment* 160, 66-74.
- Ravishankara, A.R., Daniel, J.S., Portmann, R.W., 2009. Nitrous oxide (N₂O): The dominant ozone-depleting substance emitted in the 21st century. *Science* 326, 123-125.
- Ro, K.S., Johnson, M.H., Stone, K.C., Hunt, P.G., Flesch, T., Todd, R.W., 2013. Measuring gas emissions from animal waste lagoons with an inverse-dispersion technique. *Atmospheric Environment* 66, 101-106.
- Saggar, S., Jha, N., Deslippe, J., Bolan, N.S., Luo, J., Giltrap, D.L., Kim, D.G., Zaman, M., Tillman, R.W., 2013. Denitrification and N₂O:N₂ production in temperate grasslands: Processes, measurements, modelling and mitigating negative impacts. *The Science of the total environment* 465.
- Schmidt, G.A., Ruedy, R.A., Miller, R.L., Lacis, A.A., 2010. Attribution of the present-day total greenhouse effect. *Journal of Geophysical Research-Atmospheres* 115. DOI: 10.1029/2010jd014287.
- Senbayram, M., Chen, R.R., Mühling, K.H., Dittert, K., 2009. Contribution of nitrification and denitrification to nitrous oxide emissions from soils after application of biogas waste and other fertilizers. *Rapid Communications in Mass Spectrometry* 23, 2489-2498.
- Senbayram, M., Chen, R., Budai, A., Bakken, L., Dittert, K., 2012. N₂O emission and the N₂O/(N₂O + N₂) product ratio of denitrification as controlled by available carbon substrates and nitrate concentrations. *Agriculture Ecosystems & Environment* 147, 4-12.
- Smith, K., Cumby, T., Lapworth, J., Misselbrook, T., Williams, A., 2007. Natural crusting of slurry storage as an abatement measure for ammonia emissions on dairy farms. *Biosystems Engineering* 97, 464-471.
- Snider, D.M., Schiff, S.L., Spoelstra, J., 2009. ¹⁵N/¹⁴N and ¹⁸O/¹⁶O stable isotope ratios of nitrous oxide produced during denitrification in temperate forest soils. *Geochimica et Cosmochimica Acta* 73, 877-888.
- Snyder, C.S., Bruulsema, T.W., Jensen, T.L., Fixen, P.E., 2009. Review of greenhouse gas emissions from crop production systems and fertilizer management effects. *Agriculture Ecosystems & Environment* 133, 247-266.
- Sommer, S.G., Olesen, J.E., Christensen, B.T., 1991. Effects of temperature, wind speed and air humidity on ammonia volatilization from surface applied cattle slurry. *Journal of Agricultural Science* 117, 91-100.
- Sommer, S.G., Christensen, B.T., Nielsen, N.E., Schjorring, J.K., 1993. Ammonia volatilization during storage of cattle and pig slurry: effect of surface cover. *Journal of Agricultural Science* 121, 63-71.
- Sommer, S.G., Petersen, S.O., Sogaard, H.T., 2000. Greenhouse gas emission from stored livestock slurry. *Journal of Environmental Quality* 29, 744-751.
- Stocker, T.F., Qin, D., Plattner, G.-K., Tignor, M., Allen, S.K., Boschung, J., Nauels, A., Xia, Y., Bex, V., Midgley, P.M., 2013. *Climate Change 2013: The Physical Science Basis. Contribution of Working*

- Group I to the Fifth Assessment Report of the Intergovernmental Panel on Climate Change
Cambridge University Press, Cambridge, United Kingdom and New York, NY, USA,
- Sutka, R.L., Ostrom, N.E., Ostrom, P.H., Gandhi, H., Breznak, J.A., 2003. Nitrogen isotopomer site preference of N₂O produced by *Nitrosomonas europaea* and *Methylococcus capsulatus* Bath. Rapid Communications in Mass Spectrometry 17, 738-745.
- Sutka, R.L., Ostrom, N.E., Ostrom, P.H., Gandhi, H., Breznak, J.A., 2004. Nitrogen isotopomer site preference of N₂O produced by *Nitrosomonas europaea* and *Methylococcus capsulatus* Bath (vol 18, pg 1411, 2004). Rapid Communications in Mass Spectrometry 18, 1411-1412.
- Sutka, R.L., Ostrom, N.E., Ostrom, P.H., Breznak, J.A., Gandhi, H., Pitt, A.J., Li, F., 2006. Distinguishing nitrous oxide production from nitrification and denitrification on the basis of isotopomer abundances. Applied and Environmental Microbiology 72, 638-644.
- Sutka, R.L., Adams, G.C., Ostrom, N.E., Ostrom, P.H., 2008. Isotopologue fractionation during N₂O production by fungal denitrification. Rapid Communications in Mass Spectrometry 22, 3989-3996.
- Sutton, M.A., Milford, C., Dragosits, U., Place, C.J., Singles, R.J., Smith, R.I., Pitcairn, C.E.R., Fowler, D., Hill, J., ApSimon, H.M., Ross, C., Hill, R., Jarvis, S.C., Pain, B.F., Phillips, V.C., Harrison, R., Moss, D., Webb, J., Espenhahn, S.E., Lee, D.S., Hornung, M., Ulliyett, J., Bull, K.R., Emmett, B.A., Lowe, J., Wyers, G.P., 1998. Dispersion, deposition and impacts of atmospheric ammonia: quantifying local budgets and spatial variability. Environmental Pollution 102, 349-361.
- Sutton, M.A., Oenema, O., Erisman, J.W., Leip, A., van Grinsven, H., Winiwarter, W., 2011. Too much of a good thing. Nature 472, 159-161.
- Tambone, F., Genevini, P., D'Imporzano, G., Adani, F., 2009. Assessing amendment properties of digestate by studying the organic matter composition and the degree of biological stability during the anaerobic digestion of the organic fraction of MSW. Bioresource Technology 100, 3140-3142.
- Toyoda, S., Yoshida, N., 1999. Determination of nitrogen isotopomers of nitrous oxide on a modified isotope ratio mass spectrometer. Analytical Chemistry 71, 4711-4718.
- Toyoda, S., Yoshida, N., Miwa, T., Matsui, Y., Yamagishi, H., Tsunogai, U., Nojiri, Y., Tsurushima, N., 2002. Production mechanism and global budget of N₂O inferred from its isotopomers in the western North Pacific. Geophysical Research Letters 29, 4.
- Toyoda, S., Mutoke, H., Yamagishi, H., Yoshida, N., Tanji, Y., 2005. Fractionation of N₂O isotopomers during production by denitrifier. Soil Biology & Biochemistry 37, 1535-1545.
- Toyoda, S., Yano, M., Nishimura, S., Akiyama, H., Hayakawa, A., Koba, K., Sudo, S., Yagi, K., Makabe, A., Tobar, Y., Ogawa, N.O., Ohkouchi, N., Yamada, K., Yoshida, N., 2011. Characterization and production and consumption processes of N₂O emitted from temperate agricultural soils determined via isotopomer ratio analysis. Global Biogeochemical Cycles 25. DOI: 10.1029/2009gb003769.
- Wächter, H., Mohn, J., Tuzson, B., Emmenegger, L., Sigrist, M.W., 2008. Determination of N₂O isotopomers with quantum cascade laser based absorption spectroscopy. Optics Express 16, 9239-9244.

- Weier, K.L., Doran, J.W., Power, J.F., Walters, D.T., 1993. Denitrification and the dinitrogen/nitrous oxide ratio as affected by soil water, available carbon, and nitrate. *Soil Science Society of America Journal* 57, 66-72.
- Well, R., Flessa, H., 2009. Isotopologue enrichment factors of N₂O reduction in soils. *Rapid Communications in Mass Spectrometry* 23, 2996-3002.
- Wood, J.D., Gordon, R.J., Wagner-Riddle, C., 2013. Biases in discrete CH₄ and N₂O sampling protocols associated with temporal variation of gas fluxes from manure storage systems. *Agricultural and Forest Meteorology* 171, 295-305.
- Wrage, N., Velthof, G.L., van Beusichem, M.L., Oenema, O., 2001. Role of nitrifier denitrification in the production of nitrous oxide. *Soil Biology & Biochemistry* 33, 1723-1732.
- Wulf, S., Maeting, M., Clemens, J., 2002. Application technique and slurry co-fermentation effects on ammonia, nitrous oxide, and methane emissions after spreading: I. Ammonia volatilization. *Journal of Environmental Quality* 31, 1789-1794.
- Yoshida, N., Toyoda, S., 2000. Constraining the atmospheric N₂O budget from intramolecular site preference in N₂O isotopomers. *Nature* 405, 330-334.

Chapter 2

Open-Path quantification of ammonia, methane, and nitrous oxide emissions from co-fermented anaerobic digestates stored in lagoons

Jan Reent Köster, Andreas Pacholski, Klaus Dittert, David W. T. Griffith,
Owen Tom Denmead, Deli Chen, Henning Kage, and Karl-Hermann Mühling

Open-Path quantification of ammonia, methane, and nitrous oxide emissions from co-fermented anaerobic digestates stored in lagoons

Jan Reent Köster^{1#}, Andreas Pacholski^{2,3*}, Klaus Dittert⁴, David W. T. Griffith⁵, Owen Tom Denmead^{6,7}, Deli Chen⁶, Henning Kage², Karl-Hermann Mühling¹

¹ Institute of Plant Nutrition and Soil Science, Kiel University, Hermann-Rodewald-Str. 2, 24118 Kiel, Germany

² Agronomy and Crop Science, Kiel University, Hermann-Rodewald-Str. 9, 24118 Kiel, Germany

³ Graduate School/Inkubator, Leuphana University Lüneburg, Scharnhorststr. 1, 21335 Lüneburg, Germany

⁴ Department of Crop Science, Section of Plant Nutrition and Crop Physiology University of Göttingen, Carl-Sprengel-Weg 1, 37075 Göttingen, Germany

⁵ School of Chemistry, University of Wollongong, Wollongong, Australia

⁶ School of Land and Environment, University of Melbourne, Melbourne, Australia

⁷ CSIRO Land and Water, Canberra, Australia

*Correspondence:

email: pacholski@inkubator.leuphana.de; phone: +49 4131 677 2906; fax: +49 4131 677 2411

present address: Department of Environmental Sciences, Norwegian University of Life Sciences, P.O. Box 5003, 1432 Ås, Norway

Key words: open path FTIR; Fourier transform infrared spectroscopy; biogas plant; trace gas emissions; greenhouse gas; bLS; backward Lagrangian stochastic dispersion model; WindTrax; surface crust; fermentation residues

Abstract

Biogas production for generating electricity is explicitly promoted in several European countries to reduce greenhouse gas (GHG) emissions. However, biogas energy production itself may cause significant GHG (CH_4 and N_2O) and NH_3 emissions, in particular during storage of anaerobic digestates (AD) in uncovered tanks and lagoons. However, measurements are challenging and thus data are scarce. We investigated NH_3 , CH_4 , and N_2O emissions from two open AD storage lagoons using open-path Fourier Transform infrared spectroscopy (OP FTIR) in combination with a micrometeorological dispersion model. This methodological approach was validated by trace gas release experiments, and the gas recovery rate was determined to be 113% ($\pm 17\%$; $n=106$). The trace gas emissions from both lagoons were dominated by CH_4 and NH_3 , while N_2O emissions were only detectable during summer. Destruction of a naturally occurring surface crust did not affect total CH_4 release but strongly increased NH_3 emissions. The deployed measuring approach was shown to provide good precision under rather complex micrometeorological conditions and to be well-suited for lagoon studies. The detected high trace gas emissions during AD storage clearly counteract the purpose of biogas energy, i.e. the reduction of GHG emissions, and suggest more systematic investigation. Gas tight covers on AD storage facilities are strongly recommended to reduce these emissions and to utilize additional CH_4 .

1 Introduction

Biogas production by anaerobic fermentation of energy crops and organic residues for generation of electricity and heat is explicitly promoted as a renewable energy source in several European countries (Herrmann and Rath, 2012) for reducing carbon dioxide (CO₂) emissions from fossil fuel consumption. However, it has been shown that at different steps of the biogas production chain, greenhouse gases (GHGs) and ammonia (NH₃) may be released to the atmosphere with potential to significantly affect the climate footprint of biogas energy (Meyer-Aurich et al., 2012; Claus et al., 2013; Herrmann, 2013). Expanding biogas production generates large amounts of anaerobic digestates (AD) as by-products of the fermentation process. AD are usually stored in large tanks or lagoons for many weeks up to several months before field application as organic fertilizers. A high percentage of these storage facilities are still uncovered. For example, in Germany 32% of the AD stores are not covered at all and another 15% are equipped with non-gastight covers (Daniel-Gromke et al., 2013), while in Austria recently 40% of the storage facilities have been reported to be uncovered (Braun, 2009). Under these conditions trace gases such as NH₃, methane (CH₄), and nitrous oxide (N₂O) can freely escape to the atmosphere. CH₄ and N₂O are potent GHGs (Stocker et al., 2013), while NH₃ is not a direct GHG, but emitted NH₃ is mainly deposited locally (Asman et al., 1998) and affects natural ecosystems and biodiversity (Sutton et al., 2011). Approximately 1% of deposited NH₃ is eventually converted to N₂O and released to the atmosphere (Mosier et al., 1998).

AD are typically characterized by higher ammonium (NH₄⁺) concentration and pH value compared to animal slurries due to the fermentation process (Gutser et al., 2005; Tambone et al., 2009), and therefore hold a higher potential for NH₃ volatilization. Furthermore, AD usually contain residual unfermented substrate and therefore pose a source of potentially high CH₄ emission during storage. A survey involving AD from 61 biogas plants revealed an average residual CH₄ production potential at 20 – 22°C between 1.5% (multi-stage plants) and 3.5% (single-stage plants) relative to the utilized CH₄, but differs widely amongst biogas plants (FNR, 2009). Thus, substantial CH₄ emission can occur during AD storage (Gioelli et al., 2011), potentially dominating the variability of GHG emissions of the whole biogas production process (Meyer-Aurich et al., 2012). A naturally forming surface crust can reduce NH₃ and CH₄ emissions to a certain degree, as it reduces NH₃ and NH₄⁺ diffusion to the surface (Sommer et al., 1993; Misselbrook et al., 2005), and harbors CH₄ and NH₃ oxidizing bacteria which may reduce those emissions (Nielsen et al., 2013). However, the latter might increase N₂O emissions by NH₃ oxidation and subsequent denitrification processes in the surface crust (Sommer et al., 2000; Berg et al., 2006).

Until now, only few studies on emissions from digested animal slurries during storage have been published, while data about emissions from energy crop derived AD is particularly scarce. Such information is crucial to fully evaluate GHG savings from biogas energy production systems and for national greenhouse gas inventories. In studies on emissions from stored digested cattle slurry investigated in pilot scale tanks in combination with dynamic chamber measurements considerable GHG and NH₃ emissions were found (Amon et al., 2006; Clemens et al., 2006). Another recent study investigated trace gas emissions from uncovered farm scale AD tanks using a floating chamber approach, and emissions equaling up to 11% of the CH₄ produced in the regular process and high NH₃ emissions were detected (Liebetrau et al., 2013). However, in a study deploying floating open chambers to determine CH₄ emissions from liquid slurry Husted (1993) showed large spatial variations

ranging up to a factor of 100, indicating high uncertainty of the chamber technique. Similarly, Park et al. (2010) found high spatial and temporal variability as well as flux overestimation with the floating chamber method, while Wood et al. (2013) reported that the occurrence of a surface crust on animal slurries can lead to less predictable but rather episodic and irregular flux events, leading to high uncertainties of non-continuous flux chamber measurements. Furthermore, NH_3 emissions depend largely on atmospheric turbulence (Olesen and Sommer, 1993); therefore, chamber measurements of NH_3 emissions are particularly susceptible to spatiotemporal variations and results may be flawed by up to one order of magnitude (Parker et al., 2013). Despite some significant uncertainties, the aforementioned studies indicate high potential of trace gas emissions during storage of AD and animal slurries. However, quantitatively valid flux measurements representative for the particular emission process at a source scale of several hundred square meters are still lacking.

Noninvasive micrometeorological techniques like mass balance methods, flux-gradient techniques, eddy covariance, or micrometeorological dispersion models for trace gas flux measurements integrate over larger source areas and time periods and are therefore less susceptible to spatial and temporal emission heterogeneity (Denmead, 2008; Park et al., 2010). The backward Lagrangian Stochastic dispersion technique (bLS; Flesch et al., 1995; Flesch et al., 2004) has the advantages of more flexible calculation of short-range dispersion from area sources of any shape and does not necessarily require multiple wind and concentration sensors to estimate trace gas fluxes (Flesch et al., 2004; Denmead, 2008). In studies with artificial tracer emission from area sources under ideal conditions the bLS technique achieved accuracies of 90 to 98% (Flesch et al., 2004; McBain and Desjardins, 2005). In field trials with wind disturbance, the accuracy of this technique has been shown to be lower, but still satisfying (Flesch et al., 2005). Ideally, the bLS technique is combined with one or more open-path line-average concentration sensors like open-path Tunable Diode Laser Absorption Spectroscopy (TDLAS) or open-path Fourier Transform infrared spectroscopy (OP FTIR). OP FTIR has the advantage of measuring a variety of trace gases simultaneously including NH_3 , CH_4 , N_2O , CO_2 , and H_2O (Denmead, 2008).

For obtaining first values of trace gas emissions (CH_4 , N_2O , NH_3) without disturbing the emission process, two open AD storage lagoons in Northern Germany were investigated by means of OP FTIR combined with bLS flux quantification. It was hypothesized that trace gas emissions from these AD lagoons would be high and dominated by CH_4 , because of the residual gas potential of AD, and by NH_3 volatilization due to AD's chemical properties and the lagoons' large surface area to volume ratio. Furthermore, we assumed that a natural surface crust reduces NH_3 losses during storage, but promotes N_2O formation. Measurements were carried out under contrasting weather (summer, winter) and lagoon management (crust, stirring) conditions. To evaluate the applicability of the bLS technique under suboptimal micrometeorological conditions in lagoon settings, several tracer release experiments were carried out.

2 Material and methods

2.1 Site descriptions

Two uncovered AD storage lagoons of farm biogas digesters located in the federal state of Schleswig-Holstein in Northern Germany were investigated. The lagoons were bordered by earthwork brims, which were elevated relative to the surrounding area by about 1 to 1.5 m. Farm buildings were located at 30 to 40 m distance upwind. The inner lagoon surface was lined with foil and the berm was sloping with approximately 45 degrees on the inside. AD in both lagoons was covered by surface crusts of usually 30 to 50 cm thickness.

The first lagoon (hereinafter called Lagoon 1) was part of a biogas plant with a combined heat and power unit (CHP) of 400 kW electrical power output, but operated at 200 kW only during the trials in 2012. It consisted of two consecutive continuously stirred fermenters with a total volume of 2200 m³ and a hydraulic retention time of ca. 115 days. Daily substrate input was 16 t silage from grass, wheat, and maize, and 8 t separated cattle slurry solids. The lagoon had a maximum capacity of more than 2000 m³, and current filling levels were estimated by the operating company (Table 1). The surface area was ca. 1100 m² (varying with filling level due to sloping brims). About 70% of the solid phase of the AD was separated by means of a screw press and not passed into the lagoon. During the measurements in October and November 2012 the AD had been amended with ammonium sulfate solution to raise its N fertilizer value. In July 2013 this lagoon was stirred twice for one hour at an interval of two days during the emission measurements to homogenize the surface crust prior to AD land spreading.

Table 1. Lagoon filling levels and major AD characteristics during the six lagoon trials.

| Lagoon, trial | Lagoon filling level [m ³]* | AD characteristics | | | | | |
|--------------------------|---|--------------------|-------------------------------|---|--------------------------|------|------|
| | | DM [%] | Total N [g dm ⁻³] | NH ₄ ⁺ -N [g dm ⁻³] | OM [g dm ⁻³] | C/N | pH |
| Lagoon 2, 22.-23.10.2012 | 1500 | 1.8 | 1.6 | 0.79 | n.d. | n.d. | 7.39 |
| Lagoon 1, 24.-25.10.2012 | 300-400** | 3.3 | 4.4 | 3.8 | n.d. | n.d. | 7.92 |
| Lagoon 1, 22.-24.11.2012 | 700** | n.d. | n.d. | n.d. | n.d. | n.d. | n.d. |
| Lagoon 2, 18.-20.12.2012 | 2800 | 3.4 | 1.9 | 1.1 | n.d. | n.d. | 7.56 |
| Lagoon 1, 05.-12.07.2013 | 1800 | 8.6 | 4.6 | 2.9 | 55 | 6.9 | 8.81 |
| Lagoon 2, 07.-08.08.2013 | 300 | 2.9 | 1.0 | 0.6 | 21 | 12 | 7.33 |

DM = dry matter; OM = organic matter

n.d. = not determined

*estimated by the operating farmer

**AD had been amended with ammonium sulfate solution to raise its N fertilizer value

The second lagoon (Lagoon 2) was part of a small biogas plant with a 65 kW CHP which was not used to full capacity. It was fed with dairy cattle slurry and forage wastes from the dairy farm, totaling to about 20 t per day. The biogas plant consisted of a single 700 m³ fermenter with a hydraulic retention time of 35 days. The lagoon had a total capacity of ca. 3000 m³ and a maximum surface of ca. 1200 m² (varying with filling level). In the winter 2012/2013 the fermentation process was interrupted. Therefore, during the measurements in August 2013 the lagoon contained only residual AD of ca. 150 m³ mixed with additional 150 m³ dairy cattle slurry.

During the trace gas measurements AD samples were taken from the lagoons and analyzed for dry matter (DM) gravimetrically after drying at 105°C with subsequent organic matter (OM) determination as loss on ignition at 550°C. Total N content was determined using the Kjeldahl method, while ammonium N content was measured colorimetrically (Table 1).

2.2 Instrumentation, setup, and positioning

Trace gas concentrations were measured using a bistatic OP FTIR spectrometer (M4411-S, Midac Corporation, Westfield, MA, USA). This OP FTIR instrument is equipped with a Stirling cooled mercury cadmium telluride (MCT) detector, ZnSe interferometer optics, and a 10" Newtonian telescope, in combination with a 20" IR source located at the opposite end of the optical path (postmodulated bistatic configuration). The FTIR spectrometer and the IR source were placed 1.3 m above ground along the downwind edge of the AD lagoons with an optical path length between 30 and 50 m during all measurements.

Wind data were measured using a 3D sonic anemometer (CSAT3, Campbell Scientific, Inc., Logan, UT, USA) close to the middle of the optical measuring path and recorded by a data logger (CR800, Campbell Scientific, Inc.). Additionally, atmospheric pressure, air temperature, relative humidity, and precipitation were measured (Table 2). The dimensions of the lagoons as well as positioning and alignment of instrumentation were determined by GPS (TopCon GRS-1, Topcon Positioning Systems Inc., Livermore, CA, USA), corrected via the SAPOS® high precision real-time positioning service (HEPS; ≤ 2 cm; <http://www.sapos.de/>).

Table 2. Weather conditions* during the lagoon trials.

| Lagoon, trial | Ø Temperature [°C] | Ø Wind speed [m s ⁻¹] | Ø Barometric press. [mbar] | Ø Relative humidity [%] | Ø Radiation [W] |
|--------------------------|--------------------|-----------------------------------|----------------------------|-------------------------|-----------------|
| Lagoon 2, 22.-23.10.2012 | 12.1 | 2.01 | 1026 | 93.9 | 13.5 |
| Lagoon 1, 24.-25.10.2012 | 9.6 | 2.88 | 1016 | 80.0 | 53.3 |
| Lagoon 1, 22.-24.11.2012 | 6.4 | 2.61 | 1016 | 91.1 | 16.6 |
| Lagoon 2, 18.-20.12.2012 | 2.6 | 2.46 | 1023 | 94.0 | 11.0 |
| Lagoon 1, 05.-12.07.2013 | 17.4 | 2.89 | 1026 | 71.6 | 381.9 |
| Lagoon 2, 07.-08.08.2013 | 17.5 | 1.71 | 1013 | 74.9 | 192.1 |

periods of u_ below 0.1 m s⁻¹ are excluded here, because they were not included in flux calculations

Before and/or after the trace gas measurements in the plume of the AD lagoons, the FTIR instrument was placed upwind of the lagoons to measure the atmospheric background concentrations of the target trace gases for at least one hour, which were then assumed to be constant throughout the respective trial.

Measurements were carried out preferably under favorable atmospheric conditions, i.e. periods with no or very low precipitation were chosen and wind directions with no significant upwind emission sources and major obstructions to reduce uncertainties during flux estimations. However, at both locations farm buildings were located downwind of the optical measuring path in a distance of ca. 30 to 40 m.

2.3 Trace gas concentration measurements and flux calculations using 'WindTrax'

NH₃, N₂O, and CH₄ concentrations were measured continuously usually for one or two days, but in one trial for seven days, taking advantage of a long period of favorable meteorological conditions. Single-beam FTIR spectra were collected integrating over 1.2 minutes (= 128 scans) at 0.5 cm⁻¹ spectral resolution. For NH₃ analysis passive FTIR spectra (IR source off) were subtracted from these single-beam spectra to compensate for background IR radiation (Jarvis, 2003). For CH₄ and N₂O this step was skipped, because IR background radiation in the corresponding spectral regions is negligible and subtraction of passive spectra could possibly introduce additional noise into the spectra and lead to a less robust fit during spectrum analysis. The single-beam spectra were then quantitatively analyzed for NH₃, CH₄, and N₂O concentrations using species specific absorption lines in consideration of ambient air temperature and atmospheric pressure by means of a Multi-Atmospheric Layer Transmission Model (MALT; Griffith, 1996). Based on this model, the measured single-beam spectrum was fitted to an iteratively recalculated spectrum based on line parameters from the *HITRAN* molecular spectroscopic database (2008 edition; Rothman et al., 2009) using a non-linear least square fitting algorithm (Griffith et al., 2012). For NH₃ absorption lines at the 960 - 980 cm⁻¹ spectral window were used, while for N₂O the 2150 - 2250 cm⁻¹ region was analyzed and for CH₄ the region of 3001 - 3140 cm⁻¹. The analytical precision (2σ) was at least 5 ppb for NH₃, 25 ppb for CH₄, and 3 ppb for N₂O or better (estimation based on FTIR spectra collected at 35 - 45 m optical path length under virtually clean air field conditions).

The trace gas concentrations and meteorological data were integrated to 15-minute values. The trace gas fluxes were estimated using the bLS technique (Flesch et al., 1995; Flesch et al., 2004), which is implemented in the software *WindTrax* (version 2.0.8.8; Thunder Beach Scientific, Edmonton, Alberta, Canada; <http://www.thunderbeachscientific.com/>), by simulating the displacement of particles (here: 50,000) in the atmospheric surface layer from the source area through the measuring path. For all *WindTrax* simulations a surface roughness length z_0 of 1 cm was assumed because of the rough surface crust structure, and neutral atmospheric stability was chosen as suggested by Sommer et al. (2005).

2.4 Tracer release experiments

Three experiments with controlled release of N₂O and NH₃ on a lagoon surface were carried out to validate the accuracy of the bLS technique under the given lagoon conditions. A tubing system consisting of polyvinyl chloride tubing with 0.5" ID was placed on the surface crust of the lagoons. It

was spiked with a cannula (Braun Sterican®, B. Braun Melsungen AG, Melsungen, Germany; 0.40 x 20 mm, 27G x 3/4" or 0.30 x 12 mm, 30G x 1/2") every 5 m, totaling 36 cannulas, and placed on the lagoon surface in 5 m (Lagoon 1) or 7 m distance (Lagoon 2) to obtain a regular 5 x 5 m (Lagoon 1) or 7 x 5 m pattern (Lagoon 2), respectively. Medical grade N₂O (≥ 98% v/v; Air Liquide Deutschland GmbH, Düsseldorf, Germany) or pure NH₃ (N38, ≥ 99.98% v/v; Air Liquide Deutschland GmbH) was released via the tubing system at a rate of 215 g h⁻¹ (November 2012) or 282 g h⁻¹ N₂O (July 2013), respectively, or 336 g h⁻¹ NH₃. Flow rates were controlled with a float purgometer (10A6142 Purgometer, equipped with FP-1/8-25-G-5 measuring tube and FP-CA-18 (Carboloy) float; ABB Automation Products GmbH, Alzenau, Germany). The first 30 min data after onset of the N₂O release was rejected to avoid bias caused by potential adsorption to the tubing, while in the NH₃ release trial the first 45 min data had to be rejected due to u_* being below 0.15 m s⁻¹ (see section 2.5) during the initial phase. This experimental approach is similar to the design used by Ro et al. (2013), who released CH₄ from the surface of an irrigation pond of ca. 4000 m² via a 45 m square grid to evaluate the bLS technique under comparable conditions.

The N₂O or NH₃ concentrations, respectively, averaged over ca. one hour before and after the release experiment were used as background concentrations (C_b) for calculating the trace gas recoveries. The N₂O and NH₃ emissions from both lagoons were very low during two of these trials (cold conditions), while during the third trial (summer) there was some low N₂O emission. These emissions were taken into account assuming constant C_b or, in case of the experiment during summer, a linear trend during the release experiments, and thus did not affect the results significantly. The trace gas recovery was calculated via WindTrax using settings as described in section 2.3. The ratio between the calculated trace gas flux (Q_{bLS}) and the actual trace gas release rate (Q) was calculated and tested for its deviation from 1 using Student's t-test ($\alpha = 0.05$).

2.5 Data filtering for periods of inaccurate Q_{bLS}

Estimated trace gas fluxes were filtered to eliminate phases of potentially inaccurate bLS estimates. The flux estimations by the bLS model have been shown to be affected during periods of near calm, for example during sunrise and sunset transitions (Flesch et al., 2004). A low friction velocity u_* is the best indication of inaccurate Q_{bLS} and it was suggested to discard phases of $u_* < 0.15$ m s⁻¹ (Flesch et al., 2004). u_* has been calculated according to Monteith and Unsworth (1990):

$$u = \left(\frac{u_*}{k}\right) \ln\left\{\frac{z-d}{z_0}\right\}$$

Here, u is the wind speed, k the Karman constant, z the height of the wind sensor, and d the zero-plane displacement height. During the tracer experiments, phases of $u_* < 0.15$ m s⁻¹ were ignored. For the emission measurements, however, we were less restrictive and skipped observations with $u_* < 0.1$ m s⁻¹ only, because these low wind speeds occurred almost solely during night time. Rejecting most of the night data for some trials would likely result in overestimation especially of NH₃ fluxes, which were often higher during daytime. In return we accepted supposedly lower precision for these data points. Furthermore, a larger degree of concentration sensor footprint coverage over the emission source results in better bLS accuracy (Ro et al., 2011). Therefore, data points with a lagoon footprint coverage below 20% were rejected as affected by non-optimal wind direction (Ro et al., 2013). Gaps in the data sets occurring after data filtering were filled by linear interpolation to reduce bias caused by diurnal variations when calculating day-averaged emission rates.

3 Results and discussion

3.1 Methodology and validation by tracer release/recovery experiments

The three trace gas release experiments comprised 23, 24, and 59 periods of 15-minute observations (Fig. 1a), for which the ratio of the tracer (N_2O or NH_3 , respectively) emission rate estimated using the bLS technique (Q_{bLS}) and the actual release rate (Q) was determined. One of these experiments (07/2013) consisted of two separate trials on two consecutive days with similar setup and under similar atmospheric conditions which were combined for data analysis. The tracer recovery experiments revealed an accuracy between 0.89 and 1.23 (Q_{bLS}/Q ratio; Fig. 1b). The overall Q_{bLS}/Q ratio comprising the three tracer experiments with a total of 106 15-minute periods was 1.13 ($\sigma = \pm 0.17$ (STD)) and deviated significantly from 1.

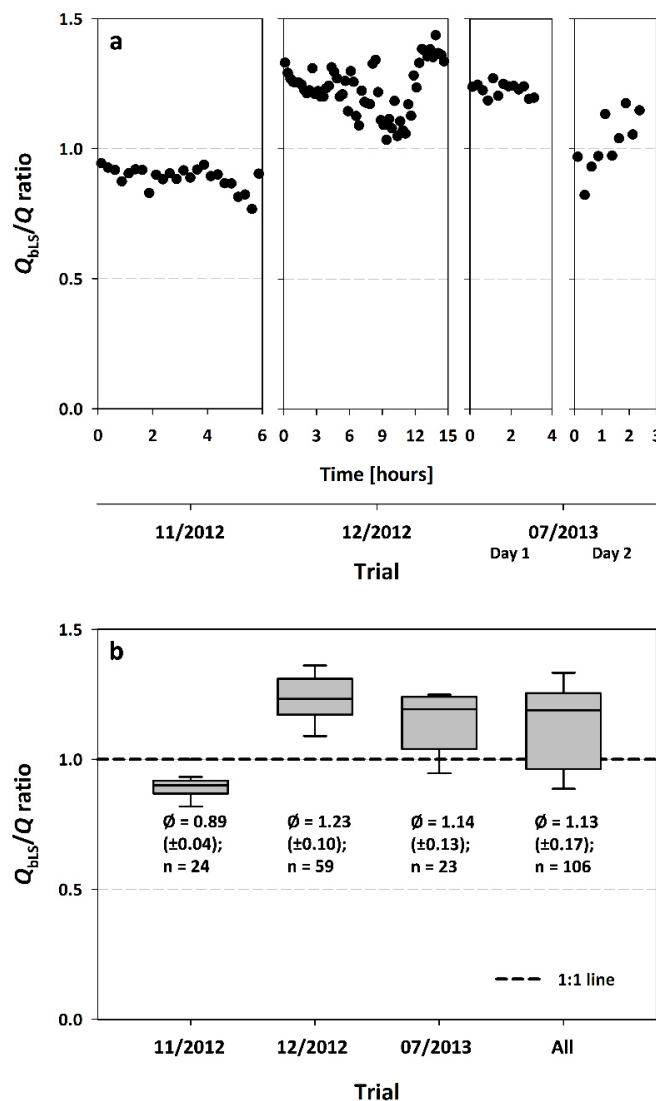


Figure 1. Validation of the methodological approach by recovering N_2O or NH_3 , respectively, released from the surface of two lagoons via a tubing system. Individual data points (a) represent 15-min values of the ratio of the measured trace gas retrieval (Q_{bLS}) and the actual released flux (Q) of N_2O (11/2012 and 07/2013) or NH_3 (12/2012). Mean Q_{bLS}/Q ratio incl. standard deviation (in brackets) of the individual trials as well as over all trials are given in (b).

The bLS technique can achieve very good accuracy for estimating fluxes from ground level sources with inaccuracies of about 2% under ideal conditions (Flesch et al., 2004; McBain and Desjardins, 2005). For situations with disturbed wind flow, which is likely to apply for the present study, the bLS technique has been shown to give estimates of lower, but still acceptable accuracy (Flesch et al., 2005; McBain and Desjardins, 2005). Ro et al. (2013) achieved Q_{bLS}/Q ratios between 0.81 (± 0.18) and 0.93 (± 0.19) with the bLS technique during CH_4 release experiments from an irrigation pond. In another tracer study investigating the applicability of OP-FTIR in combination with the bLS technique for measuring CH_4 emissions, Wang et al. (2014) reported Q_{bLS}/Q ratios of 0.86 and 0.84. Compared to these studies, the overall Q_{bLS}/Q ratio achieved in the present study indicates similar or even better accuracy, although in the present study it was not possible to calculate the Obukhov stability length L on the available data acquisition hardware and thus no data filtering to exclude periods of extreme stable or unstable stratification was done as suggested earlier (Flesch et al., 2004; Ro et al., 2013). Thus, in the present study the bLS calculations were based on the assumption of neutral stability for all measurements, as over long measuring intervals this is likely the most common atmospheric state (Sommer et al., 2005); obviously, this practice did not seriously affect the accuracy. This suggests that for longer measurement periods well-founded assumptions about atmospheric conditions can be sufficient to achieve acceptable bLS estimates. Thus, routine measurements in lagoon settings are feasible when reasonable parameters are chosen without the need of experimental determination of 'best fit' settings.

3.2 Trace gas emissions

3.2.1 NH_3 and CH_4 emissions

The fluxes of the trace gases of interest (Table 3) were found clearly higher during summer than during winter. Clear diurnal variations of the NH_3 and CH_4 fluxes were observed during the summer (Fig. 2a and 2b), while there was no such clear trend during the winter season (Fig. 3). This is most likely due to high temperature fluctuation range of the surface in the course of the day during summer due to higher solar radiation.

Highest NH_3 emissions of $3.5 \text{ g NH}_3\text{-N m}^{-2} \text{ day}^{-1}$ (equivalent to $4.2 \text{ kg NH}_3\text{-N day}^{-1}$ from the whole lagoon) were measured during the very sunny and warm summer period in 07/2013 from Lagoon 1 containing AD from energy crop co-fermentation, while lowest NH_3 emissions were observed at Lagoon 2 in 12/2012 ($0.17 \text{ g NH}_3\text{-N m}^{-2} \text{ day}^{-1}$). Clemens et al. (2006) reported average NH_3 emissions of 2.6 g or $1.0 \text{ g NH}_3\text{-N m}^{-2} \text{ day}^{-1}$ during summer or winter storage, respectively, of fermented cattle slurry in pilot scale tanks. For the summer period these results are very similar to the results of the present study, while during the winter trial those reported fluxes were clearly higher. However, in a similar study on emissions from digested dairy cattle slurry during summer using the same experimental facilities, Amon et al. (2006) reported NH_3 emissions of $0.2 \text{ g NH}_3\text{-N m}^{-2} \text{ day}^{-1}$, which is roughly one-tenth of the emissions observed from both lagoons in present study. Comparative data on emissions from AD from energy crop co-digestion is scarce (e.g. Liebetrau et al., 2013) and not detailed enough and afflicted with artificial conditions and do not allow direct comparisons to our study. Some other studies focused on emissions from lagoons with animal slurries which have similar physicochemical properties as AD. For example, Grant et al. (2013) reported NH_3 emissions from pig slurry lagoons about two to five times higher compared to the present study, and emissions from a

Table 3. NH₃ and CH₄ fluxes during the six lagoon trials.

| Lagoon, trial | Emission rate | | Whole lagoon emission rate | |
|---------------------------|--|--|---|---|
| | NH ₃ -N [g m ⁻² day ⁻¹]** | CH ₄ -C [g m ⁻³ day ⁻¹]** | NH ₃ -N [kg day ⁻¹] | CH ₄ -C [kg day ⁻¹] |
| Lagoon 2, 22.-23.10.2012 | 0.17 | 22.7 | 0.17 | 34.0 |
| Lagoon 1, 24.-25.10.2012 | 2.28 | 13.1 | 2.05 | 3.9 |
| Lagoon 1, 22.-24.11.2012 | 1.03 | 5.5 | 0.95 | 3.8 |
| Lagoon 2, 18.-20.12.2012 | 0.13 | 9.0 | 0.16 | 25.2 |
| Lagoon 1, 05.-12.07.2013* | 3.54 | 27.5 | 4.20 | 49.5 |
| Lagoon 2, 07.-08.08.2013 | 2.31 | 19.2 | 1.82 | 5.8 |

*Average trace gas fluxes before the stirring events conducted later during this trial

**NH₃-N flux is given per m² surface area because NH₃ volatilization largely depends on the emitting surface, while CH₄ production rather depends on available substrate and is thus given per m³ AD

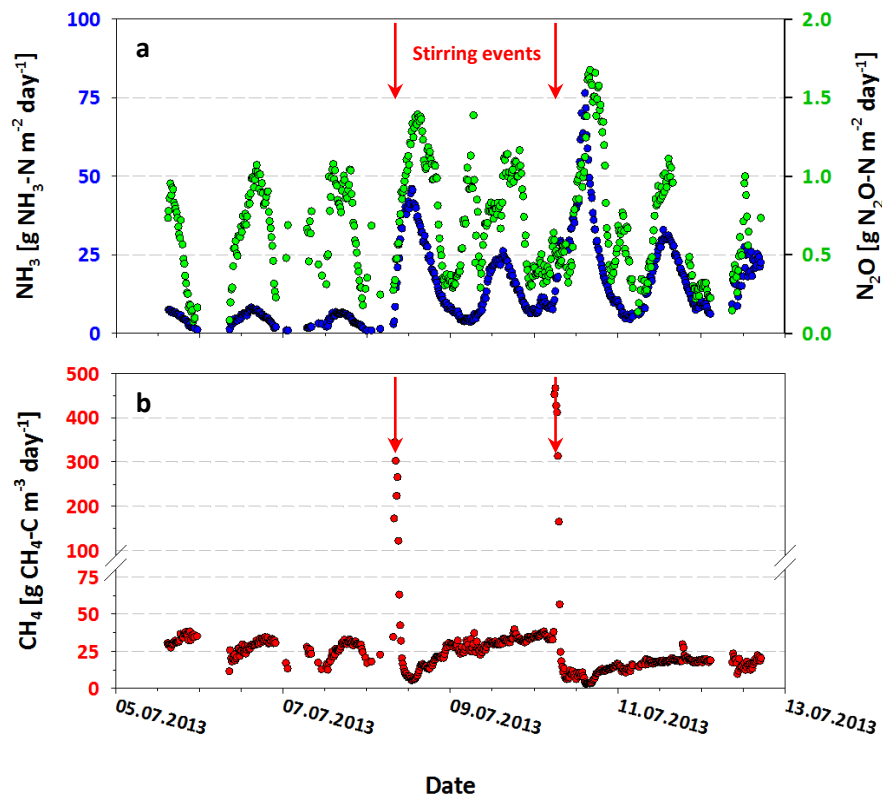


Figure 2. NH₃ and N₂O (a), and CH₄ flux (b) from Lagoon 1 measured by OP FTIR and the bLS technique during the one week trial in 07/2013 (15-minute values). The red arrows indicate the two stirring events of about one hour at a time.

dairy cattle slurry lagoon determined by McGinn et al. (2008) during summer were in the lower range compared to Grant et al. (2013), but still about two times higher than in the present study. Average ammonia flux rates reported from a pig slurry lagoon in Denmark ($0.78 \text{ kg NH}_3\text{-N m}^{-2} \text{ a}^{-1}$) (Feilberg and Sommer, 2013) were on a similar level as average values of Lagoon 1 ($0.83 \text{ kg NH}_3\text{-N m}^{-2} \text{ a}^{-1}$) and higher than average values of Lagoon 2 ($0.45 \text{ kg NH}_3\text{-N m}^{-2} \text{ a}^{-1}$). So despite in general higher ammoniacal N content and higher pH value of AD due to the fermentation process, in the present study the NH_3 emissions were not found to be higher compared to literature values on emissions from animal slurry lagoons. Possibly, NH_3 emissions were reduced due to the occurrence of massive surface crusts and lower temperatures in comparison to the aforementioned studies, but a more specific evaluation will require deeper investigation.

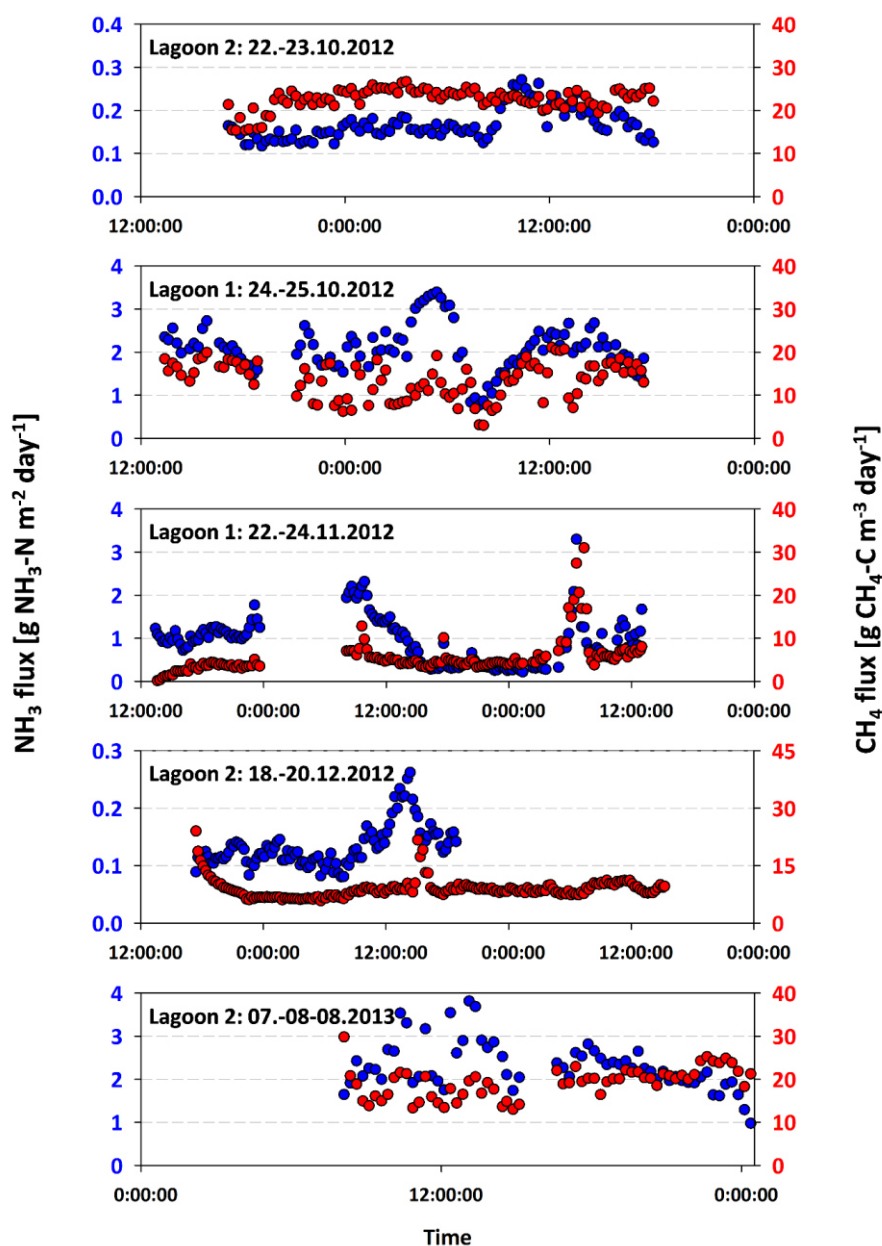


Figure 3. NH_3 and CH_4 fluxes from the two uncovered AD lagoons measured by OP FTIR and the bLS technique during the five shorter trials. Data points indicate 15-minute average values. Please note different scaling of the Y axes.

Similar to NH_3 , the highest CH_4 flux was observed at Lagoon 1 during July 2013, being about $27.5 \text{ g CH}_4\text{-C m}^{-3} \text{ day}^{-1}$ (equivalent to $49.5 \text{ kg CH}_4\text{-C day}^{-1}$ from the whole lagoon). This is about twice, or three to four times, as high as reports by Amon et al. (2006) or Clemens et al. (2006) respectively, while lowest CH_4 emissions found in the present study during the winter season (late autumn) were still about seven to ten times higher compared to winter emissions by Clemens et al. (2006) though our trial does not represent the coldest period of the winter season. CH_4 emissions from pig waste lagoons ranged from 20 to 100% compared to the present study (Sharpe et al., 2002), but also midsummer maximum emission peaks more than ten times higher have been reported (DeSutter and Ham, 2005), while CH_4 emissions from solid separated dairy cattle waste water lagoons during summer were in a similar range compared to our findings (Todd et al., 2011). It can therefore be summarized, that there exists high variation in fluxes which is partly caused by low reliability of some of the analytical approaches.

3.2.2 N_2O emissions

Highest N_2O fluxes were detected at Lagoon 1 during midsummer (07/2013). N_2O emissions from Lagoon 2 in 08/2013 were lower, and no reliable quantification was possible, because the N_2O concentrations were too close to the atmospheric background. During the four trials during the winter half year, measured N_2O concentrations were around the atmospheric background levels, indicating that N_2O emissions were negligible.

The measured average N_2O concentration in the plume of the undisturbed Lagoon 1 in 07/2013 was 25.0 ppbv above the atmospheric background concentration, determined as 310.3 ppbv (average of 36 spectra ≈ 0.75 hours; Fig. 4), and a clear diurnal pattern was observed. The last two days of this measuring series are not included in the day-averaged flux because of AD land spreading upwind to the lagoon which probably affected the N_2O background concentrations during the day for the last two days. This was indicated by the elevated N_2O concentration measured aside of the lagoon as atmospheric background concentration being 326.4 ppbv (average of 76 spectra) at the end of this trial (Fig. 4). During other trials we observed small variations in the measured atmospheric background concentration of N_2O despite the lack of any (known) significant emission sources. This could be due to a small uncertainty or drift (less than 10 ppbv) of the FTIR spectrometer affecting the N_2O measurements, possibly related to the alignment of the instrument with the IR source. The short-term stability of the N_2O measurements was sufficient for the N_2O release experiments. However, for the calculated fluxes during the trial in 07/2013 a maximum uncertainty of 10 ppbv corresponds to an uncertainty of the calculated fluxes of ca. 40%, which is in addition to the uncertainty of the bLS technique as discussed above (section 3.1).

Estimated average N_2O flux from the lagoon was $0.52 \text{ g N}_2\text{O-N m}^{-2} \text{ day}^{-1}$ (equivalent to $621.8 \text{ g N}_2\text{O-N day}^{-1}$) during the initial two days of the trial from the undisturbed lagoon (Fig. 2a). This is similar to previous studies on storage of digested dairy cattle slurry in pilot scale tanks (Amon et al., 2006; Clemens et al., 2006). It has been shown that N_2O released from stored animal slurries is primarily produced by biochemical processes within the surface crust (Sommer et al., 2000; Berg et al., 2006). In oxic zones of such crusts ammonia oxidation (nitrification) will occur, while in anoxic zones the produced nitrate and nitrite can be denitrified. Both processes may emit N_2O , and these N_2O emissions are negatively correlated with the surface crust's water content (Sommer et al., 2000) and therefore abate upon destruction of the crust (Berg et al., 2006).

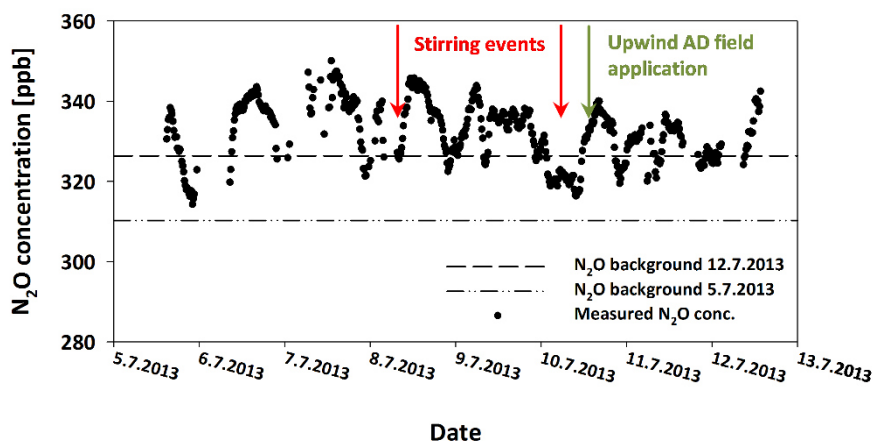


Figure 4. N₂O concentration measured by OP FTIR at Lagoon 1 during the one week trial in 07/2013. Data points indicate N₂O concentrations measured in the downwind plume of the lagoon (15-minute averages), while the dash-dotted line represents the atmospheric N₂O background concentration measured aside the lagoon before the trial (and used as background concentration for the flux calculations) and the dashed line the N₂O background concentration measured at the end of the lagoon trial which was potentially affected by N₂O emissions from upwind AD field application.

3.2.3 Effect of surface crusts and agitation on trace gas emissions

During the two stirring events in July 2013 for crust homogenization (with more thorough homogenization during the second agitation) NH₃ volatilization started to increase drastically and reached maximum emission rates of 50 and 90 kg NH₃-N day⁻¹, respectively (Fig. 2a), during midday when solar radiation and wind speed were highest, but halved already during the following day because of a gradual recovery and drying of the surface crust. Mean daily NH₃ flux was 4.2 kg NH₃-N day⁻¹ before the two stirring events, but increased to 22.6 and 31.3 kg NH₃-N day⁻¹ after the two stirring events, averaging 21.9 kg NH₃-N day⁻¹ over the four days comprising both stirring events. Thus, NH₃ emissions were reduced efficiently by the surface crust by more than 80%. This is in agreement with previous studies where NH₃ emissions were reduced by 50 – 60% (Misselbrook et al., 2005; Smith et al., 2007), or even 80% (Sommer et al., 1993). AD from energy crop co-fermentation are characterized by large shares of plant fiber, which can build a more effective surface crust than for example pig slurry. During the following days after agitation NH₃ emissions clearly decreased, because the surface crust recovered and reduced NH₃ availability at the surface (Sommer et al., 1993).

In contrast to NH₃ emissions, the CH₄ emission peaks reached their maximum the both stirring events, and emissions immediately abated after agitation was stopped (Fig. 2b), and the CH₄ flux even dropped below the initial rates. Obviously, CH₄ dissolved in AD and/or trapped underneath or in the surface crust was released, because stirring strips CH₄ from the liquid phase, resulting in temporarily reduced emission rates afterwards as suggested before (Husted, 1993). Thus, in contrast to NH₃, stirring seems not to affect the cumulated CH₄ release from the lagoon, because CH₄ production is determined by the microbial activity in the AD. It has been reported that methane-oxidizing bacteria in a surface crust of animal slurries can reduce CH₄ emissions by CH₄ oxidization of about 1 to 10 g CH₄ m⁻² day⁻¹ (Petersen and Ambus, 2006; Nielsen et al., 2013); however, the results of the present trial do not indicate significant CH₄ consumption by this process. This may possibly be explained by the fact that CH₄

emissions from slurry and digestate with incrustated surface tends to be spatially and temporally very heterogeneous due to rather episodic bubble and burst events mainly from cracks in the surface crust as observed earlier (Wood et al., 2013).

The N₂O fluxes increased during the days following AD agitation by about 50% compared to the undisturbed lagoon. This is in contrast to reports on ceasing N₂O production after surface crust destruction (Berg et al., 2006). Possibly, homogenization brought additional ammonium to the oxic surface, promoting nitrification and subsequent denitrification activity and thus N₂O production.

3.3 Potential impact of trace gas emissions from AD storage on GHG savings by biogas energy

The CO₂-equivalent weighted trace gas emissions from both AD lagoons were found to be high relative to the GHG saving potential of the respective biogas plant. This is of particular importance for the biogas plant predominantly operated with energy crops because these emissions considerably reduce the GHG balance of biogas energy. However, it has recently been shown that saving of CH₄ emissions from slurry storage due to fermentation of the slurry has a considerable effect on the GHG balance of biogas plants (Amon et al., 2006; Clemens et al., 2006; Meyer-Aurich et al., 2012). Nevertheless, CH₄ emissions observed in our study were in a similar range as those observed from farm and pilot scale slurry storages. CH₄ emissions from cattle slurry storage tanks in Sweden varied between 1.5 - 3.5 g CH₄-C m⁻³ day⁻¹ in winter and summer (Rodhe et al., 2009). In another study values up to 34.5 g CH₄-C m⁻³ day⁻¹ were observed (Husted, 1994). In a pilot scale study Sommer et al. (2007) detected emissions between 20 g CH₄-C m⁻³ day⁻¹ up to 200 g CH₄-C m⁻³ day⁻¹ (values derived from data reported in the study). However, the latter were only observed at long incubation times (>50 days) at constantly high temperatures. In our study, values for CH₄ emissions ranged between 5.5 – 27.5 g CH₄-C m⁻³ day⁻¹, which is higher as the emissions observed in Sweden and in the same range as those determined in the pilot scale study. It can be concluded, that CH₄ emissions from AD storage lagoons containing co-fermented slurry with biogas crops have about the same magnitude as those from storages with unfermented slurry. With respect to N₂O emissions, values reported for unfermented slurry were generally close to 0 (Sommer et al., 2000; Berg et al., 2006). However, the build-up of a strong floating surface crust of the coarse and fibrous AD in the present study may have triggered N₂O emissions, which have not been reported yet for unfermented slurries. As a result, co-fermented AD stored in lagoons give probably no benefit with respect to avoidance of CH₄ emission from unfermented slurries. In contrast, as the major part of the DM is derived from energy crops and additional N₂O emission spikes may occur, it can be hypothesized that GHG emissions from storage lagoons with AD of co-fermented slurries have even higher GHG emissions as those from undigested slurry. However, due to non-continuous measurement in our study and the strong influence of temperature and substrate conditions, this effect cannot precisely be quantified.

The reported data from literature as well as the present study highlight the high emission potential of AD posing a major risk to the GHG balance and sustainability of biogas energy. Together with other biogas energy related emissions AD storage derived emissions may even negate biogas GHG savings. Therefore, adequate measures like gastight covers on AD storage facilities are strongly recommended to reduce these emissions and to improve the efficiency of biogas energy by recovering additional CH₄. Neither study allows calculating whole year emissions or precise year-averaged emission factors due to the low number of observations and the high variability of emissions as affected by various factors. This underlines the need of further systematic investigation.

Acknowledgements

Jan Reent Köster thanks the German Federal Environmental Foundation (DBU) for a PhD scholarship. The authors thank the owners of the biogas plants for their great cooperation and support. Thomas Rübiger, Claas Meckelnburg, Stefan Becker, and Nils-Ole Asmussen helped with testing, setup, and operation of the instrumentation during the trials. Purchase of open-path FTIR equipment was supported by the Innovationsstiftung Schleswig-Holstein. Funding of actual measurements was granted by the Ministry of Energy, Education and Traffic of the Federal State of Schleswig-Holstein and the European Regional Development Fund (ERDF) in the framework of the joint project 'Centre of Excellence of Biomass in Schleswig-Holstein'.

References

- Amon, B., Kryvoruchko, V., Amon, T., Zechmeister-Boltenstern, S., 2006. Methane, nitrous oxide and ammonia emissions during storage and after application of dairy cattle slurry and influence of slurry treatment. *Agriculture Ecosystems & Environment* 112, 153-162.
- Asman, W.A.H., Sutton, M.A., Schjorring, J.K., 1998. Ammonia: emission, atmospheric transport and deposition. *New Phytologist* 139, 27-48.
- Berg, W., Brunsch, R., Pazsiczki, I., 2006. Greenhouse gas emissions from covered slurry compared with uncovered during storage. *Agriculture Ecosystems & Environment* 112, 129-134.
- Braun, R., 2009. *Short Report - Status Austria - 2009*; In: IEA Task 37 "Energy from Biogas and Landfill Gas". LE Petten, The Netherlands. URL: http://www.iea-biogas.net/country-reports.html?file=files/daten-redaktion/download/publications/country-reports/apr2009/austria_report4-09.pdf; accessed: 14.05.2014.
- Claus, S., Taube, F., Wienforth, B., Svoboda, N., Sieling, K., Kage, H., Senbayram, M., Dittert, K., Gericke, D., Pacholski, A., Herrmann, A., 2013. Life-cycle assessment of biogas production under the environmental conditions of northern Germany: greenhouse gas balance. *Journal of Agricultural Science FirstView*, 1-10.
- Clemens, J., Trimborn, M., Weiland, P., Amon, B., 2006. Mitigation of greenhouse gas emissions by anaerobic digestion of cattle slurry. *Agriculture, Ecosystems & Environment* 112, 171-177.
- Daniel-Gromke, J., Denysenko, V., Sauter, P., Naumann, K., Scheftelowitz, M., Krautz, A., Beil, M., Beyrich, w., Peters, W., Schicketanz, S., Schultze, C., Deumelandt, P., Reinicke, F., 2013. *Stromerzeugung aus Biomasse*; In: Deutsches Biomasseforschungszentrum (DBFZ); Leipzig, Germany; pp 47-48. URL: https://www.dbfz.de/web/fileadmin/user_upload/Referenzen/Berichte/biomassemonitoring_zwischenbericht_bf.pdf; accessed: 24.01.2014.
- Denmead, O.T., 2008. Approaches to measuring fluxes of methane and nitrous oxide between landscapes and the atmosphere. *Plant and Soil* 309, 5-24.
- DeSutter, T.M., Ham, J.M., 2005. Lagoon-biogas emissions and carbon balance estimates of a swine production facility. *Journal of Environmental Quality* 34, 198-206.
- Feilberg, A., Sommer, S.G., 2013. Ammonia and Malodorous Gases: Sources and Abatement Technologies. In: Sommer, S.G., Christensen, M.L., Schmidt, T., Jensen, L.S. (Eds.), *Animal Manure Recycling: Treatment and Management*. John Wiley & Sons Ltd., Chichester, West Sussex, pp. 153-175.
- Flesch, T.K., Wilson, J.D., Yee, E., 1995. Backward-time Lagrangian stochastic dispersion models and their application to estimate gaseous emissions. *Journal of Applied Meteorology* 34, 1320-1332.
- Flesch, T.K., Wilson, J.D., Harper, L.A., Crenna, B.P., Sharpe, R.R., 2004. Deducing ground-to-air emissions from observed trace gas concentrations: A field trial. *Journal of Applied Meteorology* 43, 487-502.
- Flesch, T.K., Wilson, J.D., Harper, L.A., 2005. Deducing ground-to-air emissions from observed trace gas concentrations: A field trial with wind disturbance. *Journal of Applied Meteorology* 44, 475-484.
- FNR, 2009. *Biogas-Messprogramm II - 61 Biogasanlagen im Vergleich*. Fachagentur Nachwachsende Rohstoffe e.V. (FNR), Gülzow, Germany. URL: http://www.fnr-server.de/ftp/pdf/literatur/pdf_385messdaten_biogasmessprogramm_ii.pdf; accessed: 01.09.2013.

- Gioelli, F., Dinuccio, E., Balsari, P., 2011. Residual biogas potential from the storage tanks of non-separated digestate and digested liquid fraction. *Bioresource Technology* 102, 10248-10251.
- Grant, R.H., Boehm, M.T., Lawrence, A.F., Heber, A.J., 2013. Ammonia emissions from anaerobic treatment lagoons at sow and finishing farms in Oklahoma. *Agricultural and Forest Meteorology* 180, 203-210.
- Griffith, D.W.T., 1996. Synthetic calibration and quantitative analysis of gas-phase FT-IR spectra. *Applied Spectroscopy* 50, 59-70.
- Griffith, D.W.T., Deutscher, N.M., Caldow, C., Kettlewell, G., Riggensbach, M., Hammer, S., 2012. A Fourier transform infrared trace gas and isotope analyser for atmospheric applications. *Atmospheric Measurement Techniques* 5, 2481-2498.
- Gutser, R., Ebertseder, T., Weber, A., Schraml, M., Schmidhalter, U., 2005. Short-term and residual availability of nitrogen after long-term application of organic fertilizers on arable land. *Journal of Plant Nutrition and Soil Science-Zeitschrift Fur Pflanzenernahrung Und Bodenkunde* 168, 439-446.
- Herrmann, A., Rath, J., 2012. Biogas Production from Maize: Current State, Challenges, and Prospects. 1. Methane Yield Potential. *Bioenergy Research* 5, 1027-1042.
- Herrmann, A., 2013. Biogas Production from Maize: Current State, Challenges and Prospects. 2. Agronomic and Environmental Aspects. *Bioenergy Research* 6, 372-387.
- Husted, S., 1993. An open chamber technique for determination of methane emission from stored livestock manure. *Atmospheric Environment Part a-General Topics* 27, 1635-1642.
- Husted, S., 1994. Seasonal Variation in Methane Emission from Stored Slurry and Solid Manures. *Journal of Environmental Quality* 23, 585-592.
- Jarvis, J.M., 2003. Open Path Spectrophotometry (UV, IR, FT-IR). In: Lipták, B.G. (Ed.), *Instrument Engineers' Handbook, Fourth Edition, Volume One: Process Measurement and Analysis: Process Measurement and Analysis*. CRC Press, Boca Raton, FL, USA, pp. 1493-1505.
- Liebetrau, J., Reinelt, T., Clemens, J., Hafermann, C., Friehe, J., Weiland, P., 2013. Analysis of greenhouse gas emissions from 10 biogas plants within the agricultural sector. *Water Science and Technology* 67, 1370-1379.
- McBain, M.C., Desjardins, R.L., 2005. The evaluation of a backward Lagrangian stochastic (bLS) model to estimate greenhouse gas emissions from agricultural sources using a synthetic tracer source. *Agricultural and Forest Meteorology* 135, 61-72.
- McGinn, S.M., Coates, T., Flesch, T.K., Crenna, B., 2008. Ammonia emission from dairy cow manure stored in a lagoon over summer. *Canadian Journal of Soil Science* 88, 611-615.
- Meyer-Aurich, A., Schattauer, A., Hellebrand, H.J., Klauss, H., Plochl, M., Berg, W., 2012. Impact of uncertainties on greenhouse gas mitigation potential of biogas production from agricultural resources. *Renewable Energy* 37, 277-284.
- Misselbrook, T.H., Brookman, S.K.E., Smith, K.A., Cumby, T., Williams, A.G., McCrory, D.F., 2005. Crusting of stored dairy slurry to abate ammonia emissions: Pilot-scale studies. *Journal of Environmental Quality* 34, 411-419.
- Monteith, J.L., Unsworth, M.H., 1990. *Principles of Environmental Physics*. Butterworth-Heinemann Ltd., Oxford, UK.
- Mosier, A., Kroeze, C., Nevison, C., Oenema, O., Seitzinger, S., van Cleemput, O., 1998. Closing the global N₂O budget: nitrous oxide emissions through the agricultural nitrogen cycle. *Nutrient Cycling in Agroecosystems* 52, 225-248.

- Nielsen, D.A., Schramm, A., Nielsen, L.P., Revsbech, N.P., 2013. Seasonal Methane Oxidation Potential in Manure Crusts. *Applied and Environmental Microbiology* 79, 407-410.
- Olesen, J.E., Sommer, S.G., 1993. Modelling effects of wind speed and surface cover on ammonia volatilization from stored pig slurry. *Atmospheric Environment Part a-General Topics* 27, 2567-2574.
- Park, K.H., Wagner-Riddle, C., Gordon, R.J., 2010. Comparing methane fluxes from stored liquid manure using micrometeorological mass balance and floating chamber methods. *Agricultural and Forest Meteorology* 150, 175-181.
- Parker, D., Ham, J., Woodbury, B., Cai, L., Spiehs, M., Rhoades, M., Trabue, S., Casey, K., Todd, R., Cole, A., 2013. Standardization of flux chamber and wind tunnel flux measurements for quantifying volatile organic compound and ammonia emissions from area sources at animal feeding operations. *Atmospheric Environment* 66, 72-83.
- Petersen, S.O., Ambus, P., 2006. Methane Oxidation in Pig and Cattle Slurry Storages, and Effects of Surface Crust Moisture and Methane Availability. *Nutrient Cycling in Agroecosystems* 74, 1-11.
- Ro, K.S., Johnson, M.H., Hunt, P.G., Flesch, T.K., 2011. Measuring Trace Gas Emission from Multi-Distributed Sources Using Vertical Radial Plume Mapping (VRPM) and Backward Lagrangian Stochastic (bLS) Techniques. *Atmosphere* 2, 553-566.
- Ro, K.S., Johnson, M.H., Stone, K.C., Hunt, P.G., Flesch, T., Todd, R.W., 2013. Measuring gas emissions from animal waste lagoons with an inverse-dispersion technique. *Atmospheric Environment* 66, 101-106.
- Rodhe, L., Ascue, J., Nordberg, A., 2009. Emissions of greenhouse gases (methane and nitrous oxide) from cattle slurry storage in Northern Europe. In: Basse, E.M., Svenning, J.C., Olesen, J.E. (Eds.), *Beyond Kyoto: Addressing the Challenges of Climate Change - Science Meets Industry, Policy and Public*. Iop Publishing Ltd, Bristol.
- Rothman, L.S., Gordon, I.E., Barbe, A., Benner, D.C., Bernath, P.E., Birk, M., Boudon, V., Brown, L.R., Campargue, A., Champion, J.P., Chance, K., Coudert, L.H., Dana, V., Devi, V.M., Fally, S., Flaud, J.M., Gamache, R.R., Goldman, A., Jacquemart, D., Kleiner, I., Lacome, N., Lafferty, W.J., Mandin, J.Y., Massie, S.T., Mikhailenko, S.N., Miller, C.E., Moazzen-Ahmadi, N., Naumenko, O.V., Nikitin, A.V., Orphal, J., Perevalov, V.I., Perrin, A., Predoi-Cross, A., Rinsland, C.P., Rotger, M., Simeckova, M., Smith, M.A.H., Sung, K., Tashkun, S.A., Tennyson, J., Toth, R.A., Vandaele, A.C., Vander Auwera, J., 2009. The HITRAN 2008 molecular spectroscopic database. *Journal of Quantitative Spectroscopy & Radiative Transfer* 110, 533-572.
- Sharpe, R.R., Harper, L.A., Byers, F.M., 2002. Methane emissions from swine lagoons in Southeastern US. *Agriculture Ecosystems & Environment* 90, 17-24.
- Smith, K., Cumby, T., Lapworth, J., Misselbrook, T., Williams, A., 2007. Natural crusting of slurry storage as an abatement measure for ammonia emissions on dairy farms. *Biosystems Engineering* 97, 464-471.
- Sommer, S.G., Christensen, B.T., Nielsen, N.E., Schjorring, J.K., 1993. Ammonia volatilization during storage of cattle and pig slurry: effect of surface cover. *Journal of Agricultural Science* 121, 63-71.
- Sommer, S.G., Petersen, S.O., Sogaard, H.T., 2000. Greenhouse gas emission from stored livestock slurry. *Journal of Environmental Quality* 29, 744-751.
- Sommer, S.G., McGinn, S.M., Flesch, T.K., 2005. Simple use of the backwards Lagrangian stochastic dispersion technique for measuring ammonia emission from small field-plots. *European Journal of Agronomy* 23, 1-7.

- Sommer, S.G., Petersen, S.O., Sorensen, P., Poulsen, H.D., Moller, H.B., 2007. Methane and carbon dioxide emissions and nitrogen turnover during liquid manure storage. *Nutrient Cycling in Agroecosystems* 78, 27-36.
- Stocker, T.F., Qin, D., Plattner, G.-K., Tignor, M., Allen, S.K., Boschung, J., Nauels, A., Xia, Y., Bex, V., Midgley, P.M., 2013. *Climate Change 2013: The Physical Science Basis. Contribution of Working Group I to the Fifth Assessment Report of the Intergovernmental Panel on Climate Change* Cambridge University Press, Cambridge, United Kingdom and New York, NY, USA.
- Sutton, M.A., Oenema, O., Erisman, J.W., Leip, A., van Grinsven, H., Winiwarter, W., 2011. Too much of a good thing. *Nature* 472, 159-161.
- Tambone, F., Genevini, P., D'Imporzano, G., Adani, F., 2009. Assessing amendment properties of digestate by studying the organic matter composition and the degree of biological stability during the anaerobic digestion of the organic fraction of MSW. *Bioresource Technology* 100, 3140-3142.
- Todd, R.W., Cole, N.A., Casey, K.D., Hagevoort, R., Auvermann, B.W., 2011. Methane emissions from southern High Plains dairy wastewater lagoons in the summer. *Animal Feed Science and Technology* 166-67, 575-580.
- Wang, W., Liu, W., Zhang, T., Lu, Y., 2014. Measuring Greenhouse-Gas Emissions from a Synthetic Tracer Source. *Journal of Applied Spectroscopy* 81, 264-272.
- Wood, J.D., Gordon, R.J., Wagner-Riddle, C., 2013. Biases in discrete CH₄ and N₂O sampling protocols associated with temporal variation of gas fluxes from manure storage systems. *Agricultural and Forest Meteorology* 171, 295-305.

Chapter 3

Cold season ammonia emissions from land spreading with anaerobic digestates from biogas production

Jan Reent Köster, Klaus Dittert, Karl-Hermann Mühling,
Henning Kage, and Andreas Pacholski

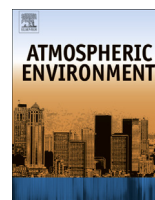
Atmospheric Environment 84 (2014) 35 – 38

DOI: [10.1016/j.atmosenv.2013.11.037](https://doi.org/10.1016/j.atmosenv.2013.11.037)



Contents lists available at ScienceDirect

Atmospheric Environment

journal homepage: www.elsevier.com/locate/atmosenv

Short communication

Cold season ammonia emissions from land spreading with anaerobic digestates from biogas production

Jan Reent Köster^{a,*}, Klaus Dittert^b, Karl-Hermann Mühling^a, Henning Kage^c,
Andreas Pacholski^{c,d}^a Institute of Plant Nutrition and Soil Science, Kiel University, Hermann-Rodewald-Str. 2, 24118 Kiel, Germany^b Department of Crop Science, Section of Plant Nutrition and Crop Physiology, University of Goettingen, Carl-Sprengel-Weg 1, 37075 Goettingen, Germany^c Agronomy and Crop Science, Institute of Crop Science and Plant Breeding, Kiel University, Hermann-Rodewald-Straße 9, 24118 Kiel, Germany^d Graduate School/Inkubator, Leuphana University Lüneburg, Scharnhorststr. 1, 21335 Lüneburg, Germany

HIGHLIGHTS

- NH₃ emission of AD land spreading measured by open path FTIR and a dispersion model.
- Continuous monitoring of NH₃ fluxes in 15-min resolution over 6 days.
- 33% of ammonium in AD emitted as NH₃ after application on predominantly frozen soil.
- To our knowledge first report on NH₃ emissions from AD land spreading in winter.

ARTICLE INFO

Article history:

Received 1 August 2013

Received in revised form

11 November 2013

Accepted 14 November 2013

Keywords:

Open path FTIR

Backward Lagrangian stochastic dispersion model

bLS

NH₃ emissions

Northern Germany

Micrometeorology

ABSTRACT

Anaerobic digestates (AD) from biogas production are applied to agricultural land as organic fertilizers, but pose an ammonia (NH₃) emission source. However, data about NH₃ emissions of cold season AD land spreading is still lacking. Therefore, in the present study NH₃ emissions of AD application under winter conditions were determined. AD was applied via trail hoses to a field plot of 27 ha in Northern Germany during the winter with temperatures around the freezing point and partly frozen soil. NH₄⁺ N application rate was, including a preceding urea application, 123 kg NH₄⁺ and urea N ha⁻¹. The NH₃ volatilization was monitored using Open Path Fourier Transform Infrared spectroscopy in combination with a micrometeorological transport model. Cumulative NH₃ volatilization during the six day measurements was 17.5 kg NH₃ N ha⁻¹ which corresponds to 33.1% of the NH₄⁺ N in applied AD. This NH₃ loss is relatively high for low temperature conditions and was most likely caused by the frozen soil restricting AD infiltration.

© 2013 Elsevier Ltd. All rights reserved.

1. Introduction

Biogas production by anaerobic fermentation of energy crops and organic wastes like animal slurries for generating electricity is explicitly promoted as renewable energy source in several European countries (Herrmann and Rath, 2012). The by-products of the biogas fermentation process, anaerobic digestates (AD), are generally applied to agricultural land as organic fertilizers to return nutrients into the production cycle. In previous studies it has been shown that during land spreading of AD large amounts of NH₃ can

be emitted to the atmosphere (Amon et al., 2006; Quakernack et al., 2012) and pose not only a loss of nitrogen (N), but also environmental threats. A large proportion of NH₃ is deposited locally and may affect natural ecosystems (Sutton et al., 1998, 2011; Hertel et al., 2013). Furthermore, it may be assumed that about 1% of NH₃ deposited to soils is transformed by microbial processes to nitrous oxide (N₂O) (IPCC, 2007), a potent greenhouse gas and ozone depleting substance, whereas NH₃ is considered a secondary greenhouse gas. As there exists substantial emission potential in AD management (Amon et al., 2006), these emissions could significantly reduce GHG savings of biogas energy.

Most studies on NH₃ emissions during AD management including field application only cover the growing season, i.e. the period between spring and early autumn. To our knowledge no data exists on NH₃ emissions from AD land spreading under cold winter conditions

* Corresponding author. Tel.: +49 431 880 3194.

E-mail addresses: jrkoester@plantnutrition.uni-kiel.de, janreent@gmx.de (J. R. Köster).

so far. This is in contrast to the common practice in Germany to apply slurry after snow melt but on still frozen soil. This is due to a better trafficability, assumed low NH_3 emissions because of low temperatures, and limitations in manure storage capacities. Later in spring slurry application may be hampered by moist soil conditions and crop damage may be comparatively high. In many cases these slurry applications are combined with the application of synthetic N fertilizers to meet crop N demand supplied by the first N dose. Therefore, a profound database about these emissions is essential for consulting on good practice in AD and slurry management.

Recently, optical remote sensing techniques combined with micrometeorological transport models are becoming more widespread for trace gas emission studies in agricultural context (e.g. Flesch et al., 2007; Jones et al., 2011). These techniques usually integrate fluxes from much larger source areas than for example chamber techniques and are rather robust against 'hot spots' and heterogeneous emission sources (Denmead, 2008).

In the present study we determined NH_3 emissions during and after AD land spreading under practical conditions using Open Path FTIR and a micrometeorological dispersion model during the winter season.

2. Materials and methods

2.1. Description of field site and fertilizer application

The field site was located in Northern Germany in the federal state of Schleswig-Holstein near the coast of the Baltic Sea ($+54^\circ 26' 31''$, $+9^\circ 56' 46''$). The soil was a sandy loam soil, classified as Stagnic Luvisol, and was cropped with winter rye, which had a height of approximately 5 cm at the time of the field trial. The dimension of the field plot, positions of instrumentation, and relative orientation to each other were determined by GPS (TopCon GRS-1, Topcon Positioning Systems Inc., Livermore, CA, USA), corrected by the SAPOS[®] high precision real-time positioning service (HEPS; ≤ 2 cm; <http://www.sapos.de/>).

The measurement campaign was carried out in co-operation with a local farmer in the winter season during the last week of February 2013. Air temperatures were fluctuating around the freezing point (average 0.2°C), but slightly increasing towards the end of the measuring period. The soil was mainly frozen to a depth of 8–10 cm, but the top 0.5–2 cm of the soil surface were occasionally thawing during the day. Average wind speed during the six days after AD application was 2.9 m s^{-1} . Temperature and wind speed over time are shown in Fig. 1. During the night from February 24th to 25th there was 0.7 mm of precipitation in form of snow, which melted during the following day.

AD applied in this field trial derived from a biogas plant which was operated by energy crop silage and pig slurry co-fermentation. Major characteristics of the AD are 6.5% dry matter, 4.97 kg N m^{-3} , $2.64\text{ kg NH}_4^+ \text{ N m}^{-3}$, and pH 8.9. About 9 h before AD application, pelletized urea (46% N) was applied to a field plot of c. 27 ha at an application rate of $150\text{ kg urea ha}^{-1}$ ($\sim 70\text{ kg urea N ha}^{-1}$). AD was applied via trail hoses to the field plot on February 22nd, starting in the afternoon. Application was paused overnight and completed in the morning of the following day downwind of our instrumentation and did therefore not affect the measurements. Target application rate was $20\text{ m}^3\text{ AD ha}^{-1}$, which is equivalent to $52.8\text{ kg NH}_4^+ \text{ N ha}^{-1}$, adding up to $122.8\text{ kg NH}_4^+ \text{ and urea N ha}^{-1}$.

2.2. OP FTIR measurements and flux calculation using 'WindTrax'

NH_3 concentrations were measured by Open Path FTIR for seven days, covering one day before and six days after start of AD land spreading. Measurements were stopped after this time span in

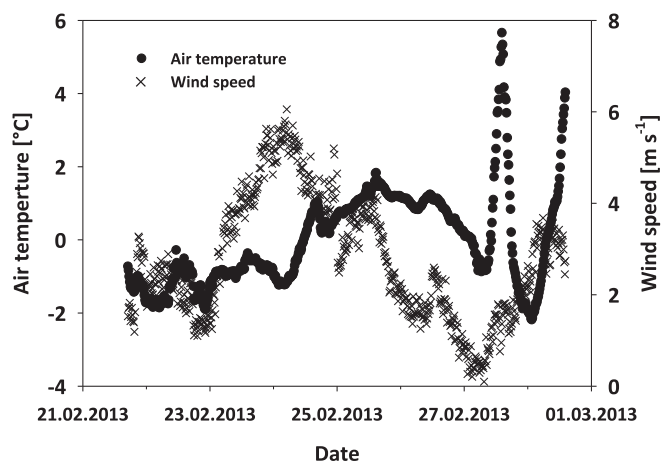


Fig. 1. Air temperature and wind speed during the field campaign. During the day the soil surface thawed occasionally to a depth of c. 0.5–2 cm.

order to avoid effects of applied urea N on the NH_3 emissions. Urea hydrolysis is very slow under cold conditions and can be neglected for the first days after application. Measurements were carried out at a height of 1.3 m above ground and 69.95 m optical path length. The deployed FTIR spectrometer (M4411-S, Midac Corporation, Westfield, MA, USA) was equipped with a Stirling cooled mercury cadmium telluride (MCT) detector, ZnSe interferometer optics, and a 10" Newtonian telescope. A 20" IR source was placed at the opposite end of the optical path. Single-beam spectra were collected integrating 128 scans at 0.5 cm^{-1} resolution over 1.2 min. The FTIR spectrometer was set up 23.5 h prior to the start of the AD application to measure the atmospheric background concentration of NH_3 , which was averaged 3.744 ppb and taken account of in the flux calculation. Wind data were measured using a 3D sonic anemometer (CSAT3, Campbell Scientific Inc., Logan, UT, USA) in the middle of the FTIR measuring path. The anemometer data was recorded at 1 Hz using a data logger (CR800, Campbell Scientific Inc.), while for the other sensors (atmospheric pressure, air temperature, precipitation) 30 s averages were collected.

The FTIR spectra were quantitatively analyzed for NH_3 concentrations using NH_3 absorption lines at the $960\text{--}980\text{ cm}^{-1}$ spectral window in consideration of ambient air temperature and atmospheric pressure by means of a Multi-Atmospheric Layer Transmission Model (MALT; Griffith, 1996). By this model, the measured single-beam spectrum is fitted to an iteratively recalculated spectrum based on line parameters from the HITRAN molecular spectroscopic database (2008 edition; Rothman et al., 2009) using a non-linear least square fitting algorithm (Griffith et al., 2012). The retrieved NH_3 concentrations and collected meteorological data were averaged to 15 min means and NH_3 fluxes were estimated using a backward Lagrangian stochastic dispersion model (bLS; Flesch et al., 1995, 2004), implemented in the software WindTrax (version 2.0.8.8; Thunder Beach Scientific, Edmonton, Alberta, Canada), simulating the displacement of 50,000 particles from the source area through the measuring path. A surface roughness length z_0 of 1.0 cm was assumed, and according to suggestions by Sommer et al. (2005) overall neutral atmospheric stability was chosen.

3. Results and discussion

Cumulated NH_3 emission determined by FTIR was $17.48\text{ kg NH}_3\text{ N ha}^{-1}$ over the initial six days after AD land spreading (Fig. 2) which corresponds to 33.1% of the applied $\text{NH}_4^+ \text{ N}$. Despite low ambient temperatures, these emissions are in a similar range or

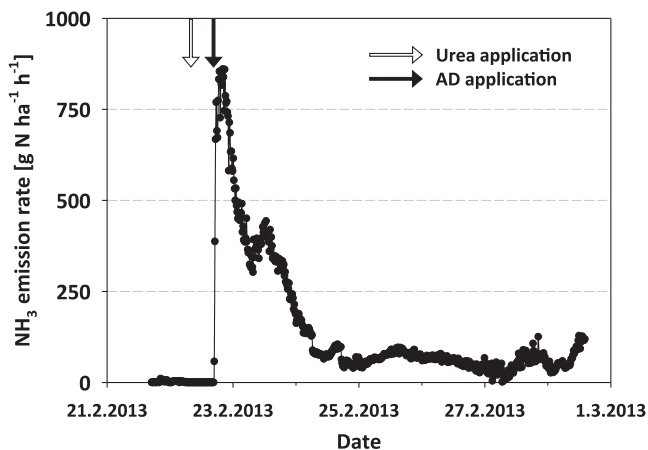


Fig. 2. NH_3 N emission rate from a field plot after AD application determined by Open Path FTIR in combination with the *bLS* dispersion technique during a field campaign in late February 2013 with temperatures oscillating around the freezing point.

higher compared to NH_3 emissions from AD land spreading with trailer hoses in the same study region in late spring (Quakernack et al., 2012). High NH_3 emissions after band spreading of slurry can particularly occur on arable land with no or low vegetation and can be similar or only slightly lower compared to splash plate application (Wulf et al., 2002).

Most of NH_3 -loss measurements from arable field sources reported in the literature are characterized by an uncertainty of at least 15% (Harper and Sharpe, 1998). Sommer et al. (2005) showed that ZINST-height measurements with long sampling intervals were afflicted with an uncertainty of at least 16% depending on measurement height. The measurement height is critical for the accuracy of the flux calculations of the *bLS* model (e.g. McBain and Desjardins, 2005; Sommer et al., 2005). The chosen measurement height in our study was close to the recommendation in Sommer et al. (2005) for the given distance between sensor and field edge of minimum 100 m (depending on wind direction) and z_0 of 1.0 cm for very short and sparse vegetation. Due to the high temporal resolution of NH_3 concentration measurements and meteorological data we assume that the accuracy of our measurements is within the range of $\pm 10\%$ reported in earlier studies applying the *bLS* technique (McBain and Desjardins, 2005; Gao et al., 2009).

As shown in Fig. 2, NH_3 emissions peaked during and directly after land spreading and abated afterwards revealing a typical NH_3 emission pattern of surface applied slurry. The major portion of ammonia was released during the first two days after land spreading, while emission rates during the following four days were clearly lower and relatively constant, but NH_3 concentrations were still significantly above atmospheric background. When the measurements were stopped six days after AD application, NH_3 volatilization was still lasting and emissions increased during the last 1.5 days of the measurement. The air temperature started rising at this point (Fig. 1) and the delayed effect of field applied urea on NH_3 emissions probably commenced. Urea was applied c. 9 h prior to AD application, but measured NH_3 concentrations remained at background levels until start of AD land spreading. Field applied urea subsequently partly covered with liquid AD (about 50% of field area) is potentially hydrolyzed faster to NH_4^+ , which will, together with the high pH value of AD, amplify NH_3 emissions. However, measurements of NH_3 emissions after urea application without AD in the same study region under similar conditions about two weeks later showed that urea hydrolysis took several days before emissions could be detected and emissions were very low (3% of applied N after four weeks; Ni et al., unpublished data). Hydrolysis of urea is

mainly temperature controlled and very slow at low temperatures (Xu et al., 1993), and applied slurry cooled down rapidly and partly froze at the surface within 1–2 h after application. In addition, applied urea was not dissolved in the slurry but was covered by a slurry layer which probably functioned as an emission barrier for urea derived NH_3 which had to diffuse to the slurry surface prior to emission. Therefore, the detected NH_3 emissions derived not from AD only but include probably small amounts of NH_3 from hydrolyzed urea, and it is likely that application of urea and AD together led to higher NH_3 emissions than staggered application of urea and AD. This particularly applies to emissions on February 27th and 28th which show with subsequently increasing emissions a typical pattern of NH_3 emission after urea application (Pacholski et al., 2006). These emissions cover about $1.72 \text{ kg NH}_3 \text{ N ha}^{-1}$. Measurements were later on stopped to avoid further effects of urea on AD emissions. If a warmer and dry period would have followed, subsequent NH_3 emissions could have been high, in the same range as those observed for AD (Ni et al., unpublished data).

The exact NH_3 contribution of urea remains uncertain. Nevertheless, these results highlight that the by far major fraction of high NH_3 emissions occurred due to AD application under cold temperature conditions. Emissions would be smaller when rain is following the cold period and NH_4^+ is washed into the soil. But it is typical for these early spring applications that they occur at rather stable cold weather conditions without precipitation. Nevertheless, probably no large subsequent emissions occurred after finishing the measurements. Estimating maximum asymptotic NH_3 loss by fitting a sigmoidal function (Demeyer et al., 1995) to the AD derived cumulated emissions measured until February 27th yielded c. $17.4 \text{ kg NH}_3 \text{ N ha}^{-1}$ ($R^2 = 1$), which corresponds to 33% of the NH_4^+ N contained in AD.

Several previous studies indicate that NH_3 volatilization is significantly affected by air temperature, especially during the initial 24 h, and that the emission event may last longer under low air temperatures (Sommer et al., 1991; Huijsmans et al., 2003). In the present study, about 50% of the total NH_3 release occurred during the initial 24 h, and after 48 h the emission levelled at a low but constant rate and was still ongoing when measurements were stopped after six days. This indicates that the emission event lasted clearly longer compared to other studies. For example, in a study applying AD to grass and wheat in late spring, about 75% of the NH_3 emission occurred during the initial 12 h (Quakernack et al., 2012), while in the present study 75% of the NH_3 were released after 48 h. We attribute this to the predominantly frozen soil by which infiltration of AD was clearly restricted, and most of applied AD remained on the soil surface. Due to the low temperature the AD on the soil surface remained moist or temporarily frozen during the whole measurement period but did not dry. So dissolved NH_4^+ remained mobile. A similar observation was reported by Sommer et al. (1991) after surface application of cattle slurry. During daytime, when AD and the upper 0.5–2 cm soil layer were thawed, NH_3 emissions were clearly higher compared to night time. Therefore we conclude that the frozen soil hampering infiltration and the freeze-thaw cycles prolonged the emission phase and increased total NH_3 volatilization above amounts which would typically be emitted under the given environmental conditions. It has been shown earlier, that infiltration of slurry into the soil influences NH_3 volatilization (Sommer et al., 2004).

4. Conclusions

Cumulative NH_3 emissions after urea application and consecutive AD land spreading account for $17.5 \text{ kg NH}_3 \text{ N ha}^{-1}$ within the first six days, while asymptotic AD derived NH_3 loss was estimated using a sigmoidal function to reach a total of $17.4 \text{ kg NH}_3 \text{ N ha}^{-1}$

(equivalent to 33% of the applied $\text{NH}_4\text{-N}$). Urea hydrolysis is slow at low temperatures, and is likely to have led to additional NH_3 loss during the following weeks. The observed emissions were higher than expected under cold temperatures around the freezing point and point out that application of organic fertilizers pose even under cold temperature conditions a significant source of NH_3 emissions. We attribute the emitted amounts and the relatively long duration of the emission event to the frozen soil restricting AD infiltration into the soil. As a conclusion, AD land spreading appears non-advisable under frozen soil conditions with respect to ammonia volatilization, and application of urea and AD should be temporally segregated as AD may foster hydrolysis of urea and NH_3 volatilization.

Acknowledgements

Jan Reent Köster thanks the German Federal Environmental Foundation (DBU) for a PhD scholarship. The authors gratefully acknowledge the support of D.W.T. Griffith (University of Wollongong, Australia) with FTIR spectra analysis and the project support of D. Holthusen and A. Seidel (Kiel University). O.T. Denmead (CSIRO Canberra, Australia) and D. Chen (The University of Melbourne, Australia) helped establishing the measurement instrumentation. R. Bonse kindly permitted and supported these measurements on his agricultural land. Purchase of Open Path FTIR equipment was supported by the Innovationsstiftung Schleswig Holstein. Funding of actual measurements was granted by the Ministry of Energy, Education and Traffic of the Federal State of Schleswig-Holstein and the EU Regional Programme 2000 in the framework of the joint project 'Centre of Excellence of Biomass in Schleswig-Holstein'.

References

- Amon, B., Kryvoruchko, V., Amon, T., Zechmeister-Boltenstern, S., 2006. Methane, nitrous oxide and ammonia emissions during storage and after application of dairy cattle slurry and influence of slurry treatment. *Agric. Ecosyst. Environ.* 112, 153–162.
- Demeyer, P., Hofman, G., van Cleemput, O., 1995. Fitting ammonia volatilization dynamics with a logistic equation. *Soil Sci. Soc. Am. J.* 59, 261–265.
- Denmead, O.T., 2008. Approaches to measuring fluxes of methane and nitrous oxide between landscapes and the atmosphere. *Plant Soil* 309, 5–24.
- Flesch, T.K., Wilson, J.D., Yee, E., 1995. Backward-time Lagrangian stochastic dispersion models and their application to estimate gaseous emissions. *J. Appl. Meteorol.* 34, 1320–1332.
- Flesch, T.K., Wilson, J.D., Harper, L.A., Crenna, B.P., Sharpe, R.R., 2004. Deducing ground-to-air emissions from observed trace gas concentrations: a field trial. *J. Appl. Meteorol.* 43, 487–502.
- Flesch, T.K., Wilson, J.D., Harper, L.A., Todd, R.W., Cole, N.A., 2007. Determining ammonia emissions from a cattle feedlot with an inverse dispersion technique. *Agric. For. Meteorol.* 144, 139–155.
- Gao, Z.L., Mauder, M., Desjardins, R.L., Flesch, T.K., van Haarlem, R.P., 2009. Assessment of the backward Lagrangian stochastic dispersion technique for continuous measurements of CH_4 emissions. *Agric. For. Meteorol.* 149, 1516–1523.
- Griffith, D.W.T., 1996. Synthetic calibration and quantitative analysis of gas-phase FT-IR spectra. *Appl. Spectrosc.* 50, 59–70.
- Griffith, D.W.T., Deutscher, N.M., Caldwell, C., Kettlewell, G., Riggenbach, M., Hammer, S., 2012. A Fourier transform infrared trace gas and isotope analyser for atmospheric applications. *Atmos. Meas. Tech.* 5, 2481–2498.
- Harper, L.A., Sharpe, R.R., 1998. Atmospheric ammonia: issues on transport and nitrogen isotope measurement. *Atmos. Environ.* 32, 273–277.
- Herrmann, A., Rath, J., 2012. Biogas production from maize: current state, challenges, and prospects. 1. Methane yield potential. *Bioenergy Res.* 5, 1027–1042.
- Hertel, O., Geels, C., Frohn, L.M., Ellermann, T., Skjoth, C.A., Løstrem, P., Christensen, J.H., Andersen, H.V., Peel, R.G., 2013. Assessing atmospheric nitrogen deposition to natural and semi-natural ecosystems – experience from Danish studies using the DAMOS. *Atmos. Environ.* 66, 151–160.
- Huijsmans, J.F.M., Hol, J.M.G., Vermeulen, G.D., 2003. Effect of application method, manure characteristics, weather and field conditions on ammonia volatilization from manure applied to arable land. *Atmos. Environ.* 37, 3669–3680.
- IPCC, 2007. In: Metz, B., Davidson, O.R., Bosch, P.R., Dave, R., Meyer, L.A. (Eds.), *Climate Change 2007: Mitigation. Contribution of Working Group III to the Fourth Assessment Report of the Intergovernmental Panel on Climate Change*. Cambridge University Press, Cambridge, United Kingdom and New York, NY, USA.
- Jones, F.M., Phillips, F.A., Naylor, T., Mercer, N.B., 2011. Methane emissions from grazing Angus beef cows selected for divergent residual feed intake. *Anim. Feed Sci. Technol.* 166–167, 302–307.
- McBain, M.C., Desjardins, R.L., 2005. The evaluation of a backward Lagrangian stochastic (bLS) model to estimate greenhouse gas emissions from agricultural sources using a synthetic tracer source. *Agric. For. Meteorol.* 135, 61–72.
- Ni, K., Kage, H., Pacholski, A. Effects of urease and nitrification inhibitors on ammonia volatilization after multiple application of urea to winter wheat in Northern Germany, unpublished data.
- Pacholski, A., Cai, G.X., Nieder, R., Richter, J., Fan, X.H., Zhu, Z.L., Roelcke, M., 2006. Calibration of a simple method for determining ammonia volatilization in the field – comparative measurements in Henan Province, China. *Nutr. Cycl. Agroecosyst.* 74, 259–273.
- Quakernack, R., Pacholski, A., Techow, A., Herrmann, A., Taube, F., Kage, H., 2012. Ammonia volatilization and yield response of energy crops after fertilization with biogas residues in a coastal marsh of Northern Germany. *Agric. Ecosyst. Environ.* 160, 66–74.
- Rothman, L.S., Gordon, I.E., Barbe, A., Benner, D.C., Bernath, P.E., Birk, M., Boudon, V., Brown, L.R., Campargue, A., Champion, J.P., Chance, K., Coudert, L.H., Dana, V., Devi, V.M., Fally, S., Flaud, J.M., Gamache, R.R., Goldman, A., Jacquemart, D., Kleiner, I., Lacome, N., Lafferty, W.J., Mandin, J.Y., Massie, S.T., Mikhailenko, S.N., Miller, C.E., Moazzen-Ahmadi, N., Naumenko, O.V., Nikitin, A.V., Orphal, J., Perevalov, V.I., Perrin, A., Predoi-Cross, A., Rinsland, C.P., Rotger, M., Simeckova, M., Smith, M.A.H., Sung, K., Tashkun, S.A., Tennyson, J., Toth, R.A., Vandaele, A.C., Vander Auwera, J., 2009. The HITRAN 2008 molecular spectroscopic database. *J. Quant. Spectrosc. Radiat. Transf.* 110, 533–572.
- Sommer, S.G., Olesen, J.E., Christensen, B.T., 1991. Effects of temperature, wind speed and air humidity on ammonia volatilization from surface applied cattle slurry. *J. Agric. Sci.* 117, 91–100.
- Sommer, S.G., Hansen, M.N., Sogaard, H.T., 2004. Infiltration of slurry and ammonia volatilisation. *Biosyst. Eng.* 88, 359–367.
- Sommer, S.G., McGinn, S.M., Flesch, T.K., 2005. Simple use of the backwards Lagrangian stochastic dispersion technique for measuring ammonia emission from small field-plots. *Eur. J. Agron.* 23, 1–7.
- Sutton, M.A., Milford, C., Dragosits, U., Place, C.J., Singles, R.J., Smith, R.I., Pitcairn, C.E.R., Fowler, D., Hill, J., ApSimon, H.M., Ross, C., Hill, R., Jarvis, S.C., Pain, B.F., Phillips, V.C., Harrison, R., Moss, D., Webb, J., Espenhahn, S.E., Lee, D.S., Hornung, M., Ulyett, J., Bull, K.R., Emmett, B.A., Lowe, J., Wyers, G.P., 1998. Dispersion, deposition and impacts of atmospheric ammonia: quantifying local budgets and spatial variability. *Environ. Pollut.* 102, 349–361.
- Sutton, M.A., Oenema, O., Erisman, J.W., Leip, A., van Grinsven, H., Winiwarter, W., 2011. Too much of a good thing. *Nature* 472, 159–161.
- Wulf, S., Maeting, M., Clemens, J., 2002. Application technique and slurry co-fermentation effects on ammonia, nitrous oxide, and methane emissions after spreading: I. Ammonia volatilization. *J. Environ. Qual.* 31, 1789–1794.
- Xu, J.G., Heeraman, D.A., Wang, Y., 1993. Fertilizer and temperature effects on urea hydrolysis in undisturbed soil. *Biol. Fertil. Soils* 16, 63–65.

Chapter 3.1

Corrigendum

Cold season ammonia emissions from land spreading with anaerobic digestates from biogas production

Jan Reent Köster, Klaus Dittert, Karl-Hermann Mühling,
Henning Kage, and Andreas Pacholski

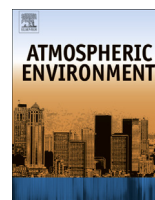
Atmospheric Environment 90 (2014) 149

DOI: [10.1016/j.atmosenv.2014.03.014](https://doi.org/10.1016/j.atmosenv.2014.03.014)



Contents lists available at ScienceDirect

Atmospheric Environment

journal homepage: www.elsevier.com/locate/atmosenv

Corrigendum

Corrigendum to 'Cold season ammonia emissions from land spreading with anaerobic digestates from biogas production' [Atmos. Environ. 84 (2014) 35–38]

Jan Reent Köster^{a,*}, Klaus Dittert^b, Karl-Hermann Mühling^a, Henning Kage^c,
Andreas Pacholski^{c,d}^a Institute of Plant Nutrition and Soil Science, Kiel University, Hermann-Rodewald-Str. 2, 24118 Kiel, Germany^b Department of Crop Science, Section of Plant Nutrition and Crop Physiology, University of Goettingen, Carl-Sprengel-Weg 1, 37075 Goettingen, Germany^c Agronomy and Crop Science, Institute of Crop Science and Plant Breeding, Kiel University, Hermann-Rodewald-Straße 9, 24118 Kiel, Germany^d Graduate School/Inkubator, Leuphana University Lüneburg, Scharnhorststr. 1, 21335 Lüneburg, Germany

In the original report on our FTIR approach for measuring ammonia emissions after land spreading of anaerobic digestates a systematic error has occurred. In our quantitative analysis of single-beam FTIR spectra, subtraction of background IR radiation has been missed out, which is necessary for the bistatic OP FTIR configuration used in the study. This is mandatory because the thermal emission of near field objects contributes to the spectral continuum, while the NH₃ absorption lines are not equally enhanced.

Therefore now, prior to quantitative analysis of single-beam spectra, passive FTIR spectra (IR source off) were subtracted from the single beam spectra to compensate for background IR radiation (Jarvis, 2003). After this correction, the NH₃ background concentration (i.e. the NH₃ concentration before AD field spreading) was determined to be 5.19 ppb, which was taken into account during the flux calculation.

Results

The corrected cumulative NH₃ loss over the whole observation period (six days) after AD land spreading was 21.46 kg NH₃-N ha⁻¹, which corresponds to 40.6% of the applied AD NH₄⁺-N. The NH₃ emissions during the last two days of the trial (February 27th and 28th), which we rather attribute to urea hydrolysis, amounted to 2.06 kg NH₃-N ha⁻¹.

So the new calculations resulted in an increase of the observed emissions throughout the emission process; however, the time course pattern remained unaffected (Fig. 2).

References

Jarvis, J.M., 2003. Open Path Spectrophotometry (UV, IR, FT-IR). In: Lipták, B.G. (Ed.), Instrument Engineers' Handbook, Fourth Edition, Volume One: Process Measurement and Analysis: Process Measurement and Analysis. CRC Press, Boca Raton, FL, USA, pp. 1493-1505.

The authors would like to apologize for any inconvenience caused.

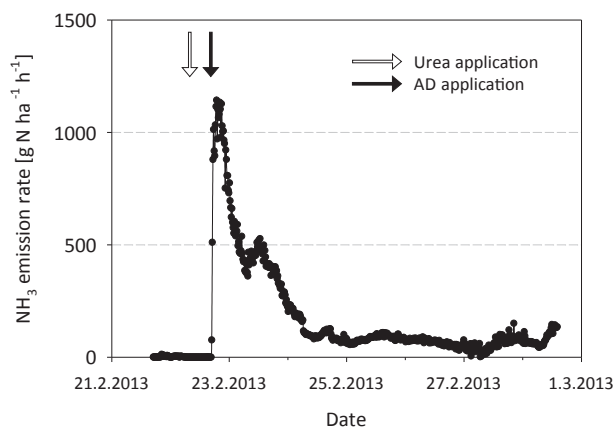


Fig. 2. NH₃-N emission rate from a field plot after AD application determined by Open Path FTIR in combination with the *bLS* dispersion technique during a field campaign in late February 2013 with temperatures oscillating around the freezing point.

DOI of original article: <http://dx.doi.org/10.1016/j.atmosenv.2013.11.037>.

* Corresponding author. Department of Environmental Sciences, Norwegian University of Life Sciences, 1430 Ås, Norway.

E-mail addresses: jan.reent.koester@nmbu.no, janreent@gmx.de (J.R. Köster).

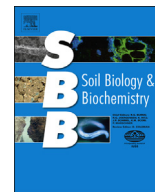
Chapter 4

Anaerobic digestates lower N₂O emissions compared to cattle slurry by affecting rate and product stoichiometry of denitrification - an N₂O isotopomer case study

Jan Reent Köster, Laura Cárdenas, Roland Bol, Dominika Lewicka-Szczebak,
Mehmet Senbayram, Reinhard Well, Anette Giesemann, and Klaus Dittert

Soil Biology & Biochemistry 84 (2015) 65 – 74

DOI: 10.1016/j.soilbio.2015.01.021



Anaerobic digestates lower N₂O emissions compared to cattle slurry by affecting rate and product stoichiometry of denitrification – An N₂O isotopomer case study

Jan Reent Köster^{a,*}, Laura M. Cárdenas^b, Roland Bol^c, Dominika Lewicka-Szczebak^d, Mehmet Senbayram^e, Reinhard Well^d, Anette Giesemann^d, Klaus Dittert^{e,f}

^a Institute of Plant Nutrition and Soil Science, Kiel University, Hermann-Rodewald-Str. 2, 24118 Kiel, Germany

^b Rothamsted Research, North Wyke, Okehampton EX20 2SB, UK

^c Terrestrial Biogeochemistry Group, Institute of Bio- and Geosciences, Agrosphere (IBG-3), Forschungszentrum Jülich GmbH, Wilhelm-Johnen-Straße, 52428 Jülich, Germany

^d Thünen Institute of Climate-Smart Agriculture, Federal Research Institute for Rural Areas, Forestry and Fisheries, Bundesallee 50, 38116 Braunschweig, Germany

^e Institute of Applied Plant Nutrition (IAPN), University of Göttingen, Carl-Sprengel-Weg 1, 37075 Göttingen, Germany

^f Department of Crop Science, Section of Plant Nutrition and Crop Physiology, University of Göttingen, Carl-Sprengel-Weg 1, 37075 Göttingen, Germany

ARTICLE INFO

Article history:

Received 22 July 2014

Received in revised form

20 January 2015

Accepted 21 January 2015

Available online 7 February 2015

Keywords:

Nitrous oxide

Organic fertilizer

Biogas

Nitrification

Site preference

N₂O reduction

Source partitioning

ABSTRACT

Assessing effects of organic fertilizer applications on N₂O emissions is of great interest because they can cause higher N₂O emissions compared to inorganic fertilizers for a given amount of added nitrogen (N). But there are also reports about enhanced N₂O reduction to climate-neutral elemental N₂ after application of organic manures to soils. Factors controlling the N₂O/(N₂O + N₂) product ratio of denitrification are interrelated, and also the ratio is difficult to study because of limitations in N₂ flux measurements. In this study, we investigated N₂O and N₂ emissions from soil treated with organic fertilizers with different C/N ratios. An N₂O isotopomer approach combined with conventional N₂O and N₂ flux measurements was employed to study underlying microbial pathways.

A grassland soil was amended with anaerobic digestate (AD) from food waste digestion (low C/N ratio) or cattle slurry (CS; high C/N ratio), respectively, adjusted to 90% WFPS, and incubated for 52 days under helium–oxygen atmosphere (10% O₂) using a soil incubation system capable of automated N₂O, N₂, and CO₂ measurements. N₂O isotopomer signatures, i.e. the δ¹⁸O and SP values (site preference between ¹⁵N at the central and the peripheral position in the N₂O molecule), were determined by Isotope Ratio Mass Spectrometry and used to model and subsequently estimate the contribution of bacterial denitrification and autotrophic nitrification to N₂O production. For this approach the direct determination of emitted N₂ is essential to take isotope effects during N₂O reduction to N₂ into account by correcting the measured isotope signatures for isotope effects during N₂O reduction using previously determined fractionation factor ranges.

The addition of both organic fertilizers to soil drastically increased the rate of gaseous N emissions (N₂O + N₂), probably due to the effects of concurrent presence of nitrate and labile C on the denitrification rate. In the initial phase of the experiment (day 1 to ~15), gaseous N emissions were dominated by N₂ fluxes in soils amended with organic manures; meanwhile, N₂O emissions were lower compared to untreated Control soils, but increased after 15–20 days relative to the initial fluxes, especially with CS. Extremely low N₂O, but high N₂ emissions in the initial phase suggest that reduction of N₂O to N₂ via denitrification was triggered when the soil was amended with organic fertilizers. In contrast in the untreated Control, N₂O release was highest during the initial phase. Total N₂O release from AD treated soil was similar to Control, while N₂O from CS treated soil was considerably higher, indicating that denitrification was triggered more by the high labile carbon content in CS, while the cumulative N₂O/(N₂O + N₂) product ratio and thus N₂O reduction were similar with both organic fertilizers.

* Corresponding author. Present address: Department of Environmental Sciences, Norwegian University of Life Sciences, P.O. Box 5003, 1432 Ås, Norway. Tel.: +47 6723 1864.

E-mail address: jan.reent.koester@nmbu.no (J.R. Köster).

The results of the N₂O source partitioning based on the isotopomer data suggest that about 8–25% (AD) and 33–43% (CS) of the cumulated N₂O emission was due to nitrification in organically amended soil, while in the untreated Control nitrification accounted for about 5–16%. The remaining N₂O production was attributed mainly to denitrification, while the poor model fit for other source pathways like fungal denitrification suggested their contribution to be of minor importance. The observed rather distinct phases with predominance first of denitrification and later of nitrification may help developing mitigation measures by addressing N₂O source processes individually with appropriate management options. The observation of relatively large shares of nitrification-derived N₂O is surprising, but may possibly be related to the low soil pH and will require further investigation.

The determination of N₂ production is essential for this isotopomer-based source partitioning approach, but so far only applicable under laboratory conditions. The results of this study indicate that the combination of N₂O δ¹⁸O and SP values is very useful in obtaining more robust source estimates as compared to using SP values alone.

© 2015 Elsevier Ltd. All rights reserved.

1. Introduction

Nitrous oxide (N₂O) is a potent greenhouse gas (GHG; Stocker et al., 2013) and ozone depleting substance affecting the stratospheric ozone layer (Ravishankara et al., 2009). Increasing atmospheric N₂O concentrations are caused by anthropogenic activities, in particular by the intensification of agriculture production and introduction of huge amounts of reactive nitrogen (N) species into the global N cycle (Galloway et al., 2004).

N₂O mainly derives from agricultural soils, where high N fertilizer inputs are directly related to N₂O production (Mosier et al., 1998; Galloway et al., 2004), resulting in 2–2.5% conversion of fertilizer N to N₂O (Davidson, 2009). However, understanding of factors controlling N₂O production and consumption processes in soils has still to be improved to implement more advanced mitigation strategies to reduce undesirable side effects of fertilizer use.

Renewable energy sources like biogas produced from various organic substrates like food waste, animal wastes, and energy crops for generating electricity and heat are explicitly promoted and gained importance in several European countries (Herrmann and Rath, 2012). The residues of the biogas fermentation process, anaerobic digestates (AD), are mostly applied to agricultural land as 'organic' fertilizers. However, AD may, similar to other organic fertilizers (e.g. livestock manures, human waste), increase N₂O emissions from soils compared to mineral N fertilizers (e.g. Senbayram et al., 2009; Köster et al., 2011), because residual organic carbon substrates favor microbial denitrification, the respiratory nitrate reduction, in soils (Robertson and Groffman, 2007).

Various stable isotope techniques have been developed to study N transitions and to differentiate N₂O source processes as reviewed by Baggs (2008). However, they are all afflicted with various shortcomings. Recently, the analysis of isotopomers, the intramolecular ¹⁵N distribution in the linear asymmetric N₂O molecule, has been introduced as a mean of differentiating source processes (Toyoda and Yoshida, 1999; Yoshida and Toyoda, 2000). In addition to bulk isotope signatures, the parameter 'site preference' (SP), defined as the difference of δ¹⁵N at the central (α) and the peripheral (β) position of the N₂O molecule has been proposed. Distinct N₂O δ¹⁵N^{bulk}, δ¹⁸O, and SP signatures have been identified to be specific for bacterial denitrification (including nitrifier denitrification), nitrification (i.e. ammonium oxidation via hydroxylamine), or fungal denitrification (Sutka et al., 2003, 2004, 2006, 2008; Toyoda et al., 2005), and the SP is considered to be independent of the isotopic signature of the precursor species (Toyoda et al., 2002). However, this approach may be complicated by some overlap of signatures of autotrophic nitrification and fungal denitrification (Sutka et al., 2006, 2008), and by N₂O reduction to N₂

altering the N₂O SP (Ostrom et al., 2007). Additional information may be obtained by the relationship of N₂O δ¹⁸O and SP values, which have been shown to be linearly correlated with the SP in N₂O significantly affected by N₂O reduction (Jinuntuya-Nortman et al., 2008; Well and Flessa, 2009a; Köster et al., 2013b), but interpretation of isotopomer results still remains challenging (Decock and Six, 2013). However, this approach can provide valuable information on N₂O releasing soil processes, especially when combined with other techniques like direct measurements of the main denitrification products N₂O and N₂.

Recent developments and application of improved process models promote the understanding of isotope effects during N₂O production and consumption processes and associated fractionation factors, thus allowing better estimations on source processes (Toyoda et al., 2011; Lewicka-Szczebak et al., 2014).

The objectives of this study were to compare organic fertilizers of different C/N ratio for their effect on total N₂O and N₂ losses by denitrification and associated changes in the N₂O/(N₂O + N₂) product ratio. Therefore, an incubation experiment was carried out under conditions favorable for denitrification. The use of an N₂-free helium-oxygen incubation atmosphere in an automated soil incubation system allowed direct simultaneous measurement of N₂O, N₂, and CO₂. Denitrification was expected to be the major microbial pathway contributing to N₂O production, though also nitrification (i.e. ammonium oxidation via hydroxylamine) was expected to play a role following the application of AD and cattle slurry (CS) as ammonium based organic fertilizers. This was to be confirmed by applying the N₂O isotopomer approach, as nitrification-derived N₂O is characterized by higher δ¹⁸O and SP values. ¹⁸O and site-specific ¹⁵N fractionation factors may vary over relative wide ranges, which thus was taken into account. N₂O source partitioning was conducted independently using N₂O δ¹⁸O and SP signatures, respectively, to cross-check the N₂O source estimates.

2. Materials and methods

2.1. Sampling and properties of soil and organic fertilizers

The soil was collected in Rowden Moor (50°46'26"N, 03°55'47"W; 162 m above sea level), Okehampton, Devon, UK. This soil is classified as a Hallsworth Series soil, which is a clayey non-calcareous Pelostagnogley in head from clay shale (Harrod and Hogan, 2008). The bulk density was about 0.9–1 g cm⁻³. The sampling site had previously been in grassland use but it has been left fallow for the last ten years. The upper 2 cm of soil and roots

were removed and the 10–15 cm soil horizon beneath was collected.

AD from food waste was collected from a commercial biogas plant in Holsworthy, Devon, UK. This biogas plant is mainly fed with food residues including liquid waste from abattoirs and some municipal waste and has a hydraulic retention time of about 53 days. The digestate sample was taken directly from the digester.

CS was collected at a dairy farm in Southwick, Dumfries, Scotland, UK. The slurry and digestate samples were stored at ca. 4 °C till onset of the experiment.

Dry matter (DM) content of samples from fresh soil and organic fertilizer samples was determined gravimetrically after drying at 105 °C and organic matter (OM) was measured as loss on ignition at 550 °C. The pH value was determined after suspending soil in deionized water, while in the liquid organic fertilizers it was measured directly. Mineral N (nitrate and exchangeable ammonium) was extracted with 2 M KCl and analyzed colorimetrically by segmented flow analysis. Total N was determined in fresh soil and organic fertilizer samples using Kjeldahl digestion with steam distillation and subsequent titration. Water-extractable organic carbon (WEOC) of soil and organic fertilizer samples was extracted with Millipore® water (18.2 MΩ), filtered, and total C and inorganic C were determined using a Skalar Formacs^{HT} TOC Analyser; afterwards, WEOC was calculated. Total C was determined on air dried soil samples and organic fertilizer samples dried at 60 °C using an elemental analyzer (Carlo Erba NA 2500 CE Instruments, Thermo Quest Italia S.p.A., Milano, Italy). Prior to mass spectrometric analysis of the ¹⁵N/¹⁴N isotope ratio organic fertilizer were acidified using HCl to a pH of ~2 (to avoid ammonia volatilization during desiccation), dried, and analyzed on an isotope ratio mass spectrometer 20-20 Stable Isotope Analyser (PDZ Europa Ltd., Crewe, UK). The properties of the soil, digestate, and slurry are given in Table 1.

2.2. Automated soil incubation experiment and trace gas measurements

The incubation experiment was carried out under fully controlled conditions using an automated soil incubation system consisting of twelve stainless steel incubation vessels as described by Cárdenas et al. (2003). Fresh soil was sieved through a sieve with 4 mm mesh size and repacked 10.5 cm high into steel cylinders to cores of 1686 g dry weight with a bulk density of 1 g cm⁻³. Soil moisture was adjusted to 90% water-filled pore space (WFPS), taking the liquid fertilizers' water content into account. The soil cores were placed in the incubation vessels, which were then sealed. The incubation atmosphere was replaced by a helium–oxygen (He/O₂) mixture containing 10% oxygen to remove

atmospheric nitrogen. Thus, soil conditions promoting denitrification were established, which may occur after precipitation events or in subsoil. During a two-day pre-incubation phase atmospheric air was purged from the vessels from the bottom to the top of the incubation vessels, whereas during the main incubation phase He/O₂ was directed through an inlet in the lid with a flow rate of 6 ml vessel⁻¹ min⁻¹ to simulate air movement with a low wind speed. The organic fertilizers or deionized water as the Control treatment were applied to the soil via a helium-flushed amendment vessel mounted to the lid aiming at a target rate of 152.4 mg NH₄⁺ – N (kg dry soil)⁻¹ (equiv. to 160 kg NH₄⁺ – N ha⁻¹; actual application rate was around 138 mg NH₄⁺ – N (kg dry soil)⁻¹), resulting in highest N input in treatment CS due to its high N_{org} content (see Table 2). After fertilizer application no further additions were made. Soil cores of each treatment were set up in triplicate. The soil was incubated for 52 days at 20 °C. Gas samples were taken automatically from the incubation vessels about 16 times per day and analyzed online. N₂O and CO₂ concentrations were measured on a Philips PU 4500 (Philips Scientific, Cambridge, UK) gas chromatograph (GC) equipped with an electron capture detector (ECD). N₂ was quantified by a second GC equipped with a Pulsed Discharge Detector (D-2-I-220; VICI Valco Instruments Co. Inc., Houston, TX, USA) operated in Helium Ionization Mode (Cárdenas et al., 2003). Typical analytical precision (1σ) for N₂O was better than 1%, while for N₂ and CO₂ it was better than 3%. The calibration of both GCs was checked daily. In addition for isotope analysis, gas samples were collected from all treatments at frequent intervals. N₂O δ¹⁵N^{bulk}, δ¹⁵N^α, and δ¹⁸O values were determined by isotope ratio mass spectrometry at the Thünen Institute Braunschweig, Germany, by analyzing *m/z* 44, 45, and 46 of intact N₂O⁺ molecular ions and *m/z* 30 and 31 of NO⁺ fragment ions (Toyoda and Yoshida, 1999) on a Delta V Plus isotope ratio mass spectrometer (Thermo Fisher Scientific, Bremen, Germany). The typical analytical precision was 0.2, 0.4, and 0.3‰ for δ¹⁵N^{bulk}, δ¹⁵N^α, and δ¹⁸O, respectively (Köster et al., 2013a). The ¹⁵N–N₂O value was corrected for ¹⁷O according to Brand (1995).

2.3. Statistical data analyses

The incubation experiment was conducted in a completely randomized design. The area under the curve calculation for the cumulative trace gas emissions was performed by linear interpolation between individual data points. Mineralization and nitrification were calculated using a mass balance approach. For generation of GC calibration equations the REG procedure of the statistical software package SAS 9.0 (SAS Institute Inc., Cary, North Carolina, USA) was used. The Tukey test (Tukey's range test; α = 0.05) was carried out for multiple comparisons assuming

Table 1
Characteristics of soil and organic fertilizers. Mean values (±standard deviation).

| | Soil | Anaerobic digestate | Cattle slurry |
|---|----------------|---------------------|----------------|
| Dry Matter [DM; %] | 73.5 (±0.12) | 3.9 (±0.02) | 8.7 (±0.05) |
| Kjeldahl N [mg (kg soil DM) ⁻¹ or kg (org. waste FM) ⁻¹] | 2333 (±28.7) | 8607 (±187.7) | 2977 (±55.1) |
| NH ₄ ⁺ – N [mg (kg soil DM) ⁻¹ or kg (org. waste FM) ⁻¹] | 2.94 (±0.428) | 5443 (±251.7) | 1067 (±78.0) |
| NO ₃ ⁻ – N [mg (kg soil DM) ⁻¹ or kg (org. waste FM) ⁻¹] | 31.25 (±1.364) | 0.345 (±0.037) | 0.499 (±0.209) |
| Total C [% DM] | 3.41 (±0.07) | 35.60 (±0.23) | 35.12 (±0.43) |
| Organic matter [% DM; LOI ^a] | 9.69 (±0.05) | 69.21 (±0.27) | 63.17 (±0.59) |
| WEOC ^b [mg (kg FM) ⁻¹] | 44.2 (±4.58) | 2053 (±35.74) | 2717 (±13.35) |
| C/N ratio | 9.19 | 1.29 | 8.5 |
| pH | 4.9 | 8.4 | 8.1 |
| δ ¹⁵ N [vs N ₂ air; ‰] | 5.7 (±0.18) | 6.37 (±0.1) | 4 (±0.28) |

n = 3; except for pH (n = 1).

^a LOI = Loss on ignition.

^b WEOC = Water extractable organic carbon.

Table 2
Organic fertilizer application and resulting N and C input.

| Treatment | Application [g (kg soil DM) ⁻¹] | Resulting N and C input | | | | |
|---------------------|--|--|--|--|--|---|
| | | NH ₄ ⁺ – N [mg (kg soil DM) ⁻¹] | NO ₃ ⁻ – N [mg (kg soil DM) ⁻¹] | N _{org} [mg (kg soil DM) ⁻¹] | WEOC [mg (kg soil DM) ⁻¹] | Total C [mg (kg soil DM) ⁻¹] |
| Anaerobic digestate | 25.3 | 138.0 | 0.009 | 80.12 | 52.0 | 349.8 |
| Cattle Slurry | 129.0 | 137.7 | 0.064 | 246.3 | 350.5 | 3937.3 |

normality and homogeneity of variance using the “SimTestDiff” procedure from the SimComp package (Hasler, 2012), which is capable of handling unbalanced data sets, within the statistical software package R (version 3.0.2; The R Foundation for Statistical Computing, Vienna, Austria).

2.4. Model-based N₂O source partitioning

Different N₂O production pathways may be distinguished based on N₂O isotopomer information, which requires knowledge about the isotopic signatures of N₂O that is unaffected by N₂O reduction (δ_{N_2O-0}). These have been estimated based on the signatures of residual N₂O (δ_{N_2O-r}) that has not been reduced, the relative N₂O reduction rate calculated from the measured N₂ production, and the isotope effect during N₂O reduction. Afterwards, a two end-member isotopic mass balance was applied to decipher the relative contribution to N₂O production based on the SP and $\delta^{18}O$ values of emitted N₂O. Initially, the most probable scenario was considered comprising heterotrophic bacterial denitrification (including nitrifier denitrification with similar N₂O isotope signatures) and autotrophic nitrification (i.e. NH₄⁺ oxidation pathway via hydroxylamine) as end-members for the isotopic mass balance assuming only one homogeneously distributed substrate pool. A certain range of variation for these end-member isotope signatures as well as for the isotopic fractionation factors during N₂O reduction according to literature values was taken into account in these calculations, which thus resulted in a broader range of estimates for each contributing process. Also, another scenario involving fungal denitrification as N₂O source process was taken into account and will be briefly discussed in the following.

The incubation experiment was performed in a He incubation system where N₂ fluxes were measured directly and the N₂O/(N₂O + N₂) product ratio is known, thus the isotopic signatures of initially produced N₂O (δ_{N_2O-0} values: SP₀ and $\delta^{18}O_0$), i.e. of N₂O unaffected by N₂O reduction, can be estimated assuming closed system isotope dynamics using the Rayleigh equation (Mariotti et al., 1981; Fry, 2006):

$$\delta_{N_2O-r} = \delta_{N_2O-0} + \eta_r \cdot \ln\left(\frac{C}{C_0}\right) \quad (1)$$

with η_r being the net isotope effect (NIE; according to Jinuntuya-Nortman et al. (2008)) associated with N₂O reduction, and C and C₀ the residual and the initial substrate concentration, i.e. the expression (C/C₀) represents the product ratio (N₂O/(N₂O + N₂)). The δ_{N_2O-0} results obtained from this equation are very vulnerable to the precisely measured product ratio. Very low product ratios observed for some phases of this experiment (Fig. 1) cannot be determined precisely enough, and therefore for these calculations only very robust data have been accepted (N₂O/(N₂O + N₂) > 0.11).

Estimating δ_{N_2O-0} values according to Eq. (1) requires information about the fractionation factors associated with N₂O reduction. These factors have recently been analyzed in depth for various experimental approaches, and it was indicated that their large variations depend on the experimental conditions (Lewicka-Szczebak et al., 2014). That study also included He incubations,

where N₂O production and reduction occurred simultaneously (similar to this study), and less negative η_{180} values (about -7‰) when compared to previous studies (about -15‰) were found (Menyailo and Hungate, 2006; Ostrom et al., 2007; Jinuntuya-Nortman et al., 2008; Well and Flessa, 2009a; Lewicka-Szczebak et al., 2014). Hence, for η_{180} the range of -15 to -7‰ ($\emptyset = -11‰$) was adopted for Eq. (1). The η_{SP} values of all the available literature data are very robust and vary in a narrow range from -7 to -3‰ ($\emptyset = -5‰$) (Ostrom et al., 2007; Jinuntuya-Nortman et al., 2008; Well and Flessa, 2009a; Lewicka-Szczebak et al., 2014), which was also adopted in our calculations (Eq. (1)). The δ_{N_2O-0} values were calculated using the upper and the lower values of these ranges, which provides the results for minimum and maximum δ_{N_2O-0} values, respectively (Table 5).

The source partitioning of N₂O production was based on the two end-member isotopic mass balance equation:

$$\delta^{18}O_{N_2O-0} = \delta^{18}O_D \cdot f_{D-0} + \delta^{18}O_N \cdot f_{N-0} \quad (2)$$

$$SP_{N_2O-0} = SP_D \cdot f_{D-SP} + SP_N \cdot f_{N-SP} \quad (3)$$

The most probable scenario assumes denitrification (D) and nitrification (N) as two major N₂O sources, thus f_D and f_N represent the contribution of denitrification and nitrification, respectively. These contributions were calculated independently based on a $\delta^{18}O$ (Eq. (2): f_{D-0}, f_{N-0}) or SP (Eq. (3): f_{D-SP}, f_{N-SP}) isotopic mass balance. The ranges of end-member isotopic signatures were defined according to literature data: SP_D from -11 to 0‰ ($\emptyset = -5‰$) (Toyoda et al., 2005; Sutka et al., 2006) and SP_N from +33 to +37‰ ($\emptyset = +35‰$) (Sutka et al., 2006), while $\delta^{18}O_D$ from +10 to +20‰ ($\emptyset = +15‰$) (Toyoda et al., 2005; Snider et al., 2013; Lewicka-Szczebak et al., 2014) and $\delta^{18}O_N$ from +40 to +50‰ ($\emptyset = +45‰$) (Sutka et al., 2006; Heil et al., 2014). For defining the $\delta^{18}O_N$ and $\delta^{18}O_D$ ranges we used several experimental studies, which most probably used distilled tap water for their experiments. Some of these references provide information on the water- $\delta^{18}O$ values: e.g. ca. -7.5‰ (Lewicka-Szczebak et al., 2014), -9.2‰ (Toyoda et al., 2005), and -9.5‰ (Snider et al., 2013). Actually, there is only small variation in water- $\delta^{18}O$ among those studies when compared to the ranges of $\delta^{18}O_N$ and $\delta^{18}O_D$. Our water signature is most likely very close to these values, taking into account the geographical location (United Kingdom) and water source (distilled tap water) and the fact that there is little variation $\delta^{18}O$ of local water supplies (Bowen et al., 2005). In our experiment we can thus expect similar ranges of $\delta^{18}O_N$ and $\delta^{18}O_D$ because the possible deviation of our water- $\delta^{18}O$ is very probably much smaller than the assumed $\delta^{18}O_D$ range of +10 to +20‰. An impact of water- $\delta^{18}O$ on the $\delta^{18}O_D$ range can only be expected if water- $\delta^{18}O$ is extremely variable as shown by Lewicka-Szczebak et al. (2014), where waters with $\delta^{18}O$ of -13.5 to -2.6‰ were used, and the $\delta^{18}O$ of produced N₂O ranged from +5 to +16‰. The $\delta^{15}N^{bulk}$ signatures of the emitted N₂O were not included in the source partitioning approach, as the ¹⁵N signatures of mineral N, i.e. NO₃⁻ and NH₄⁺, cannot be assumed to be constant throughout the incubation phase, but will rather change due to fractionation during mineralization, nitrification, and denitrification processes. Monitoring of these isotope dynamics would

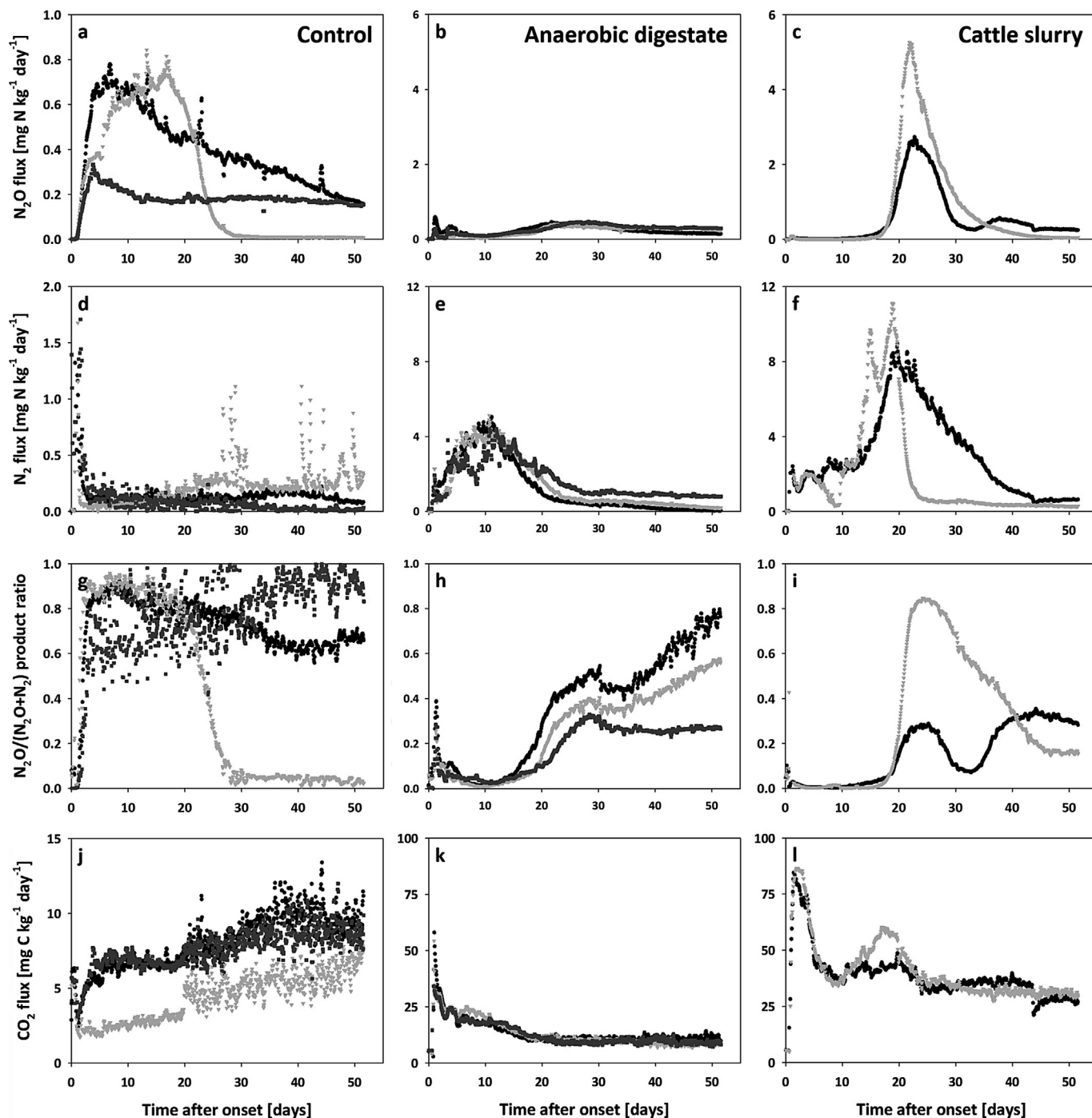


Fig. 1. N_2O -N flux (a, b, c), N_2 -N flux (d, e, f), the $\text{N}_2\text{O}/(\text{N}_2\text{O} + \text{N}_2)$ product ratio (g, h, i), and CO_2 -C flux (j, k, l) of soil left unamended (Control), or amended with Anaerobic digestate or Cattle slurry, respectively, at a target rate of $152 \text{ mg NH}_4^+ - \text{N} (\text{kg soil DM})^{-1}$ during incubation for 52 days at 90% WFPS and 0.1 atm p_{O_2} . Different symbols/colors indicate individual replications. Please be aware of differing ordinate scaling in the control treatment.

require frequent soil sampling, which was not possible with the deployed experimental setup, as incubation vials had to hold their airtight sealing to avoid N_2 contamination.

In the model calculations, the upper as well as the lower values of the given ranges were considered. We have also simulated an additional scenario involving bacterial denitrification and fungal denitrification, where the following end-member isotope signatures were used for the isotopic mass balance (Eqs. (2) and (3), with f_F representing fungal denitrification): $\text{SP}_D = -5\%$, SP_F from +34

to +37‰, $\delta^{18}\text{O}_D = +15\%$, and $\delta^{18}\text{O}_F$ from +30 to +40‰ (Sutka et al., 2008; Rohe et al., 2014).

3. Results and discussion

3.1. Trace gas emissions

Both added organic substrates induced a significant increase in soil respiration (CO_2 emission), but the time course of this

Table 3
Cumulated N₂O, N₂, and CO₂ emissions. Mean values per treatment (±standard deviation).

| Treatment | N ₂ O–N [mg (kg soil DM) ⁻¹] | N ₂ [mg (kg soil DM) ⁻¹] | N _{emitted} [mg (kg soil DM) ⁻¹] | N ₂ O/(N ₂ O + N ₂) ratio | CO ₂ –C [mg (kg soil DM) ⁻¹] | N ₂ O emission factor (N _{min} applied) [%] | N ₂ O emission factor (TN* applied) [%] |
|---------------------|--|--|--|--|--|--|---|
| Control | 14.1 (±5.5) ^a | 8.0 (±3.3) ^a | 22.1 (±6.7) ^a | 0.63 (±0.11) ^a | 342.3 (±100.6) ^a | / | / |
| Anaerobic digestate | 12.6 (±0.9) ^a | 73.0 (±9.6) ^b | 85.6 (±10.4) ^b | 0.15 (±0.01) ^b | 669.5 (±18.2) ^b | 9.12 (±0.66) ^a | 5.77 (±0.42) ^a |
| Cattle slurry | 34.1 (±8.0) ^b | 125.4 (±41.7) ^b | 159.4 (±33.7) ^c | 0.22 (±0.10) ^b | 2030.5 (±70.4) ^c | 24.72 (±5.83) ^b | 8.87 (±2.01) ^a |

n = 3 for Control and Anaerobic digestate; n = 2 for Cattle slurry.

Superscript letters indicate Tukey grouping (p < 0.05) (different letters indicate significant differences).

* TN = total N.

Table 4
N_{min} and WEOC concentrations in the soil after incubation. Mean values per treatment (±standard deviation).

| Treatment | NO ₃ ⁻ –N [mg (kg soil DM) ⁻¹] | NH ₄ ⁺ –N [mg (kg soil DM) ⁻¹] | N _{min} [mg (kg soil DM) ⁻¹] | WEOC [mg (kg soil DM) ⁻¹] | N _{mineralized} (net) [mg (kg soil DM) ⁻¹] | N _{nitrified} [mg (kg soil DM) ⁻¹] | Total N _{inorg} * recovered [mg (kg soil DM) ⁻¹] |
|---------------------|---|---|--|--|--|--|--|
| Control | 31.1 (±26.2) ^a | 5.3 (±8.5) ^a | 36.4 (±17.8) ^a | 13.6 (±5.8) ^a | 24.31 (±15.26) ^a | 19.03 (±23.76) ^a | 58.50 (±15.26) ^a |
| Anaerobic digestate | 111.1 (±36.1) ^a | 44.9 (±17.6) ^a | 156.1 (±18.9) ^b | 8.2 (±3.6) ^a | 69.45 (±8.58) ^b | 162.52 (±25.82) ^b | 241.65 (±8.58) ^b |
| Cattle slurry | 97.2 (±56.2) ^a | 17.6 (±23.2) ^a | 114.8 (±33.0) ^b | 31.5 (±4.0) ^b | 102.25 (±0.70) ^b | 222.33 (±22.55) ^b | 274.20 (±0.70) ^b |

n = 3 for Control and Anaerobic digestate; n = 2 for Cattle slurry.

Superscript letters indicate Tukey grouping (p < 0.05) (different letters indicate significant differences).

* Including N₂O–N, N₂, NO₃⁻–N, and NH₄⁺–N.

stimulation varied greatly among the substrates. The observed CO₂ production in organically amended soils decreased gradually during the incubation (Fig. 1k and l) and the cumulative CO₂ emission from the AD treatment were twice as high as in the Control, while CO₂ release with CS application was about six times higher than the Control (Table 3). The latter clearly indicates that CS has significantly higher labile C content than AD. Assuming that the mineralization of soil organic carbon is unaffected by the amendments (i.e. no priming effect), cumulative CO₂ losses for the entire incubation can be used to calculate the approximate fraction of the added carbon substrates which are mineralized during the incubation. The mineralization of the substrate C can then be estimated as the difference between cumulative CO₂–C evolved in amended soil and the Control. The calculated share of mineralized AD-C and CS-C was about 94 and 43%, respectively. The very high percentage of carbon mineralization in AD is surprising, as one may expect that the biogas fermentation process consumes most rapidly fermented fractions in the organic substrates, and only the most recalcitrant compounds remain (Tambone et al., 2013). However, food waste as fermentation substrate for biogas production is usually highly degradable, and may therefore lead to very low concentrations of residual undegraded organic C. Thus, the organic matter in AD was almost completely mineralized within 25 days after its application to soil. With CS application elevated CO₂ release indicated ongoing C mineralization from applied CS during the entire incubation.

Rates and cumulative N₂O fluxes in soils treated with CS and AD varied significantly. Interestingly, the addition of organic fertilizers to the soil did not induce an immediate N₂O peak, obviously because N₂O was further reduced to N₂. Maximum N₂O emission

rates were found 8, 25, and 23 days after onset of treatments in Control, AD, and CS treatment, respectively, and fluxes gradually decreased afterwards, reaching background levels about 40 days after start of the experiment. Here, cumulative N₂O emissions were highest in treatment CS (34.1 mg N₂O–N (kg soil DM)⁻¹), being more than twice as high than in AD or Control (12.6 and 14.1 mg N₂O–N (kg soil DM)⁻¹, respectively). This is in contrast to previous findings by Senbayram et al. (2009) who found similar (or even slightly higher) N₂O emissions from soil treated with AD (originating from maize digestion) compared to CS. This deviation likely originates from differences in the physicochemical properties of the applied AD, as AD originating from food waste digestion has usually a finer texture and contains less fibrous material. The higher digestibility of food wastes allows more complete mineralization of the substrates during the fermentation process (also depending on digester properties), and thus the content of inorganic N is usually higher, while the content of residual organic C is lower.

N₂O release per unit of applied N_{min} (i.e. the short-term N₂O emission factor) was significantly lower with AD (9.1%) compared to CS (24.7%), which was attributed to the lower labile C content of AD per unit N_{min} applied, resulting in lower microbial activity and thus lower denitrification (Table 3). Interpretation of these emission factors, however, requires some caution as the experimental conditions were rather artificial and intended to promote denitrification; thus, these factors cannot be transferred agricultural cropping systems, where emissions factors are usually found to be around 0.5–2% even with AD or CS application (e.g. Senbayram et al., 2014). It has been reported that the N₂O mitigation potential of AD compared to CS may depend largely on interactions

Table 5
The inputs and results of isotopic calculations: δ_{N₂O–r} – measured residual N₂O isotopic signatures; δ_{N₂O–0} – calculated (Eq. (1)) initially produced N₂O isotopic signatures; f_{N–SP} – contribution of SP-enriched end-member; f_{N–O} – contribution of O-enriched end-member. The given ranges of minimal (min) and maximal (max) values result from application of literature range of isotopic fractionation factors for N₂O reduction (η¹⁸O from –15 to –7% and η_{SP} from –7 to –3‰). The mean end-members values were used (for denitrification SP = –5‰, δ¹⁸O = 15‰; for nitrification SP = 35‰, δ¹⁸O = 45‰), see Section 3.2 for details. Mean values per treatment (±standard deviation). The f values represent the calculated cumulative contribution over the whole incubation time (f values of individual measurements are weighted for the respective N₂O fluxes).

| Treatment | δ _{N₂O–r} | | δ _{N₂O–0} | | δ _{N₂O–0} | | f _{N–O} min [%] | f _{N–SP} min [%] | f _{N–O} max [%] | f _{N–SP} max [%] |
|---------------------|-------------------------------|-------------|--------------------------------------|--------------------------------------|-------------------------------|-----------------------|--------------------------|---------------------------|--------------------------|---------------------------|
| | δ ¹⁸ O [‰] | SP [‰] | δ ¹⁸ O _{min} [‰] | δ ¹⁸ O _{max} [‰] | SP _{min} [‰] | SP _{max} [‰] | | | | |
| Control | 22.9 (±9.8) | –1.4 (±3.8) | 15.2 (±9.0) | 18.1 (±7.4) | –4.7 (±3.6) | –3.3 (±2.9) | 5.2 (±5.0) | 0.2 (±0.2) | 33.8 (±9.8) | 16.0 (±1.7) |
| Anaerobic digestate | 32.6 (±5.2) | 5.4 (±5.5) | 17.6 (±7.1) | 26.6 (±4.2) | 0.1 (±4.4) | 4.6 (±3.2) | 8.1 (±3.5) | 8.0 (±1.8) | 36.4 (±4.8) | 25.1 (±2.0) |
| Cattle slurry | 34.5 (±5.0) | 12.1 (±9.2) | 18.8 (±8.2) | 28.3 (±3.5) | 11.4 (±5.8) | 16.2 (±5.0) | 10.4 (±10.5) | 32.7 (±5.6) | 43.1 (±13.8) | 47.9 (±4.4) |

between soil type, digestion process conditions, and organic substrates used for the fermentation process, as observed effects of AD on N_2O emissions from soil were found to be inconsistent, being higher or lower compared to non-digested CS (Abubaker et al., 2013).

Cumulative N_2 release was ca. 9 and 15 times higher in treatment AD and CS, respectively, compared to Control. Although cumulative N_2 fluxes were clearly higher in CS than in AD, this difference was not significant due to high variation between the individual replicates in both treatments. In contrast to N_2O , significant N_2 fluxes occurred immediately after organic soil amendment. This highlights the importance of N_2O reduction to N_2 during the initial phase after organic fertilizer application, which is known to be a kind of temporal hotspot in terms of N_2O production and reduction processes. Maximum N_2 fluxes were clearly higher than the maximum N_2O fluxes in the organic treatments and occurred prior to the maximum N_2O peaks, while in the Control N_2O emissions occurred immediately after onset and reached higher levels than the N_2 flux. With AD, maximum N_2 fluxes were observed about ten days earlier than with CS, which was probably caused by earlier C_{org} depletion in treatment AD and thus abating N_2O reduction. In a previous study applying AD to soil with high moisture (85% water holding capacity), it has been observed that nitrate concentrations started to increase about ten days after application, while at the same time significant N_2O emissions emerged, which was attributed to decreasing N_2O reduction (Sembayram et al., 2009). Significant nitrification during the incubation phase was confirmed by the high nitrate and low ammonium contents of the soil at the end of the incubation phase (Table 4). Hence, the combined effect of accumulation of NO_3^- and simultaneous depletion of readily available C likely caused the decline in N_2O reduction in both organic treatments in the present study.

Total emissions of gaseous N compounds, i.e. N_2O and N_2 , differed significantly in all treatments and were extremely high in the organic treatments with the maximum in treatment CS. The higher N_{org} content of CS resulted in higher total N input and higher N mineralization; however, the calculated N mineralization would only explain a fraction of the observed differences between CS and AD. Supposedly, the relative high anaerobicity and the absence of significant N sinks like plants promoted high denitrification particularly in the fertilized treatments. Higher $N_2O + N_2$ release can be attributed to the labile C fraction of the organic fertilizers, promoting microbial respiration and thus, heterotrophic denitrification (e.g. Weier et al., 1993). In the present study, cumulative ($N_2O + N_2$)-N fluxes were positively correlated with respiration rates with $R^2 = 0.82$ ($p < 0.01$). Additionally, the overall $N_2O/(N_2O + N_2)$ product ratio was significantly higher in Control (0.63) compared to the treatments AD and CS, where it was relatively similar (0.15 and 0.22, respectively; Table 3). This lower $N_2O/(N_2O + N_2)$ product ratio in the organic treatments can clearly be attributed to the promoting effect of organic C input on N_2O reduction via denitrification when the soil NO_3^- content is low which was shown in previous studies (Weier et al., 1993; Sembayram et al., 2012). The similarity of the $N_2O/(N_2O + N_2)$ product ratios between the treatments AD and CS despite the significant difference in organic C input and the resulting differences in the NO_3^-/C_{ratio} in the soil was most likely caused by the high C input rate and the fertilizer application on top of the soil, leading to very low NO_3^-/C ratios in the upper soil layer and thus to NO_3^- limitation and almost complete N_2O reduction to N_2 (Sembayram et al., 2012). During the initial period of the present experiment the $N_2O/(N_2O + N_2)$ product ratio was close to zero in AD and CS treatments (Fig. 1h and i) indicating almost complete reduction of N_2O to N_2 . At later stages, however, the ratio increased in both, AD

and CS treatment, most likely for the following two reasons: i) the decreasing demand for electron acceptors in later stages of the experiment due to depletion of labile C; ii) an inhibitory effect of the increasing NO_3^- concentration in the soil (due to nitrification) on N_2O reduction (Weier et al., 1993; Sembayram et al., 2012). Here, the $N_2O/(N_2O + N_2)$ product ratio increased more rapidly in AD than in CS, in parallel CO_2 emissions decreased more rapidly in AD than in CS, indicating the key role of labile C content in the soil on the $N_2O/(N_2O + N_2)$ product ratio. However, the much higher C/N ratio of CS and thus the resulting higher C input did not significantly affect to overall $N_2O/(N_2O + N_2)$ product ratio, while it caused significantly higher $N_2O + N_2$ emissions.

3.2. Isotopomer-based N_2O source partitioning approach

The observed shifts in N_2O isotope values (Fig. 2) may be caused by variable contributions of different microbial N_2O production pathways with different source specific N_2O isotope signatures (Toyoda et al., 2005; Sutka et al., 2006, 2008) and by N_2O reduction to N_2 , leading to enrichment of heavy isotopes in residual N_2O (Bol et al., 2003; Ostrom et al., 2007; Well and Flessa, 2009a). Thus, apportioning N_2O fluxes to individual production pathways is challenging.

The N_2O source apportioning approach was based on an isotopic mass balance assuming autotrophic nitrification and denitrification as its two end-members. The calculations were based on isotope effects during N_2O production and reduction determined in previous studies (see Section 2.3). For determination of the δ_{N_2O-0} values closed system isotope dynamics were assumed. As discussed before, isotope fractionation during N_2O reduction in soils is most probably characterized by a mixture of processes following open and closed isotope dynamics as discussed previously (Decock and Six, 2013). However, open system models can only be applied when the system is in steady state, i.e. substrate concentration as well as reaction rate are constant (Fry, 2006), which is not fulfilled here. The incubations were carried out under very high soil moisture (90% WFPS) and such conditions favor the accumulation of N_2O in soil microsites prior to its reduction, which results in closed system-like conditions and thus justifies the assumption of closed system isotope dynamics. In a previous study using a similar incubation approach we observed clearly closed system-like isotope dynamics (Köster et al., 2013b). Nevertheless, we have examined the effect of using open system equations, and the calculated cumulative contribution of nitrification was always higher when compared to the presented results calculated with closed system equation and the maximum difference reached 25%.

Fig. 3 shows the range of possible variations of f_N values during the incubation time based on the adopted range of fractionation factors and end-members isotopic signatures. The lower and upper limits of the presented ranges are defined by the lowest and highest results in any of the calculated scenarios of individual incubation vessels, while the true N_2O contribution of nitrification may be expected within the overlap region of f_{N-0} and f_{N-SP} . Although in some cases our model gave a relative wide range of results, the trends of the calculated f_{N-0} and f_{N-SP} fractions were similar and the mean difference between them was 7%. However, calculations based on the SP provided clearly higher precision, i.e. the range of variations for f_{N-SP} was smaller, since the fractionation factors as well as end-member isotope signatures were much more robust for SP than for $\delta^{18}O$ (Table 5).

The assumption of one homogenous NO_3^- pool as substrate for denitrification may not be valid in the present study, as previous studies indicated the contribution of different N pools to N_2O production in soils after adding glucose/nitrate solution to the soil surface (Meijide et al., 2010; Bergstermann et al., 2011). In the

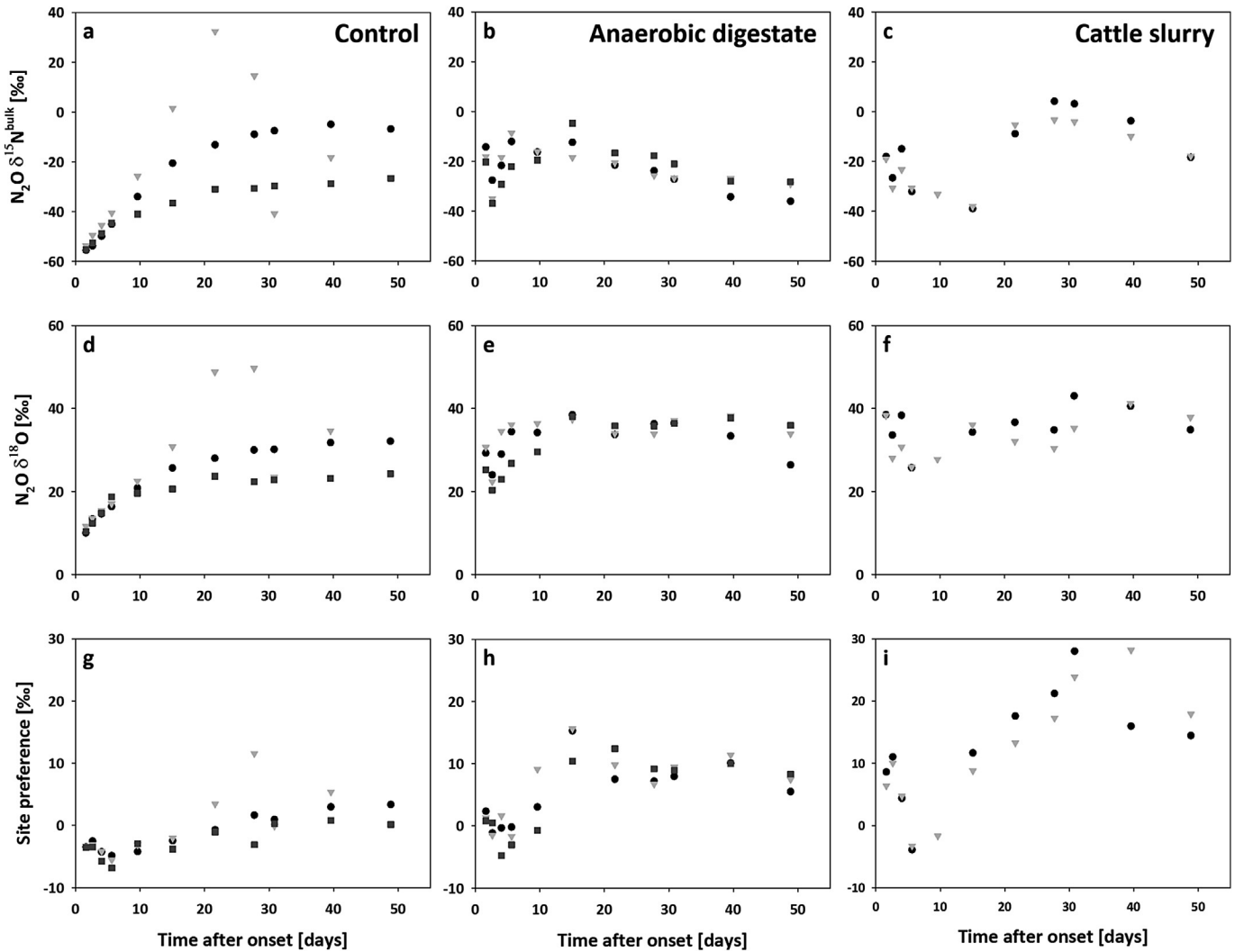


Fig. 2. $N_2O \delta^{15}N^{bulk}$ (a, b, c), $\delta^{18}O$ (d, e, f), and SP (g, h, i) during incubation period of 52 days of unamended soil (Control), or after amendment with Anaerobic digestate or Cattle slurry, respectively, at a target rate of $152 \text{ mg } NH_4^+ - N \text{ (kg soil DM)}^{-1}$, 90% WFPS, and 0.1 atm p_{O_2} . Different symbols/colors indicate individual replications. Please note that some data points overlap each other.

present study the variation in the $N_2O \delta^{15}N^{bulk}$ pattern could also be explained by two substrate pools consisting of NO_3^- mineralized from organic fertilizer on top of the soil and soil-derived NO_3^- initially present. However, the existence of more than one substrate

pool would not affect the conclusions based on $\delta^{18}O$ and SP values, because the SP is independent of the isotopic signatures of the precursors (Toyoda et al., 2002), and O is mainly exchanged with soil water and thus also largely independent of the substrate's

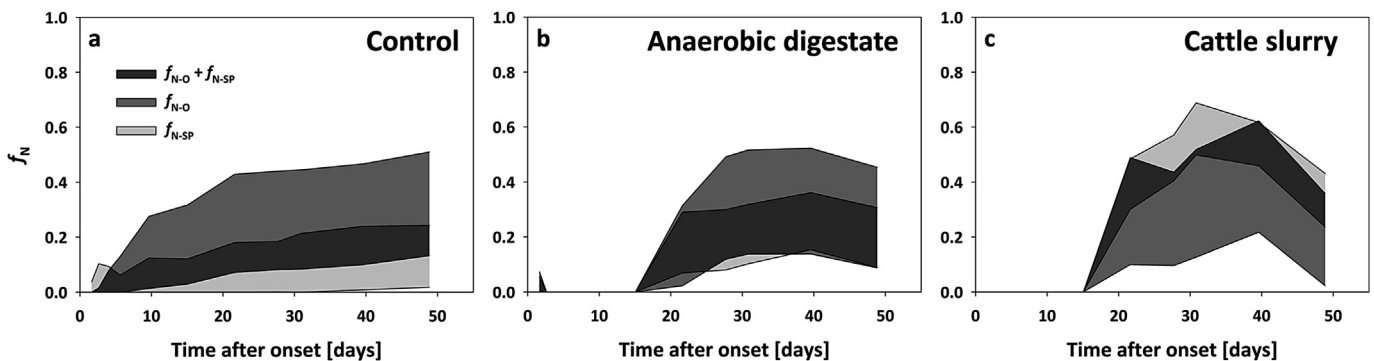


Fig. 3. N_2O contribution of nitrification, estimation based on $N_2O \delta^{18}O$ (f_{N-O}) and SP values (f_{N-SP}), during the course of the 52 day incubation of unamended soil (Control; a), or after amendment with Anaerobic digestate (b) or Cattle slurry (c), respectively, at a target rate of $152 \text{ mg } NH_4^+ - N \text{ (kg soil DM)}^{-1}$, 90% WFPS, and 0.1 atm p_{O_2} . Dark gray area fill indicates the range of agreement of f_{N-O} and f_{N-SP} in which the actual value is expected, while middle gray indicates f_{N-O} and light gray f_{N-SP} estimate ranges, which do not agree with each other.

signatures (Kool et al., 2009; Well and Flessa, 2009b; Lewicka-Szczebak et al., 2014).

Furthermore, alternative N₂O production pathways may also contribute to some extent to N₂O production. Fungal denitrification produces N₂O with high SP values around 37‰, being close to those of nitrification (Sutka et al., 2008; Rohe et al., 2014). However, in the alternative scenario comprising bacterial denitrification and fungal denitrification as major N₂O sources, a worse fit of f_{F-SP} and f_{F-O} was achieved (average deviation of 14% compared to an average deviation between f_{N-O} and f_{N-SP} of 7%), indicating that fungal denitrification had rather minor contribution to N₂O production. Nitrifier denitrification shares the same NO₂⁻ reduction pathway with heterotrophic denitrifiers and thus, the resulting SP values of produced N₂O are identical, and also the δ¹⁸O signatures were found to be relatively close to those of denitrification (Sutka et al., 2006). Thus, the N₂O production attributed to denitrification comprises those of nitrifier denitrification as well. The observed SP trends in the present study, however, show clear contribution of an N₂O source process characterized by higher SP values, i.e. nitrification.

We may underline again that the source partitioning calculations applied in this study only provide rough estimates of the pathways contributing to N₂O production and rather give information on general trends but not on precise absolute shares, since the fractionation factors associated with various pathways of N₂O production and consumption processes cannot yet be determined exactly and minor contribution of other N₂O sources cannot be excluded. Nevertheless, the presented approach taking advantage of both, N₂O SP and δ¹⁸O values in combination with measured N₂ emission, allows to narrow the uncertainty of estimates significantly compared to approaches solely based on the SP.

3.3. N₂O isotopomer trends and source processes

In Fig. 2 the N₂O isotope trends during the course of the experiment are shown. Initial substrate δ¹⁵N of soil and organic fertilizers are given in Table 1. The δ¹⁵N^{bulk} values of emitted N₂O were generally found between -56‰ and +5‰ (except for some more 'extreme' values occurring in one replicate of Control; see Fig. 2). The δ¹⁸O values of N₂O ranged from +10‰ to +50‰, and SP values were between -7‰ and +29‰. In Control, the clearest trends were observed, with all isotope values increasing during the incubation time. In contrast, in treatment AD such increase was only observed during the initial two weeks; afterwards, the isotope values remained relatively constant or even decreased (δ¹⁵N^{bulk}). In CS a short decrease in all isotope values was observed in the initial phase (about five days), followed by an increase until day 30, and another slight decrease towards the end of the incubation phase.

The relative N₂O contribution of nitrification (f_N) and denitrification (f_D) was estimated as discussed above (3.2). In general, lower mean f_N (f_{N-SP} and f_{N-O}) values (i.e. relative contribution of nitrification) were found with Control soils, increasing from 0 to roughly 25% (i.e. f_D decreased from 100 to about 75%) than in the fertilized treatments, where the mean f_N values were lower for treatment AD (increasing from 0 to around 35%) than for treatment CS (increasing from -0 to around 50% with short-term maximum f_N up to 67%). Similarly, when comparing the mean cumulated f_N values (Table 5), they are lowest in the Control and highest with CS. It may be speculated that the increase in nitrification rates in the Control treatment was caused by increasing mineralization of N_{org} as CO₂ production increased as well, which led to higher ammonium availability and thus higher nitrification rates. In the fertilized treatments the similar trend, i.e. increasing contribution from nitrification in the course of the experiment, was probably caused by increasing O₂ availability due to the decreasing respiration rates. This identification of distinct phases with predominance of

individual N₂O source processes may help developing mitigation option, e.g. tackling nitrification peaks with nitrification inhibitors or possibly even promoting denitrification to further reduce N₂O to N₂ under conditions where options for reducing denitrification are not successful. The high amounts of N₂O produced by nitrification, though mostly being lower than N₂O release from denitrification, are remarkable as the experimental conditions with relatively high soil moisture and reduced O₂ availability are typically expected to predominantly favor N₂O production via heterotrophic denitrification. Results from earlier studies on N₂O emissions from organically amended soils under comparable incubation conditions suggested that most N₂O rather derived from denitrification, while there was only minor contribution of nitrification, especially during phases with high N₂O fluxes (Senbayram et al., 2009; Köster et al., 2011). Usually, in fertilized soils, N₂O production via nitrification is relatively low; however, Khalil et al. (2004) showed that under reduced oxygen availability the N₂O production via nitrification may increase by a factor of ten compared to atmospheric O₂ concentrations, reaching up to 1.5% of the nitrified N, though their labeling approach did not allow differentiation between hydroxylamine oxidation and nitrifier denitrification. When the soil pH is below 5 as in the present study, N₂O production by nitrification might even be higher (Mørkved et al., 2007).

3.4. Conclusions

In the present soil incubation study we demonstrated that following organic fertilizer application to soil under high moisture conditions, N₂ and N₂O fluxes can lead to extremely high losses of fertilizer N. During the initial phase after organic soil amendment the importance of N₂O reduction to N₂ was clearly shown, while significant N₂O fluxes appeared after a couple of days.

A source apportioning approach based on N₂O isotopomer signatures of emitted N₂O was used to narrow down its major source processes. This approach was based on the N₂O δ¹⁸O as well as the SP values, making the source estimations more robust compared to the sole use of N₂O SP values.

Hereby, denitrification was found to be the main source of emitted N₂O in untreated soil. In soils organically treated with anaerobic digestate or with cattle slurry, absolute denitrification rates were much higher compared to Control; but nevertheless, relative nitrification rates gained high importance at later stages of the incubation phase, peaking temporarily up to 67% of the N₂O production and contributing up to about 40% of the total N₂O release. The identification of the N₂O source processes is limited to laboratory studies so far, but information and better understanding about the dominating N₂O source pathways and their temporal dynamics is important for developing N₂O mitigation strategies, as this could facilitate countering the dominating N₂O source pathways with appropriate management options.

Acknowledgments

Jan Reent Köster thanks the German Federal Environmental Foundation (DBU) for a PhD scholarship. Rothamsted Research receives strategic funding by the Biotechnology and Biological Sciences Research Council (BBSRC), UK. This project was done under the grant number BB/K001051/1. The authors thank Mark Butler, Andrew Bristow, Liz Dixon, Neil Donovan, Trish Butler (all RRes), and Martina Heuer (TI) for their laboratory support. Dave Chadwick and David Hatch (both formerly RRes) contributed with ideas and useful discussions. Jamie Gascoigne (Greenfinch Ltd., Milton Ernest, Bedfordshire, UK), Neil Pollard, and Jake Prior (both Andigestion Ltd., Holsworthy, Devon, UK) provided cattle slurry and anaerobic digestate.

References

- Abubaker, J., Odlare, M., Pell, M., 2013. Nitrous oxide production from soils amended with biogas residues and cattle slurry. *Journal of Environmental Quality* 42, 1046–1058.
- Baggs, E.M., 2008. A review of stable isotope techniques for N₂O source partitioning in soils: recent progress, remaining challenges and future considerations. *Rapid Communications in Mass Spectrometry* 22, 1664–1672.
- Bergstermann, A., Cárdenas, L., Bol, R., Gilliam, L., Goulding, K., Meijide, A., Scholefield, D., Vallejo, A., Well, R., 2011. Effect of antecedent soil moisture conditions on emissions and isotopologue distribution of N₂O during denitrification. *Soil Biology and Biochemistry* 43, 240–250.
- Bol, R., Toyoda, S., Yamulki, S., Hawkins, J.M.B., Cárdenas, L.M., Yoshida, N., 2003. Dual isotope and isotopomer ratios of N₂O emitted from a temperate grassland soil after fertiliser application. *Rapid Communications in Mass Spectrometry* 17, 2550–2556.
- Bowen, G.J., Winter, D.A., Spero, H.J., Zierenberg, R.A., Reeder, M.D., Cerling, T.E., Ehleringer, J.R., 2005. Stable hydrogen and oxygen isotope ratios of bottled waters of the world. *Rapid Communications in Mass Spectrometry* 19, 3442–3450.
- Brand, W.A., 1995. PRECON: a fully automated interface for the pre-GC concentration of trace gases in air for isotopic analysis. *Isotopes in Environmental and Health Studies* 31, 277–284.
- Cárdenas, L.M., Hawkins, J.M.B., Chadwick, D., Scholefield, D., 2003. Biogenic gas emissions from soils measured using a new automated laboratory incubation system. *Soil Biology and Biochemistry* 35, 867–870.
- Davidson, E.A., 2009. The contribution of manure and fertilizer nitrogen to atmospheric nitrous oxide since 1860. *Nature Geoscience* 2, 659–662.
- Decock, C., Six, J., 2013. How reliable is the intramolecular distribution of ¹⁵N in N₂O to source partition N₂O emitted from soil? *Soil Biology and Biochemistry* 65, 114–127.
- Fry, B., 2006. *Stable Isotope Ecology*. Springer Science+Business Media, LLC, New York, NY, USA.
- Galloway, J.N., Dentener, F.J., Capone, D.G., Boyer, E.W., Howarth, R.W., Seitzinger, S.P., Asner, G.P., Cleveland, C.C., Green, P.A., Holland, E.A., Karl, D.M., Michaels, A.F., Porter, J.H., Townsend, A.R., Vorosmarty, C.J., 2004. Nitrogen cycles: past, present, and future. *Biogeochemistry* 70, 153–226.
- Harrod, T.R., Hogan, D.V., 2008. *The Soils of North Wyke and Rowden. Revised Edition of Original Report by T.R. Harrod, Soil Survey of England and Wales (1981)*. URL: <http://www.rothamsted.ac.uk/sites/default/files/SoilsNWRowden.pdf> (accessed 20.05.14).
- Hasler, M., 2012. SimComp: Simultaneous Comparisons for Multiple Endpoints. R Package Version 1.7.0. URL: <http://CRAN.R-project.org/package=SimComp>.
- Heil, J., Wolf, B., Brüggemann, N., Emmenegger, L., Tuzson, B., Vereecken, H., Mohn, J., 2014. Site-specific ¹⁵N isotopic signatures of abiotically produced N₂O. *Geochimica et Cosmochimica Acta* 139, 72–82.
- Herrmann, A., Rath, J., 2012. Biogas production from maize: current state, challenges, and prospects. 1. methane yield potential. *BioEnergy Research* 5, 1027–1042.
- Jinuntuya-Nortman, M., Sutka, R.L., Ostrom, P.H., Gandhi, H., Ostrom, N.E., 2008. Isotopologue fractionation during microbial reduction of N₂O within soil mesocosms as a function of water-filled pore space. *Soil Biology and Biochemistry* 40, 2273–2280.
- Khalil, K., Mary, B., Renault, P., 2004. Nitrous oxide production by nitrification and denitrification in soil aggregates as affected by O₂ concentration. *Soil Biology and Biochemistry* 36, 687–699.
- Kool, D.M., Wrage, N., Oenema, O., Harris, D., Van Groenigen, J.W., 2009. The ¹⁸O signature of biogenic nitrous oxide is determined by O exchange with water. *Rapid Communications in Mass Spectrometry* 23, 104–108.
- Köster, J.R., Cárdenas, L., Senbayram, M., Bol, R., Well, R., Butler, M., Mühling, K.H., Dittert, K., 2011. Rapid shift from denitrification to nitrification in soil after biogas residue application as indicated by nitrous oxide isotopomers. *Soil Biology and Biochemistry* 43, 1671–1677.
- Köster, J.R., Well, R., Tuzson, B., Bol, R., Dittert, K., Gieseemann, A., Emmenegger, L., Manninen, A., Cárdenas, L., Mohn, J., 2013a. Novel laser spectroscopic technique for continuous analysis of N₂O isotopomers – application and intercomparison with isotope ratio mass spectrometry. *Rapid Communications in Mass Spectrometry* 27, 216–222.
- Köster, J.R., Well, R., Dittert, K., Gieseemann, A., Lewicka-Szczepak, D., Mühling, K.H., Herrmann, A., Lammel, J., Senbayram, M., 2013b. Soil denitrification potential and its influence on N₂O reduction and N₂O isotopomer ratios. *Rapid Communications in Mass Spectrometry* 27, 2363–2373.
- Lewicka-Szczepak, D., Well, R., Köster, J.R., Fuß, R., Senbayram, M., Dittert, K., Flessa, H., 2014. Experimental determinations of isotopic fractionation factors associated with N₂O production and reduction during denitrification. *Geochimica et Cosmochimica Acta* 134, 55–73.
- Mariotti, A., Germon, J.C., Hubert, P., Kaiser, P., Letolle, R., Tardieux, A., Tardieux, P., 1981. Experimental determination of nitrogen kinetic isotope fractionation: some principles; illustration for the denitrification and nitrification processes. *Plant and Soil* 62, 413–430.
- Meijide, A., Cárdenas, L.M., Bol, R., Bergstermann, A., Goulding, K., Well, R., Vallejo, A., Scholefield, D., 2010. Dual isotope and isotopomer measurements for the understanding of N₂O production and consumption during denitrification in an arable soil. *European Journal of Soil Science* 61, 364–374.
- Menyailo, O.V., Hungate, B.A., 2006. Stable isotope discrimination during soil denitrification: production and consumption of nitrous oxide. *Global Biogeochemical Cycles* 20. <http://dx.doi.org/10.1029/2005gb002527>.
- Mørkved, P.T., Dörsch, P., Bakken, L.R., 2007. The N₂O product ratio of nitrification and its dependence on long-term changes in soil pH. *Soil Biology and Biochemistry* 39, 2048–2057.
- Mosier, A., Kroeze, C., Nevison, C., Oenema, O., Seitzinger, S., van Cleemput, O., 1998. Closing the global N₂O budget: nitrous oxide emissions through the agricultural nitrogen cycle. *Nutrient Cycling in Agroecosystems* 52, 225–248.
- Ostrom, N.E., Pitt, A., Sutka, R., Ostrom, P.H., Grandy, A.S., Huizinga, K.M., Robertson, G.P., 2007. Isotopologue effects during N₂O reduction in soils and in pure cultures of denitrifiers. *Journal of Geophysical Research-Biogeosciences* 112. <http://dx.doi.org/10.1029/2006JG00287>.
- Ravishankara, A.R., Daniel, J.S., Portmann, R.W., 2009. Nitrous oxide (N₂O): the dominant ozone-depleting substance emitted in the 21st century. *Science* 326, 123–125.
- Robertson, G.P., Groffman, P.M., 2007. Nitrogen transformations. In: Paul, E.A. (Ed.), *Soil Microbiology, Biochemistry, and Ecology*. Springer, New York, NY, USA, pp. 341–364.
- Rohe, L., Anderson, T.-H., Braker, G., Flessa, H., Gieseemann, A., Lewicka-Szczepak, D., Wrage-Mönnig, N., Well, R., 2014. Dual isotope and isotopomer signatures of nitrous oxide from fungal denitrification – a pure culture study. *Rapid Communications in Mass Spectrometry* 28, 1893–1903.
- Senbayram, M., Chen, R.R., Mühling, K.H., Dittert, K., 2009. Contribution of nitrification and denitrification to nitrous oxide emissions from soils after application of biogas waste and other fertilizers. *Rapid Communications in Mass Spectrometry* 23, 2489–2498.
- Senbayram, M., Chen, R., Budai, A., Bakken, L., Dittert, K., 2012. N₂O emission and the N₂O(N₂O + N₂) product ratio of denitrification as controlled by available carbon substrates and nitrate concentrations. *Agriculture Ecosystems & Environment* 147, 4–12.
- Senbayram, M., Chen, R., Wienforth, B., Herrmann, A., Kage, H., Mühling, K.H., Dittert, K., 2014. Emission of N₂O from biogas crop production systems in Northern Germany. *BioEnergy Research* 7, 1223–1236.
- Snider, D.M., Venkiteswaran, J.J., Schiff, S.L., Spoelstra, J., 2013. A new mechanistic model of δ¹⁸O-N₂O formation by denitrification. *Geochimica et Cosmochimica Acta* 112, 102–115.
- Stocker, T.F., Qin, D., Plattner, G.-K., Tignor, M., Allen, S.K., Boschung, J., Nauels, A., Xia, Y., Bex, V., Midgley, P.M., 2013. *Climate Change 2013: the Physical Science Basis. Contribution of Working Group I to the Fifth Assessment Report of the Intergovernmental Panel on Climate Change*. Cambridge University Press, Cambridge, United Kingdom and New York, NY, USA.
- Sutka, R.L., Ostrom, N.E., Ostrom, P.H., Gandhi, H., Breznak, J.A., 2003. Nitrogen isotopomer site preference of N₂O produced by *Nitrosomonas europaea* and *Methylococcus capsulatus* bath. *Rapid Communications in Mass Spectrometry* 17, 738–745.
- Sutka, R.L., Ostrom, N.E., Ostrom, P.H., Gandhi, H., Breznak, J.A., 2004. Nitrogen isotopomer site preference of N₂O produced by *Nitrosomonas europaea* and *Methylococcus capsulatus* bath (vol. 18, pg 1411, 2004). *Rapid Communications in Mass Spectrometry* 18, 1411–1412.
- Sutka, R.L., Ostrom, N.E., Ostrom, P.H., Breznak, J.A., Gandhi, H., Pitt, A.J., Li, F., 2006. Distinguishing nitrous oxide production from nitrification and denitrification on the basis of isotopomer abundances. *Applied and Environmental Microbiology* 72, 638–644.
- Sutka, R.L., Adams, G.C., Ostrom, N.E., Ostrom, P.H., 2008. Isotopologue fractionation during N₂O production by fungal denitrification. *Rapid Communications in Mass Spectrometry* 22, 3989–3996.
- Tambone, F., Adani, F., Gigliotti, G., Volpe, D., Fabbri, C., Provenzano, M.R., 2013. Organic matter characterization during the anaerobic digestion of different biomasses by means of CPMAS ¹³C NMR spectroscopy. *Biomass and Bioenergy* 48, 111–120.
- Toyoda, S., Yoshida, N., 1999. Determination of nitrogen isotopomers of nitrous oxide on a modified isotope ratio mass spectrometer. *Analytical Chemistry* 71, 4711–4718.
- Toyoda, S., Yoshida, N., Miwa, T., Matsui, Y., Yamagishi, H., Tsunogai, U., Nojiri, Y., Tsurushima, N., 2002. Production mechanism and global budget of N₂O inferred from its isotopomers in the western North Pacific. *Geophysical Research Letters* 29, 4.
- Toyoda, S., Mutoke, H., Yamagishi, H., Yoshida, N., Tanji, Y., 2005. Fractionation of N₂O isotopomers during production by denitrifier. *Soil Biology and Biochemistry* 37, 1535–1545.
- Toyoda, S., Yano, M., Nishimura, S., Akiyama, H., Hayakawa, A., Koba, K., Sudo, S., Yagi, K., Makabe, A., Tobar, Y., Ogawa, N.O., Ohkouchi, N., Yamada, K., Yoshida, N., 2011. Characterization and production and consumption processes of N₂O emitted from temperate agricultural soils determined via isotopomer ratio analysis. *Global Biogeochemical Cycles* 25. <http://dx.doi.org/10.1029/2009gb003769>.
- Weier, K.L., Doran, J.W., Power, J.F., Walters, D.T., 1993. Denitrification and the dinitrogen/nitrous oxide ratio as affected by soil water, available carbon, and nitrate. *Soil Science Society of America Journal* 57, 66–72.
- Well, R., Flessa, H., 2009a. Isotopologue enrichment factors of N₂O reduction in soils. *Rapid Communications in Mass Spectrometry* 23, 2996–3002.
- Well, R., Flessa, H., 2009b. Isotopologue signatures of N₂O produced by denitrification in soils. *Journal of Geophysical Research-Biogeosciences* 114. <http://dx.doi.org/10.1029/2008JG000804>.
- Yoshida, N., Toyoda, S., 2000. Constraining the atmospheric N₂O budget from intramolecular site preference in N₂O isotopomers. *Nature* 405, 330–334.

Chapter 5

Soil denitrification potential and its influence on N₂O reduction and N₂O isotopomer ratios

Jan Reent Köster, Reinhard Well, Klaus Dittert, Anette Giesemann,
Dominika Lewicka-Szczebak, Karl-Hermann Mühling, Antje Herrmann,
Joachim Lammel, and Mehmet Senbayram

Rapid Communications in Mass Spectrometry 27 (2013) 2363 – 2373

DOI: 10.1002/rcm.6699

Rapid Commun. Mass Spectrom. 2013, 27, 2363–2373
(wileyonlinelibrary.com) DOI: 10.1002/rcm.6699

Soil denitrification potential and its influence on N₂O reduction and N₂O isotopomer ratios

Jan Reent Köster¹, Reinhard Well², Klaus Dittert³, Anette Giesemann²,
Dominika Lewicka-Szczebak², Karl-Hermann Mühling¹, Antje Herrmann⁴, Joachim Lammel⁵
and Mehmet Senbayram^{5,6*}

¹Institute of Plant Nutrition and Soil Science, Kiel University, Hermann-Rodewald-Str. 2, D-24118 Kiel, Germany

²Thünen Institute of Climate-Smart Agriculture, Federal Research Institute for Rural Areas, Forestry and Fisheries, Bundesallee 50, D-38116 Braunschweig, Germany

³Department of Crop Science, Section of Plant Nutrition and Crop Physiology, University of Goettingen, Carl-Sprengel-Weg 1, D-37075 Goettingen, Germany

⁴Institute of Crop Science and Plant Breeding, Kiel University, Hermann-Rodewald-Str. 9, D-24118 Kiel, Germany

⁵Institute of Plant Nutrition and Environmental Science, Research Center Hanninghof, Yara Int. ASA, Hanninghof 35, D-48249 Duermen, Germany

⁶Institute of Applied Plant Nutrition, University of Goettingen, Carl-Sprengel-Weg 1, D-37075 Goettingen, Germany

RATIONALE: N₂O isotopomer ratios may provide a useful tool for studying N₂O source processes in soils and may also help estimating N₂O reduction to N₂. However, remaining uncertainties about different processes and their characteristic isotope effects still hamper its application. We conducted two laboratory incubation experiments (i) to compare the denitrification potential and N₂O/(N₂O+N₂) product ratio of denitrification of various soil types from Northern Germany, and (ii) to investigate the effect of N₂O reduction on the intramolecular ¹⁵N distribution of emitted N₂O.

METHODS: Three contrasting soils (clay, loamy, and sandy soil) were amended with nitrate solution and incubated under N₂-free He atmosphere in a fully automated incubation system over 9 or 28 days in two experiments. N₂O, N₂, and CO₂ release was quantified by online gas chromatography. In addition, the N₂O isotopomer ratios were determined by isotope-ratio mass spectrometry (IRMS) and the net enrichment factors of the ¹⁵N site preference (SP) of the N₂O-to-N₂ reduction step (η_{SP}) were estimated using a Rayleigh model.

RESULTS: The total denitrification rate was highest in clay soil and lowest in sandy soil. Surprisingly, the N₂O/(N₂O+N₂) product ratio in clay and loam soil was identical; however, it was significantly lower in sandy soil. The IRMS measurements revealed highest N₂O SP values in clay soil and lowest SP values in sandy soil. The η_{SP} values of N₂O reduction were between –8.2 and –6.1 ‰, and a significant relationship between $\delta^{18}O$ and SP values was found.

CONCLUSIONS: Both experiments showed that the N₂O/(N₂O+N₂) product ratio of denitrification is not solely controlled by the available carbon content of the soil or by the denitrification rate. Differences in N₂O SP values could not be explained by variations in N₂O reduction between soils, but rather originate from other processes involved in denitrification. The linear $\delta^{18}O$ vs SP relationship may be indicative for N₂O reduction; however, it deviates significantly from the findings of previous studies. Copyright © 2013 John Wiley & Sons, Ltd.

Nitrous oxide (N₂O) is one of the most important greenhouse gases (GHG) and ozone depleting substances released by agriculture.^[1,2] High nitrogen (N) fertilizer inputs in intensified cropping systems lead to high N₂O release into the atmosphere from agricultural soils as the main source.^[3,4] In these soils N₂O is mainly produced by biological nitrification and denitrification processes, especially under oxygen (O₂)-limited conditions.^[5] During denitrification, nitrate (NO₃) is

used as an alternative electron acceptor to O₂ and gradually reduced to molecular nitrogen (N₂) via the intermediate products NO₂, NO, and N₂O, of which gaseous NO and N₂O can escape into the atmosphere.^[6] The net N₂O release from the soil is the balance of N₂O production and consumption, i.e. reduction to N₂, by denitrification processes in the soil. The N₂O/(N₂O+N₂) product ratio may be used as an adequate measure containing information about both, N₂O production and reduction rates.

The determination of denitrification rates is challenging because of the difficulties of direct N₂ measurements. Most techniques applied are affected by shortcomings and, thus, only a limited number of studies under laboratory conditions has involved direct N₂ measurements.^[7] The N₂O production and consumption rates via denitrification are controlled by

* Correspondence to: M. Senbayram, Institute of Applied Plant Nutrition, University of Goettingen, Carl-Sprengel-Weg 1, D-37075 Goettingen, Germany.
E-mail: mehmetzenbayram6@yahoo.co.uk

different factors, e.g. availability of substrates (organic carbon (C) as electron donor and nitrogen oxides or O₂ as electron acceptors), soil moisture, pH, temperature, and microbial community structure.^[8–11] At high concentrations NO₃⁻ inhibits N₂O reduction to N₂,^[8] and thus raises the N₂O/(N₂O+N₂) product ratio.^[12] It has also been reported that N₂O reduction and denitrification are reduced when the soil pH is low.^[13,14] In a recent study on South Asian agricultural soils it has been shown that long-term intensification of agricultural production with high N fertilizer input leads to soil acidification, resulting in a higher N₂O/(N₂O+N₂) denitrification product ratio, and therefore higher N₂O emissions may occur.^[15]

Different stable isotope approaches are routinely used to study the global N cycle but N₂O partitioning to source processes remains challenging.^[16] During the last decade the intramolecular ¹⁵N distribution in the linear asymmetric N₂O molecule, i.e. the ¹⁵N site preference (SP), moved into focus as a potential tool to apportion N₂O to its source processes.^[17–19] The SP indicates the difference between the δ¹⁵N^α (= ¹⁵N/¹⁴N ratio of the central N atom in the N₂O molecule) and the δ¹⁵N^β value (= ¹⁵N/¹⁴N ratio of the peripheral N atom)^[20] and is considered to be independent of the isotopic signature of the N₂O precursor species.^[21] In pure culture studies, N₂O from nitrification and bacterial denitrification has been shown to express clearly distinct ranges in SP.^[19,22] However, deploying N₂O SP values for N₂O source apportioning is still complicated by overlapping SP signatures with fungal denitrification.^[18] Furthermore, only little knowledge exists about novel N₂O production pathways such as archaeal nitrification and denitrification, anammox, and DNRA and their related isotopic signals.^[23] Moreover, it has not yet been proven that findings obtained from a limited number of isolated microbial strains in pure culture can be applied on observations under soil conditions with complex microbial communities without further adjustments. In recent studies, it has been shown that microbial reduction of N₂O to N₂ causes ¹⁵N enrichment at the α-position relative to the β-position of residual N₂O, i.e. to raise the SP.^[24–26]

The use of isotopomer ratios for N₂O source apportioning requires much better understanding of isotope effects during N₂O reduction, alongside the isotope signals of N₂O production via different pathways. Therefore, we set up two laboratory incubation experiments with three typical but contrasting soils from northern Germany with the objectives (i) to compare the

denitrification potential and N₂O/(N₂O+N₂) product ratio of denitrification of these soils, and (ii) to investigate the effect of N₂O reduction on the intramolecular ¹⁵N distribution of the emitted N₂O.

EXPERIMENTAL

Soil sampling and site description

Samples from three diverging soils were collected in autumn 2011 from the upper 15 cm soil horizon of unfertilized plots at three experimental field sites in the federal state of Schleswig-Holstein (Northern Germany). The basic soil properties are listed in Table 1. A sandy loam, classified as Stagnic Luvisol, was sampled at Hohenschulen experimental farm of Kiel University where the mean annual precipitation is 778 mm and the average temperature is 8.9°C. At Karkendamm experimental farm a sandy soil, classified as Gleyic Podzol, was collected. The annual precipitation in this region is 868 mm and the average temperature is 9.0°C. The third soil, a heavy silt-clayey soil containing ca 40% clay and 55% silt, was classified as Fluvimollic Gleysol. It was collected at an experimental site in the coastal marsh region at the west coast of Schleswig-Holstein in northern Germany, with 855 mm annual precipitation and 8.2°C average temperature. All soil samples were carefully air dried to allow sieving with a 4 mm mesh sieve, but complete drying out was avoided to minimize mineralization after rewetting. Several days prior to the incubation experiments the soil was rewetted to ca 40–50% water holding capacity (WHC). After the incubation, soil mineral nitrogen was extracted with 0.01 M CaCl₂ solution (1:4 w/v) and the NO₃⁻ and NH₄⁺ concentrations were determined colorimetrically by segmented flow analysis. The δ¹⁵N and δ¹⁸O values of the applied and residual nitrate in the soil solution were determined using the denitrifier method.^[27,28]

Automated soil incubation experiments

Two soil incubation experiments were carried out in a fully automated continuous-flow incubation system at Hanninghof Research Station in Duermen, Germany. In the first experiment (Experiment 1), 1.5 kg fresh loam soil (Hohenschulen soil) or clay soil (Marsh soil) was repacked into each incubation vessel, while in the second experiment (Experiment 2) 1.6 kg of the

Table 1. Soil properties (± standard deviation)

| Soil properties | Sampling site | | |
|--|-------------------------|--------------------------|---------------------|
| | Karkendamm (sandy soil) | Hohenschulen (loam soil) | Marsch (clay soil) |
| Soil type | Gleyic Podzol | Stagnic Luvisol | Fluvimollic Gleysol |
| pH | 4.96 | 6.92 | 7.12 |
| Total N [%] | 0.104 (±0.006) | 0.153 (±0.018) | 0.233 (±0.0003) |
| Total C [%] | 1.49 (±0.044) | 1.5 (±0.06) | 2.32 (±0.006) |
| C/N | 14.39 (±0.395) | 9.85 (±0.791) | 9.96 (±0.011) |
| NH ₄ ⁺ -N [mg kg ⁻¹ dry soil] | 0.56 (±0.053) | 0.55 (±0.069) | 0.63 (±0.276) |
| NO ₃ ⁻ -N [mg kg ⁻¹ dry soil] | 7.90 (±0.077) | 14.21 (±0.442) | 33.04 (±0.099) |

loam soil and the sandy soil (Karkendamm soil) was used. The cylindrical incubation vessels consisted of acrylic glass (Röhm (Schweiz) AG, Brüttisellen, Switzerland) with an inner diameter of 140 mm, 10 mm wall thickness and 200 mm height. Pre-wetted soils (loam soil, sandy soil, and clay soil) were treated with 0 or 30 (Experiment 1) and 15 mM KNO₃ solution (Experiment 2) prior to the incubation. Each incubation vessel was equipped with a porous ceramic plate at the bottom which allowed adjustment of the soil moisture. Each repacked soil core was flooded with 1200 mL nitrate solution and drained to ca 65% WHC by applying a vacuum to the ceramic plate. Flooding and draining were repeated twice in order to reach homogeneity in nitrate concentration in the soil solution and water content and thus to establish homogenous conditions for denitrifiers. After soil moisture adjustment, the final NO₃⁻ concentration in the soils was 64.9 ± 1.29 and 109.8 ± 1.23 mg NO₃⁻-N kg⁻¹ soil DM in loamy and clay soil, respectively (Experiment 1), and 37.2 ± 1.18 and 15.6 ± 0.24 mg NO₃⁻-N kg⁻¹ soil DM in loamy and sandy soil, respectively (Experiment 2). The incubation vessels were then sealed and the atmospheric air in the vessels was replaced by pure He (≥99.999% He; AIR LIQUIDE Deutschland GmbH, Düsseldorf, Germany) by applying vacuum and filling with He in several cycles. Subsequently, the vessel headspace was continuously flushed with He at a flow rate of ca 20–22 mL min⁻¹. In Experiment 1 the soil was incubated under anoxic conditions (pure He) for 9 days. In Experiment 2 the soil was incubated for 21 days under anoxic conditions followed by 7 days under oxic conditions (20% O₂, 80% He).

For online trace gas concentration analysis of N₂O, N₂, and CO₂, a gas sample from each vessel outlet was directed to a gas chromatograph (450-GC, Varian B.V., Middelburg, The Netherlands) sequentially via two multi-positional valves (12 and 16 ports) with electric actuator (Flow-through (SF) selectors, VICI Valco, Waterbury, TX, USA) controlled by Trilution software (Gilson Inc., Middleton, WI, USA) and an interface module (508 interface module, Gilson Inc.). The gas sample was then analyzed by the gas chromatograph, deploying a thermal conductivity detector (TCD) for N₂, O₂, and CO₂, and an electron capture detector (ECD) for N₂O quantification.

Mass spectrometry

At regular intervals, gas samples were taken from each incubation vessel by attaching 120 mL serum bottles (20 mm crimp neck) to the outlets in flow-through mode for several hours as described previously.^[29] These gas samples were analyzed by IRMS for N₂O δ¹⁵N^α, δ¹⁵N^β, and δ¹⁸O isotope ratio values. In brief, the N₂O isotopomer signatures were determined by analyzing *m/z* 44, 45, and 45 of intact N₂O⁺ ions as well as *m/z* 30 and 31 of NO⁺ fragment ions using a Delta V isotope ratio mass spectrometer (Thermo Scientific, Bremen, Germany), and the δ¹⁵N^α, δ¹⁵N^β, and δ¹⁸O values were calculated according to Toyoda and Yoshida.^[20] All isotope ratio values are expressed as ‰ deviation from the ¹⁵N/¹⁴N and ¹⁸O/¹⁶O ratios of the reference materials (i.e. atmospheric N₂ and Vienna Standard Mean Ocean Water (VSMOW)). The δ¹⁵N-N₂O value was corrected for ¹⁷O according to the method described by Brand.^[30]

Statistical data analysis

Statistical data analysis was carried out using R (version 2.15.1; The R Foundation for Statistical Computing; Vienna, Austria). As the replication numbers were unbalanced in some cases, a Tukey test (Tukey's range test; α = 0.05) was carried out using the "SimTestDiff" procedure from the *SimComp* package by Hasler^[31] which is capable of handling unbalanced data sets. Net isotope effects (NIE; η)^[24] for SP and δ¹⁸O values during N₂O reduction were estimated by fitting the logarithmic Rayleigh equation^[32] to the measured data using the software package SigmaPlot/SigmaStat (version 11; Systat Software Inc., San José, CA, USA).

RESULTS AND DISCUSSION

Trace gas fluxes and the N₂O/(N₂O+N₂) product ratio

In Experiment 1, fluxes and cumulative N₂O emissions in non-fertilized control soils were very low and not significantly different for the two soil types (Table 2). Here, cumulative fluxes of N₂O over 9 days were less than 0.3 mg kg⁻¹ dry soil and almost all the N₂O was released during the first day after the onset of the experiment; afterwards, fluxes of N₂O were approximating zero. As expected, with the addition of KNO₃ to both soils, N₂O emission increased significantly, and the time course of this stimulation was almost identical in loam and clay soil (Fig. 1(a)). In soils treated with KNO₃, maximum N₂O fluxes were found within the first 24 h of the incubation period. Afterwards, N₂O release from both soil types decreased exponentially. Overall, the cumulative emissions of N₂O-N of KNO₃-treated clay soil (4.4 mg kg⁻¹ dry soil) were significantly higher than those of the loamy soil (3.6 mg kg⁻¹ dry soil).

Significant N₂ fluxes started 12 h after the onset of the treatments in both soils (Fig. 1(b)). N₂ emissions in non-fertilized control soils sharply decreased to levels close to zero 3 days after onset of the treatments which was probably due to complete depletion of NO₃⁻ in the soil. The N₂ emission rate clearly declined more slowly than the rapid decrease in the N₂O emission rate in non-fertilized control soils. The latter indicates that 24 h after the onset of the treatments almost all the N₂O produced during denitrification was further reduced to N₂ due to the lack of electron acceptors. In situations when soil microorganisms experience a shortage of nitrate and nitrite, the relative N₂O reduction rate increases and approaches the N₂O production rate.^[8] In contrast to the control soils, the N₂ emission rate in the KNO₃-treated soils was almost constant over the whole experimental period, but higher in the clay soil.

Similar to the cumulative N₂ and N₂O emissions, cumulative CO₂ production was also higher in clay soil than in loamy soil (Fig. 1(c) and Table 2). This clearly indicates a higher soil respiration rate resulting in higher denitrification rates (i.e. N₂O+N₂ production; Fig. 1(d)) in the clay soil, which we mainly attributed to its higher organic carbon content. The N₂O/(N₂O+N₂) product ratio (Fig. 1(e)) of denitrification showed very high variation, ranging between 0 and 0.4 within all treatments. The lowest N₂O/(N₂O+N₂) product ratios were observed in non-fertilized soils; these ratios were close to zero and significantly lower than in KNO₃-treated soils. Here, it was highest immediately after the onset of the treatments and decreased gradually from ca 0.4 to ca 0.1 during the experiment,

Table 2. Cumulative emissions of N₂O-N, N₂, and CO₂-C during soil incubation (± standard deviation)

| Experiment | Soil (treatment) | N ₂ O-N [mg kg ⁻¹ soil DM] | N ₂ -N [mg kg ⁻¹ soil DM] | (N ₂ O+N ₂)-N [mg kg ⁻¹ soil DM] | CO ₂ -C [mg kg ⁻¹ soil DM] | N ₂ O/(N ₂ O+N ₂) |
|---------------------------|--------------------------|---|--|---|---|---|
| Experiment 1 (9 days) | Loam (control) | 0.012 (± 0.003) ^a | 3.69 (± 1.784) ^a | 3.702 (± 1.778) ^a | 20.201 (± 1.242) ^a | 0.005 (± 0.005) ^a |
| | Clay (control) | 0.296 (± 0.221) ^a | 7.468 (± 0.926) ^a | 7.764 (± 0.776) ^a | 38.497 (± 1.225) ^c | 0.039 (± 0.03) ^a |
| | Loam (KNO ₃) | 3.566 (± 0.228) ^b | 16.683 (± 2.895) ^b | 20.249 (± 3.029) ^b | 22.059 (± 1.213) ^a | 0.178 (± 0.022) ^b |
| Experiment 2 (28 days) | Clay (KNO ₃) | 4.446 (± 0.22) ^c | 22.49 (± 2.326) ^c | 26.937 (± 2.333) ^c | 33.726 (± 1.356) ^b | 0.166 (± 0.017) ^b |
| | Loam (KNO ₃) | 2.347 (± 0.197) ^b | 42.85 (± 2.675) ^b | 45.197 (± 2.757) ^b | 70.272 (± 2.406) ^a | 0.052 (± 0.004) ^a |
| | Sand (KNO ₃) | 4.89 (± 0.096) ^b | 17.706 (± 0.396) ^a | 22.547 (± 0.457) ^a | 76.881 (± 3.595) ^a | 0.215 (± 0.002) ^b |

Different superscript letters indicate significant differences according to Tukey's range test with $\alpha = 0.05$; n = 4 (Experiment 1 – KNO₃) or n = 3 (Experiment 1 – control and Experiment 2).

as observed in previous incubation studies where NO₃⁻ was subject to gradual depletion.^[33,34] A higher N₂O/(N₂O+N₂) product ratio of denitrification in KNO₃-treated soils reflects the well-known effect of increasing ratio of available electron acceptor to electron donors resulting in decreasing N₂O reduction.^[8] Therefore, the high NO₃⁻ addition to the soils promoted N₂O emission relatively more than N₂ emission.^[8,12]

Similarly, van Cleemput^[35] concluded that nitrate usually inhibits or retards N₂O reduction, resulting in higher N₂O emission from fertilized soils. Surprisingly, we did not observe any significant difference in the N₂O/(N₂O+N₂) product ratio of denitrification when comparing the two soil types. As described above, the clay soil had a higher C content and greater denitrification rate. Therefore, due to its higher electron acceptor demand a higher rate of N₂O reduction would be expected. However, both soil types had almost identical N₂O/(N₂O+N₂) product ratios of denitrification in both non-fertilized and KNO₃ treatments. Apparently, factors favoring higher N₂O reduction to N₂ in the clay soil than in the loam soil (including organic C, pH, and lower gas diffusivity) have been stabilized by other factors leading to the opposite effect. We may speculate that this could be due to differences in microbial community structure.^[11,36,37]

In Experiment 2, very sharp N₂O peaks were observed in the initial phase of the anoxic period in both soil types (sandy soil and loamy soil; Fig. 1(f)), which is similar to Experiment 1. The maximum N₂O fluxes were higher in sandy soil, but they declined more rapidly than in the loamy soil. In addition, the cumulative N₂O emission in sandy soil during the anoxic period was twice as high as in the loamy soil. N₂ production (Fig. 1(g)) was highest during the initial 3 days after onset of treatments. In the loamy soil it decreased slowly, while it decreased more rapidly in sandy soil during the anoxic period. The latter suggests that denitrification became limited by substrate availability (NO_x) in sandy soil in the later stages of the anoxic period. In contrast to N₂O, the cumulative N₂ production and total denitrification rate (i.e. N₂O+N₂; Fig. 1(i)) in the loamy soil was more than twice as high as in the sandy soil during the anoxic phase. The higher denitrification potential in loamy soil than in sandy soil might be attributed to its physicochemical properties; however, CO₂ release and therefore the total soil microbial activity were similar in both soils (Fig. 1(h)). After 21 days of anoxic incubation, the incubation atmosphere was switched to aerobic conditions, i.e. 20% O₂, for additional 7 days. The N₂ production in both soils decreased towards zero within hours which indicates immediate inhibition of N₂O reductase activity by O₂. The N₂O release in the sandy soil peaked for 1 day and decreased afterwards; in contrast, N₂O release from the loamy soil further decreased at the start of the aerobic phase.

The N₂O/(N₂O+N₂) product ratio (Fig. 1(j) and Table 2) was four times higher in the sandy soil than in the loamy soil, indicating that the N₂O reduction rate was clearly limited in the sandy soil. Even under conditions of severe substrate depletion, the N₂O/(N₂O+N₂) product ratio of denitrification in sandy soil was surprisingly high suggesting that the reduction of N₂O to N₂ is restricted in this soil. The latter may be attributed to differences in the denitrifier community structure and/or lower soil pH of the sandy soil. It has been shown that expression of the denitrification genes *nirS* and *cnorB* is strongly affected at pH 5 compared with pH 6–8,^[38]

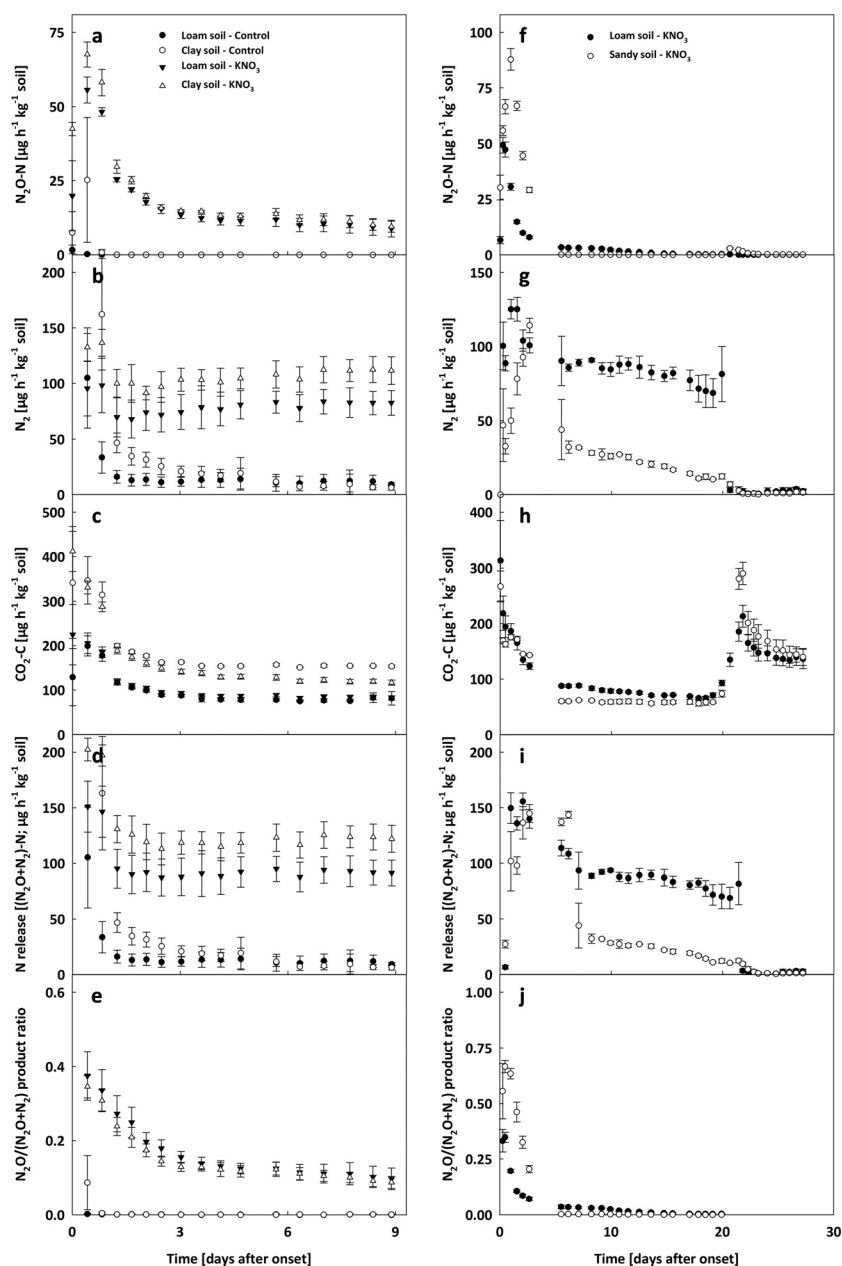


Figure 1. Experiment 1: Cumulative N₂O (a), N₂ (b), CO₂ (c), total N release (d), and the cumulative N₂O/(N₂O+N₂) product ratio (e) during anaerobic incubation of a loam and a clay soil after application of 30 mM KNO₃ solution or water (control), respectively, at a soil moisture of ca 65% WHC. n = 3 (control; treated with water) or n = 4 (KNO₃-treated). Experiment 2: Cumulative N₂O (f), N₂ (g), CO₂ (h), total N release (i), and the cumulative N₂O/(N₂O+N₂) product ratio (j) during incubation of a loamy and a sandy soil treated with 15 mM KNO₃ solution at a moisture of ca 65% WHC. The anaerobic phase lasted for the first 21 days, the aerobic phase for the following 7 days. n = 3 (n = 2 for sandy soil in (g), (i), and (j) due to a small leak corrupting the N₂ analysis in one replicate).

but also that correct translation of transcripts of the *nosZ* gene can be completely corrupted under low pH.^[39] Therefore, the ability of denitrifying bacteria to reduce N₂O is restricted under low soil pH; hence, the N₂O/(N₂O+N₂) product ratio is also affected.^[13,15,40] Compared with Experiment 1,

the N₂O/(N₂O+N₂) product ratio of the loamy soil was clearly lower in Experiment 2 (Day 9: 0.097 ± 0.009 in KNO₃-treated loamy soil, compared with 0.178 ± 0.022 in Experiment 1) which was probably due to the lower rate of applied KNO₃ in Experiment 2.^[12]

Isotopic signatures of N₂O and isotope effects of N₂O reduction

In Experiment 1, N₂O isotopomer analysis was only conducted on gas samples from KNO₃-treated soils, as the N₂O concentrations in stored gas samples of the non-fertilized control treatments were too low for reliable IRMS analysis. The δ¹⁵N^{bulk} values of N₂O released during the initial phase of the experiment were -36.8‰ (±0.53) and -31.9‰ (±1.25) in clay and loamy soil, respectively, with δ¹⁵N^{bulk} values in clay soil being significantly lower than in the loamy soil during the first three samplings. However, δ¹⁵N^{bulk} values increased and were similar in both soil types at the end of the experiment (ca -19‰; Fig. 2(a)). The latter shows that the emitted N₂O was becoming gradually less depleted in ¹⁵N relative to the initial ¹⁵N signature of the soil nitrate pool with the δ¹⁵N value of the applied KNO₃ being 6.5‰ which can be attributed to ongoing ¹⁵N enrichment of the diminishing NO₃ pool undergoing denitrification due to isotope fractionation as shown before.^[41,42] The initial N₂O δ¹⁵N^{bulk} values of both soils were within the range of δ¹⁵N^{bulk} values known to be indicative of N₂O derived from denitrification (ca -54 to -10‰ relative to the substrate)^[43,44] but also fall within the range reported for nitrification

(ca -90 to -40‰) as summarized by Baggs.^[16] In the present study we may assume that N₂O was produced almost entirely by heterotrophic denitrification, as this process was explicitly favored under the anaerobic incubation conditions. Hence our δ¹⁵N^{bulk} data are in line with previous denitrification studies. Similar to ¹⁵N enrichment in the residual soil nitrate pool, N₂O is enriched in ¹⁵N during N₂O reduction to N₂ by denitrifiers.^[25,41] During N₂O reduction lighter N₂O is preferentially consumed, which results in ¹⁵N enrichment of the remaining N₂O, i.e. in raising N₂O δ¹⁵N^{bulk} values. In the present study, N₂O has been continuously removed from the incubation vessel head space by the continuous-flow incubation technique. However, N₂O reduction was clearly higher in the later phase of the incubation as indicated by the strong decrease in the N₂O/(N₂O+N₂) product ratio (see Fig. 1(e)). Therefore, the higher N₂O δ¹⁵N^{bulk} values towards the end of the experiment can be attributed to both ongoing ¹⁵N enrichment of NO₃ and decreasing N₂O/(N₂+N₂O) product ratio.

The δ¹⁸O values were not significantly different between the two soil types (Fig. 2(b)). During the incubation period the δ¹⁸O values increased by 6–7‰ in both soils. The δ¹⁸O value of N₂O has been shown to reflect mainly the isotope signature of the soil water and the isotope effect during

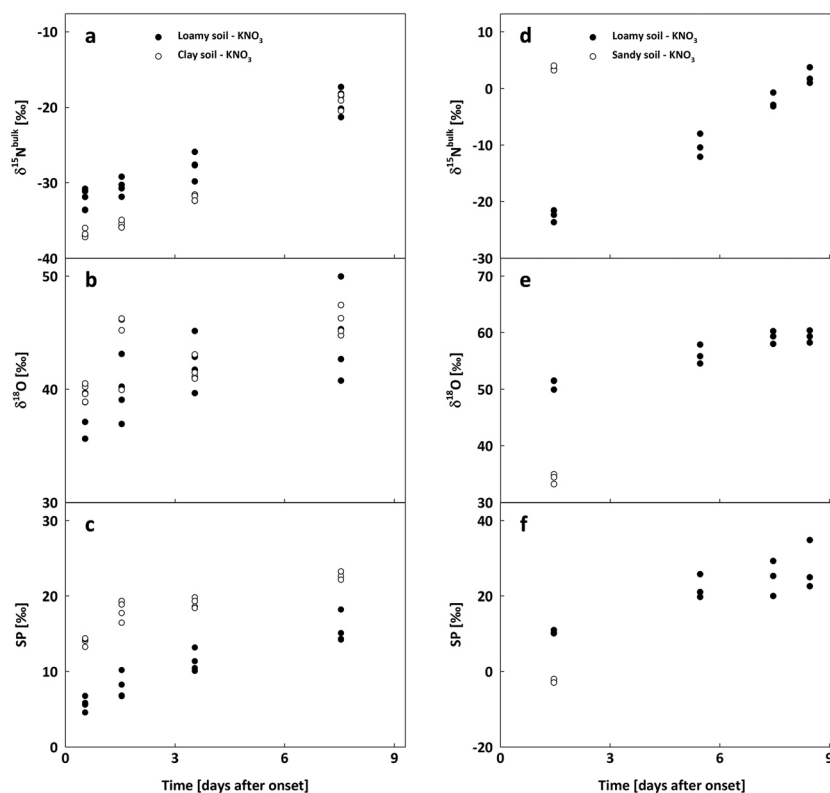


Figure 2. Experiment 1: δ¹⁵N^{bulk} values (a), δ¹⁸O values (b), and ¹⁵N site preference values (SP; c) of N₂O emitted in Experiment 1 during the 9 day incubation of a loam and a clay soil. Soil solution contained 30 mM KNO₃. No N₂O isotope data is available from untreated soil as N₂O release was too low for isotope analysis. δ¹⁵N^{bulk} values (d), δ¹⁸O values (e), and SP values (f) of N₂O emitted in Experiment 2 during the initial 9 days of the 28 day incubation of a loam and a sandy soil. Soil solution contained 15 mM KNO₃. Only a few data points are available from sandy soil as N₂O release declined rapidly and N₂O concentrations became too low for isotope analysis.

O-exchange between N₂O and water.^[45,46] It has been found that O is almost completely exchanged with O of water during denitrification in many soils,^[47] and, to some extent, also during nitrification.^[48] Therefore, it may be assumed that the δ¹⁸O value of N₂O produced by denitrification has been almost constant as observed previously in soil incubations when N₂O reduction was inhibited.^[26] This can be expected in the present study because the isotopic water signature should have been fairly constant. The observed δ¹⁸O shift of 6–7‰ therefore probably reflects the isotope effect of the increasing N₂O reduction rate.^[25,26] Surprisingly, in the residual nitrate only slight enrichment in ¹⁸O was found compared with applied nitrate. It should be expected that residual nitrate will be enriched in ¹⁸O in a similar manner as in ¹⁵N due to preferential reduction of molecules with light isotopes.^[49] However, we observed only a low ¹⁵N enrichment of 4.3 and 1.5‰ in loam and clay soil, respectively. This might suggest that the nitrate isotopic signature is also influenced by the ¹⁸O signature of the soil water. This supports the suggestion by Kool *et al.*^[50] about the reversibility of the reduction steps, which may result in the indirect exchange of O isotopes between soil water and nitrate.

As mentioned above, N₂O produced by microbial or fungal soil processes is characterized by a more or less distinct SP. Typical SP values for denitrification-derived N₂O (including nitrifier denitrification) range from –11 to 0‰,^[19,22] while SP values from nitrification (i.e. NH₄⁺ oxidation via hydroxylamine) have been found to be around 31 to 36‰.^[19] Fungal denitrification may complicate interpretation of SP by producing N₂O with SP values around 37‰, which is close to the isotopic signature of nitrification-derived N₂O.^[18] In the present study, the N₂O SP values during the initial phase of Experiment 1 were 5.7‰ (±0.9) and 14‰ (±0.51) in the loamy and the clay soil, respectively (Fig. 2(c)). These SP values are clearly higher than expected for N₂O solely derived from denitrification, especially in the clay soil. It has been shown that N₂O reduction to N₂ raises the SP of N₂O, because N₂O with ¹⁴N at the α position is preferentially reduced to N₂, causing ¹⁵N enrichment at the α position in the remaining N₂O and so increasing SP values.^[24,25] Thus, that the observed SP values are higher than literature values may to some extent be attributed to isotopic fractionation during N₂O reduction. In both soils the SP values increased during the experiment by 9–10‰, reaching 15.5‰ (±1.88) and 22.8‰ (±0.53) after 1 week. The N₂O/(N₂O+N₂) product ratio of both soils decreased during the incubation phase from ca 0.4 to 0.1, which correlated well with the increasing SP, caused by rising N₂O reduction. The N₂O/(N₂O+N₂) product ratios and their trends were identical in both soils throughout the whole incubation period; however, the SP values were constantly higher in clay soil (ca 8‰). It is obvious that fractionation during N₂O reduction alone cannot explain these distinct SP values from the two soils, because the relative reduction rates of N₂O were almost identical. The differences rather originate from influences of other processes related to N₂O production in soil, such as fungal denitrification,^[18] or other processes of which isotope signals have not been investigated so far (e.g. archaeal N₂O production, DNRA, and anammox).^[23]

In Experiment 2, N₂O isotopomer analysis on gas samples from the sandy soil was only possible for the first sampling (ca 30 h after onset) due to a very rapid decrease in N₂O release, while the N₂O concentrations in gas samples of the loam soil

were sufficient for IRMS analysis during the first 9 days after the onset of the experiment. The δ¹⁵N^{bulk} value of the released N₂O (Fig. 2(d)) during the second day of the experiment was –22.5‰ (±1.04) in the loam soil, while it was significantly higher in the sandy soil (+3.5 (±0.43)). During the following 7 days the δ¹⁵N^{bulk} values in the loamy soil increased linearly by almost 25‰ to 2.1‰ (±1.41). In contrast to Experiment 1, the δ¹⁸O values (Fig. 2(e)) were significantly different between the two soils during the first sampling, being 51‰ (±0.91) in the loamy soil and 34.2‰ (±0.89) in the sandy soil, and increased in the loamy soil to 59.3‰ (±1.05). The SP values were 10.5‰ (±4.7) in the loamy soil, increasing to 27.5‰ (±6.51), and –2.6‰ (±0.5) during the first sampling in the sandy soil (Fig. 2(f)). Overall, the isotope values and trends in the loamy soil were similar to those in Experiment 1. However, the N₂O isotope values of the sandy soil were clearly different, with δ¹⁵N^{bulk} values being much higher, but δ¹⁸O and SP values being significantly lower than in the loamy soil, but even more so than in the clay soil in Experiment 1. Here, a crucial point is the 4 times higher N₂O/(N₂O+N₂) product ratio in the sandy soil, indicating significantly lower relative N₂O reduction. The latter may at least partly explain the lower N₂O δ¹⁸O and SP values found in the sandy soil. However, this cannot explain the high N₂O δ¹⁵N^{bulk} values, which are close to the δ¹⁵N value of the applied nitrate and do not seem to be affected by fractionation during nitrate and N₂O reduction. As discussed for Experiment 1, nitrate reduction may enrich ¹⁵N in the remaining substrate pool, although this was not observed in the sandy soil (Table 3). In contrast, the soil nitrate δ¹⁵N values in the sandy soil were slightly lower at the end of the incubation relative to the applied nitrate. Probably, the ¹⁵N enrichment of the nitrate pool was obscured by the isotopic signature of nitrate produced via mineralization and nitrification in the sandy soil during the 7 day aerobic incubation phase at the end of the experiment as nitrification is known to favor lighter isotopes.^[51] Similarly, the strong decrease in the nitrate δ¹⁸O values by ca 26‰ in both soils (Table 3) may be attributed to nitrification during the oxic incubation phase, but also by O exchange with water as discussed earlier.^[50]

Based on the measured SP and δ¹⁸O values the NIE (η) of the N₂O-to-N₂ reduction step was estimated. The isotopic fractionation during N₂O reduction can be described by the Rayleigh model,^[25,32] which assumes a closed system in which no substrate (i.e. N₂O) is added (via production) nor removed, and the substrate is used up over time.^[52] However, as discussed by Decock and Six,^[53] in reality mostly a mixture of open and closed system isotope dynamics should occur in soil and they revealed in a simulation that N₂O reduction only increases SP drastically when more than 80% of all the substrate is consumed following closed system dynamics. This applies in the present study and the observed data can be described by a logarithmic function, which is characteristic for closed systems. Therefore, we suppose that it is adequate to analyze the experimental results in the present study using the Rayleigh model (Eqn. (1)):

$$\delta_s = \delta_{s0} + \eta \ln \left(\frac{C}{C_0} \right) \quad (1)$$

in which δ_s is the isotope signature of the remaining substrate (i.e. the N₂O SP or δ¹⁸O value), δ_{s0} the signature of the initial substrate, and C and C₀ the residual and initial substrate

Table 3. Soil mineral N content and $\delta^{15}\text{N}$ and $\delta^{18}\text{O}$ values of applied NO_3^- and residual NO_3^- in soil solution (\pm standard deviation)

| | Soil (treatment) | Applied NO_3^- -N [mg kg ⁻¹ soil DM] | Residual NO_3^- -N [mg kg ⁻¹ soil DM] | NH_4^+ -N [mg kg ⁻¹ soil DM] | $\delta^{15}\text{N}$ [‰] of residual NO_3^- | $\delta^{18}\text{O}$ [‰] of residual NO_3^- |
|--------------------------|--------------------------|---|--|---|--|--|
| Experiment 1 (9 days) | Loam (control) | 0 | 2.19 (± 0.178) ^a | < LOQ [#] | -4.0 (± 0.92) ^a | -0.4 (± 1.21) ^a |
| | Clay (control) | 0 | 5.53 (± 0.142) ^a | < LOQ [#] | 8.8 (± 0.35) ^b | 2.9 (± 0.26) ^b |
| | Loam (KNO ₃) | 64.9 (± 1.29) | 34.08 (± 1.274) ^b | < LOQ [#] | 21.3 (± 1.4) ^c | 27.1 (± 0.63) ^d |
| Experiment 2 (28 days) | Clay (KNO ₃) | 109.8 (± 1.23) | 45.88 (± 4.095) ^c | < LOQ [#] | 26.1 (± 1.8) ^d | 24.3 (± 0.66) ^c |
| | Loam (KNO ₃) | 37.2 (± 1.18) | 7.61 (± 0.904) ^a | < LOQ [#] | 18.8 (± 6.96) ^b | -3.1 (± 1.77) |
| KNO ₃ applied | Sand (KNO ₃) | 15.6 (± 0.24) | 8.52 (± 0.274) ^a | < LOQ [#] | 5.6 (± 0.2) ^a | -2.9 (± 0.31) |
| | | | | | 6.5 (± 0.02) | 22.8 (± 0.27) |

Different superscript letters indicate significant differences according to Tukey's range test with $\alpha = 0.05$; n = 4 (Experiment 1 – KNO₃) or n = 3 (Experiment 1 – control and Experiment 2).

[#]Below limit of quantification (LOQ) of 2.4 mg NH_4^+ -N kg⁻¹

concentrations (here N_2O and ($\text{N}_2\text{O} + \text{N}_2$)). The SP_0 value of the produced N_2O is not exactly known, but it may be assumed to be constant during the course of experiment, because it depends largely on the soil microbial community structure. Oxygen is largely exchanged with soil water during nitrate reduction.^[47] Therefore, we hypothesize also that the $\delta^{18}\text{O}_0$ signature of N_2O (i.e. the $\delta^{18}\text{O}$ value of N_2O unaffected by N_2O reduction) is approximately constant throughout the experiment as the isotopic signature of soil water is also constant. Hence, the η value can be approximated from the relationship between the δ_5 value and (C/C_0). The logarithmic function was fitted to the measured data using an iterative least squares algorithm (SigmaStat) to determine the respective η_{SP} and $\eta_{18\text{O}}$ values. This approach is demonstrated graphically in Fig. 3.

For the loam soil the isotope data of both experiments was combined to cover a wider $\text{N}_2\text{O}/(\text{N}_2\text{O} + \text{N}_2)$ product ratio range. The SP net isotope effects of N_2O reduction (η_{SP}) were -6.1‰ (clay soil; Fig. 3(a)) and -8.2‰ (loam soil). These values match very well with enrichment factors reported by Well and Flessa,^[26] who found η_{SP} values of -7.9 to -3.6 in a study investigating N_2O reduction in soil and with findings by Ostrom *et al.*^[25] in pure culture experiments of *Pseudomonas stutzeri* and *Pseudomonas denitrificans*, expressing η_{SP} values of -6.8 to -5.0‰. Jinuntuya-Nortman *et al.*^[24] observed lower ¹⁵N enrichment during N_2O reduction in soil mesocosms and reported enrichments factors of -4.5 to -2.9‰. The initial N_2O SP values (SP_0) during N_2O production were calculated to be ca -4‰ (loamy soil) and 8‰ (clay soil). The SP_0 value of the loamy soil matches with published values on denitrification-derived N_2O ,^[19,22] the SP_0 value of the clay soil, however, is clearly higher. This might indicate significant contribution of fungal denitrification to N_2O production, which is characterized by much higher SP values.^[18] Since fungi are lacking in N_2O reductase,^[54] fungal N_2O production could have balanced the other factors stimulating N_2O reduction (higher C_{org} and pH; lower O_2 diffusivity) and thus have led to a similar $\text{N}_2\text{O}/(\text{N}_2 + \text{N}_2\text{O})$ product ratio to that of the loamy soil. The calculation of NIE during N_2O reduction for the sandy soil was not possible, because there were only three data points available. However, the SP_0 value (the initial N_2O SP) of the sandy soil was estimated using the Rayleigh equation (Eqn. (1)). Here, the η_{SP} value was assumed to be similar to those of the two other soils. Based on this assumption, the SP_0 was calculated to be between -10 and -6‰. This is clearly lower than for the two other soils and also lower than most published SP values.

The $\delta^{18}\text{O}$ net isotope effects ($\eta_{\delta^{18}\text{O}}$) for N_2O reduction were calculated as -8.6 and -3.4‰ for the loamy and the clay soil, respectively (Fig. 3(b)); for the clay soil, however, the R^2 of $\eta_{\delta^{18}\text{O}}$ was relatively low. These $\eta_{\delta^{18}\text{O}}$ values are clearly smaller than published values of -20 to -11‰ from N_2O reduction in soils,^[26] or -30.5‰ during N_2O reduction in the ocean,^[55] and are in the lowest range of pure cultured denitrifiers (-25 to -5‰).^[25]

Our estimations of η_{SP} are based on a number of assumptions and are therefore subject to some uncertainties. For example, we postulate that the isotope fractionation follows closed system dynamics, which might not be completely fulfilled, and that both SP_0 and η_{SP} were constant during the incubation. Strict constancy in η_{SP} is not expected, however, because changes in the denitrifier community

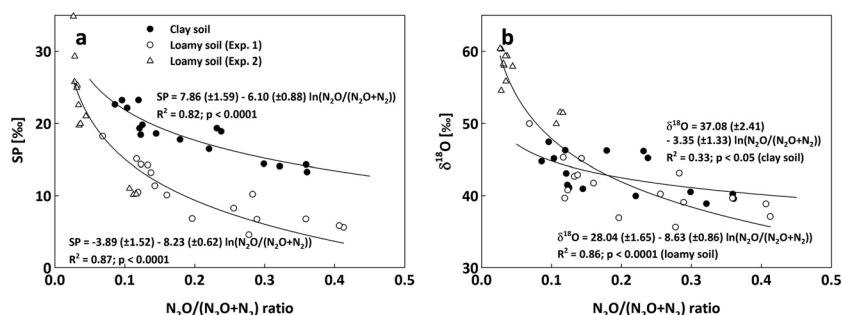


Figure 3. SP (a) and $\delta^{18}\text{O}$ (b) values of N₂O vs the N₂O/(N₂O+N₂) product ratio during the incubation of two soils treated with KNO₃ solution. Isotope values are expressed as a function of the N₂O/(N₂O+N₂) product ratio according to the Rayleigh model (Eqn. (1)); n = 28 (loam soil) or n = 16 (clay soil).

structure with subsequent effect on $\eta_{\text{SP}}^{[23]}$ could probably have occurred during the incubation resulting from exhaustion of substrates and from adaptation to conditions favoring denitrification. Similarly, the assumption about the constant $\delta^{18}\text{O}_0$ signature may not be fulfilled due to incomplete O-isotope exchange with soil water.^[47] Moreover, to constrain the SP₀ of the sandy soil we assumed that the η_{SP} was similar to those of the other soils which is questionable in view of the reported variations in η_{SP} .^[26] To further validate our results and obtain more precise estimates of $\eta_{\text{SP}}/\eta_{\delta^{18}\text{O}}$ and SP₀, combined modeling of N₂O production and reduction and associated isotope effects is needed, which is beyond the scope of this paper.

Calculation of the $\eta_{\delta^{15}\text{N}}^{\text{bulk}}$ values of N₂O reduction was not possible as the isotopic signature of the nitrate pool in the soil was not constant but subject to gradual ¹⁵N enrichment. Estimating $\delta^{15}\text{N}^{\text{bulk}}$ reduction effects requires a more sophisticated modeling approach, which is part of ongoing efforts of our group and will be further discussed elsewhere.

Ostrom *et al.*^[25] suggested that N₂O reduction can clearly be recognized in the correlations (or lack thereof) between $\delta^{18}\text{O}$ and $\delta^{15}\text{N}^{\text{bulk}}$ values, and $\delta^{18}\text{O}$ and $\delta^{15}\text{N}^{\alpha}$ values, and between $\delta^{18}\text{O}$ and SP values, and found in pure cultured denitrifiers a $\delta^{18}\text{O}$ vs SP relationship of 2.2 to be indicative for N₂O reduction. Similar observations were reported by Well and Flessa,^[26] who found a $\delta^{18}\text{O}$ vs SP relationship of around 2.5 for N₂O reduction in soils. However, in this study, this relationship was between 0.69 and 0.93 (Fig. 4). These differences might be attributed to a basically different experimental setup, because in the two aforementioned studies N₂O had been added to the head space of the incubation flasks. Prior to reduction, the added N₂O had to diffuse into the soil solution and pass into the microbial cell. Meanwhile diffusive fractionation would occur affecting ¹⁸O rather than SP signatures, and, thus, affect the $\delta^{18}\text{O}$ vs SP relationship. In the case of *in situ* produced N₂O in our study, however, isotopically lighter N₂O will more rapidly escape from denitrifying micro-sites by diffusion which might to some extent favor accumulation and subsequent reduction of isotopically heavier N₂O. This effect counteracts the enzymatic $\delta^{18}\text{O}$ and $\delta^{15}\text{N}$ effects as suggested earlier^[56] and might thus explain why our estimates of $\eta^{18}\text{O}$ yielded smaller values than in the literature data. In groundwater, the

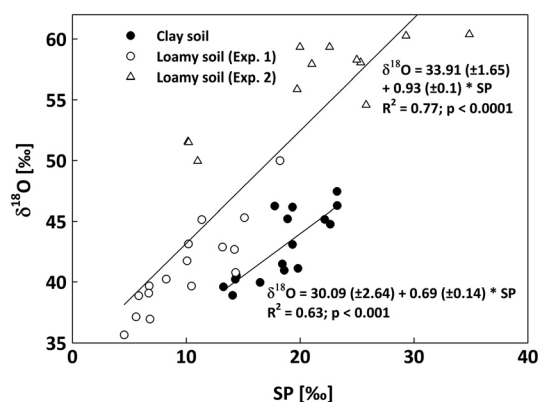


Figure 4. The N₂O $\delta^{18}\text{O}$ vs SP relationship during the incubation of a loam and a clay soil; n = 28 (loam soil) or n = 16 (clay soil).

$\delta^{18}\text{O}$ vs SP relationship was found to be closer to our findings, with values between 0.2 and 1.14.^[49,57] This was attributed to the small isotope effect during N₂O diffusion in water^[49] which thus also supports our above hypothesis.

CONCLUSIONS

The results of the two incubation experiments clearly show that the similarity of N₂O/(N₂O+N₂) product ratios in different soils could not be explained by soil physicochemical properties only. We suspect that differences in physicochemical properties between the loamy and the clay soil might have been balanced by fungal denitrification.

The estimated SP₀ values differed greatly between the different soils. This indicates that processes other than bacterial denitrification, possibly fungal denitrification, may have contributed significantly to N₂O production in the clay soil, and strengthens our hypothesis based on the observed N₂O/(N₂O+N₂) product ratios, although this requires further verification. The N₂O SP values were strongly affected by N₂O reduction and the η_{SP} values of the N₂O-to-N₂ reduction step are in agreement with previous studies; however, the $\delta^{18}\text{O}$ values were less affected by N₂O reduction than previously reported. This may be attributed to differences

in the experimental setup, i.e. N₂O addition to the head space vs N₂O being produced in denitrifying cells in the present study.

These results clearly demonstrate that further efforts are required to deepen the knowledge not only on isotopic signatures from different N₂O source pathways, but also on reduction effects on the relation of ¹⁸O and ¹⁵N signatures. Better understanding of these processes including their associated isotope signals may lead to a simplified isotopomer approach to be used for measuring N₂O source contributions and to estimate N₂O reduction.

Acknowledgements

Jan Reent Köster thanks the German Federal Environmental Foundation (DBU) for a PhD scholarship. The authors thank Martina Heuer and Bärbel Biegler for laboratory support, Anna Techow for supplying soil samples, and Nathaniel Ostrom and an anonymous reviewer for their comments on an earlier version of this manuscript.

REFERENCES

- [1] A. R. Ravishankara, J. S. Daniel, R. W. Portmann. Nitrous oxide (N₂O): The dominant ozone-depleting substance emitted in the 21st century. *Science* **2009**, 326, 123.
- [2] *Climate Change 2007: Mitigation. Contribution of Working Group III to the Fourth Assessment Report of the Intergovernmental Panel on Climate Change*, (Eds: B. Metz, O. R. Davidson, P. R. Bosch, R. Dave, L. A. Meyer). Cambridge University Press, Cambridge, UK and New York, NY, USA, **2007**.
- [3] A. R. Mosier, C. Kroeze, C. Nevison, O. Oenema, S. Seitzinger, O. van Cleemput. Closing the global N₂O budget: nitrous oxide emissions through the agricultural nitrogen cycle. *Nutr. Cycl. Agroecosyst.* **1998**, 52, 225.
- [4] A. R. Mosier, J. M. Duxbury, J. R. Freney, O. Heinemeyer, K. Minami. Assessing and mitigating N₂O emissions from agricultural soils. *Clim. Change* **1998**, 40, 7.
- [5] K. Khalil, B. Mary, P. Renault. Nitrous oxide production by nitrification and denitrification in soil aggregates as affected by O₂ concentration. *Soil Biol. Biochem.* **2004**, 36, 687.
- [6] N. Wrage, G. L. Velthof, M. L. van Beusichem, O. Oenema. Role of nitrifier denitrification in the production of nitrous oxide. *Soil Biol. Biochem.* **2001**, 33, 1723.
- [7] P. M. Groffman, M. A. Altabet, J. K. Bohlke, K. Butterbach-Bahl, M. B. David, M. K. Firestone, A. E. Giblin, T. M. Kana, L. P. Nielsen, M. A. Voytek. Methods for measuring denitrification: Diverse approaches to a difficult problem. *Ecol. Appl.* **2006**, 16, 2091.
- [8] K. L. Weier, J. W. Doran, J. F. Power, D. T. Walters. Denitrification and the dinitrogen/nitrous oxide ratio as affected by soil water, available carbon, and nitrate. *Soil Sci. Soc. Am. J.* **1993**, 57, 66.
- [9] M. Maag, F. P. Vinther. Nitrous oxide emission by nitrification and denitrification in different soil types and at different soil moisture contents and temperatures. *Appl. Soil Ecol.* **1996**, 4, 5.
- [10] R. Knowles. Denitrification. *Microbiol. Rev.* **1982**, 46, 43.
- [11] P. Dörsch, G. Braker, L. R. Bakken. Community-specific pH response of denitrification: experiments with cells extracted from organic soils. *FEMS Microbiol. Ecol.* **2012**, 79, 530.
- [12] M. Senbayram, R. Chen, A. Budai, L. Bakken, K. Dittert. N₂O emission and the N₂O/(N₂O + N₂) product ratio of denitrification as controlled by available carbon substrates and nitrate concentrations. *Agric. Ecosyst. Environ.* **2012**, 147, 4.
- [13] M. Šimek, J. E. Cooper. The influence of soil pH on denitrification: progress towards the understanding of this interaction over the last 50 years. *Eur. J. Soil Sci.* **2002**, 53, 345.
- [14] J. Čuhel, M. Šimek, R. J. Laughlin, D. Bru, D. Chèneby, C. J. Watson, L. Philippot. Insights into the effect of soil pH on N₂O and N₂ emissions and denitrifier community size and activity. *Appl. Environ. Microbiol.* **2010**, 76, 1870.
- [15] N. Raut, P. Dörsch, B. K. Sitaula, L. R. Bakken. Soil acidification by intensified crop production in South Asia results in higher N₂O/(N₂+N₂O) product ratios of denitrification. *Soil Biol. Biochem.* **2012**, 55, 104.
- [16] E. M. Baggs. A review of stable isotope techniques for N₂O source partitioning in soils: recent progress, remaining challenges and future considerations. *Rapid Commun. Mass Spectrom.* **2008**, 22, 1664.
- [17] S. Park, T. Pérez, K. A. Boering, S. E. Trumbore, J. Gil, S. Marquina, S. C. Tyler. Can N₂O stable isotopes and isotopomers be useful tools to characterize sources and microbial pathways of N₂O production and consumption in tropical soils? *Global Biogeochem. Cycles* **2011**, 25. DOI: 10.1029/2009gb003615.
- [18] R. L. Sutka, G. C. Adams, N. E. Ostrom, P. H. Ostrom. Isotopologue fractionation during N₂O production by fungal denitrification. *Rapid Commun. Mass Spectrom.* **2008**, 22, 3989.
- [19] R. L. Sutka, N. E. Ostrom, P. H. Ostrom, J. A. Breznak, H. Gandhi, A. J. Pitt, F. Li. Distinguishing nitrous oxide production from nitrification and denitrification on the basis of isotopomer abundances. *Appl. Environ. Microbiol.* **2006**, 72, 638.
- [20] S. Toyoda, N. Yoshida. Determination of nitrogen isotopomers of nitrous oxide on a modified isotope ratio mass spectrometer. *Anal. Chem.* **1999**, 71, 4711.
- [21] S. Toyoda, N. Yoshida, T. Miwa, Y. Matsui, H. Yamagishi, U. Tsunogai, Y. Nojiri, N. Tsurushima. Production mechanism and global budget of N₂O inferred from its isotopomers in the western North Pacific. *Geophys. Res. Lett.* **2002**, 29, 4.
- [22] S. Toyoda, H. Mutoke, H. Yamagishi, N. Yoshida, Y. Tanji. Fractionation of N₂O isotopomers during production by denitrifier. *Soil Biol. Biochem.* **2005**, 37, 1535.
- [23] N. E. Ostrom, P. H. Ostrom, in *Handbook of Environmental Isotope Geochemistry*, vol. I, (Ed.: M. Baskaran). Springer, Berlin Heidelberg, **2012**, pp. 453–476.
- [24] M. Jinuntuya-Nortman, R. L. Sutka, P. H. Ostrom, H. Gandhi, N. E. Ostrom. Isotopologue fractionation during microbial reduction of N₂O within soil mesocosms as a function of water-filled pore space. *Soil Biol. Biochem.* **2008**, 40, 2273.
- [25] N. E. Ostrom, A. Pitt, R. Sutka, P. H. Ostrom, A. S. Grandy, K. M. Huizinga, G. P. Robertson. Isotopologue effects during N₂O reduction in soils and in pure cultures of denitrifiers. *J. Geophys. Res.* **2007**, 112. DOI: 10.1029/2006JG000287.
- [26] R. Well, H. Flessa. Isotopologue enrichment factors of N₂O reduction in soils. *Rapid Commun. Mass Spectrom.* **2009**, 23, 2996.
- [27] K. L. Casciotti, D. M. Sigman, M. G. Hastings, J. K. Bohlke, A. Hilker. Measurement of the oxygen isotopic composition of nitrate in seawater and freshwater using the denitrifier method. *Anal. Chem.* **2002**, 74, 4905.
- [28] D. M. Sigman, K. L. Casciotti, M. Andreani, C. Barford, M. Galanter, J. K. Bohlke. A bacterial method for the nitrogen isotopic analysis of nitrate in seawater and freshwater. *Anal. Chem.* **2001**, 73, 4145.

- [29] R. Well, I. Kurganova, V. L. de Gerenyu, H. Flessa. Isotopomer signatures of soil-emitted N₂O under different moisture conditions – A microcosm study with arable loess soil. *Soil Biol. Biochem.* **2006**, *38*, 2923.
- [30] W. A. Brand. PRECON: A fully automated interface for the pre-GC concentration of trace gases in air for isotopic analysis. *Isot. Environ. Health Stud.* **1995**, *31*, 277.
- [31] M. Hasler. SimComp: Simultaneous Comparisons for Multiple Endpoints. *R package version 1.7.0*, **2012**, <http://CRAN.R-project.org/package=SimComp>.
- [32] A. Mariotti, J. C. Germon, P. Hubert, P. Kaiser, R. Letolle, A. Tardieux, P. Tardieux. Experimental determination of nitrogen kinetic isotope fractionation: Some principles; illustration for the denitrification and nitrification processes. *Plant Soil* **1981**, *62*, 413.
- [33] A. Bergstermann, L. M. Cárdenas, R. Bol, L. Gilliam, K. W. T. Goulding, A. Meijide, D. Scholefield, A. Vallejo, R. Well. Effect of antecedent soil moisture conditions on emissions and isotopologue distribution of N₂O during denitrification. *Soil Biol. Biochem.* **2011**, *43*, 240.
- [34] A. Meijide, L. M. Cárdenas, R. Bol, A. Bergstermann, K. Goulding, R. Well, A. Vallejo, D. Scholefield. Dual isotope and isotopomer measurements for the understanding of N₂O production and consumption during denitrification in an arable soil. *Eur. J. Soil Sci.* **2010**, *61*, 364.
- [35] O. van Cleemput. Subsoils: chemo- and biological denitrification, N₂O and N₂ emissions. *Nutr. Cycl. Agroecosyst.* **1998**, *52*, 187.
- [36] G. Braker, P. Dörsch, L. R. Bakken. Genetic characterization of denitrifier communities with contrasting intrinsic functional traits. *FEMS Microbiol. Ecol.* **2012**, *79*, 542.
- [37] L. Holtan-Hartwig, P. Dörsch, L. R. Bakken. Comparison of denitrifying communities in organic soils: kinetics of NO₃ and N₂O reduction. *Soil Biol. Biochem.* **2000**, *32*, 833.
- [38] S. Saleh-Lakha, K. E. Shannon, S. L. Henderson, C. Goyer, J. T. Trevors, B. J. Zebarth, D. L. Burton. Effect of pH and temperature on denitrification gene expression and activity in *Pseudomonas mandelii*. *Appl. Environ. Microbiol.* **2009**, *75*, 3903.
- [39] L. Bergaust, Y. J. Mao, L. R. Bakken, Å. Frostegård. Denitrification response patterns during the transition to anoxic respiration and posttranscriptional effects of suboptimal pH on nitrogen oxide reductase in *Paracoccus denitrificans*. *Appl. Environ. Microbiol.* **2010**, *76*, 6387.
- [40] B. B. Liu, P. T. Mørkved, Å. Frostegård, L. R. Bakken. Denitrification gene pools, transcription and kinetics of NO, N₂O and N₂ production as affected by soil pH. *FEMS Microbiol. Ecol.* **2010**, *72*, 407.
- [41] C. C. Barford, J. P. Montoya, M. A. Altabet, R. Mitchell. Steady-state nitrogen isotope effects of N₂ and N₂O production in *Paracoccus denitrificans*. *Appl. Environ. Microbiol.* **1999**, *65*, 989.
- [42] O. V. Menyailo, B. A. Hungate. Stable isotope discrimination during soil denitrification: Production and consumption of nitrous oxide. *Global Biogeochem. Cycle* **2006**, *20*. DOI: 10.1029/2005gb002527.
- [43] T. Pérez, D. Garcia-Montiel, S. Trumbore, S. Tyler, P. De Camargo, M. Moreira, M. Piccolo, C. Cerri. Nitrous oxide nitrification and denitrification ¹⁵N enrichment factors from Amazon forest soils. *Ecol. Appl.* **2006**, *16*, 2153.
- [44] R. Well, H. Flessa. Isotopologue signatures of N₂O produced by denitrification in soils. *J. Geophys. Res.* **2009**, *114*. DOI: 10.1029/2008JG000804.
- [45] D. M. Snider, J. J. Venkiteswaran, S. L. Schiff, J. Spoelstra. Deciphering the oxygen isotope composition of nitrous oxide produced by nitrification. *Global Change Biol.* **2012**, *18*, 356.
- [46] D. M. Snider, J. J. Venkiteswaran, S. L. Schiff, J. Spoelstra. A new mechanistic model of δ¹⁸O-N₂O formation by denitrification. *Geochim. Cosmochim. Acta* **2013**, *112*, 102.
- [47] D. M. Kool, N. Wrage, O. Oenema, D. Harris, J. W. Van Groenigen. The ¹⁸O signature of biogenic nitrous oxide is determined by O exchange with water. *Rapid Commun. Mass Spectrom.* **2009**, *23*, 104.
- [48] D. M. Kool, C. Müller, N. Wrage, O. Oenema, J. W. Van Groenigen. Oxygen exchange between nitrogen oxides and H₂O can occur during nitrifier pathways. *Soil Biol. Biochem.* **2009**, *41*, 1632.
- [49] R. Well, W. Eschenbach, H. Flessa, C. von der Heide, D. Weymann. Are dual isotope and isotopomer ratios of N₂O useful indicators for N₂O turnover during denitrification in nitrate-contaminated aquifers? *Geochim. Cosmochim. Acta* **2012**, *90*, 265.
- [50] D. M. Kool, N. Wrage, O. Oenema, C. Van Kessel, J. W. Van Groenigen. Oxygen exchange with water alters the oxygen isotopic signature of nitrate in soil ecosystems. *Soil Biol. Biochem.* **2011**, *43*, 1180.
- [51] P. Högberg. Tansley review No. 95 – ¹⁵N natural abundance in soil-plant systems. *New Phytol.* **1997**, *137*, 179.
- [52] B. Fry. *Stable Isotope Ecology*. Springer Science+Business Media, LLC, New York, NY, USA, **2006**.
- [53] C. Decock, J. Six. How reliable is the intramolecular distribution of ¹⁵N in N₂O to source partition N₂O emitted from soil? *Soil Biol. Biochem.* **2013**, *65*, 114.
- [54] H. Shoun, D. H. Kim, H. Uchiyama, J. Sugiyama. Denitrification by fungi. *FEMS Microbiol. Lett.* **1992**, *94*, 277.
- [55] H. Yamagishi, M. B. Westley, B. N. Popp, S. Toyoda, N. Yoshida, S. Watanabe, K. Koba, Y. Yamanaka. Role of nitrification and denitrification on the nitrous oxide cycle in the eastern tropical North Pacific and Gulf of California. *J. Geophys. Res.* **2007**, *112*. DOI: 10.1029/2006JG000227.
- [56] R. Well, H. Flessa, in *Proceedings of the 4th International Symposium on Isotopomers*, (Ed: N. Yoshida), **2009**, pp. 86–93.
- [57] K. Koba, K. Osaka, Y. Tobar, S. Toyoda, N. Ohte, M. Katsuyama, N. Suzuki, M. Itoh, H. Yamagishi, M. Kawasaki, S. J. Kim, N. Yoshida, T. Nakajima. Biogeochemistry of nitrous oxide in groundwater in a forested ecosystem elucidated by nitrous oxide isotopomer measurements. *Geochim. Cosmochim. Acta* **2009**, *73*, 3115.

Chapter 6

Experimental determinations of isotopic fractionation factors associated with N₂O production and reduction during denitrification in soils

Dominika Lewicka-Szczebak, Reinhard Well, Jan Reent Köster, Roland Fuß,
Klaus Dittert, Mehmet Senbayram, Klaus Dittert, and Heiner Flessa

Geochimica et Cosmochimica Acta 134 (2014) 55 – 73

DOI: 10.1016/j.gca.2014.03.010

Experimental determinations of isotopic fractionation factors associated with N₂O production and reduction during denitrification in soils

Dominika Lewicka-Szczebak^{a,b,*}, Reinhard Well^a, Jan Reent Köster^c,
Roland Fuß^a, Mehmet Senbayram^{d,e}, Klaus Dittert^f, Heiner Flessa^a

^a Thünen Institute of Climate-Smart Agriculture, Federal Research Institute for Rural Areas, Forestry and Fisheries, Bundesallee 50, D-38116 Braunschweig, Germany

^b Institute of Geological Sciences, University of Wrocław, Cybulskiego 30, PL-50-205 Wrocław, Poland

^c Institute of Plant Nutrition and Soil Science, Kiel University, Hermann-Rodewald-Str. 2, D-24118 Kiel, Germany

^d Institute of Plant Nutrition and Environmental Science, Research Center Hanninghof, Yara Int. ASA, Hanninghof 35, D-48249 Dülmen, Germany

^e Institute of Applied Plant Nutrition, University of Göttingen, Carl-Sprengel-Weg 1, D-37075 Göttingen, Germany

^f Department of Crop Science, Section of Plant Nutrition and Crop Physiology, University of Göttingen, Carl-Sprengel-Weg 1, D-37075 Göttingen, Germany

Received 26 December 2013; accepted in revised form 7 March 2014; Available online 24 March 2014

Abstract

Quantifying denitrification in arable soils is crucial in predicting nitrogen fertiliser losses and N₂O emissions. Stable isotopologue analyses of emitted N₂O ($\delta^{15}\text{N}$, $\delta^{18}\text{O}$ and $\text{SP} = {}^{15}\text{N}$ site preference within the linear N₂O molecule) may help to distinguish production pathways and to quantify N₂O reduction to N₂. However, such interpretations are often ambiguous due to insufficient knowledge on isotopic fractionation mechanisms. Here we present a complex experimental approach to determine the net fractionation factors (η) associated with denitrification. This determination is based on three laboratory experiments differing in their experimental set-up and soil properties. Static and dynamic incubation techniques were compared. All available methods for independent determination of N₂O reduction contribution were used, namely, N₂-free atmosphere incubation, acetylene inhibition technique and ¹⁵N gas-flux method.

For N₂O production: (i) the determined difference in $\delta^{18}\text{O}$ between soil water and produced N₂O vary from +18‰ to +42‰ and show very strict negative correlation with soil water saturation; (ii) the determined $\eta^{15}\text{N}$ of N₂O production vary from –55‰ to –38‰ and the fractionation decreases with decreasing substrate availability; (iii) the determined SP of produced N₂O vary from –3‰ to +9‰. For N₂O reduction: (i) the determined $\eta^{18}\text{O}$ and $\eta^{15}\text{N}$ of N₂O reduction vary in very wide ranges from –18‰ to +4‰ and from –11‰ to +12‰, respectively, and depend largely on the differences in experimental setups; whereas (ii) the determined ηSP of N₂O reduction shows a very consistent value with all previous studies and varies in a rather narrow range from –2‰ to –8‰. It can be concluded that η values of N₂O production determined during laboratory incubations yield only roughly estimates for respective values expectable under field study conditions. $\eta^{18}\text{O}$ and $\eta^{15}\text{N}$ associated with N₂O reduction may vary largely, probably depending on spatial and temporal coincidence of N₂O production and reduction, and are hence not yet predictable for natural conditions. However, the ηSP

* Corresponding author at: Thünen Institute of Climate-Smart Agriculture, Federal Research Institute for Rural Areas, Forestry and Fisheries, Bundesallee 50, D-38116 Braunschweig, Germany. Tel.: +49 531 596 2668; fax: +49 531 596 2699.

E-mail address: dominika.lewicka-szczebak@ti.bund.de (D. Lewicka-Szczebak).

of N₂O reduction appeared to be relatively robust and a most probable value of about -5% can be used to constrain N₂O reduction based on SP of soil emitted N₂O.

© 2014 Elsevier Ltd. All rights reserved.

1. INTRODUCTION

Denitrification is an anaerobic microbial process of successive reduction of nitrate to N₂O and N₂ (Firestone and Davidson, 1989). It is supposed to be a dominant N₂O emission source from agricultural temperate soils (Opdyke et al., 2009; Ostrom et al., 2010). Hence, the understanding and ability to quantify this process is crucial in mitigating the microbial consumption of nitrogen fertilisers as well as in reducing N₂O emission, which significantly contributes to global warming and stratospheric ozone depletion (IPCC, 2013). Owing to the recent developments of analytical methods we are not only able to analyse isotopic composition of N₂O ($\delta^{15}\text{N}$ and $\delta^{18}\text{O}$), but also to determine the site preference (SP), *i.e.*, the difference in $\delta^{15}\text{N}$ between the central and the peripheral N atom of linear N₂O molecule (Brenninkmeijer and Röckmann, 1999; Toyoda and Yoshida, 1999). While isotopologue signatures of soil-emitted N₂O have been determined in a variety of soil and climatic conditions to explore the environmental impact on isotopologue signatures and their spatio-temporal variability (Perez et al., 2001; Yamulki et al., 2001; Bol et al., 2003; Well et al., 2006), only recently first attempts have been made to use this approach to estimate N₂O reduction to N₂ (Opdyke et al., 2009; Park et al., 2011; Toyoda et al., 2011).

However, in order to provide precise quantitative information about the contribution of particular pathways based on isotopologue measurements, the isotopic fractionation must be well understood. Unfortunately, isotope fractionation factors related to denitrification are still poorly examined due to the complexity of this process. Denitrification is a multistep process of a successive reduction of nitrate through the following reduction steps: $\text{NO}_3^- \rightarrow \text{NO}_2^- \rightarrow \text{NO} \rightarrow \text{N}_2\text{O} \rightarrow \text{N}_2$ (Firestone and Davidson, 1989). Each of these steps represents an individual microbial enzymatic reaction mediated by a different enzyme and, consequently, each step is associated with individual characteristic isotopic fractionation (Ostrom and Ostrom, 2011). The commonly applied analytical techniques enable us to analyse only the last intermediate of the whole process, namely N₂O. Therefore, here we try to deepen the knowledge about the isotopic fractionation affecting the final isotopic signature of N₂O as an intermediate product of denitrification. This signature results from all the successive enzymatic reactions leading to N₂O synthesis, which we combine here in a simplified step called N₂O production (NO_3^- -N₂O reaction step). Moreover, during partial consumption of the produced N₂O by reduction to N₂, the isotopic signature of the remaining N₂O is further modified.

The net isotope effects (η) for such multistep processes are actually a result of a several intrinsic isotopic effects (ϵ) occurring due to the successive enzymatic reactions as well as during physical processes like, *e.g.*, substrate

transport, adsorption, and formation of substrate-enzyme complexes (Elsner et al., 2005; Ostrom and Ostrom, 2011; Well et al., 2012). Thus, the intrinsic isotopic effects (ϵ) are stable and characteristic for a particular process and net isotope effects (η) are determined for a more complex sequences of chemical and physical processes and represent an interaction between them, and hence may differ due to changes in *e.g.*, environmental conditions, process rates or substrate availability (Elsner, 2010; Ostrom and Ostrom, 2011). The variations in η values can be quite well explained by the balance between isotopic fractionation associated with enzymatic reactions and with substrate and product diffusion. For denitrification processes the Farquhar equation was proposed as mathematical description for η values (Jinuntuya-Nortman et al., 2008; Ostrom and Ostrom, 2011). However, observed isotope effects can be additionally influenced by other phenomena, like, *e.g.*, an inhomogeneous substrate dispersion, the formation of isolated micro-sites like dead-end pores and spatial and temporal heterogeneity of reaction rates (Well et al., 2012), which are not included in the definition of η . The eventual isotope effects, taking into account all the possibly contributing processes, are defined as apparent isotope effects (AIE). Hence, whereas η represents the true isotopic fractionation associated with particular process, which can be theoretically fully explained, by a balance between enzymatic and diffusion fractionation factors, and predicted for the given conditions, AIE is the apparent effect, which is a result of all possible coexisting factors, often not yet fully understood and mathematically defined. Based on the current knowledge, we are still not able to precisely quantify all the factors contributing to the AIE of denitrification processes. Hence, in this study, for calculation purposes we assumed we were dealing with η , but simultaneously kept in mind that the actual AIEs may be more complex.

Current knowledge about the fractionation factors associated with denitrification processes is mainly based on pure culture studies (Barford et al., 1999; Casciotti et al., 2002; Toyoda et al., 2005; Sutka et al., 2006, 2008). Additionally, there are also a few studies with intact soils concerning N₂O production (Mariotti et al., 1981; Menyailo and Hungate, 2006; Perez et al., 2006; Well and Flessa, 2009b) and N₂O reduction (Ostrom et al., 2007; Vieten et al., 2007; Well and Flessa, 2009a). The reported ranges of AIEs are very wide and explanations for these large variations are still ambiguous. The most common explanation is a balance between fractionation factors associated with enzymatic reactions and with substrate diffusion (Jinuntuya-Nortman et al., 2008; Ostrom and Ostrom, 2011). Moreover, a theory of non-steady fractionation due to transient kinetics of enzymatic reactions has been proposed, taking into

account biomass and enzyme dynamics (Maggi and Riley, 2009, 2010).

However, no studies conducted so far have determined the fractionation factors under in situ conditions, or even under experimental conditions, where production and reduction occur simultaneously. Here we present the first attempt to determine both fractionation factors associated with simultaneously occurring N_2O production and reduction in the course of denitrification in soils, *i.e.*, with heterogeneous distribution of substrates, transformation and transport rates and in presence of diverse soil microbial communities. We propose two original approaches for investigations of isotopic effects during denitrification based on simultaneous determination of both reaction steps, *i.e.*, production and reduction. Such an approach has a clear advantage over experiments which separate these two reaction steps. Namely, under natural conditions production and reduction occur simultaneously within the same soil micro-sites or even the same microbial cells. Thus, artificial separation of these processes may lead to pronounced experimental artefacts as already suggested by Well and Flessa (2009a).

The main difficulty in conducting an experiment analysing the whole denitrification process is the unknown contribution of N_2O reduction. Hence, for a reliable modelling of fractionation factors of both N_2O production and reduction, independent quantitative data of N_2O reduction are necessary. There are several methods available for determining the N_2O reduction: direct N_2 -measurements (incubations under the N_2 -free atmosphere), ^{15}N tracing (incubations with addition of ^{15}N -labelled NO_3^-) and the reduction inhibition method (incubations with acetylene application). Here we show and compare the results obtained by using all of these methods in different experimental approaches.

The objective of our study was to determine fractionation factors associated with N_2O production and reduction during denitrification. Moreover, we wanted to elucidate factors controlling the magnitude of the apparent isotope effects. This was done by comparing different experimental approaches to assess fractionation factors and by covering a range of soil types and conditions.

2. METHODS

2.1. Experimental set-ups

The summary of all experimental conditions in various incubation treatments used for this study is presented in Table 1.

2.1.1. Experiment 1 – indirect method, static incubation

The static incubation technique was applied in an anoxic atmosphere (N_2). Two arable soil types were used: a *Luvisol* with loamy sand texture (experiment 1A–D) and *Haplic Luvisol* (experiment 1E–F) with silt loam texture, characterised by total C content of 1.43% and 1.62%, total N content of 0.10% and 0.13%, and pH (in 0.01 M CaCl_2) of 5.67 and 7.38, respectively.

The soil was air dried to a water content of 14.1 and 17.2 wt.% for the loamy sand and silt loam, respectively, and sieved at 2 mm mesh size. Afterwards, the soil was rewetted

to obtain a WFPS (water filled pore space) of 80% and fertilised with 50 mg N-NO_3 per kg soil. This was achieved by evenly distributed addition of nitrate solution of adequate concentration and volume depending on the targeted treatment. Then soils were thoroughly mixed to obtain the homogenous distribution of water and fertilizer and equivalent of 100 g of dry soil was repacked into each incubation jar with bulk densities of 1.3 g cm^{-3} for the silt loam soil and 1.6 g cm^{-3} for the loamy sand soil. The 0.8 L Weck jars (J. WECK GmbH u. Co. KG, Wehr, Germany) were used with airtight rubber seal and with two three-way valves installed in their glass cover to enable sampling and jars flushing. The jars were flushed with N_2 with ca. 500 mL min^{-1} for 10 min to create anoxic conditions. Immediately after flushing acetylene (C_2H_2) was added to inhibit N_2O reduction in selected jars, by replacing 80 mL of N_2 with C_2H_2 , which resulted in 10 kPa C_2H_2 in the headspace. The soils were incubated for ca. 25 h and four sample collections were performed in 4 to 10 h intervals by transferring 30 mL of headspace gases into two preevacuated 12-mL Labco Exetainer® (Labco Limited, Ceredigion, UK). The volume of taken sample was immediately replaced by pure N_2 gas.

In order to precisely determine the O-exchange with soil water we applied various treatments differing in soil water and soil nitrate isotopic signatures (similar to Snider et al. (2009)). This was achieved by rewetting the soils with two different waters of very distinct isotopic signatures: *heavy water* ($\delta^{18}\text{O}_{\text{H}_2\text{O}} = -1.5\text{‰}$) and *light water* ($\delta^{18}\text{O}_{\text{H}_2\text{O}} = -14.8\text{‰}$) and by adding two different nitrate fertilisers: natural *Chile saltpeter* (ca. $\delta^{15}\text{N}_{\text{NO}_3} = 1\text{‰}$; $\delta^{18}\text{O}_{\text{NO}_3} = 56\text{‰}$) and *synthetic NaNO_3* (ca. $\delta^{15}\text{N}_{\text{NO}_3} = 6\text{‰}$; $\delta^{18}\text{O}_{\text{NO}_3} = 27\text{‰}$). Additional treatments with addition of ^{15}N -labelled NaNO_3 (98 at.% ^{15}N) were used to control the efficiency of acetylene inhibition and to determine the product ratio in not-inhibited treatments. Inhibition was applied to all treatments with synthetic nitrate and to half of the treatments with Chile saltpeter and ^{15}N -labelled nitrate. As a result, eight different incubation treatments were prepared for each soil type. Each treatment was incubated in three replicates. The incubation of the silt loam soil was conducted under controlled temperature of 22 °C (experiment 1E–F). Two incubations were conducted for the sandy soil: under 22 °C (experiment 1C–D) and 8 °C (experiment 1A–B – see Table 1) to check if the isotopic fractionation associated with O-exchange process is temperature-dependent.

2.1.2. Experiment 2 – indirect method, dynamic incubation

The soil incubation procedure has been described in detail by (Well and Flessa, 2009b). Here we present only briefly the general approach. The dynamic incubation technique in anoxic atmosphere (N_2) was applied. Two arable soils were used: classified as *Haplic Luvisol* (experiment 2C–D) and as *Gleyic Podsol* (experiment 2A–B) characterised by total C content of 1.48% and 2.30%, total N content of 0.16% and 0.14%, and pH of 6.1 and 5.6, respectively. Soil samples were packed into 400-mL screw-cap jars (8 cm height, 8.2 cm i.d.) to a height of 5 cm with bulk densities of 1.2 g cm^{-3} for the silt loam soil, and 1.5 g cm^{-3} for the sandy soil, giving dry weights per jar of 316 g and

Table 1
Experimental conditions applied in the experiments 1, 2, and 3.

| Experiment | Soil | WFPS | Temp. | Fertiliser amendment | mgN–NO ₃ /kg dry soil | $\delta^{15}\text{N}(\text{NO}_3)$ [‰] | $\delta^{18}\text{O}(\text{NO}_3)$ [‰] | $\delta^{18}\text{O}(\text{H}_2\text{O})$ [‰] | Incubation | Product ratio determination | |
|------------|------|------------|-------|----------------------|----------------------------------|--|--|---|-------------------------|--|--|
| 1 | 1A | Loamy sand | 83 | 8 °C | Chile saltpeter | 60.3 | 2.0 ^a | 38.2 ^a | –9.2/–13.5 ^c | Static in N ₂ , 25 h | C ₂ H ₂ addition combined with ¹⁵ N-tracing |
| | 1B | | 83 | | NaNO ₃ | 59.1 | 7.0 ^a | 17.0 ^a | | | |
| | 1C | | 81 | 22 °C | Chile saltpeter | 56.1 | 2.3 ^a | 42.4 ^a | | | |
| | 1D | | 78 | | NaNO ₃ | 56.0 | 6.3 ^a | 19.3 ^a | | | |
| | 1E | Silt loam | 82 | 22 °C | Chile saltpeter | 77.5 | 2.3 ^a | 31.8 ^a | –2.6/–8.7 ^c | | |
| | 1F | | 83 | | NaNO ₃ | 78.7 | 5.4 ^a | 15.8 ^a | | | |
| 2 | 2A | Sand | 66 | 15 °C | No | 47.5 | –0.5 ^a | 8.5 ^a | –6.1 ^c | Dynamic in N ₂ , N ₂ flow 5–10 mL min ^{–1} , 3 days | C ₂ H ₂ addition |
| | 2B | | 66 | | KNO ₃ | 145.4 | 3.0 ^a | 20.7 ^a | | | |
| | 2C | Silt loam | 72 | | No | 62.4 | –5.7 ^a | 13.7 ^a | –4.2 ^c | | |
| | 2D | | 72 | | KNO ₃ | 205.9 | –4.2 ^a | 23.7 ^a | | | |
| 3 | 3A | Silty clay | 49 | 20 °C | KNO ₃ | 109.8 | 6.5 ^b | 22.8 ^b | ca. –8 ^d | Dynamic in He, He flow 20–22 mL min ^{–1} , up to 10 days | Direct online measurements of N ₂ emissions |
| | 3B | Sandy loam | 47 | | | 64.9 | | | | | |
| | 3C | | 54 | | KNO ₃ | 38.2 | | | | | |
| | 3D | | 54 | | KNO ₃ + urea | 40.4 | | | | | |
| | 3E | | 53 | | KNO ₃ | 37.2 | | | | | |

^a The soil nitrate extracts after fertiliser amendment were analysed at the beginning of the experiment.

^b Fertiliser solution analysed (the soil solution was replaced by fertiliser solution).

^c Soil water extracted and analysed; given values for treatment with heavy/light water, respectively.

^d Soil water not analysed, estimated with $\pm 2\%$.

396 g, respectively. The jars were sealed airtight with plastic-coated metal lids equipped with fittings for inlet and outlet flow lines. Four replicates per treatments were then integrated into a previously described microcosm system (Well and Flessa, 2009b) which enabled continuous flushing of the headspace with a controlled flow of N₂ (Westfalengas, Münster, Germany) at 5 to 10 mL min^{–1}. Triplicate gas samples were collected using one 115-mL serum bottle sealed with grey butyl crimp-cap septa (Part # 611012, Altmann, Holzkirchen, Germany) and two 12-mL Labco Exetainer® (Labco Limited, Ceredigion, UK) which were connected in line with the exhaust air of the microcosms. Flow rates were measured at the exhaust before each sampling using a high precision digital flow meter (Alltech Associates Inc., Deerfield, IL, USA).

Microcosms were incubated at 15 °C for three days. Samples were collected daily. In half of the treatments, N₂O reduction was inhibited by establishing 5 kPa C₂H₂ (Westfalengas, Münster, Germany, purity >99.6%) in the intake air flow, which was achieved by mixing controlled flows of N₂ and C₂H₂.

2.1.3. Experiment 3 – N₂-free incubations

The soil incubation procedure has been described in detail by Köster et al. (2013). Here we present only briefly the general approach. Laboratory incubations were carried out under N₂-free atmosphere, where the fluxes of both N₂O and N₂ were analysed continuously (in approx. 10 h intervals) fully automated by gas chromatography and samples for N₂O isotopologue analysis were collected once a day. Two different arable soil types were used for the incubation: sandy loam, classified as *Stagnic Luvisol* (experiment 3A) and silty clay soil, classified as *Fluvisollic Gleysol* (experiment 3B–E) characterised by total C content of 1.53% and 2.33%, total N content of 0.15% and 0.23%, and pH of 6.92 and 7.12, respectively. The soil solution was exchanged with fertiliser solution (KNO₃) by repeated saturation and drainage of the soil. In experiment 3D soil was additionally fertilised with urea. The water content was about 14 and 21 wt.% for the sandy loam and silty clay soils, respectively, which corresponds to ca. 50% WFPS.

Each soil was incubated under anaerobic conditions in four replicates. 1.5 kg (3A and B) or 1.6 kg (3C–E) fresh

soil was repacked into each incubation vessel. The vessels were continuously flushed with He at a flow rate of ca. 20–22 mL min⁻¹. The incubation lasted nine days under controlled temperature (20 °C) under anoxic conditions.

2.2. Chromatographic analyses

In Experiments 1 and 2 the samples for gas concentration analyses were collected in Labco Exetainer® (Labco Limited, Ceredigion, UK) vials. Samples from Experiment 1 were analysed using an Agilent 7890A gas chromatograph (Agilent Technologies, Santa Clara, CA, USA) equipped with an electron capture detector (ECD) and from Experiment 2 using a Fisons GC 8000 gas chromatograph (Fisons Instruments S.p.A., Milano, Italy). Precision as given by the standard deviation (1σ) of four standard gas mixtures was typically 1.5%.

In Experiment 3, online trace gas concentration analysis of N₂O and N₂ was performed with a Varian gas chromatograph (450-GC, Varian B.V., Middelburg, The Netherlands) using a thermal conductivity detector (TCD) for N₂ measurements and an electron capture detector (ECD) for N₂O measurements. The measurements precision was better than 20 ppb for N₂O and 2 ppm for N₂.

2.3. Isotopic analyses

2.3.1. Natural abundance N₂O

N₂O samples from Experiments 1 and 3 were analysed using a Delta V isotope ratio mass spectrometer (Thermo Scientific, Bremen, Germany) coupled to automatic preparation system: Precon + Trace GC Isolink (Thermo Scientific, Bremen, Germany) where N₂O was pre-concentrated, separated and purified. Samples from Experiment 2 were measured using a modified Precon connected to Delta XP isotope ratio mass spectrometer (Thermo Scientific, Bremen, Germany) as described by Well and Flessa (2009b).

In the mass spectrometer, N₂O isotopomer signatures were determined by measuring *m/z* 44, 45, and 46 of intact N₂O⁺ ions as well as *m/z* 30 and 31 of NO⁺ fragments ions. This allows the determination of average δ¹⁵N (δ¹⁵N^{bulk}), δ¹⁵N^α (δ¹⁵N of the central N position of the N₂O molecule), and δ¹⁸O (Toyoda and Yoshida, 1999). δ¹⁵N^β (δ¹⁵N of the peripheral N position of the N₂O molecule) is calculated from δ¹⁵N^{bulk} = (δ¹⁵N^α + δ¹⁵N^β)/2. The ¹⁵N site preference (SP) is defined as SP = δ¹⁵N^α - δ¹⁵N^β. The scrambling factor and ¹⁷O-correction have been taken into account (Röckmann et al., 2003). Pure N₂O was used as the reference gas and this was analysed for isotopologue signatures in the laboratory of the Tokyo Institute of Technology using calibration procedures reported previously (Toyoda and Yoshida, 1999; Westley et al., 2007).

All isotopic signatures are expressed as ‰ deviation from the ¹⁵N/¹⁴N and ¹⁸O/¹⁶O ratios of the reference materials (*i.e.*, atmospheric N₂ and Vienna Standard Mean Ocean Water (V-SMOW), respectively). The analytical precision determined as standard deviation (1σ) of the internal standards for measurements of δ¹⁵N, δ¹⁸O and SP was typically 0.1%, 0.1%, and 0.5‰, respectively.

2.3.2. ¹⁵N-labelled N₂O

The gas samples from the ¹⁵N-labelled treatments in Experiment 1 were analysed for *m/z* 29 and 30 of N₂ using a modified GasBench II preparation system coupled to MAT 253 isotope ratio mass spectrometer (Thermo Scientific, Bremen, Germany) according to Lewicka-Szczepak et al. (2013). This system allows determination of the N₂ concentration originating from the ¹⁵N labelled pool and hence the contribution of N₂O reduction as well as the ¹⁵N enrichment in the denitrifying pool.

2.3.3. Soil analyses

Soil nitrates were extracted by shaking 11 g soil in 110 mL 0.01 M CaCl₂ solution at room temperature for one hour and NO₃⁻ concentrations were determined colorimetrically. δ¹⁵N and δ¹⁸O of initial and residual nitrate in the soil solution were determined using the bacterial denitrification method (Sigman et al., 2001; Casciotti et al., 2002). For Experiment 1 and 2 the initial nitrate means a mixture of soil and fertilizer nitrate and for Experiment 3 this is the fertilizer solution replacing the original soil solution.

Soil water was extracted with the method described by Königer et al. (2011) and δ¹⁸O of water samples was measured at the Centre for Stable Isotope Research and Analysis (University of Göttingen) using Delta V plus isotope ratio mass spectrometer coupled to a Thermal Combustion Elemental Analyser (Thermo Scientific, Bremen, Germany).

2.4. Determination of fractionation factors

All the determined η values are expressed as product-to-substrate fractionation (η_{P-S}). This means that negative η values indicate product depletion in heavy isotopes in relation to substrate.

2.4.1. η of N₂O production (η₁)

¹⁵N bulk: δ¹⁵N of produced N₂O are governed by the isotopic fractionation factor between soil nitrate (substrate) and N₂O (product). Moreover, during the reaction progress the residual nitrate is gradually enriched in heavy isotopes. This enrichment can be calculated applying Rayleigh distillation equations (Mariotti et al., 1981):

$$\delta_S \cong \delta_{IS} + \eta_1 * \ln f_1 \quad (1)$$

where: δ_S and δ_{IS} are the isotopic signatures of residual and initial nitrate, respectively, *f*₁ is the fraction of the residual nitrate-N calculated by subtracting the initial nitrate concentration (N_{NO₃⁻*i*) and the cumulative N emission as denitrification products (N_{N₂+N₂O}) for each time step of the process:}

$$f_1 = (N_{NO_3^-i} - N_{N_2+N_2O})/N_{NO_3^-i} \quad (2)$$

And η₁ is the net isotope effect for N₂O production.

Having determined δ_S, δ_P (isotopic composition of the instantaneously produced N₂O) can be calculated as follows:

$$\delta_P \cong \delta_S + \eta_1 \quad (3)$$

Eq. (3) can be applied for dynamic incubations (Experiment 2 and 3), since δ_P is obtained from isotopic analysis gas samples obtained during continuous flushing of the

headspace. For the static incubations (Experiment 1) where N₂O was accumulated during the experiment, the following modified Rayleigh equation was used (Fry, 2006):

$$\delta_{AP} \cong \delta_{IS} - \eta_1 * \left(\frac{f_1}{1 - f_1} * \ln f_1 \right) \quad (4)$$

where δ_{AP} is the isotopic signature of accumulated product.

For Experiments 1 and 2 the η_1^{15N} was calculated directly from the results of the acetylated treatments, where N₂O reduction was inhibited; hence the measured N₂O isotopic signature is a result of fractionation during N₂O production by denitrification.

¹⁸O: δ^{18O} of produced N₂O are additionally influenced by the process of O-exchange with soil water, which may be very high or even nearly complete (Kool et al., 2009; Snider et al., 2009). But the amount of this exchange cannot be assumed a priori, and hence the initial isotopic signature of the O-precursor is actually not known. Therefore, in this case the η_1^{18O} cannot be easily calculated and actually only the Δ values representing the difference between product and the potential substrate can be given. Using the $\delta^{18O}_{N_2O}$ of acetylated treatments for Experiments 1 and 2 we have calculated these values for two extreme cases: (i) that the O-precursor is entirely water ($\Delta^{18O}_{N_2O-H_2O}$), *i.e.*, assuming the full exchange with soil water or (ii) that the O-precursor is entirely nitrate ($\Delta^{18O}_{N_2O-NO_3}$), *i.e.*, assuming there is no exchange with soil water at all.

SP: The ¹⁵N site preference of produced N₂O (SP) is independent of the isotopic signature of the substrates and is mainly governed by the species contribution in active soil microbial community (Sutka et al., 2003). Therefore, the SP_{N₂O} measured in the acetylated treatments (Experiments 1 and 2) represent the characteristic η_1 SP (Well and Flessa, 2009b).

2.4.2. η of N₂O reduction (η_2)

The process of N₂O reduction to N₂ can be also described with Rayleigh fractionation, hence Eq. (1) in the following form was applied:

$$\delta_R \cong \delta_P + \eta_2 * \ln f_2, \quad (5)$$

where δ_R stands for the isotopic composition of residual N₂O directly measured in all experiments; δ_P is the produced N₂O unaffected by reduction, which was either directly measured (Experiments 1 and 2, acetylated treatments), or modelled (Experiment 3, see next section); f_2 is the product ratio of the reduction process (N₂O/(N₂O + N₂)), calculated either based on comparison of acetylated and non-acetylated treatments (Experiments 1 and 2) or direct measurements of N₂O and N₂ fluxes. In Experiment 1, the product ratio was additionally checked by the incubation with ¹⁵N-labelled nitrate.

2.4.3. Modelling approach for Experiment 3

In Experiment 3, η of N₂O production was not directly determined because there was no treatment with inhibited N₂O reduction, *i.e.*, N₂O production and N₂O reduction always occurred simultaneously. Therefore, a modelling approach has been applied for determining η values for both processes (η_1 for N₂O production and η_2 for N₂O

reduction). For this purpose the Eqs. (1)–(3) and (5) were applied to describe the whole process of denitrification. The starting values of η_1 and η_2 for numerical optimization were adopted from the estimates of previous literature reports. For η_1 following values were used: (i) $\eta_1^{15N} = -50\text{‰}$ (Well and Flessa, 2009b); (ii) η_1 SP = 5‰ (Well and Flessa, 2009b); (iii) $\delta^{18O}_{\text{produced N}_2\text{O}} = +40\text{‰}$ (Snider et al., 2009). For ¹⁸O and SP values a constant production signature was assumed, since δ^{18O} of produced N₂O is mainly governed by the isotopic exchange of O-isotopes with soil water (Kool et al., 2009; Snider et al., 2009), which can be assumed to show little variation during incubation in enclosures due to minimal evaporation. Assuming a nearly full O-exchange with soil water, the enrichment in ¹⁸O of the residual nitrate can be neglected. The SP of produced N₂O is independent of the isotopic signature of the substrates and is mainly governed by the species contribution in active soil microbial community (Sutka et al., 2003). We have assumed this community is not changing significantly during the experiment, thus the SP of emitted N₂O (η_1 SP) should be stable. For η_2 the following initial values were used for model fitting: (i) $\eta_2^{15N} = -7\text{‰}$; (ii) η_2 SP = -6‰ ; (iii) $\eta_2^{18O} = -15\text{‰}$ (Well and Flessa, 2009a).

The best fit values were found by minimizing the sum of squared errors. This was done in two ways, (i) using the Microsoft Office Excel 2007 Solver tool applying simplex method and (ii) using the R 3.0.1 (R Core Team, 2013) applying Levenberg–Marquardt (LM) method. For the latter approach Markov chain Monte Carlo (MCMC) simulations as implemented in package FME were conducted subsequently to access parameter uncertainty (Soetaert, 2010; Soetaert and Petzoldt, 2010). The results obtained by these two methods were in excellent agreement, and only the results of the LM + MCMC approach are presented and discussed here, as they provide additional information on parameter uncertainty. In Supplementary materials as Appendix 1 we provide an example of R code illustrating how the fractionation models were fitted and parameter uncertainties derived using MCMC. The highest probability estimates from the MCMC simulation are presented as the final results.

2.5. Statistical methods

Statistical analyses were performed using the Microsoft Office Excel 2007 ‘data analysis’ tool and R 3.0.1 (R Core Team, 2013). For results comparisons, ANOVA variance analysis was used with the significance level α of 0.05. The uncertainty values provided for the measured parameters represent the standard deviation (1 σ) of the replicates. The standard errors given for the directly calculated (not modelled) values of fractionation factors are calculated using Gauss’s error propagation equation taking into account standard errors of all individual parameters.

3. RESULTS

3.1. Experiment 1

During this experiment four samples were collected in the course of 25 h and the results showed some clear time

trends. The complete data obtained for all samplings are presented in [Supplementary materials \(Appendix 2\)](#). The average process rates and δ values obtained from acetylated treatments used for the determination of η_1 are presented in [Table 2](#). The average process rates and δ values obtained from non-acetylated treatments used for the determination of η_2 are presented in [Table 3](#).

Gross N_2O production determined in acetylated treatments varied between $2843 \mu\text{g N kg}^{-1} \text{d}^{-1}$ for the sandy soil at low temperature (1A) and $8915 \mu\text{g N kg}^{-1} \text{d}^{-1}$ at higher temperature (1D). At the same temperature conditions the loamy sand soil showed higher production than the silt loam soil by about $2000 \mu\text{g N kg}^{-1} \text{d}^{-1}$, but this difference was not statistically significant ($P = 0.05$). Net N_2O production in absence of C_2H_2 varied between 2202 and $7502 \mu\text{g N kg}^{-1} \text{d}^{-1}$. N_2O reduction calculated based on the parallel ^{15}N -labelled incubations ranged from 670 to $3272 \mu\text{g N kg}^{-1} \text{d}^{-1}$, showing the highest value for the silt loam soil (1E). Consequently, the N_2O -to- $(N_2 + N_2O)$ product ratio of denitrification was significantly ($P < 0.001$) lower for silt loam soil (1E) when compared to loamy sand (1A, 1C). But no significant differences ($P = 0.2$) in the product ratio were found for different temperatures treatments (1A to 1C).

$\delta^{18}\text{O}$ of produced N_2O in treatments with C_2H_2 varied from 4.8‰ to 16.3‰ and were about 5‰ higher in treatments with heavy water when compared the treatments with light water ([Table 2](#)). This difference clearly reflects the differences in $\delta^{18}\text{O}$ of soil water ([Table 1](#)). Consequently, the calculated $\Delta^{18}\text{O}_{N_2O-H_2O}$, showing the difference in $\delta^{18}\text{O}$ between soil water and produced N_2O , were quite homogeneous for all treatments. Hence, the average $\Delta^{18}\text{O}_{N_2O-H_2O}$ value of $19.0 \pm 0.7\text{‰}$ can be stated as representative for all treatments. Conversely, the $\Delta^{18}\text{O}_{N_2O-NO_3}$ varied in a very wide range from -37.4‰ to -0.5‰ .

$\delta^{15}\text{N}$ of produced N_2O varied between -43.0‰ and -30.9‰ and were always significantly ($P < 0.001$) lower for the treatments with Chile saltpeter (1A, 1C, 1E) than with synthetic NaNO_3 (1B, 1D, 1F) and this difference was clearly higher in the lower temperature treatment (1A to 1B). The calculated $\eta_1^{15}\text{N}$ showed larger isotopic fractionation for treatments amended with Chile saltpeter when compared to synthetic NaNO_3 . However, this difference was only significant ($P < 0.001$) at a low temperature (1A to 1B).

The $\eta_1\text{SP}$ varied in a very narrow range from -3.6‰ to -2.1‰ . Even though the differences between three various treatments with different soils and different temperatures (1A/1C/1E; 1B/1D/1F) were very low, about 1‰ , they were always statistically significant ($P < 0.001$). However, there were no significant differences ($P = 0.3$) between the treatments with different fertilisers (1A/1B; 1C/1D; 1E/1F).

All three signatures analysed ($\delta^{18}\text{O}$, $\delta^{15}\text{N}$, and SP) always showed lower values in acetylated treatments when compared to the respective non-acetylated treatments. Therefore, the corresponding η_2 values were always negative. $\eta_2^{18}\text{O}$ varied in a narrow range around -17.4 ± 0.9 , $\eta_2^{15}\text{N}$ showed wider range between -4.6‰ and -11.0‰ and $\eta_2\text{SP}$ varied in a very narrow range around $-6.0 \pm 0.4\text{‰}$ without significant differences between different treatments.

Table 2
Gross N_2O production rates (pN_2O) and isotopic signatures (presented as average of all samplings with standard deviation) determined for experiment 1 and 2 in acetylated treatments. Isotopic fractionation factors of the NO_3^- -to N_2O step (η_1) were calculated with Eq. (1).

| | pN_2O [$\mu\text{g N/kg/d}$] | $\delta^{18}\text{O}$ [‰] | | $\delta^{15}\text{N}$ [‰] | SP [‰] | $\Delta^{18}\text{O}_{N_2O-H_2O}$ [‰] | | $\Delta^{18}\text{O}_{N_2O-NO_3}$ [‰] | | $\eta^{15}\text{N}_{NO_3-N_2O}$ [‰] | $\eta\text{SP}_{NO_3-N_2O}$ [‰] |
|--------------|----------------------------------|---------------------------|------------|---------------------------|------------|---------------------------------------|------------|---------------------------------------|-------------|-------------------------------------|---------------------------------|
| | | Heavy w. | Light w. | | | Heavy w. | Light w. | Heavy w. | Light w. | | |
| <i>Exp 1</i> | | | | | | | | | | | |
| 1A | 2843 ± 660 | 11.0 ± 0.6 | 6.1 ± 0.5 | -42.0 ± 1.5 | -2.3 ± 0.5 | 20.2 ± 0.8 | 19.6 ± 0.7 | -27.2 ± 1.2 | -32.1 ± 1.1 | -44.7 ± 1.4 | -2.3 ± 0.4 |
| 1B | 3010 ± 841 | 10.6 ± 0.5 | 5.9 ± 0.5 | -33.9 ± 1.9 | -2.1 ± 0.8 | 19.8 ± 0.7 | 19.4 ± 0.7 | -6.4 ± 1.1 | -11.1 ± 1.1 | -41.6 ± 0.9 | -2.1 ± 0.7 |
| 1C | 8792 ± 2022 | 10.0 ± 0.7 | 5.0 ± 0.7 | -36.0 ± 3.3 | -3.3 ± 0.9 | 19.2 ± 0.9 | 18.5 ± 0.9 | -32.4 ± 1.2 | -37.4 ± 1.2 | -40.3 ± 2.1 | -3.3 ± 0.8 |
| 1D | 8915 ± 2238 | 9.8 ± 0.4 | 4.8 ± 0.5 | -30.9 ± 3.3 | -3.6 ± 0.8 | 19.0 ± 0.6 | 18.3 ± 0.7 | -9.5 ± 1.1 | -14.5 ± 1.1 | -39.2 ± 2.1 | -3.6 ± 0.6 |
| 1E | 6624 ± 2795 | 16.3 ± 0.8 | 10.2 ± 0.6 | -43.0 ± 2.6 | -2.5 ± 0.9 | 18.9 ± 0.9 | 19.1 ± 0.8 | -15.5 ± 1.3 | -21.6 ± 1.2 | -46.5 ± 1.8 | -2.5 ± 0.8 |
| 1F | 6820 ± 2952 | 15.3 ± 0.5 | 9.5 ± 0.6 | -38.6 ± 2.5 | -2.8 ± 0.6 | 17.9 ± 0.7 | 18.4 ± 0.8 | -0.5 ± 1.1 | -6.3 ± 1.2 | -45.1 ± 1.8 | -2.8 ± 0.5 |
| <i>Exp 2</i> | | | | | | | | | | | |
| 2A | 1120 ± 59 | 21.7 ± 2.5 | 21.7 ± 2.5 | -35.4 ± 2.2 | 3.4 ± 2.1 | 24.8 ± 5.0 | 24.8 ± 5.0 | 4.9 ± 3.0 | 4.9 ± 3.0 | -47.1 ± 3.3 ^a | 1.7 ± 2.9 |
| 2B | 955 ± 86 | 21.3 ± 1.0 | 21.3 ± 1.0 | -42.5 ± 1.3 | -0.2 ± 1.0 | 25.1 ± 3.6 | 25.1 ± 3.6 | -6.2 ± 1.0 | -6.2 ± 1.0 | -50.0 ± 1.2 ^a | -1.0 ± 1.4 |
| 2C | 1976 ± 237 | 11.9 ± 1.3 | 11.9 ± 1.3 | -39.9 ± 2.1 | -5.4 ± 1.6 | 15.7 ± 1.8 | 15.7 ± 1.8 | -3.0 ± 2.1 | -3.0 ± 2.1 | -51.6 ± 1.3 ^a | -4.7 ± 1.9 |
| 2D | 1611 ± 320 | 17.4 ± 1.2 | 17.4 ± 1.2 | -45.8 ± 1.0 | -4.9 ± 2.1 | 20.0 ± 2.7 | 20.0 ± 2.7 | -11.1 ± 1.0 | -11.1 ± 1.0 | -52.8 ± 1.5 ^a | -4.5 ± 1.9 |

^a The results published before in [Well and Flessa \(2009b\)](#).

* Various treatments regarding added soil water in experiment 1 (isotopically depleted – 'light w.' and enriched water – 'heavy w.' was used).

Table 3
Net N₂O production (pN₂O) and reduction (rN₂O) rates and isotopic signatures (presented as average of all samplings with standard deviation) determined for experiment 1 and 2 in non-acetylated treatments. Isotopic fractionation factors of the N₂O-to-N₂ step (η_2) were calculated with Eq. (5) based on comparison of acetylated and non-acetylated treatments.

| Exp | pN ₂ O [$\mu\text{g N/kg/d}$] | rN ₂ O [$\mu\text{g N/kg/d}$] | N ₂ O/ (N ₂ + N ₂ O) | $\delta^{18}\text{O}$ [‰] | | $\delta^{15}\text{N}$ [‰] | SP [‰] | $\eta^{18}\text{O}_{\text{N}_2\text{-N}_2\text{O}}$ [‰] | $\eta^{15}\text{N}_{\text{N}_2\text{-N}_2\text{O}}$ [‰] | $\eta^{\text{SP}}_{\text{N}_2\text{-N}_2\text{O}}$ [‰] |
|--------------|--|--|--|---------------------------|------------|---------------------------|------------|---|---|--|
| | | | | Heavy w.* | Light w.* | | | | | |
| Exp 1 | | | | | | | | | | |
| 1A | 2202 ± 348 | 670 ± 348 ^a | 0.74 ± 0.04 ^a | 15.7 ± 2.3 | 10.2 ± 1.7 | -40.8 ± 1.4 | -0.6 ± 1.0 | -17.6 ± 1.3 | -15.7 ± 0.8 | -4.6 ± 6.3 |
| 1C | 7502 ± 1875 | 2778 ± 1339 ^a | 0.79 ± 0.06 ^a | 15.8 ± 3.9 | 10.5 ± 3.5 | -32.3 ± 1.9 | -1.5 ± 1.7 | -17.9 ± 0.2 | -17.1 ± 0.7 | -11.0 ± 3.7 |
| 1E | 3659 ± 1501 | 3272 ± 829 ^a | 0.60 ± 0.03 ^a | 26.8 ± 1.6 | 20.1 ± 0.8 | -38.7 ± 1.9 | 0.8 ± 1.0 | -18.4 ± 7.5 | -17.6 ± 8.5 | -7.0 ± 2.5 |
| Exp 2 | | | | | | | | | | |
| 2A | 263 ± 36 | 857 ± 69 ^b | 0.23 ± 0.04 ^b | 24.4 ± 2.5 | | -47.5 ± 1.6 | 6.3 ± 1.8 | -2.5 ± 1.8 | 7.6 ± 1.6 | -2.3 ± 2.0 |
| 2B | 359 ± 25 | 596 ± 90 ^b | 0.36 ± 0.04 ^b | 22.8 ± 2.0 | | -51.8 ± 1.3 | 2.8 ± 1.6 | -1.8 ± 1.4 | 8.6 ± 1.4 | -3.4 ± 1.4 |
| 2C | 944 ± 297 | 1032 ± 380 ^b | 0.43 ± 0.12 ^b | 11.9 ± 1.5 | | -49.4 ± 1.2 | -1.7 ± 2.2 | -1.6 ± 2.3 | 9.8 ± 2.8 | -6.2 ± 3.3 |
| 2D | 1158 ± 121 | 453 ± 342 ^b | 0.65 ± 0.03 ^b | 13.6 ± 0.6 | | -53.7 ± 0.6 | -3.6 ± 1.2 | 8.9 ± 3.4 | 16.2 ± 3.6 | -5.4 ± 3.8 |

* Various treatments regarding added soil water in experiment 1 (isotopically depleted – 'light w.' and enriched water – 'heavy w.' was used).

^a Calculated based on the parallel ¹⁵N-labelled incubations.

^b Calculated based on comparison of acetylated and non-acetylated treatments.

3.2. Experiment 2

The results of Experiment 2 were already partially published by Well and Flessa (2009b), but only in regard to η_1 values, *i.e.*, only the results from the acetylated treatments were presented. Moreover, the results presented by Well and Flessa (2009b) were not evaluated according to the currently accepted procedure for ¹⁷O correction (Toyoda and Yoshida, 1999; Röckmann et al., 2003); hence, the corrected values for $\eta_1\text{SP}$ and $\Delta^{18}\text{O}$ differ from the previously published values. Therefore, here these corrected data are presented again. Additionally, the values from acetylated treatments are compared with new data of the non-acetylated treatments of the same experiment, which enabled us to determine also the η_2 values.

During Experiment 2 three samples were collected within 3 incubation days. The complete data obtained for all the three following samplings are presented in Supplementary materials (Appendix 3). The average process rates and δ values obtained from acetylated treatments used for the determination of η_1 are presented in Table 2. The average process rates and δ values obtained from non-acetylated treatments used for the determination of η_2 are presented in Table 3. The results from the first sampling were used for determination of fractionation factors between soil nitrate and produced N₂O ($\eta_1^{15}\text{N}$ and $\Delta^{18}\text{O}_{\text{N}_2\text{O}-\text{NO}_3}$), since the isotopic signatures of soil nitrate were analysed for the beginning of the experiment only, and with incubation time may undergo isotopic fractionation, which is difficult to assess. Conversely, for the determination of η_2 the results of the last two samplings were used, because in the first sampling the product ratio derived by comparing the acetylated and non-acetylated treatments was very unstable and was hence disregarded as not representative for the whole experiment.

Gross N₂O production determined in acetylated treatments ranged from 955 $\mu\text{g N kg}^{-1} \text{d}^{-1}$ for sand soil to 1976 $\mu\text{g N kg}^{-1} \text{d}^{-1}$ for silt loam soil. For both soils no significant differences ($P = 0.01$) were found between the fertilised and non-fertilised treatment. Net N₂O production in absence of C₂H₂ varied between 263 and 1158 $\mu\text{g N kg}^{-1} \text{d}^{-1}$. N₂O reduction, calculated as the difference between acetylated and not acetylated treatment, ranged from 453 to 1032 $\mu\text{g N kg}^{-1} \text{d}^{-1}$. The reduction rate of the non-fertilised treatments (2A, 2C) was significantly higher ($P < 0.001$) compared to the fertilised treatments (2B, 2D). This N-effect was also reflected in the product ratio (N₂O/(N₂ + N₂O)), which was lower for both soils in the unfertilised treatments (0.23 and 0.43) compared to the fertilised treatments (0.36 and 0.65).

$\delta^{18}\text{O}$ of produced N₂O in treatments with C₂H₂ were significantly ($P < 0.001$) higher for sand soil (2A, 2B) than for silt loam soil (2C, 2D). The calculated $\Delta^{18}\text{O}_{\text{N}_2\text{O}-\text{H}_2\text{O}}$ ranged from 15.7‰ for silt loam to 25.1‰ for sand soil. The calculated $\Delta^{18}\text{O}_{\text{N}_2\text{O}-\text{NO}_3}$ varied strongly between -11.1‰ and +4.9‰. $\delta^{15}\text{N}$ of produced N₂O were significantly ($P < 0.001$) higher for unfertilised treatments. The calculated $\eta_1^{15}\text{N}$ ranged from -52.8‰ to -47.1‰, as previously shown in Well and Flessa (2009b). The $\eta_1\text{SP}$ varied between -4.7‰ and +1.7‰ and differed significantly

($P < 0.001$) between the two soils but no significant differences ($P = 0.1$) were observed within one soil for different fertilising treatments.

$\eta_2^{18}\text{O}$ varied around -2‰ except from the treatment 2D where it was strongly positive (Table 3). $\delta^{15}\text{N}$ of all acetylated treatments were significantly higher when compared to non-acetylated treatments ($P < 0.05$). The corresponding $\eta_2^{15}\text{N}$ were thus positive and varied between 7.6‰ and 16.2‰ . For the silt loam soil, $\eta_2^{15}\text{N}$ were larger ($>9.8\text{‰}$) compared to the sand soil ($<8.6\text{‰}$). The SP of the acetylated treatments was always lower compared to non-acetylated treatments. The corresponding $\eta_2\text{SP}$ ranged from -6.2 to -2.3‰ .

3.3. Experiment 3

The results of this experiment have been described in detail elsewhere (Köster et al., 2013). Here, in Table 4, we only summarise the reaction rates and isotope values used for modelling of the η values.

Net N_2O production ranged from $236 \mu\text{g N kg}^{-1} \text{d}^{-1}$ for the sandy loam with low fertilisation (3D) to $643 \mu\text{g N kg}^{-1} \text{d}^{-1}$ for the silty clay which received high fertilisation (3A). N_2O reduction, measured directly as N_2 flux, varied between 1992 and $3464 \mu\text{g N kg}^{-1} \text{d}^{-1}$, showing the highest value for the sandy loam amended with KNO_3 and urea (3D). The product ratio was more variable in treatments with lower fertilisation (3C, 3D). The average product ratios tended to be higher for these treatments but the difference to higher fertilised treatments (3A, 3B) was not statistically significant ($P = 0.2$).

The analysed isotopic signatures of the residual N_2O ranged from 41.2‰ to 48.1‰ for $\delta^{18}\text{O}$, from -30.9‰ to -15.8‰ for $\delta^{15}\text{N}$, and from 10.1‰ to 18.5‰ for SP. All these values showed larger variations for the treatments with lower fertilisation (3C, 3D) due to a more variable product ratio. SP did not show significant differences ($P = 0.3$) between the various treatments of the sandy loam soil (3B, 3C, 3D), but was significantly higher ($P < 0.001$) for the silty clay soil.

η values shown in Table 4 are the results obtained with MCMC approach (as described in Section 2.4.3). The best fit pairs of modelled η values with standard error are given. In the Supplementary data (Appendix 4) we provide the graphs of probability density distribution for all MCMC model runs for each experiment and additionally the range of possible results within 95% confidence is given. From these graphs we can estimate the robustness of the results provided by the MCMC method based on the distribution of parameter estimates. The higher covariance of parameter estimates, larger standard error and wider range of values within the lower and upper 95% confidence limits are indicators for the higher uncertainty of the results. All these parameters are given in Appendix 4 for each experimental treatment. The best modelling results were obtained for the experiments 3C and 3D, where we got the lowest standard error of the estimated η values (Table 4) and the lowest covariance of parameter estimates (Appendix 4). The estimations for the experiments 3A and 3B were not as good as 3C and 3D, but still very valuable. Worst estimations were

Table 4

Net N_2O production (pN_2O) and reduction (rN_2O) rates and isotopic signatures (presented as average of all samplings with standard deviation). Isotopic fractionation factors of the NO_3^- -to N_2O step (η_1) and N_2O -to- N_2 step (η_2) were modelled with the MCMC method.

| Exp | 3 | pN_2O [$\mu\text{g N/kg/d}$] | rN_2O [$\mu\text{g N/kg/d}$] | $\text{N}_2\text{O}/(\text{N}_2 + \text{N}_2\text{O})$ | $\delta^{18}\text{O}$ [‰] | $\delta^{15}\text{N}$ [‰] | SP [‰] | Production, η_1 | | Reduction, η_2 | | |
|-----|-----------|--|--|--|---------------------------|---------------------------|------------|---------------------------|-------------------------|---------------------------|---|-------------------------|
| | | | | | | | | $\delta^{18}\text{O}$ [‰] | $\eta^{15}\text{N}$ [‰] | $\delta^{18}\text{O}$ [‰] | $\eta^{18}\text{ON}_2\text{-N}_2\text{O}$ [‰] | $\eta^{15}\text{N}$ [‰] |
| 3A | 643 ± 491 | 2681 ± 459 | 0.18 ± 0.09 | 42.9 ± 2.9 | -30.9 ± 7.3 | 18.5 ± 3.3 | 33.9 ± 2.5 | -54.8 ± 2.6 | 6.0 ± 1.5 | -4.6 ± 1.3 | -5.8 ± 1.2 | -6.5 ± 0.8 |
| 3B | 526 ± 385 | 1992 ± 445 | 0.19 ± 0.10 | 41.2 ± 3.7 | -27.3 ± 5.2 | 10.1 ± 4.0 | 31.0 ± 2.5 | -41.0 ± 2.1 | -3.0 ± 1.9 | -6.1 ± 1.4 | -0.5 ± 1.0 | -7.7 ± 1.1 |
| 3C | 255 ± 303 | 2164 ± 1129 | 0.28 ± 0.38 | 45.9 ± 12.4 | -21.3 ± 9.7 | 11.0 ± 8.0 | 24.4 ± 1.0 | -40.3 ± 0.7 | -2.9 ± 1.5 | -9.4 ± 0.3 | -2.2 ± 0.2 | -6.1 ± 0.6 |
| 3D | 236 ± 259 | 3464 ± 1823 | 0.24 ± 0.39 | 48.1 ± 11.9 | -15.8 ± 13.7 | 13.4 ± 7.3 | 27.0 ± 1.2 | -37.8 ± 1.0 | 2.8 ± 1.3 | -7.2 ± 0.5 | -1.4 ± 0.2 | -3.9 ± 0.4 |

* Estimated from measured N_2 fluxes.

** Determined with MCMC modelling (for details see Appendix 1 and 4).

obtained for the experiment 3E, where the ranges of possible η values were extremely wide (Appendix 4), which was also reflected in larger standard errors (Appendix 4). It appeared that this experiment was not well suited for the modelling approach, as the variations of product ratio were very small during the whole experiment. Hence, the η values cannot be estimated robustly. Therefore, we also tried to apply the modelling jointly for all the experiments with sandy loam amended with KNO_3 fertiliser (3B, 3C, 3E), which provided more input data for the model. These results were very robust and in good agreement with the results from experiments 3B and 3C, which further proved their correctness. However, this also shows that the estimates obtained for experiment 3E are biased due to too low variability of input data. Hence, these data were disregarded from the further discussion and are not shown in Table 4.

The estimated $\eta_1^{15}\text{N}$ varied around -40.7 for sandy loam amended with KNO_3 (3B, 3C), without significant differences ($P = 0.2$) between various fertilisations. A slightly, but significantly lower ($P < 0.001$) value of -37.8‰ was obtained for the treatment with urea amendment (3D), and much lower value of -54.8‰ was found for the silty clay soil. The $\delta^{18}\text{O}$ of the produced N_2O were significantly higher ($P < 0.001$) for treatments with higher fertilisation, 32.5‰ (3A, 3B), when compared to lower fertilisation, 25.7‰ (3C, 3D). The $\eta_1\text{SP}$ varied around -3.0‰ for sandy loam amended with KNO_3 (3B, 3C), without significant differences ($P = 0.5$) between different fertilisations. This value was significantly higher ($P < 0.001$) for the treatment with addition of urea, $+2.8\text{‰}$. A very different $\eta_1\text{SP}$ was obtained for silty clay soil, $+6.0\text{‰}$.

The estimated $\eta_2^{18}\text{O}$ varied in the range from -9.4‰ to -4.6‰ and were significantly lower ($P < 0.001$) for the treatments with lower fertilisation (3C, 3D). $\eta_2^{15}\text{N}$ varied between -5.8‰ and -0.5‰ with the lowest value for silty clay soil, whereas sandy loam soil showed much smaller fractionation. $\eta_2\text{SP}$ varied around -6.8‰ for the KNO_3 treatments (3A, 3B, 3C) and did not show significant differences among them ($P > 0.01$), but a significantly ($P < 0.001$) higher value of -3.9‰ was obtained for the treatment with urea addition (3D).

4. DISCUSSION

4.1. η_1 – Fractionation factors of N_2O production

There are only few studies which determined isotope effects associated with N_2O production via denitrification in whole soil microbial communities (Mariotti et al., 1981; Menyailo and Hungate, 2006; Perez et al., 2006; Snider et al., 2009; Well and Flessa, 2009b). The range of the results reported by those studies is summarised and presented in Fig. 1 in comparison to our experimental results. The previous results show a very wide range of variations, and partially indicate much smaller isotope effects when compared to our results. Such an effect might be due to coexistence of N_2O reduction, which would result in large enrichment of the residual analysed N_2O . The previous studies mostly used addition of C_2H_2 to inhibit N_2O reduction (Menyailo and Hungate, 2006; Perez et al.,

2006; Well and Flessa, 2009b). However, some of them were performed without C_2H_2 addition (Snider et al., 2009, 2013), hence the isotope effects reported in those studies refer to the whole denitrification process and not particularly to the N_2O production and consequently are not directly comparable to our data. Moreover, Perez et al. (2006) applied an unconventional C_2H_2 inhibition method, *i.e.*, aerobic incubation of pre-acetylated soil, which had not been tested for the completeness of the reduction inhibition. And indeed, these studies show the highest η_1 values, *i.e.*, $\eta_1^{15}\text{N}$ up to -10‰ (Snider et al., 2013) and -9‰ (Perez et al., 2006); $\Delta^{18}\text{O}_{\text{N}_2\text{O}-\text{H}_2\text{O}}$ up to ca. $+60\text{‰}$ (Snider et al., 2013) or $+57\text{‰}$ (Perez et al., 2006); $\eta_1\text{SP}$ up to $+17.5\text{‰}$ (Perez et al., 2006; Park et al., 2011). These values are very different from the results presented by Menyailo and Hungate (2006) and Well and Flessa (2009b), where the established C_2H_2 inhibition technique in absence of O_2 (Nadeem et al., 2013) was applied. These studies reported much lower η_1 values, *i.e.*, $\eta_1^{15}\text{N}$ from -54‰ to -24‰ ; $\Delta^{18}\text{O}_{\text{N}_2\text{O}-\text{H}_2\text{O}}$ from $+16\text{‰}$ to $+26\text{‰}$; $\eta_1\text{SP}$ from $+3\text{‰}$ to $+8\text{‰}$ (Menyailo and Hungate, 2006; Well and Flessa, 2009b). These ranges are also much closer to the values obtained in this study (see Fig. 1 – bolded bars). Hence, we suppose that the other values provided by the studies not inhibiting or not completely inhibiting N_2O reduction are not directly comparable to our data, since they do not provide the fractionation factors associated only with N_2O production, but are characteristic for the whole denitrification reaction chain. This would explain the very wide range obtained by those studies, as the N_2O reduction may vary largely during an experiment.

$\Delta^{18}\text{O}_{\text{N}_2\text{O}-\text{H}_2\text{O}}$ was generally quite stable for particular experiments, however there are large differences between the experiments. Experiment 1 was particularly designed to determine the $\Delta^{18}\text{O}_{\text{N}_2\text{O}-\text{H}_2\text{O}}$ and its controlling factors; therefore soil waters and fertilisers with different $\delta^{18}\text{O}$ were applied. However, the $\Delta^{18}\text{O}_{\text{N}_2\text{O}-\text{H}_2\text{O}}$ in this experiment varied in a very narrow range and was independent of various isotopic signatures of soil water and fertiliser, of different temperatures, of N_2O production rate and of the soil type. We found a stable shift between the soil water isotopic signature and the produced N_2O . Since waters of various isotopic signatures were used in this experiment, the method described by Snider et al. (2009) can be applied to determine the mean fraction of O-exchange between H_2O and N_2O and the associated isotopic fractionation. This method is based on the correlation between $\delta^{18}\text{O}$ of N_2O and H_2O (expressed as ‰ deviation from the $^{18}\text{O}/^{16}\text{O}$ ratios of soil nitrate), where the slope of linear regression represents the fraction of O-exchange and the intercept stands for the net isotope effect. From the results of Experiment 1 we obtained the following equation for linear regression: $\delta^{18}\text{O}_{\text{N}_2\text{O}} = 0.99 * \delta^{18}\text{O}_{\text{H}_2\text{O}} + 18.2$ ($R^2 = 0.997$; $n = 12$), which indicates the O-exchange between produced N_2O and soil water of 0.99 and the net isotopic fractionation between soil water and produced N_2O of 18.2‰ .

The obtained value for O-fractionation is very close to the observed isotopic difference between soil water and produced N_2O ($\Delta^{18}\text{O}_{\text{N}_2\text{O}-\text{H}_2\text{O}} = 19.0 \pm 0.7\text{‰}$, Table 2) because the O-exchange with soil water was almost complete in this experiment. The expected isotopic fractionation for

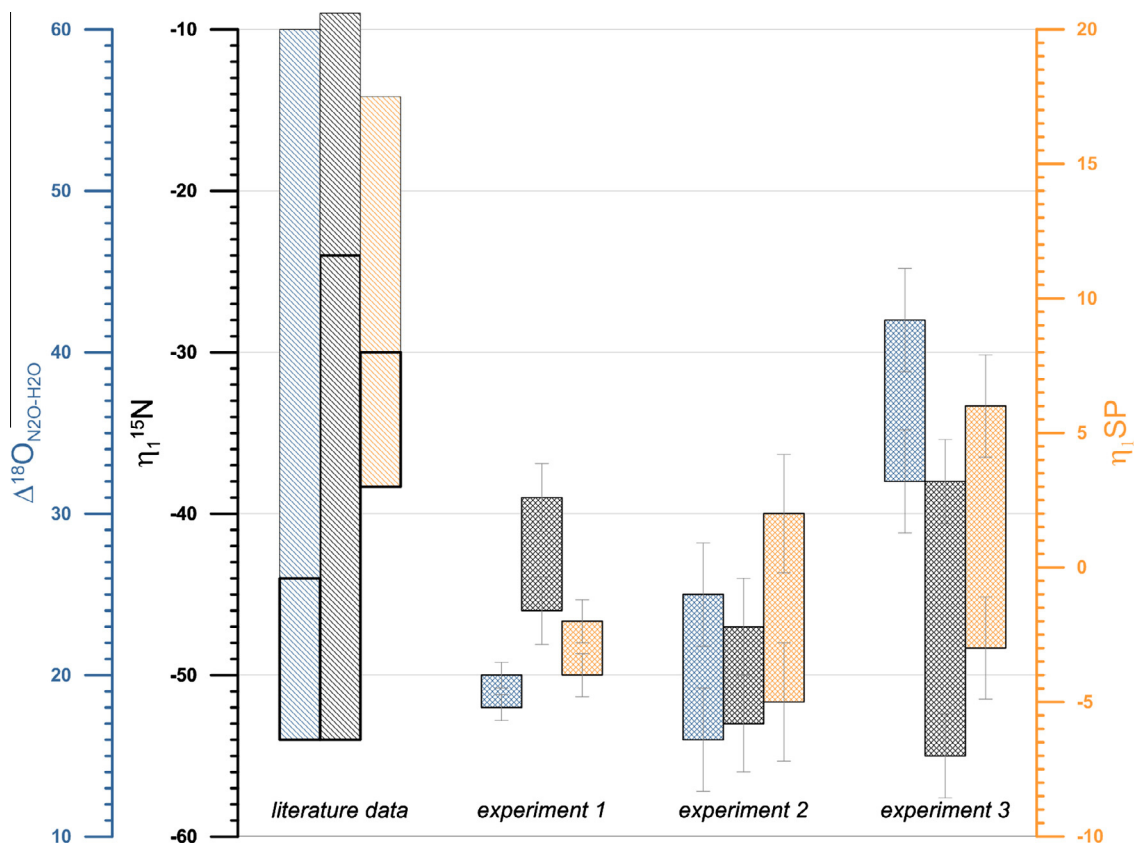


Fig. 1. Fractionation factors associated with N₂O production (η_1): reported previously in the literature (striped bars) (Mariotti et al., 1981; Menyailo and Hungate, 2006; Perez et al., 2006; Snider et al., 2009, 2013; Well and Flessa, 2009b; Menyailo and Hungate, 2006; Perez et al., 2006; Snider et al., 2009, 2013; Well and Flessa, 2009b) and determined in our experiments (checkered bars). $\Delta^{18}\text{O}$ (blue bars), $\eta_1^{15}\text{N}$ (black bars) and $\eta_1\text{SP}$ (orange bars) are shown. The literature data which are not potentially influenced by N₂O reduction (see discussion) are marked with bold bars (Mariotti et al., 1981; Menyailo and Hungate, 2006; Well and Flessa, 2009b). Error bars indicate the standard error. (For interpretation of the references to colour in this figure legend, the reader is referred to the web version of this article.)

O-exchange with water is slightly lower – about 14‰ (Casciotti et al., 2007) compared to our estimate of 18.2‰. Most probably, the additional several ‰ are due to the fractionation associated with the last step of N₂O production, *i.e.*, reduction of NO to N₂O, which takes place presumably after O-exchange with soil water (Rohe et al., submitted for publication; Snider et al., 2013).

However, the $\Delta^{18}\text{O}_{\text{N}_2\text{O}-\text{H}_2\text{O}}$ appeared to be very different for the other experiments. A very significant negative correlation between water saturation in particular experiments and observed $\Delta^{18}\text{O}_{\text{N}_2\text{O}-\text{H}_2\text{O}}$ was found ($R^2 = 0.87$; $n = 20$; see Fig. 2). As already shown the O-exchange with soil water in Experiment 1 was almost complete (99%). Unfortunately, the magnitude of O-exchange cannot be determined for two other experiments, as the method requires different isotopic signatures of waters used for incubations (Snider et al., 2009). We hypothesise that the magnitude of O-exchange decreases with decreasing WFPS and this results in higher $\Delta^{18}\text{O}_{\text{N}_2\text{O}-\text{H}_2\text{O}}$ (Fig. 2). Such a hypothesis was already proposed by Snider et al. (2013). They have shown that at low O-exchange with soil water the kinetic isotope effects associated with reduction of NO₃⁻ and NO₂⁻ (so called ‘branching effects’) result in significant ¹⁸O enrichment of the final N₂O.

Conversely, if the O-exchange is larger, these effects are diminished by the later exchange of oxygen atoms between the intermediate products (NO₂⁻ and/or NO) and H₂O and the apparent isotope effects are smaller.

But why should the lower WFPS be associated with lower extent of O-exchange with soil water? A possible explanation might be provided by the study of denitrification mechanisms by Aerssens et al. (1986) who showed that the magnitude of O-exchange decreases with the increasing nitrite (NO₂⁻) concentration. It is possible that higher WFPS favours lower NO₂⁻ concentration, due to larger dilution of the produced intermediate nitrite, its faster transportation, and consequently, faster dehydration. Unfortunately, based on results from this study we are not able to definitely prove this hypothesis. Further studies are needed to confirm the oxygen isotopic fractionation dependence on WFPS and to properly explain this correlation.

The $\eta_1^{15}\text{N}$ in all three experiments was quite similar, within the range from -55‰ to -38‰. Our experiments covered quite a wide range of N₂O production rates from about 200 to 9000 μg N kg⁻¹ d⁻¹, but no statistically significant correlation was found between production rates and $\eta_1^{15}\text{N}$ (Spearman Rank Correlation Test: $\rho = 0.03$, $P = 0.93$,

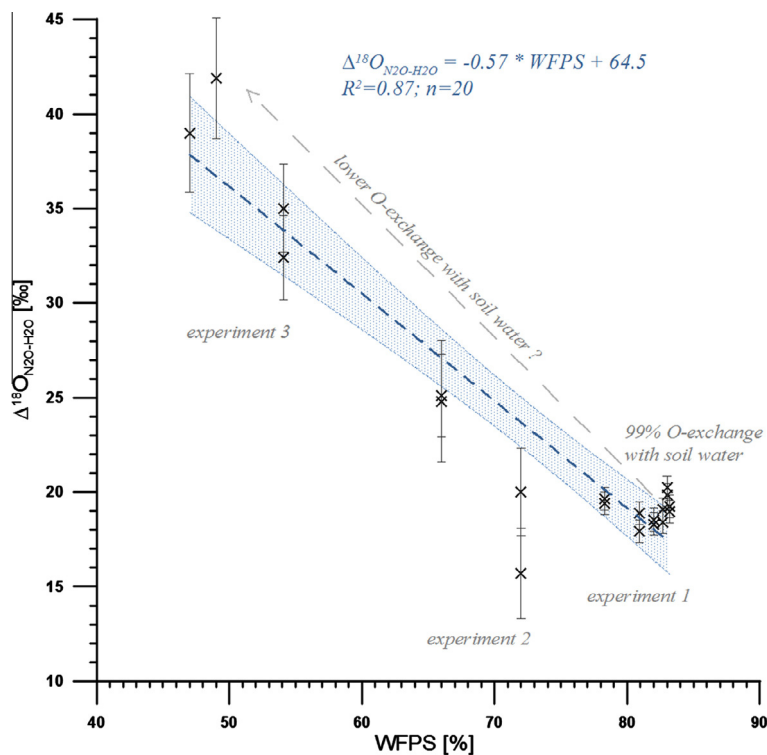


Fig. 2. Difference in $\delta^{18}\text{O}$ between soil water and produced N_2O ($\Delta^{18}\text{O}_{\text{H}_2\text{O}-\text{N}_2\text{O}}$) in relation to the water filled pore space (WFPS) of the incubated soils. The confidence band for the linear fit shown was determined for the confidence level of 95%. All the experimental data from this study (Experiments 1, 2, 3) are shown. The amount of O-exchange with soil water was precisely determined for Experiment 1 only. Error bars indicate the standard error.

$n = 14$). However, when analysing the particular experiments individually, usually the largest fractionation (represented by lower $\eta_1^{15}\text{N}$ values) was observed for the higher fertilised treatments (e.g., 1E, 1F, 3A). Hence, it could be hypothesised that the larger the substrate supply is, the larger the isotopic fractionation is, resulting in more negative $\eta_1^{15}\text{N}$ values. However, this relation cannot be proven easily based on the presented average values (Tables 2 and 4), which are individually affected by the time course of substrate consumption during the experiments, which depends on the experimental setups and process rates of the soils. Hence, the initial amount of nitrate supplied may have very different impact on the final $\eta_1^{15}\text{N}$. But for Experiment 1 the data from individual measurements (Appendix 2) can be used to analyse the relation between the residual nitrate fraction and the determined $\eta_1^{15}\text{N}$. The further the nitrate fraction was consumed, the smaller the isotopic fractionation. This correlation is statistically significant (Spearman Rank Correlation Test: $R = -0.63$; $p < 0.001$; $n = 140$). This relationship is also confirmed by the data from Experiment 2, where lower $\eta_1^{15}\text{N}$ was obtained for the unfertilised treatments. This effect could be explained by a rapid enrichment of residual NO_3^- in denitrifying sites. In our calculation approach (Eq. 1) we assume a homogenous isotopic enrichment of the substrate, whereas the $\delta^{15}\text{N}_{\text{NO}_3}$ in the active micro-sites can be much higher than bulk soil value. In such a case the observable apparent isotope effect will be lower than the actual net isotope effect occurring at the active site. This discrepancy increases with

growing difference between the bulk soil and active micro-site $\delta^{15}\text{N}_{\text{NO}_3}$. Moreover, it becomes more pronounced with ongoing consumption of substrate, which we clearly observe in Experiment 1. Therefore, the values of apparent isotope effects obtained at the beginning of the experiment, when the substrate distribution is most homogenous, can be assumed to be nearest to the net isotope effects at the active sites.

The $\eta_1\text{SP}$ vary within all three experiments in quite a narrow range from -3‰ to $+6\text{‰}$. The variations of $\eta_1\text{SP}$ mostly depend on the soil microbial community (Schmidt et al., 2004; Ostrom and Ostrom, 2011) which may be associated with different soil types and different soil properties or various experimental conditions. However, from our results we cannot indicate any consistent trends depending on soil texture, soil properties (like C or N content, pH) or experimental setup.

4.2. Fractionation of the residual nitrate

The determined fractionation factors for N_2O production should be also reflected in the isotopic signature of the residual nitrate. Fig. 3 shows the measured shift in isotopic composition of applied and residual nitrate together with the theoretical modelled values. They were calculated using Eq.1 assuming that the $\eta_1^{15}\text{N}$ determined for N_2O production ($\text{NO}_3^- \rightarrow \text{N}_2\text{O}$ step; Table 2 and 4) control the isotopic signature of the residual substrate. Results are only presented for Experiments 1 and 3, because the fraction

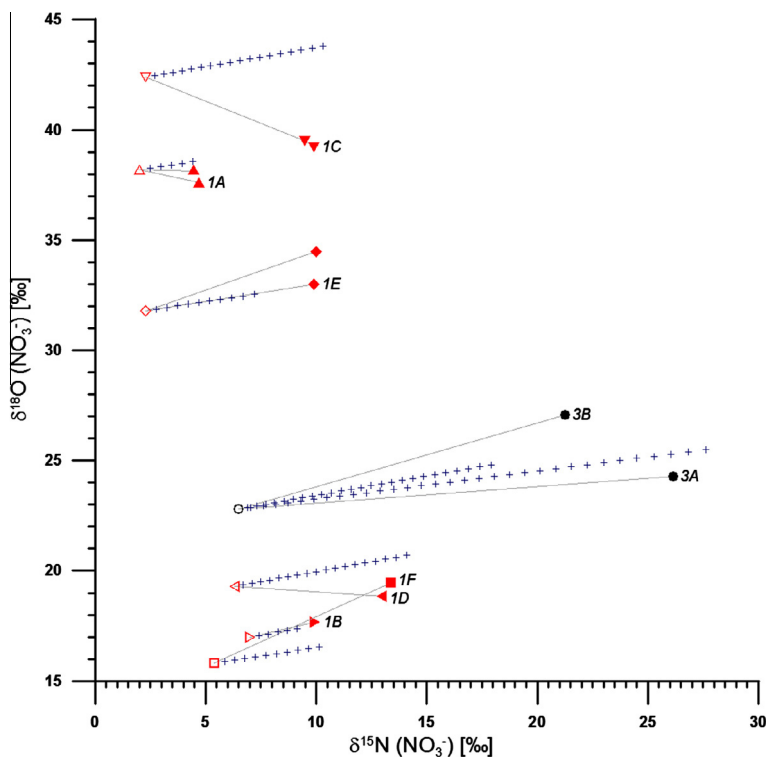


Fig. 3. Change in ^{18}O and ^{15}N isotopic signatures of nitrate during experiments 1 (red symbols) and 3 (black symbols). The initial (open symbols) and final (filled symbols) measured $\delta^{15}\text{N}_{\text{NO}_3}$ are shown. Also the theoretical values of residual nitrate with reaction progress are shown (blue crosses). They were calculated assuming the determined $\eta^{15}\text{N}$ values (Tables 2 and 4) and $\eta^{18}\text{O}$ value after literature data (-7‰ (Böttcher et al., 1990; Knöller et al., 2011)). (For interpretation of the references to colour in this figure legend, the reader is referred to the web version of this article.)

of the consumed nitrate during Experiment 2 was very low ($<5\%$) and no significant changes in nitrate isotopic signatures could have been observed.

In most cases, the modelled and measured values are quite consistent for $\delta^{15}\text{N}_{\text{NO}_3}$. However, in experiments 1E, 1F and 3B the modelled value largely underestimates the real nitrate fractionation, *i.e.*, the measured values are higher than the calculated ones. This is most probably due to the inhomogeneous microbial activity, which may lead to formation of active micro-sites. This is in accordance with the $\delta^{15}\text{N}_{\text{N}_2\text{O}}$ results discussed above, where also the significance of micro-sites dynamics has been shown.

The controls for $\delta^{18}\text{O}_{\text{NO}_3}$ are more complex, since due to O-exchange with soil water during denitrification the fractionation of residual nitrate is not related to the isotope effects observed for the produced N_2O (see discussion above). Therefore, for our simulation in Fig. 3 we have adopted the literature values for nitrate oxygen fractionation, which vary from about -8‰ (Böttcher et al., 1990) to about -6‰ (Knöller et al., 2011), hence the mean value of -7‰ was assumed. However, these values were determined for aquifers, thus may be not transferable to unsaturated soils. Rates and diffusive exchange within active and inactive sites in waters and soils can be completely different, but unfortunately the characteristic isotope effects for unsaturated soils are not known. Moreover, recently it has been shown that the $\delta^{18}\text{O}_{\text{NO}_3}$ may be also affected by the O-exchange with water (Kool et al., 2011; Wunderlich

et al., 2013) due to nitrite re-oxidation. We observed rather chaotic $\delta^{18}\text{O}_{\text{NO}_3}$ values, higher than expected for experiments 1E, 1F and 3B, and significantly lower, showing even an inverse isotope effect, for the experiments 1C and 1D (Fig. 3). The observed depletion of residual nitrate in ^{18}O may support the hypothesis that O-exchange may affect the nitrate isotopic signature (Kool et al., 2011). Nevertheless, our results show that the O isotopic fractionation of residual nitrate may be very different, both positive and negative, and thus no consistent isotope effect can be determined. The direction and magnitude of this effect is most probably dependent on the soil microbial community, *e.g.*, on the abundance of microbes capable of performing nitrite re-oxidation (Wunderlich et al., 2013).

4.3. η_2 – Fractionation factors of N_2O reduction

There are only few studies which determined isotope effects associated with N_2O reduction by denitrification using the whole soil microbial community (Menyailo and Hungate, 2006; Ostrom et al., 2007; Vieten et al., 2007; Jinuntuya-Nortman et al., 2008; Well and Flessa, 2009a). The range of the results reported by those studies are summarised and presented in Fig. 4 in comparison to our experimental results. In general, the literature data are quite consistent for $\eta_2^{15}\text{N}$ and η_2^{SP} but indicate very wide range of values for $\eta_2^{18}\text{O}$. All of the experimental results from our study confirm the range of η_2^{SP} values found in previous

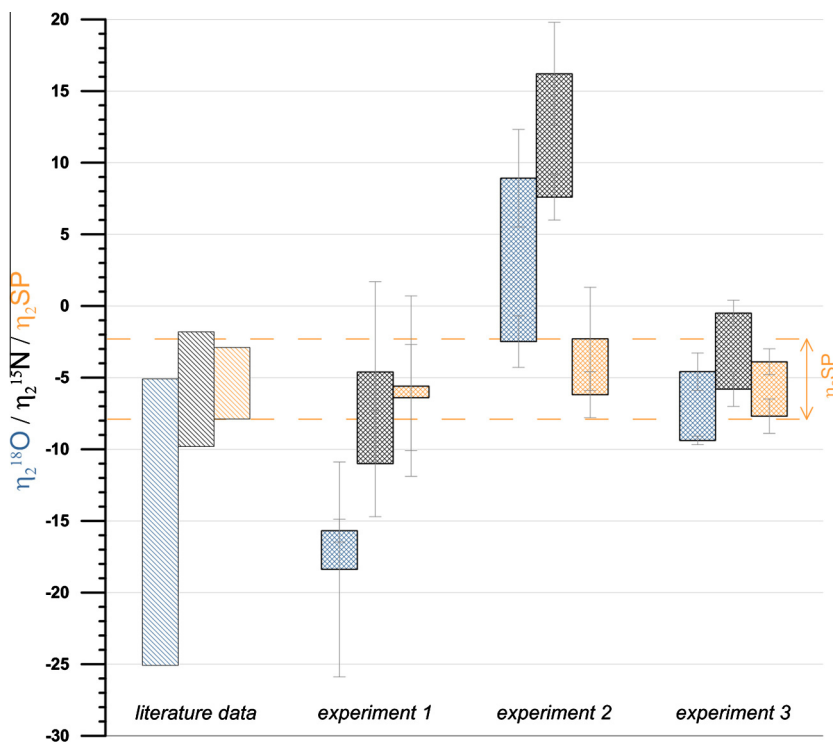


Fig. 4. Fractionation factors associated with N_2O reduction (η_2): reported previously in literature (striped bars) (Menyailo and Hungate, 2006; Ostrom et al., 2007; Jinuntuya-Nortman et al., 2008; Well and Flessa, 2009a) and determined in our experiments (checked bars). $\eta_2^{18}\text{O}$ (blue bars), $\eta_2^{15}\text{N}$ (black bars) and η_2^{SP} (orange bars) are shown. The confirmed range for η_2^{SP} is shown with dashed orange lines. Error bars indicate the standard error. (For interpretation of the references to colour in this figure legend, the reader is referred to the web version of this article.)

studies (Jinuntuya-Nortman et al., 2008; Well and Flessa, 2009a). In contrast, our values of $\eta_2^{15}\text{N}$ and $\eta_2^{18}\text{O}$ show very wide variations and are not always consistent with literature data (Fig. 4).

The η_2^{SP} obtained in different experiments (1, 2 and 3) did not show significant differences between each other ($P > 0.2$) and all varied around -5‰ . Hence, the range of η_2^{SP} from -2‰ to -8‰ reported previously (Jinuntuya-Nortman et al., 2008; Well and Flessa, 2009a) is fully confirmed by our study. Interestingly, no significant differences were found for very different treatments applied in this study, which indicates that η_2^{SP} is relatively robust and that potential impacts from different experimental approaches (static or dynamic), different temperatures, various soil types or various soil saturation levels are either not existent or relatively small and masked by errors in assessing η_2^{SP} .

For the other two isotope effects, $\eta_2^{15}\text{N}$ and $\eta_2^{18}\text{O}$, relatively close values to the average literature data were observed for Experiment 1 (Fig. 4). Only this experiment was conducted as a static incubation in closed vessels, whereas the other two experiments (1 and 3) were conducted as dynamic incubation in a flow-through system. Similarly, all the previous experiments, which determined the reduction fractionation factors, used closed static incubation technique, where N_2O was added to the headspace of nitrate-free anaerobic soil incubation (Menyailo and

Hungate, 2006; Ostrom et al., 2007; Vieten et al., 2007; Jinuntuya-Nortman et al., 2008; Well and Flessa, 2009a). Hence, we suppose that the experimental approach can have a crucial influence on the obtained results. In soil denitrification, there are two coexisting routes for N_2O reduction: (1) N_2O is being reduced immediately following N_2O production, *i.e.*, within the same denitrifying micro-site, or even the same denitrifying cell, prior to its potential escape; (2) N_2O previously escaped from the denitrifying micro-sites, re-enters a denitrifying cell where it is fully or partially reduced (Ostrom et al., 2007). These two routes may be associated with different η_2 values due to different combination of enzymatic and diffusion effects (Fig. 5). Namely, enzymatic effects are associated with negative isotopic fractionation, and, as a result, the residual unreduced N_2O is enriched in heavy isotopes. Diffusion also favours light molecules, hence the residual gas is enriched in heavy isotopes. During the reduction route (2) both diffusion and enzymatic effects (ϵ_d and ϵ_e , respectively) show a common direction of fractionation process, *i.e.*, preferentially light N_2O molecules diffuse into the denitrifying micro-site, and preferentially light N_2O molecules are reduced. Consequently, the residual unreduced N_2O is always enriched in heavy isotopes and the net isotope effect associated with this route is always negative (see also Table 5). This is the case for N_2O addition experiments (Menyailo and Hungate, 2006; Ostrom et al., 2007; Vieten et al., 2007; Jinuntuya-Nortman

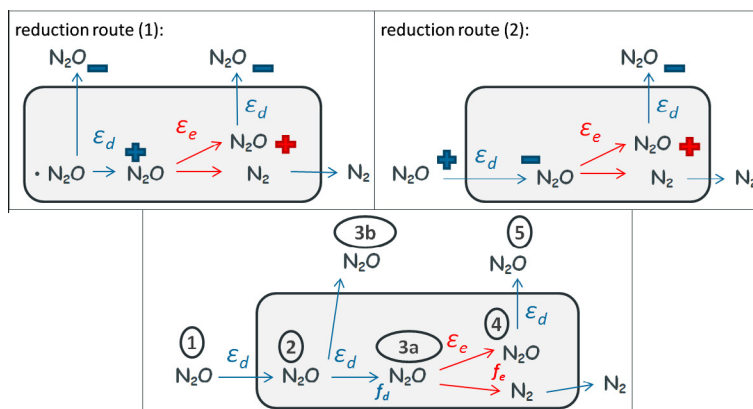


Fig. 5. Two possible routes for N_2O reduction with the associated intrinsic isotopic fractionation during diffusion (ϵ_d) and enzymatic reduction (ϵ_e). ‘+’ and ‘-’ represent N_2O enrichment and depletion in heavy isotopes, respectively, due to the occurring processes. In route (1), N_2O diffusion causes enrichment of N_2O prior to its reduction, whereas the opposite is the case in route (2). Below a summary isotope model for coexistence of both routes is presented. Based on this model the expected final net isotope effects for various residual fractions of diffusion (f_d) and enzymatic reduction (f_e) of N_2O were calculated in Table 5.

Table 5

Model calculations of net isotope effects (η) assuming various residual fractions of diffusion (f_d) and enzymatic reduction (f_e) of N_2O . $\delta^{15}N(N_2O)$ values for the following steps from (1 to 5) as presented in Fig. 5 are calculated. We assumed: $\epsilon_d = -2\text{‰}$, $\epsilon_e = -10\text{‰}$, $\delta^{15}N_1 = -40\text{‰}$. The fractionation step 1 to 2 and 4 to 5 were ignored, as they will cause identical fractionation for all the considered cases. $\delta^{15}N_{3a}$ was calculated as: $\delta^{15}N_{3a} = \delta^{15}N_1 + \epsilon_d \cdot \ln(f_d)$, and $\delta^{15}N_5$ was calculated as: $\delta^{15}N_5 = \delta^{15}N_{3a} + \epsilon_e \cdot \ln(f_e)$. $\delta^{15}N_{3b}$ was calculated from the isotopic mass balance of $\delta^{15}N_1$ and $\delta^{15}N_{3a}$. The final diffused out $\delta^{15}N_{total}$ was calculated from the isotopic mass balance of $\delta^{15}N_{3b}$ and $\delta^{15}N_5$. The final η_{total} was calculated as: $\eta_{total} = (\delta^{15}N_{total} - \delta^{15}N_1) / \ln(f_d \cdot f_e)$.

| f_d | f_e | $\delta^{15}N_{3a}$ | $\delta^{15}N_{3b}$ | $\delta^{15}N_5$ | $\delta^{15}N_{total}$ | $\eta_{total}^{15}N$ |
|-------|-------|---------------------|---------------------|--|------------------------|----------------------|
| 0.5 | 0.5 | -38.6 | -41.4 | -31.7 | -38.2 | -1.3 |
| 0.1 | 0.5 | -35.4 | -40.5 | -28.5 | -39.9 | 0.0 |
| 0.9 | 0.5 | -39.8 | -41.9 | -32.9 | -34.5 | -6.9 |
| 0.1 | 0.1 | -35.4 | -40.5 | -12.4 | -40.2 | 0.0 |
| 0.9 | 0.1 | -39.8 | -41.9 | -16.8 | -30.0 | -4.2 |
| 0.1 | 0.9 | -35.4 | -40.5 | -34.3 | -40.0 | 0.0 |
| 0.9 | 0.9 | -39.8 | -41.9 | -38.7 | -39.1 | -4.4 |
| 0.1 | 0 | -35.4 | -40.5 | <i>all not diffused N_2O is reduced</i> | -40.5 | 0.2 |
| 0.9 | 0 | -39.8 | -41.9 | | -41.9 | 18.0 |
| 0.5 | 0 | -38.6 | -41.4 | | -41.4 | 2.0 |

et al., 2008; Well and Flessa, 2009a), where only this route can be traced. Indeed, the literature data always reported the negative fractionation factors (Fig. 4). However, if we deal with the reduction route (1) we may have the inverse diffusion effect (ϵ_d) preceding the enzymatic effect, when the part of produced N_2O diffuses out of the denitrifying micro-site before reduction. Such a diffusion results in enrichment of the residual N_2O and afterwards, this enriched residuum undergoes reduction. Assuming the whole of this residuum is reduced, enzymatic fractionation effect may even have no influence at all on the final N_2O isotopic signature (see Table 5). Consequently, we may observe an inverse isotope effect, i.e., that the residual N_2O is depleted in heavy isotopes. Obviously, if not the whole residuum is fully reduced, the final net isotope effect will result from the contribution of two fractionation effects of opposite direction: positive for diffusion (ϵ_d) and negative for enzymatic reduction (ϵ_e) (see Table 5). The last effect associated with diffusion out of the denitrifying micro-site (ϵ_d) should be similar in both routes, and its contribution to the

final net isotope effect depends only on the contribution of diffused N_2O . This step has no impact on the net isotope effect if all of the residual N_2O diffuses out of the denitrifying micro-sites. The balance between enzymatic and diffusive isotopic fractionation and its possible impact on the observed η values is illustrated with an example calculation model for $\eta_{15}N$ in Table 5.

We suppose that in our experiments the large variations in the observed $\eta_{18}O$ and $\eta_{15}N$ result from the contribution of different reduction pathways, as demonstrated in the theoretical calculations presented in Table 5. Principally, both routes can be assumed to exist in static and dynamic systems, with route (1) preceding route (2) (Fig. 5). In the static experiments, the route (2) might be more effective due to accumulation of N_2O which may re-enter the denitrifying micro-sites and undergo further reduction. Indeed, for the static incubation (Experiment 1) we observe the most negative $\eta_{18}O$ and $\eta_{15}N$ values, which are typical for the reduction route (2) (Fig. 4). The highest, mainly positive, $\eta_{18}O$ and $\eta_{15}N$ values

were noted for the dynamic incubation (Experiment 2). It suggests that reduction route (1) must dominate there and that the diffusion effect of N₂O escape (ϵ_d) was more significant than the enzymatic one (ϵ_e). In Experiment 3 we actually observe the $\eta_2^{18}\text{O}$ and $\eta_2^{15}\text{N}$ values showing approximately the average of Experiments 1 and 2. If the hypothesis of the stronger impact of route (2) in the static Experiment 1 compared to the dynamic Experiment 2 is true, then the values found for Experiment 3 indicate that N₂O accumulation and associated reduction via route (2) was less pronounced compared to Experiment 2. However, because the experimental setup was quite similar regarding the possibility of simultaneous N₂O production and reduction, there must be another cause for this difference. A possible explanation would be the lower product ratio of denitrification in Experiment 3 (f from 0.18 to 0.28, Table 4) when compared to Experiment 2 (f from 0.23 to 0.65, Table 3), *i.e.*, N₂O reduction in relation to gross N₂O production was much larger. Moreover, the absolute N₂O reduction rates were also much higher in Experiment 3. It has been shown that $\eta_2^{18}\text{O}$ and $\eta_2^{15}\text{N}$ increase with increasing reaction rate (Jinuntuya-Nortman et al., 2008) due to alterations in balance of diffusive and enzymatic isotope effects. However, as that study used the N₂O addition method which excludes route (1), it is impossible to directly compare those results with ours. Nevertheless, most probably similar mechanism may explain our results, *i.e.*, in Experiment 3, the larger reduction contribution could be due to higher N₂O accumulation of produced N₂O in pore space resulting from inhibited diffusive efflux and/or higher gross N₂O production with subsequent enhanced reduction of accumulated N₂O via route (2).

The above presented hypothesis explaining the variability in $\eta_2^{18}\text{O}$ and $\eta_2^{15}\text{N}$ by various contribution of diffusive effects is further supported by the very consistent $\eta_2\text{SP}$ observed in all our experiments as well as in all the previous studies (Ostrom et al., 2007; Jinuntuya-Nortman et al., 2008; Well and Flessa, 2009a). Since there is no fractionation for SP associated with diffusion, the apparent isotope effect for SP only depends on the enzymatic fractionation. Hence, this effect is independent of the actual reduction route. Conversely, for $\eta_2^{18}\text{O}$ and $\eta_2^{15}\text{N}$ we deal with quite significant diffusive effects (Well and Flessa, 2008), hence we observe large variations due to shifts in dominant N₂O reduction pathway.

While the interaction between diffusive and enzymatic isotope effects apparently impairs the use of $\eta_2^{15}\text{N}$ and $\eta_2^{18}\text{O}$ for estimating N₂O reduction, these values might be used as indicators for the balance between reduction and diffusive emission of N₂O following its release to and accumulation in the soil pore space. This balance probably plays a key role in the control of N₂O emission from soils (Blagodatsky and Smith, 2012). Future research might reveal whether the $\eta_2^{18}\text{O}/\eta_2\text{SP}$ and $\eta_2^{15}\text{N}/\eta_2\text{SP}$ ratios of denitrification might be useful for better understanding the control of N₂O reduction in soils. In this study these ratios varied largely between the various experimental setups. For the static Experiment 1 the $\eta_2^{18}\text{O}/\eta_2\text{SP}$ ratio from 2.7 to 3.2 and $\eta_2^{15}\text{N}/\eta_2\text{SP}$ ratios from 0.7 to 2.0 were comparable to the previous literature data (Jinuntuya-Nortman et al., 2008; Well and Flessa, 2009a). But for the dynamic

experiments they were significantly lower (below 1.8 and 0.9, respectively), showing even negative values for Experiment 2 (up to -1.7 and -3.3 , respectively). This may suggest that the lower values of these ratios indicate the larger contribution of the reduction route (1).

4.4. Calculation approach: closed vs. open system

The closed system approach has been applied here for both N₂O production and N₂O reduction. This approach is quite obvious for N₂O production where the nitrate pool is gradually consumed and continuously enriched in heavy isotopes. This pool might also be theoretically renewed by nitrate originating from nitrification processes, but these can be excluded due to the application of anoxic atmosphere in all experiments presented here. However, N₂O reduction, when occurring simultaneously with N₂O production, as it is the case for our experiments, may seem to work as an open system, as the substrate – N₂O – is continuously produced and afterwards partially reduced. However, the application of open-system equations for calculation of isotopic fractionation factors is strictly only then justified if we deal with a ‘steady-state’ system, *i.e.*, the substrate input and consumption are equal (Fry, 2006). This is because the equations for open-system calculations are derived from mass balance equations and adopt an assumption about balanced in- and out-fluxes (Fry, 2006). Such a simplification is not justified for the N₂O reduction process, because the product ratio during the experiment is not stable and consequently the N₂O substrate pool is not at ‘steady-state’ which is required for ‘open-system’ equations (Fry, 2006; Decock and Six, 2013). Moreover, for physical reasons soils cannot act as a perfectly open system because there is always transient N₂O accumulation in pore space (Heincke and Kaupenjohann, 1999; Clough et al., 2005) due to inhibited diffusive efflux, which depends on the volume and geometry of water- and air-filled pores, and this property is the prerequisite for the existence of reduction route (2). Finally, the obtained results from experiments where production and reduction occurred simultaneously and the reduction contribution was known, show the logarithmic correlation between the isotopic signature of N₂O and the fraction of residual substrate (Köster et al., 2013). If the ‘open-system’ dynamics were applicable, a linear correlation should be expected (Fry, 2003, 2006). Hence, this shows that the reduction process can be mathematically better described with ‘closed-system’ equations. However, we cannot rule out that process dynamics consisted of a mix of open and closed system dynamics as proposed by Decock and Six (2013).

4.5. Significance for quantification of soil denitrification

The most important question for the future application of the determined fractionation factors is how far they are transferable to natural conditions and how robust they are for calculating the reduction contribution and for quantifying the whole nitrogen loss due to denitrification. To enable such calculations both η_1 and η_2 must be precisely predictable for a particular soil and ambient conditions. Since we

are currently able to measure three isotopic characteristics, $\delta^{18}\text{O}$, average $\delta^{15}\text{N}$, and SP, it would be enough to precisely estimate both η values for at least one of those signatures. Of course, if more of them could be estimated, the robustness of calculated quantities would further increase.

Looking at the determined η_1 values we can conclude that they are already quite well determined and our understanding of their variability is quite good for $\eta_1^{15}\text{N}$, where it mainly depends on the substrate availability, and $\eta_1\text{SP}$, that varies due to differences in soil microbial community. Nevertheless, those values cannot yet be robustly predicted for a particular soil without conducting laboratory experiments, because the range of variations is rather pronounced. However, this may be attainable with growing supply of experimental data. Although we noticed the largest range of variations for $\eta_1^{18}\text{O}$, we also showed that it may be possible to estimate $\eta_1^{18}\text{O}$ based on the presumed strict relation of oxygen isotope effect and soil WFPS (Fig. 2). If this relation was universally applicable, this would enable us to predict the $\delta^{18}\text{O}$ of N_2O produced in the course of denitrification.

Proper determination of η_2 values seem to be more complicated due to experimental difficulties. We showed that the experimental setup is a crucial factor for the measured isotope effects. The large variability of $\eta_2^{18}\text{O}$ and $\eta_2^{15}\text{N}$ is most probably due to the coexistence of diffusive and enzymatic fractionation, which may cause an opposite isotope effect. For N_2O reduction we deal with two different reduction routes that show very different interaction of diffusion and enzymatic fractionation, and consequently result in very different net isotope effects. Hence, it is still impossible to predict which mechanism is dominating for the natural conditions and which factors can be accepted for field studies. Here we showed that the application of values obtained from N_2O addition experiments (Menyailo and Hungate, 2006; Ostrom et al., 2007; Jinuntuya-Nortman et al., 2008; Well and Flessa, 2009a) may be not representative for natural conditions, as only one of two possible reduction pathways has been investigated there. However, the values obtained for $\eta_2\text{SP}$ are very consistent in our, as well as in previous, experiments (Ostrom et al., 2007; Jinuntuya-Nortman et al., 2008; Well and Flessa, 2009a), hence the range of -2‰ to -8‰ with a most probable estimate of -5‰ can be universally adopted. This is because the SP effect is only due to enzymatic processes and hence independent of differences in reduction routes.

5. SUMMARY

In this study we provide experimental determination of isotopic fractionation factors associated with N_2O production and reduction during denitrification based on three laboratory incubations which differed largely in their experimental set-up. We applied both static and dynamic incubation techniques and all available methods allowing for determination of N_2O reduction contribution, *i.e.*, incubations in helium atmosphere, acetylene inhibition technique and ^{15}N tracing method. Moreover, a wide variety of soil properties and water contents was applied in different experiments.

The apparent isotope effects during N_2O production were quite consistent with previous literature data and their variability can be explained quite well by varied incubation conditions. We suppose that if a larger data base can be provided by future studies, *e.g.*, regarding larger range of soil types and soil moisture levels, these values can be predicted quite well for given soil properties and environmental conditions. The apparent isotope effects for $\delta^{18}\text{O}$ and $\delta^{15}\text{N}$ associated with N_2O reduction appeared to depend largely on the experimental setup, presumably due to varying impact of diffusive isotopic effects. However, the apparent isotope effects for SP during N_2O reduction is independent of diffusion and shows a very consistent value in this and previous studies. Therefore, we suggest that the value of ca. -5‰ can be commonly adopted as typical for N_2O reduction process.

ACKNOWLEDGEMENTS

This study was supported by German Research Foundation (DFG We/1904-4). Many thanks are due to Anette Gieseemann and Martina Heuer for help in N_2O isotopic analyses; Jens Dyckmanns and Reinhard Langel for $\delta^{18}\text{O}$ analyses of extracted soil water; Kerstin Gilke for help in chromatographic analyses and Maciej Lewicki for supplying the isotopically depleted water from Tatra Mountains, Poland. We would like to thank Professor Nathaniel Ostrom and one anonymous reviewer for their constructive comments which helped us to improve this manuscript.

APPENDIX A. SUPPLEMENTARY DATA

Supplementary data associated with this article can be found, in the online version, at <http://dx.doi.org/10.1016/j.gca.2014.03.010>.

REFERENCES

- Aerenss E., Tiedje J. M. and Averill B. A. (1986) Isotope labeling studies on the mechanism of N–N bond formation in denitrification. *J. Biol. Chem.* **261**, 9652–9656.
- Barford C. C., Montoya J. P., Altabet M. A. and Mitchell R. (1999) Steady-state nitrogen isotope effects of N-2 and N_2O production in *Paracoccus denitrificans*. *Appl. Environ. Microb.* **65**, 989–994.
- Blagodatsky S. and Smith P. (2012) Soil physics meets soil biology: towards better mechanistic prediction of greenhouse gas emissions from soil. *Soil Biol. Biochem.* **47**, 78–92.
- Bol R., Toyoda S., Yamulki S., Hawkins J. M. B., Cardenas L. M. and Yoshida N. (2003) Dual isotope and isotopomer ratios of N_2O emitted from a temperate grassland soil after fertiliser application. *Rapid Commun. Mass Spectrom.* **17**, 2550–2556.
- Böttcher J., Strebel O., Voerkelius S. and Schmidt H. L. (1990) Using isotope fractionation of nitrate nitrogen and nitrate oxygen for evaluation of microbial denitrification in a sandy aquifer. *J. Hydrol.* **114**, 413–424.
- Brenninkmeijer C. A. M. and Röckmann T. (1999) Mass spectrometry of the intramolecular nitrogen isotope distribution of environmental nitrous oxide using fragment-ion analysis. *Rapid Commun. Mass Spectrom.* **13**, 2028–2033.
- Casciotti K. L., Bohlke J. K., McIlvin M. R., Mroczkowski S. J. and Hannon J. E. (2007) Oxygen isotopes in nitrite: analysis, calibration, and equilibration. *Anal. Chem.* **79**, 2427–2436.

- Casciotti K. L., Sigman D. M., Hastings M. G., Bohlke J. K. and Hilkert A. (2002) Measurement of the oxygen isotopic composition of nitrate in seawater and freshwater using the denitrifier method. *Anal. Chem.* **74**, 4905–4912.
- Clough T. J., Sherlock R. R. and Rolston D. E. (2005) A review of the movement and fate of N_2O in the subsoil. *Nutr. Cycl. Agroecosys.* **72**, 3–11.
- Decock C. and Six J. (2013) How reliable is the intramolecular distribution of ^{15}N in N_2O to source partition N_2O emitted from soil? *Soil Biol. Biochem.* **65**, 114–127.
- Elsner M. (2010) Stable isotope fractionation to investigate natural transformation mechanisms of organic contaminants: principles, prospects and limitations. *J. Environ. Monitor* **12**, 2005–2031.
- Elsner M., Zwank L., Hunkeler D. and Schwarzenbach R. P. (2005) A new concept linking observable stable isotope fractionation to transformation pathways of organic pollutants. *Environ. Sci. Technol.* **39**, 6896–6916.
- Firestone M. K. and Davidson E. A. (1989) Microbial basis of NO and N_2O production and consumption in soil. In *Exchange of Trace Gases Between Terrestrial Ecosystems and the Atmosphere* (eds. M. O. Andreae and D. S. Schimel). John Wiley and Sons, New York, pp. 7–21.
- Fry B. (2003) Steady state models of stable isotopic distributions. *Isot. Environ. Health Stud.* **39**, 219–232.
- Fry B. (2006) *Stable Isotope Ecology*. Springer, NY, USA.
- Heincke M. and Kaupenjohann M. (1999) Effects of soil solution on the dynamics of N_2O emissions: a review. *Nutr. Cycle Agroecosys.* **55**, 133–157.
- IPCC (2013) *Climate Change 2013: The Physical Science Basis. Contribution of Working Group I to the Fifth Assessment Report of the Intergovernmental Panel on Climate Change* (eds. T. F. Stocker, D. Qin, G. K. Plattner, M. Tignor, S. K. Allen, J. Boschung, A. Nauels, Y. Xia, V. Bex and P. M. Midgley). Cambridge University Press, Cambridge, United Kingdom and New York, NY, USA, pp. 1535.
- Jinuntuya-Nortman M., Sutka R. L., Ostrom P. H., Gandhi H. and Ostrom N. E. (2008) Isotopologue fractionation during microbial reduction of N_2O within soil mesocosms as a function of water-filled pore space. *Soil Biol. Biochem.* **40**, 2273–2280.
- Knöller K., Vogt C., Haupt M., Feisthauer S. and Richnow H. H. (2011) Experimental investigation of nitrogen and oxygen isotope fractionation in nitrate and nitrite during denitrification. *Biogeochemistry* **103**, 371–384.
- Königer P., Marshall J. D., Link T. and Mulch A. (2011) An inexpensive, fast, and reliable method for vacuum extraction of soil and plant water for stable isotope analyses by mass spectrometry. *Rapid Commun. Mass Spectrom.* **25**, 3041–3048.
- Kool D. M., Wrage N., Oenema O., Harris D. and Van Groenigen J. W. (2009) The O-18 signature of biogenic nitrous oxide is determined by O exchange with water. *Rapid Commun. Mass Spectrom.* **23**, 104–108.
- Kool D. M., Wrage N., Oenema O., Van Kessel C. and Van Groenigen J. W. (2011) Oxygen exchange with water alters the oxygen isotopic signature of nitrate in soil ecosystems. *Soil Biol. Biochem.* **43**, 1180–1185.
- Köster J. R., Well R., Dittter K., Giesemann A., Lewicka-Szczebak D., Mühling K. H., Herrmann A., Lammel J. and Senbayram M. (2013) Soil denitrification potential and its influence on the N_2O reduction and N_2O isotopomer ratios. *Rapid Commun. Mass Spectrom.* **27**, 2363–2373.
- Lewicka-Szczebak D., Well R., Giesemann A., Rohe L. and Wolf U. (2013) An enhanced technique for automated determination of ^{15}N signatures of N_2 , $(N_2 + N_2O)$ and N_2O in gas samples. *Rapid Commun. Mass Spectrom.* **27**, 1548–1558.
- Maggi F. and Riley W. J. (2009) Transient competitive complexation in biological kinetic isotope fractionation explains non-steady isotopic effects: Theory and application to denitrification in soils. *J. Geophys. Res.-Biogeo.*, 114.
- Maggi F. and Riley W. J. (2010) Mathematical treatment of isotopologue and isotopomer speciation and fractionation in biochemical kinetics. *Geochim. Cosmochim. Acta* **74**, 1823–1835.
- Mariotti A., Germon J. C., Hubert P., Kaiser P., Letolle R., Tardieux A. and Tardieux P. (1981) Experimental-determination of nitrogen kinetic isotope fractionation – some principles – illustration for the denitrification and nitrification processes. *Plant Soil* **62**, 413–430.
- Menyailo O. V. and Hungate B. A. (2006) Stable isotope discrimination during soil denitrification: production and consumption of nitrous oxide. *Global Biogeochem. Cycles* **20**.
- Nadeem S., Dorsch P. and Bakken L. R. (2013) Autoxidation and acetylene-accelerated oxidation of NO in a 2-phase system: implications for the expression of denitrification in ex situ experiments. *Soil Biol. Biochem.* **57**, 606–614.
- Opdyke M. R., Ostrom N. E. and Ostrom P. H. (2009) Evidence for the predominance of denitrification as a source of N_2O in temperate agricultural soils based on isotopologue measurements. *Global Biogeochem Cycles* **23**.
- Ostrom N. E. and Ostrom P. H. (2011) The isotopomers of nitrous oxide: analytical considerations and application to resolution of microbial production pathways In *Handbook of Environmental Isotope Geochemistry* (ed. M. Baskaran). Springer, pp. 453–477.
- Ostrom N. E., Pitt A., Sutka R., Ostrom P. H., Grandy A. S., Huizinga K. M. and Robertson G. P. (2007) Isotopologue effects during N_2O reduction in soils and in pure cultures of denitrifiers. *J. Geophys. Res.-Biogeo.* **112**.
- Ostrom N. E., Sutka R., Ostrom P. H., Grandy A. S., Huizinga K. M., Gandhi H., von Fischer J. C. and Robertson G. P. (2010) Isotopologue data reveal bacterial denitrification as the primary source of N_2O during a high flux event following cultivation of a native temperate grassland. *Soil Biol. Biochem.* **42**, 499–506.
- Park S., Perez T., Boering K. A., Trumbore S. E., Gil J., Marquina S. and Tyler S. C. (2011) Can N_2O stable isotopes and isotopomers be useful tools to characterize sources and microbial pathways of N_2O production and consumption in tropical soils? *Global Biogeochem. Cycles* **25**.
- Perez T., Garcia-Montiel D., Trumbore S., Tyler S., De Camargo P., Moreira M., Piccolo M. and Cerri C. (2006) Nitrous oxide nitrification and denitrification N-15 enrichment factors from Amazon forest soils. *Ecol. Appl.* **16**, 2153–2167.
- Perez T., Trumbore S. E., Tyler S. C., Matson P. A., Ortiz-Monasterio I., Rahn T. and Griffith D. W. T. (2001) Identifying the agricultural imprint on the global N_2O budget using stable isotopes. *J. Geophys. Res.-Atmos.* **106**, 9869–9878.
- R Core Team (2013) R: A language and environment for statistical computing. R Foundation for Statistical Computing, Vienna, Austria, URL: <<http://www.R-project.org/>>.
- Röckmann T., Kaiser J., Brenninkmeijer C. A. M. and Brand W. A. (2003) Gas chromatography/isotope-ratio mass spectrometry method for high-precision position-dependent N-15 and O-18 measurements of atmospheric nitrous oxide. *Rapid Commun. Mass Spectrom.* **17**, 1897–1908.
- Rohe L., Anderson T. -H., Braker G., Flessa H., Giesemann A., Lewicka-Szczebak D., Wrage-Mönnig N. and Well R. (submitted for publication). Dual isotope and isotopomer signatures of nitrous oxide from fungal denitrification – a pure culture study. *Rapid Commun Mass Spectrom.*
- Schmidt H. L., Werner R. A., Yoshida N. and Well R. (2004) Is the isotopic composition of nitrous oxide an indicator for its origin from nitrification or denitrification? A theoretical approach

- from referred data and microbiological and enzyme kinetic aspects. *Rapid Commun. Mass Spectrom.* **18**, 2036–2040.
- Sigman D. M., Casciotti K. L., Andreani M., Barford C., Galanter M. and Bohlke J. K. (2001) A bacterial method for the nitrogen isotopic analysis of nitrate in seawater and freshwater. *Anal. Chem.* **73**, 4145–4153.
- Snider D. M., Schiff S. L. and Spoelstra J. (2009) N-15/N-14 and O-18/O-16 stable isotope ratios of nitrous oxide produced during denitrification in temperate forest soils. *Geochim. Cosmochim. Acta* **73**, 877–888.
- Snider D., Venkiteswaran J. J., Schiff S. L. and Spoelstra J. (2013) A new mechanistic model of d18O–N₂O formation by denitrification. *Geochim. Cosmochim. Acta* **112**, 102–115.
- Soetaert K. (2010) R Package FME: Inverse Modelling, Sensitivity, Monte Carlo Applied to a Nonlinear Model. <<http://cran.r-project.org/web/packages/FME/vignettes/FMEother.pdf>>.
- Soetaert K. and Petzoldt T. (2010) Inverse modelling, sensitivity and monte carlo analysis in R using package FME. *J. Stat. Softw.*, 33.
- Sutka R. L., Adams G. C., Ostrom N. E. and Ostrom P. H. (2008) Isotopologue fractionation during N₂O production by fungal denitrification. *Rapid Commun. Mass Spectrom.* **22**, 3989–3996.
- Sutka R. L., Ostrom N. E., Ostrom P. H., Breznak J. A., Gandhi H., Pitt A. J. and Li F. (2006) Distinguishing nitrous oxide production from nitrification and denitrification on the basis of isotopomer abundances. *Appl. Environ. Microbiol.* **72**, 638–644.
- Sutka R. L., Ostrom N. E., Ostrom P. H., Gandhi H. and Breznak J. A. (2003) Nitrogen isotopomer site preference of N₂O produced by *Nitrosomonas europaea* and *Methylococcus capsulatus* bath. *Rapid Commun. Mass Spectrom.* **17**, 738–745.
- Toyoda S., Mutoh H., Yamagishi H., Yoshida N. and Tanji Y. (2005) Fractionation of N₂O isotopomers during production by denitrifier. *Soil Biol. Biochem.* **37**, 1535–1545.
- Toyoda S., Yano M., Nishimura S., Akiyama H., Hayakawa A., Koba K., Sudo S., Yagi K., Makabe A., Tobar Y., Ogawa N. O., Ohkouchi N., Yamada K. and Yoshida N. (2011) Characterization and production and consumption processes of N₂O emitted from temperate agricultural soils determined via isotopomer ratio analysis. *Global Biogeochem. Cycles* **25**.
- Toyoda S. and Yoshida N. (1999) Determination of nitrogen isotopomers of nitrous oxide on a modified isotope ratio mass spectrometer. *Anal. Chem.* **71**, 4711–4718.
- Vieten B., Blunier T., Neftel A., Alewell C. and Conen F. (2007) Fractionation factors for stable isotopes of N and O during N₂O reduction in soil depend on reaction rate constant. *Rapid Commun. Mass Spectrom.* **21**, 846–850.
- Well R., Eschenbach W., Flessa H., von der Heide C. and Weymann D. (2012) Are dual isotope and isotopomer ratios of N₂O useful indicators for N₂O turnover during denitrification in nitrate-contaminated aquifers? *Geochim. Cosmochim. Acta* **90**, 265–282.
- Well R. and Flessa H. (2008) Isotope fractionation factors of N(2)O diffusion. *Rapid Commun. Mass Spectrom.* **22**, 2621–2628.
- Well R. and Flessa H. (2009a) Isotopologue enrichment factors of N₂O reduction in soils. *Rapid Commun. Mass Spectrom.* **23**, 2996–3002.
- Well R. and Flessa H. (2009b) Isotopologue signatures of N₂O produced by denitrification in soils. *J. Geophys. Res.-Biogeo.* **114**.
- Well R., Kurganova I., de Gerenyu V. L. and Flessa H. (2006) Isotopomer signatures of soil-emitted N₂O under different moisture conditions – a microcosm study with arable loess soil. *Soil Biol. Biochem.* **38**, 2923–2933.
- Westley M. B., Popp B. N. and Rust T. M. (2007) The calibration of the intramolecular nitrogen isotope distribution in nitrous oxide measured by isotope ratio mass spectrometry. *Rapid Commun. Mass Spectrom.* **21**, 391–405.
- Wunderlich A., Meckenstock R. U. and Einsiedl F. (2013) A mixture of nitrite-oxidizing and denitrifying microorganisms affects the delta O-18 of dissolved nitrate during anaerobic microbial denitrification depending on the delta O-18 of ambient water. *Geochim. Cosmochim. Acta* **119**, 31–45.
- Yamulki S., Toyoda S., Yoshida N., Veldkamp E., Grant B. and Bol R. (2001) Diurnal fluxes and the isotopomer ratios of N₂O in a temperate grassland following urine amendment. *Rapid Commun. Mass Spectrom.* **15**, 1263–1269.

Associate editor: Jack J. Middelburg

Chapter 7

Novel laser spectroscopic technique for continuous analysis of N₂O isotopomers – application and intercomparison with isotope ratio mass spectrometry

Jan Reent Köster, Reinhard Well, Béla Tuzson, Roland Bol, Klaus Dittert, Anette Giesemann,
Lukas Emmenegger, Albert Manninen, Laura Cárdenas, and Joachim Mohn

Rapid Communications in Mass Spectrometry 27 (2013) 216 – 222

DOI: 10.1002/rcm.6434

Rapid Commun. Mass Spectrom. 2013, 27, 216–222
(wileyonlinelibrary.com) DOI: 10.1002/rcm.6434

Novel laser spectroscopic technique for continuous analysis of N₂O isotopomers – application and intercomparison with isotope ratio mass spectrometry

Jan Reent Köster^{1*}, Reinhard Well², Béla Tuzson³, Roland Bol⁴, Klaus Dittert^{1,5}, Anette Giesemann², Lukas Emmenegger³, Albert Manninen³, Laura Cárdenas⁶ and Joachim Mohn³

¹Institute of Plant Nutrition and Soil Science, Kiel University, Hermann-Rodewald-Str. 2, D-24118, Kiel, Germany

²Institute of Agricultural Climate Research, Johann Heinrich von Thünen Institut, Federal Research Institute for Rural Areas, Forestry and Fisheries, Bundesallee 50, D-38116 Braunschweig, Germany

³Laboratory for Air Pollution & Environmental Technology, EMPA, Überlandstr. 129, CH-8600, Dübendorf, Switzerland

⁴Terrestrial Biogeochemistry Group, Institute of Bio- and Geosciences, Agrosphere (IBG-3), Forschungszentrum Jülich GmbH, D-52425 Jülich, Germany

⁵Department of Crop Science, Section of Plant Nutrition and Crop Physiology, University of Goettingen, Carl-Sprengel-Weg 1, D-37075 Göttingen, Germany

⁶Rothamsted Research, North Wyke, Okehampton EX20 2SB, UK

RATIONALE: Nitrous oxide (N₂O), a highly climate-relevant trace gas, is mainly derived from microbial denitrification and nitrification processes in soils. Apportioning N₂O to these source processes is a challenging task, but better understanding of the processes is required to improve mitigation strategies. The N₂O site-specific ¹⁵N signatures from denitrification and nitrification have been shown to be clearly different, making this signature a potential tool for N₂O source identification. We have applied for the first time quantum cascade laser absorption spectroscopy (QCLAS) for the continuous analysis of the intramolecular ¹⁵N distribution of soil-derived N₂O and compared this with state-of-the-art isotope ratio mass spectrometry (IRMS).

METHODS: Soil was amended with nitrate and sucrose and incubated in a laboratory setup. The N₂O release was quantified by FTIR spectroscopy, while the N₂O intramolecular ¹⁵N distribution was continuously analyzed by online QCLAS at 1 Hz resolution. The QCLAS results on time-integrating flask samples were compared with those from the IRMS analysis.

RESULTS: The analytical precision (2σ) of QCLAS was around 0.3 ‰ for the δ¹⁵N^{bulk} and the ¹⁵N site preference (SP) for 1-min average values. Comparing the two techniques on flask samples, excellent agreement (R² = 0.99; offset of 1.2 ‰) was observed for the δ¹⁵N^{bulk} values while for the SP values the correlation was less good (R² = 0.76; offset of 0.9 ‰), presumably due to the lower precision of the IRMS SP measurements.

CONCLUSIONS: These findings validate QCLAS as a viable alternative technique with even higher precision than state-of-the-art IRMS. Thus, laser spectroscopy has the potential to contribute significantly to a better understanding of N turnover in soils, which is crucial for advancing strategies to mitigate emissions of this efficient greenhouse gas. Copyright © 2012 John Wiley & Sons, Ltd.

Nitrous oxide (N₂O) contributes significantly to global warming and climate change (e.g. IPCC 2007),^[1] and it is an efficient ozone-depleting substance^[2] with agricultural soils being the dominant sector of anthropogenic N₂O emission.^[1]

Advanced N₂O mitigation strategies for agricultural production systems rely on improved understanding of N₂O formation in soils and partitioning to the main N₂O source processes, i.e. nitrification and denitrification. The microbial

enzymatic pathways associated with N₂O production from nitrification and denitrification induce ¹⁵N depletion in the emitted N₂O which is considerably higher for nitrifying bacteria than for denitrifying bacteria.^[3,4] Therefore, measurement of the ¹⁵N content in N₂O (δ¹⁵N^{bulk} value) is an excellent tool to study these processes, although it has to be considered that its δ¹⁵N^{bulk} value also depends on the precursor signature, fractionation during N₂O to N₂ reduction,^[5] and transport limitations as well as physiological controls.^[6,7] In addition to the bulk ¹⁵N isotopic composition of N₂O, the site preference (SP = δ¹⁵N^α – δ¹⁵N^β), which specifies the intramolecular ¹⁵N distribution on the central (α) and the end (β) positions of the linear asymmetric N₂O molecule, has been shown to differ significantly between different microbial N₂O-releasing

* Correspondence to: J. R. Köster, Institute of Plant Nutrition and Soil Science, Kiel University, Hermann-Rodewald-Str. 2, D-24118 Kiel, Germany.
E-mail: jrkoester@plantnutrition.uni-kiel.de

processes in soil. SP values for nitrification (i.e. NH₃ oxidation via hydroxylamine) were found to be between 31 and 37 ‰, and in the range of -10 to 0 ‰ for denitrification (heterotrophic as well as nitrifier denitrification).^[8–11] Therefore, analysis of the N₂O site-specific isotopic composition to allocate N₂O production processes in soil studies is of increasing interest.^[12–16] However, N₂O isotopic source signatures for distinct microbial processes are still based on a limited number of pure culture studies. Furthermore, a simple two source mixing model might not always be adequate as, for example, N₂O production by fungal denitrification (ca. 37 ‰)^[7] and N₂O to N₂ reduction by heterotrophic denitrifiers (εSP = 2.9 – 6.8 ‰)^[12,17] significantly increase the N₂O site preference and might result in an overestimation of nitrification-derived N₂O.

Most reported studies analyzing N₂O isotopomers are based on mass spectrometric determination of molecular (N₂O⁺) and fragment (NO⁺) ions of N₂O, allowing the calculation of δ¹⁵N^{bulk} and SP values.^[18,19] In contrast, novel spectroscopic techniques such as Fourier transform infrared (FTIR) spectroscopy,^[20] or quantum cascade laser absorption spectroscopy (QCLAS),^[21–23] enable the direct quantification of N₂O isotopomers based on their characteristic rotational-vibrational absorption spectra, and hold advantages over isotope ratio mass spectrometry (IRMS) in terms of field applicability.

The aim of the present study was to demonstrate the feasibility of continuous N₂O isotopomer analysis by laser spectroscopy for source identification of soil-derived N₂O and its validation by intercomparison with IRMS as standard technique.

EXPERIMENTAL

Setup

An arable soil, which had been used in previous studies,^[24,25] taken from the top horizon of a Luvisol at the Hohenschulen experimental farm of Kiel University, Germany, was sieved and ca. 3 dm³ soil was repacked into 4.25 L glass jars to a bulk density of 1.4 g cm⁻³. Potassium nitrate and sucrose solution were applied on top of the soil at rates equivalent to 0.21 g sucrose and 0.025 g nitrate-N kg⁻¹ soil dry matter (DM) (equivalent to 1200 kg sucrose ha⁻¹ and 60 kg nitrate-N ha⁻¹, respectively) to foster N₂O production by heterotrophic denitrification. The soil moisture was adjusted to 80 % water-filled pore space. A control treatment was amended with nitrate only. Both treatments were set up in triplicate.

Pressurized air (Messer Schweiz AG, Lenzburg, Switzerland) was passed through the headspace of each incubation vessel at a flow rate of 20 mL min⁻¹ (Fig. 1). To assess the variability between different soil cores and to perform an offline intercomparison between QCLAS and IRMS on N₂O isotopomer concentrations, the outlet air of individual soil cores was sampled in Tedlar[®] bags deploying a peristaltic pump (Ecoline VC-MS/CA 8–6 with Tygon LFL tubing i.d. 0.63 or 0.89 mm; Ismatec, IDEX Health & Science SA, Glattbrugg, Switzerland) at 3.5 mL min⁻¹ (nitrate sucrose treatment) and 6 mL min⁻¹ (control treatment). The remaining outflow gas from the replicates of each treatment was combined and directed to a FTIR spectrometer for trace gas analysis (N₂O, CO₂). For the nitrate-sucrose treatment a FTIR spectrometer

(Avatar 370, Thermo Fisher Scientific, Waltham, MA, USA) with a low-volume (50 mL) flow-through gas cell with a 1 m optical path length (model LFT-210; Axiom Analytical Inc., Tustin, CA, USA) and InSb detector was applied.^[26] For the control cores, a FTIR spectrometer (CX4000; Gaset Technologies Oy, Helsinki, Finland), with a 9.8 m optical path cell and MCT detector was deployed. Continuous trace gas analysis was initiated 8 h prior to fertilizer addition and continued until the N₂O mixing ratios decreased to background concentrations.

Prior to online N₂O isotopomer analysis by QCLAS, H₂O and CO₂ were quantitatively removed from the gas flow of the nitrate sucrose-treated soil cores, by means of a permeation drier (MD-070-24S; Perma Pure Inc., Toms River, NY, USA) and a chemical trap filled with Ascarite (20 g, 10–35 mesh; Sigma Aldrich, Buchs, Switzerland) bracketed by Mg(ClO₄)₂ (2 × 8 g; Sigma Aldrich). For N₂O concentrations above 100 ppm, the dried and CO₂-scrubbed sample gas was dynamically diluted with synthetic air (Messer Schweiz AG) to a constant N₂O mixing ratio (100 ppm) using a LabVIEW[™] controlled mass flow controller (MFC, Red-y Smart series; Vögtlin Instruments AG, Aesch, Switzerland), based on the N₂O concentrations determined by FTIR spectroscopy. This experimental setup greatly reduced the need for non-linearity corrections of the QCLAS results and allowed optimal accuracy.

Laser spectroscopy

The laser spectrometer consisted of a single-mode, pulsed QCL (Alpes Lasers SA, Neuchâtel, Switzerland) emitting at 2188 cm⁻¹, a multipass absorption cell (AMAC-56; optical path length 56 m, volume 500 mL; Aerodyne Research Inc., Billerica, MA, USA) and a detection scheme with pulse normalization.^[22] Laser control, data acquisition and simultaneous quantification of the three main N₂O isotopic species (¹⁴N¹⁴N¹⁶O, ¹⁵N¹⁴N¹⁶O, ¹⁴N¹⁵N¹⁶O) were accomplished by TDLWintel software (Aerodyne Research Inc.) taking into account the path length, gas temperature (≈ 305 K), pressure (8 kPa) and laser line width (0.0068 cm⁻¹). The laser spectrometer was operated in a continuous flow through mode with a back pressure regulator (GSK-A3TA-FF22; Vögtlin Instruments AG) mounted upstream of the cell to maintain a constant cell pressure and a scroll pump (TriScroll 300; Agilent Technologies, Santa Clara, CA, USA) with a manual flow adjustment valve downstream.

The relative differences of the isotopic ratios δ¹⁵N^α and δ¹⁵N^β were determined by deploying a set of laboratory calibration gases produced from pure medical N₂O (Messer Schweiz AG) supplemented with distinct amounts of isotopically pure (>98 %) ¹⁵N¹⁴N¹⁶O and ¹⁴N¹⁵N¹⁶O (Cambridge Isotope Laboratories, Andover, MA, USA).^[23] Primary laboratory standards were analyzed for their δ¹⁵N^α, δ¹⁵N^β and δ¹⁵N^{bulk} values by IRMS at the Tokyo Institute of Technology.^[19] Secondary working standards applied in the presented project were measured against primary standards by QCLAS: standard 1: δ¹⁵N^α = 2.1 ± 0.1 ‰, δ¹⁵N^β = 2.0 ± 0.2 ‰, 246.9 ± 0.1 ppm N₂O; standard 2: δ¹⁵N^α = 25.0 ± 0.1 ‰, δ¹⁵N^β = 24.8 ± 0.2 ‰, 249.1 ± 0.1 ppm N₂O (the precision indicated is the standard error of the mean) and diluted to 100 ppm with synthetic air prior to QCLAS analysis. To account for drift effects, standard 1 was analyzed once per hour. For N₂O concentrations between 60 and 100 ppm, the δ¹⁵N^α and δ¹⁵N^β values were corrected for dependency on

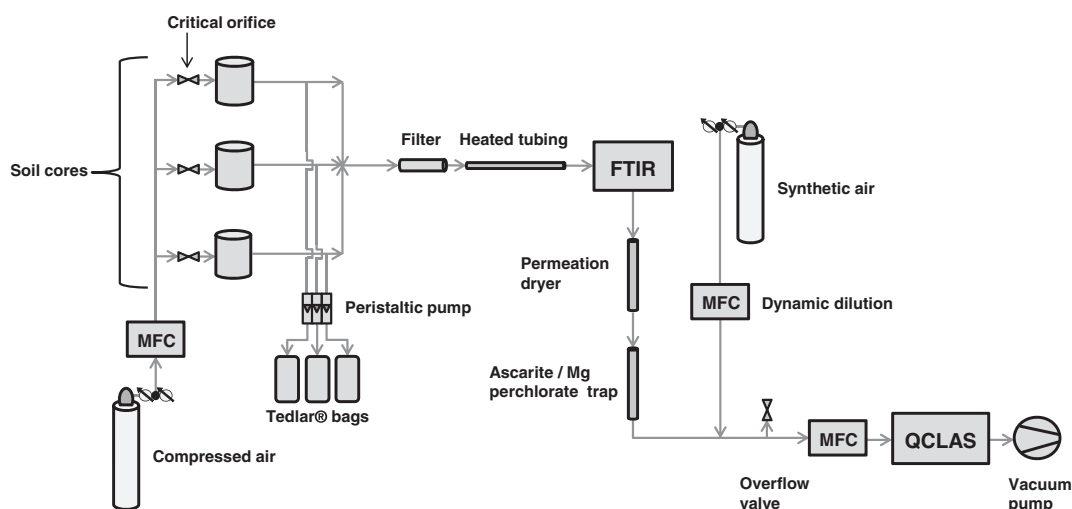


Figure 1. Experimental setup (MFC – mass flow controller; FTIR – Fourier transform infrared spectrometer; QCLAS – quantum cascade laser absorption spectrometer).

the N_2O mixing ratio. The Tedlar[®] bag samples were subsequently analyzed for their $\delta^{15}\text{N}^\alpha$ and $\delta^{15}\text{N}^\beta$ values by QCLAS; for concentrations above 10 ppm N_2O in a continuous flow through mode, for lower concentrations after preconcentration applying a liquid nitrogen-free preconcentration device. During preconcentration N_2O is adsorbed on a porous polymer adsorption trap (HayeSep D 100–120 mesh; Hayes Separations Inc., Bandera, TX, USA) at -150°C . Desorption is accomplished by resistive heating of the trap to $+10^\circ\text{C}$ and purging the released N_2O with 10 mL min^{-1} of synthetic air into the evacuated multipass cell of the laser spectrometer.^[21,22] To confirm the accuracy of our measurements, N_2O isotopomer concentrations in the pressurized air were measured by QCLAS after preconcentration. The observed N_2O mixing ratios (329.8 ± 0.2 ppb) as well as the N_2O SP value of $17.7 \pm 0.3\text{‰}$ ($\delta^{15}\text{N}^\alpha = 15.2 \pm 0.1\text{‰}$ and $\delta^{15}\text{N}^\beta = -2.5 \pm 0.1\text{‰}$) are consistent with background air (SP of $18.7 \pm 2.2\text{‰}$)^[27] with minor contributions of a ^{15}N -depleted N_2O emission source.

Mass spectrometry

The gas samples collected in the Tedlar[®] bags were analyzed for their $\delta^{15}\text{N}^\alpha$, $\delta^{15}\text{N}^\beta$, and $\delta^{18}\text{O}$ value by IRMS as a direct intercomparison between the two techniques at the von Thuenen Institute in Braunschweig, Germany. Isotopologue signatures of N_2O were determined by analyzing m/z 44, 45, and 46 of intact N_2O^+ molecular ions as well as m/z 30, 31 of NO^+ fragment ions.^[19] A modified preconcentration unit consisting of a set of automated cryotrap (PreCon; ThermoFinnigan, Bremen, Germany) equipped with an autosampler (Combi-PAL; CTC-Analytics, Zwingen, Switzerland) was coupled to a gas chromatograph (Trace GC Ultra; Thermo Fisher Scientific, Bremen, Germany) which was connected via a ConFlo IV interface to a Delta V isotope ratio mass spectrometer (Thermo Fisher Scientific). Simultaneous detection of m/z 30, 31, 44, 45, and 46 was hence possible. N-exchange between N_2O^+ and NO^+ in the ion source of the mass spectrometer, the so-called scrambling factor, was determined by analyzing defined mixtures of non-labeled N_2O with a N_2O standard labeled at the β -N position

(98 atom %; CK Gas Products Ltd., Hook, UK) as described by Röckmann *et al.*,^[28] giving a scrambling factor of 0.08 (a scrambling factor of 0.5 would mask the site preference entirely). The isotopologue ratios of $^{15}\text{R}^{\text{bulk}}$, ^{18}R and $^{15}\text{R}^\alpha$ were determined, and $^{15}\text{R}^\beta$ was obtained by the relationship of $^{15}\text{R}^{\text{bulk}} = (^{15}\text{R}^\alpha + ^{15}\text{R}^\beta)/2$, where $^{15}\text{R}^\alpha = [^{14}\text{N}^{15}\text{N}^{16}\text{O}]/[^{14}\text{N}^{14}\text{N}^{16}\text{O}]$, $^{15}\text{R}^\beta = [^{15}\text{N}^{14}\text{N}^{16}\text{O}]/[^{14}\text{N}^{14}\text{N}^{16}\text{O}]$, $^{18}\text{R} = [^{14}\text{N}^{14}\text{N}^{18}\text{O}]/[^{14}\text{N}^{14}\text{N}^{16}\text{O}]$. The isotopologue ratios of a sample (R_{sample}) were expressed as ‰ deviation from the $^{15}\text{N}/^{14}\text{N}$ and $^{18}\text{O}/^{16}\text{O}$ ratios of the standard materials (R_{std} ; i.e. atmospheric N_2 and standard mean ocean water (SMOW)), respectively: $\delta X = (R_{\text{sample}} / R_{\text{std}} - 1) \times 1000$, where $X = ^{15}\text{N}^{\text{bulk}}$, $^{15}\text{N}^\alpha$, $^{15}\text{N}^\beta$, or ^{18}O . The typical analytical precision was 0.2, 0.4, and 0.3 ‰ for $\delta^{15}\text{N}^{\text{bulk}}$, $\delta^{15}\text{N}^\alpha$, and $\delta^{18}\text{O}$ values, respectively. The detection limit for N_2O -N was 1.5 nM. Pure N_2O (purity >99.995; Linde, Munich, Germany) was used as reference gas which was analyzed for isotopologue signatures in the laboratory of the Tokyo Institute of Technology using the calibration procedures developed earlier.^[19] This reference signature was used to correct the raw $\delta^{15}\text{N}^\alpha$ value determined by our IRMS instrumentation. The linear regression between the $\delta^{15}\text{N}^\alpha$ value and m/z 30 peak areas, as determined by analysis of reference gas standards with concentrations between 200 and 10000 ppb, was used to correct for non-linearity of the NO^+ isotope ratios. The m/z 30 and m/z 44 peak areas were used to determine N_2O concentrations. The correction for ^{17}O for the $\delta^{15}\text{N}$ - N_2O value was made according to the method described by Brand.^[29]

RESULTS AND DISCUSSION

Continuous analysis of trace gas concentrations and N_2O isotope ratios by infrared spectroscopy

Figure 2 displays the N_2O and CO_2 concentration profile as analyzed by FTIR spectroscopy. Microbial activity in the nitrate sucrose-treated soil cores was considerably enhanced, as indicated by the N_2O and CO_2 mixing ratios in the offgas reaching up to 360 and 3300 ppm, respectively, while the control treatment revealed lower mixing ratios. The site-specific

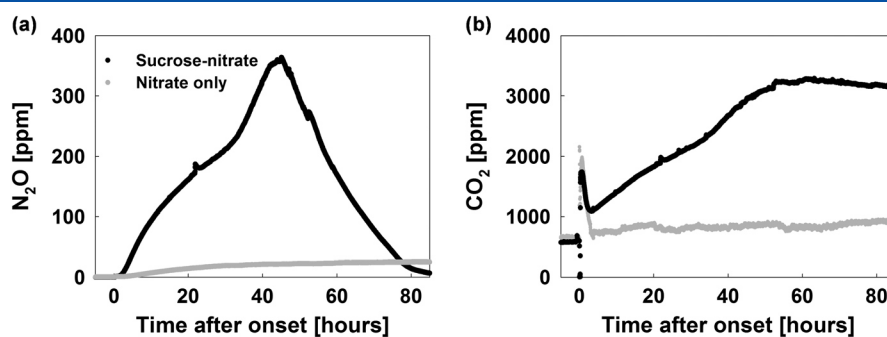


Figure 2. N₂O (a) and CO₂ (b) concentrations from nitrate sucrose-treated soil and the control treatment (nitrate only) during 4 days of incubation.

isotopic composition ($\delta^{15}\text{N}^\alpha$ and $\delta^{15}\text{N}^\beta$) of N₂O emitted from the nitrate sucrose-treated soil cores was analyzed online by QCLAS over 3 days at 1 Hz temporal resolution (Figs. 3(a) and 3(b) show 1-min average values). To our knowledge this study constitutes the first published example of a real-time analysis of N₂O isotopomers. During incubation the ¹⁵N content of the emitted N₂O ($\delta^{15}\text{N}^{\text{bulk}}$) changed considerably. Initially, the $\delta^{15}\text{N}^{\text{bulk}}$ values were around -35% , but they then increased by more than 50% in an almost linear way, reaching $+16\%$ after 3 days (Fig. 3(a)). Similar results were reported by Meijide *et al.*^[30] who observed an increase in $\delta^{15}\text{N}^{\text{bulk}}$ values by almost 40% within 4 days. The observed N₂O $\delta^{15}\text{N}^{\text{bulk}}$ values (relative to the applied nitrate $\delta^{15}\text{N}$ value of $-3.8 \pm 0.1\%$) are within the range reported for denitrification-derived N₂O as summarized by Baggs.^[4] Although the emphasis of this study is on the implementation of a novel analytical technique and intercomparison measurements and the detailed discussion of the involved microbial

source processes is beyond its scope, it should be pointed out that $\delta^{15}\text{N}^{\text{bulk}}$ value observed in this study is in agreement with typical values reported for microbial N₂O production processes.

The ¹⁵N site preference (SP, Fig. 3(b)) of the N₂O released from the nitrate sucrose treatment was -1% at the beginning of the incubation experiment and declined to around -2 to -3% within the first day after onset. Two short-term shifts in SP and N₂O mixing ratios within this period (around 20 and 55 h after onset) are due to pressure fluctuations in the headspace caused by replacement of the Ascarite/Mg(ClO₄)₂ trap. The SP reached a maximum value of $+5\%$ around 40 h after fertilizer addition, which coincided with the highest N₂O emissions (Fig. 2). Subsequently, the SP decreased to around $+3\%$ before it leveled out at $+5\%$. The observed range of SP values is consistent with the dominance of heterotrophic denitrification as the main N₂O source process for the nitrate sucrose-amended soil cores. The predominance of

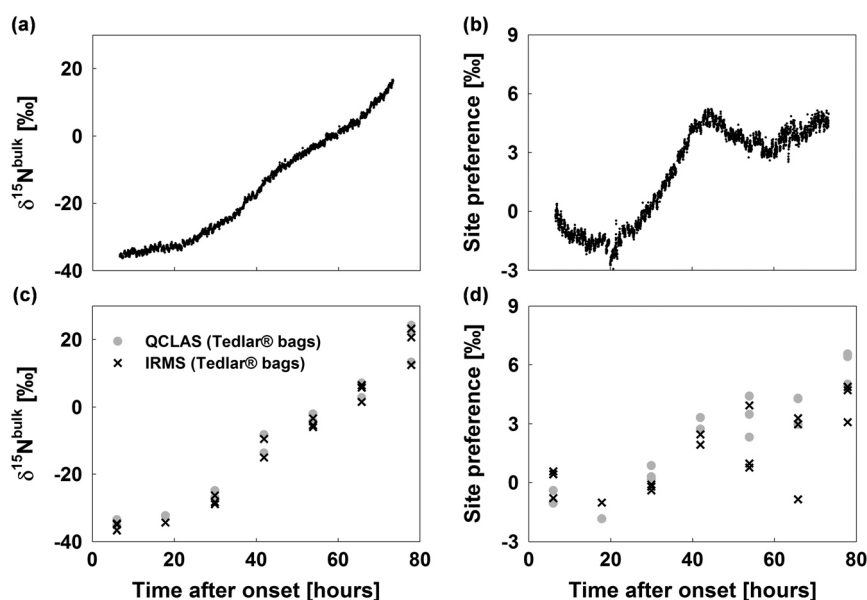


Figure 3. Continuous laser spectroscopic analysis of soil-emitted N₂O for $\delta^{15}\text{N}^{\text{bulk}}$ values (a) and ¹⁵N site preference (SP; b) after nitrate sucrose treatment. Individual data points are 1-min average values. Analysis of gas samples (Tedlar® bags) integrating over 12 h (nitrate sucrose treatment) for QCLAS-IRMS intercomparison of N₂O $\delta^{15}\text{N}^{\text{bulk}}$ values (c) and ¹⁵N site preference (SP; d).

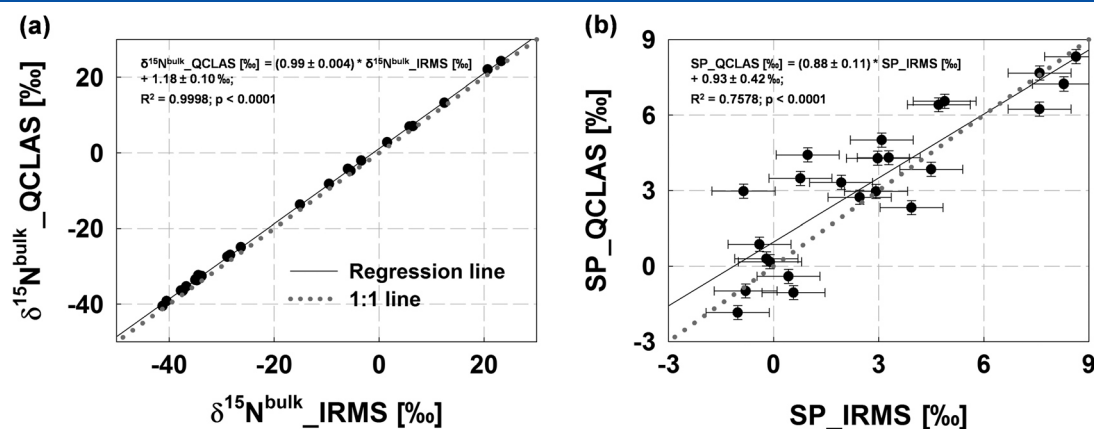


Figure 4. Intercomparison of QCLAS and IRMS results on integrating gas samples from nitrate sucrose and control treatment for N_2O $\delta^{15}\text{N}^{\text{bulk}}$ values (a) and ^{15}N site preference (SP; b). Error bars indicate precision of both techniques ($\pm 2\sigma$).

denitrification-derived N_2O is congruent with other soil studies under similar conditions.^[16,31] While SP values around 0 ‰ or slightly negative have been reported for N_2O production by denitrification (heterotrophic as well as nitrifier denitrification),^[8–11] it has been shown that fractionation during partial N_2O reduction favors $^{15}\text{N}^{14}\text{N}^{16}\text{O}$ reduction relative to $^{14}\text{N}^{15}\text{N}^{16}\text{O}$ reduction, resulting in increasing SP.^[12,17,31] The increase in SP in the nitrate sucrose-addition treatment, therefore, could be explained by an increasing importance of N_2O reduction with rising N_2O emissions. However, as nitrification and fungal denitrification have been reported to produce N_2O with SP values of 31 to 37 ‰ or 37 ‰, respectively, we cannot exclude a contribution of these processes to the observed SP shift.^[7,9]

For the control treatment, no continuous N_2O isotopic analysis was conducted, but Tedlar[®] bag gas samples were analyzed by IRMS and QCLAS. The $\delta^{15}\text{N}^{\text{bulk}}$ values of the emitted N_2O displayed only a minor, but still significant increase from -38.7 to -34.2 ‰ (QCLAS) from day 1 to day 3 (data not shown), while the N_2O SP increased from 4.3 to 7.7 ‰ (QCLAS). These results are included in the following section on the method intercomparison without detailed discussion of the underlying microbial production processes.

Intercomparison of QCLAS and IRMS

In addition to real-time $\delta^{15}\text{N}^{\text{bulk}}$ and SP analysis by QCLAS performed on N_2O from the nitrate sucrose-treated soil cores, N_2O isotopomers were determined in time-integrating bag samples by laser spectroscopy and IRMS. Figures 3(a)–3(d) indicate a considerable agreement between online N_2O SP isotopic composition and offline analysis of Tedlar[®] bag gas samples by laser spectroscopy and IRMS. The results of both techniques follow a similar trend and exhibit an excellent correlation, with $R^2 = 0.99$ and $p < 0.0001$ (Fig. 4(a)). However, the $\delta^{15}\text{N}^{\text{bulk}}$ values determined by QCLAS show a systematic offset of 1.2 ± 0.1 ‰ ($p < 0.0001$) compared with those for the Tedlar[®] bag samples analyzed by IRMS. The source of this disagreement has not yet been identified, and it might be due to any one (or both) of the involved methods. As similar $\delta^{15}\text{N}^{\text{bulk}}$ values were obtained with both techniques for N_2O calibration gases, the discrepancy might be due to differences in the gas matrix (e.g. CO_2), transportation, or gas

conditioning prior to analysis, and this will be the subject of an upcoming research project. For SP the level of agreement is clearly lower (Fig. 4(b), $R^2 = 0.76$; $p < 0.0001$). However, the SP values from the two techniques were not significantly different. Both may be explained to some extent by the considerably higher uncertainty of IRMS for SP (1 ‰, 2σ) than for $\delta^{15}\text{N}^{\text{bulk}}$ (0.4 ‰, 2σ) as SP includes the uncertainties of the $\delta^{15}\text{N}^{\alpha}$ and $\delta^{15}\text{N}^{\text{bulk}}$ values.^[32] In contrast, the analytical precision (2σ) of the laser spectrometer at current elevated N_2O mixing ratios (100 ppm) is higher, around 0.3 ‰ for both $\delta^{15}\text{N}^{\text{bulk}}$ and SP, for 1-min average values.

CONCLUSIONS

This study demonstrates the performance of QCLAS in terms of precision and temporal resolution when measuring N_2O isotopomers. Laser spectroscopy was applied for the first time for the continuous analysis of the site-specific ^{15}N isotopic composition of soil-derived N_2O at high temporal resolution. In our intercomparison study using time-integrating bag samples, excellent agreement was observed for the N_2O $\delta^{15}\text{N}^{\text{bulk}}$ value between the QCLAS results and the IRMS analysis. For the ^{15}N site preference, the correlation suffered from the lower precision of IRMS for SP. These results confirm that laser spectroscopy is a feasible alternative technique to IRMS that will facilitate a large range of new process studies based on its capability for real-time N_2O isotopic analysis. Moreover, the higher precision of QCLAS than of IRMS will enable more accurate analysis of isotope ratios of soil-derived N_2O which will improve the investigation of N_2O processes using the isotopomer approach. Currently, the amount of sample needed for QCLAS is significantly larger than for IRMS. However, this will soon be significantly improved as more sensitive laser spectrometers become available. In addition, we expect that laser spectrometers will be capable of providing data on N_2O $\delta^{18}\text{O}$ values in addition to $\delta^{15}\text{N}^{\alpha}$ and $\delta^{15}\text{N}^{\beta}$ values in the near future. This may allow the investigation of further processes, such as N_2O reduction, based on additional isotopic discrimination patterns. Finally, robust field instruments will enable extended field studies with the additional advantage of immediate data availability.

Acknowledgements

Jan Reent Köster thanks the German Federal Environmental Foundation (DBU) for a PhD scholarship and the COST Action ES0806 SIBAE for travel support. The QCLAS work was funded by the Swiss National Science Foundation (SNF). Rothamsted Research is grant funded by the Biotechnology and Biological Sciences Research Council (BBSRC), UK. The authors would like to thank Naohiro Yoshida and Sakae Toyoda from Tokyo Institute of Technology for analysis of the site-specific isotopic composition of primary N₂O calibration gases. Professor Karl H. Mühling is acknowledged for his valuable support and Martina Heuer for her efforts in the laboratory. The authors thank two anonymous reviewers and Nathaniel Ostrom for their comments on an earlier version of this manuscript.

REFERENCES

- [1] *Climate Change 2007: Mitigation. Contribution of Working Group III to the Fourth Assessment Report of the Intergovernmental Panel on Climate Change*, (Eds: B. Metz, O. R. Davidson, P. R. Bosch, R. Dave, L. A. Meyer). Cambridge University Press, Cambridge and New York, 2007.
- [2] A. R. Ravishankara, J. S. Daniel, R. W. Portmann. Nitrous oxide (N₂O): The dominant ozone-depleting substance emitted in the 21st century. *Science* **2009**, *326*, 123.
- [3] L. Y. Stein, Y. L. Yung. Production, isotopic composition, and atmospheric fate of biologically produced nitrous oxide. *Annu. Rev. Earth Planet. Sci.* **2003**, *31*, 329.
- [4] E. M. Baggs. A review of stable isotope techniques for N₂O source partitioning in soils: recent progress, remaining challenges and future considerations. *Rapid Commun. Mass Spectrom.* **2008**, *22*, 1664.
- [5] H. Yamagishi, M. B. Westley, B. N. Popp, S. Toyoda, N. Yoshida, S. Watanabe, K. Koba, Y. Yamanaka. Role of nitrification and denitrification on the nitrous oxide cycle in the eastern tropical North Pacific and Gulf of California. *J. Geophys. Res.* **2007**, *112*. DOI: 10.1029/2006JG000227.
- [6] K. L. Casciotti. Inverse kinetic isotope fractionation during bacterial nitrite oxidation. *Geochim. Cosmochim. Acta* **2009**, *73*, 2061.
- [7] R. L. Sutka, G. C. Adams, N. E. Ostrom, P. H. Ostrom. Isotopologue fractionation during N₂O production by fungal denitrification. *Rapid Commun. Mass Spectrom.* **2008**, *22*, 3989.
- [8] R. L. Sutka, N. E. Ostrom, P. H. Ostrom, H. Gandhi, J. A. Breznak. Nitrogen isotopomer site preference of N₂O produced by *Nitrosomonas europaea* and *Methylococcus capsulatus* Bath. *Rapid Commun. Mass Spectrom.* **2004**, *17*, 738.
- [9] R. L. Sutka, N. E. Ostrom, P. H. Ostrom, J. A. Breznak, H. Gandhi, A. J. Pitt, F. Li. Distinguishing nitrous oxide production from nitrification and denitrification on the basis of isotopomer abundances. *Appl. Environ. Microbiol.* **2006**, *72*, 638.
- [10] S. Toyoda, H. Mutobe, H. Yamagishi, N. Yoshida, Y. Tanji. Fractionation of N₂O isotopomers during production by denitrifier. *Soil Biol. Biochem.* **2005**, *37*, 1535.
- [11] C. H. Frame, K. L. Casciotti. Biogeochemical controls and isotopic signatures of nitrous oxide production by a marine ammonia-oxidizing bacterium. *Biogeosciences* **2010**, *7*, 2695.
- [12] N. E. Ostrom, A. Pitt, R. Sutka, P. H. Ostrom, A. S. Grandy, K. M. Huizinga, G. P. Robertson. Isotopologue effects during N₂O reduction in soils and in pure cultures of denitrifiers. *J. Geophys. Res.* **2007**, *112*. DOI: 10.1029/2006JG000287.
- [13] N. E. Ostrom, R. Sutka, P. H. Ostrom, A. S. Grandy, K. M. Huizinga, H. Gandhi, J. C. von Fischer, G. P. Robertson. Isotopologue data reveal bacterial denitrification as the primary source of N₂O during a high flux event following cultivation of a native temperate grassland. *Soil Biol. Biochem.* **2010**, *42*, 499.
- [14] R. Well, I. Kurganova, V. L. de Gerenyu, H. Flessa. Isotopomer signatures of soil-emitted N₂O under different moisture conditions - A microcosm study with arable loess soil. *Soil Biol. Biochem.* **2006**, *38*, 2923.
- [15] M. R. Opdyke, N. E. Ostrom, P. H. Ostrom. Evidence for the predominance of denitrification as a source of N₂O in temperate agricultural soils based on isotopologue measurements. *Global Biochem. Cycles.* **2009**, *23*. DOI: 10.1029/2009GB003523.
- [16] J. R. Köster, L. Cárdenas, M. Senbayram, R. Bol, R. Well, M. Butler, K. H. Mühling, K. Dittert. Rapid shift from denitrification to nitrification in soil after biogas residue application as indicated by nitrous oxide isotopomers. *Soil Biol. Biochem.* **2011**, *43*, 1671.
- [17] M. Jinuntuya-Nortman, R. L. Sutka, P. H. Ostrom, H. Gandhi, N. E. Ostrom. Isotopologue fractionation during microbial reduction of N₂O within soil mesocosms as a function of water-filled pore space. *Soil Biol. Biochem.* **2008**, *40*, 2273.
- [18] C. A. M. Brenninkmeijer, T. Röckmann. Mass spectrometry of the intramolecular nitrogen isotope distribution of environmental nitrous oxide using fragment-ion analysis. *Rapid Commun. Mass Spectrom.* **1999**, *13*, 2028.
- [19] S. Toyoda, N. Yoshida. Determination of nitrogen isotopomers of nitrous oxide on a modified isotope ratio mass spectrometer. *Anal. Chem.* **1999**, *71*, 4711.
- [20] D. W. T. Griffith, S. D. Parkes, V. Haverd, C. Paton-Walsh, S. R. Wilson. Absolute calibration of the intramolecular site preference of ¹⁵N fractionation in tropospheric N₂O by FT-IR spectroscopy. *Anal. Chem.* **2009**, *81*, 2227.
- [21] J. Mohn, C. Guggenheim, B. Tuzson, M. K. Vollmer, S. Toyoda, N. Yoshida, L. Emmenegger. A liquid nitrogen-free preconcentration unit for measurements of ambient N₂O isotopomers by QCLAS. *Atmos. Meas. Tech.* **2010**, *3*, 609.
- [22] J. Mohn, B. Tuzson, A. Manninen, N. Yoshida, S. Toyoda, W. A. Brand, L. Emmenegger. Site selective real-time measurements of atmospheric N₂O isotopomers by laser spectroscopy. *Atmos. Meas. Tech.* **2012**, *5*, 1601.
- [23] H. Wächter, J. Mohn, B. Tuzson, L. Emmenegger, M. W. Sigrist. Determination of N₂O isotopomers with quantum cascade laser based absorption spectroscopy. *Opt. Express* **2008**, *16*, 9239.
- [24] R. Horn. Division S-1 - Soil physics - Time dependence of soil mechanical properties and pore functions for arable soils. *Soil Sci. Soc. Am. J.* **2004**, *68*, 1131.
- [25] M. Senbayram, R. R. Chen, K. H. Mühling, K. Dittert. Contribution of nitrification and denitrification to nitrous oxide emissions from soils after application of biogas waste and other fertilizers. **2009**, *23*, 2489.
- [26] J. Mohn, M. J. Zeeman, R. A. Werner, W. Eugster, L. Emmenegger. Continuous field measurements of δ¹³C-CO₂ and trace gases by FTIR spectroscopy. *Isot. Environ. Health Stud.* **2008**, *44*, 241.
- [27] N. Yoshida, S. Toyoda. Constraining the atmospheric N₂O budget from intramolecular site preference in N₂O isotopomers. *Nature* **2000**, *405*, 330.
- [28] T. Röckmann, J. Kaiser, C. A. M. Brenninkmeijer, W. A. Brand. Gas chromatography/isotope-ratio mass spectrometry method for high-precision position-dependent

- ¹⁵N and ¹⁸O measurements of atmospheric nitrous oxide. *Rapid Commun. Mass Spectrom.* **2003**, *17*, 1897.
- [29] W. A. Brand. PRECON: A fully automated interface for the pre-GC concentration of trace gases in air for isotopic analysis. *Isot. Environ. Health Stud.* **1995**, *31*, 277.
- [30] A. Meijide, L. M. Cárdenas, R. Bol, A. Bergstermann, K. Goulding, R. Well, A. Vallejo, D. Scholefield. Dual isotope and isotopomer measurements for the understanding of N₂O production and consumption during denitrification in an arable soil. *Eur. J. Soil Sci.* **2010**, *61*, 364.
- [31] R. Well, H. Flessa. Isotopologue signatures of N₂O produced by denitrification in soils. *J. Geophys. Res.* **2009**, *114*. DOI: 10.1029/2008JG000804.
- [32] R. Well, H. Flessa, L. Xing, X. T. Ju, V. Römheld. Isotopologue ratios of N₂O emitted from microcosms with NH₄⁺ fertilized arable soils under conditions favoring nitrification. *Soil Biol. Biochem.* **2008**, *40*, 2416.

Chapter 8

General discussion

8 General Discussion

High anthropogenic GHG emissions are known to increase radiative forcing and thus to induce global warming and climate change, and the agricultural sector contributes significantly to these emissions (Stocker et al., 2013).

The presented thesis was designed to contribute to the understanding of agriculture related GHG emissions and thus to participate in adapting more sustainable agricultural practice.

The use of renewable energy source is explicitly promoted in several European countries to replace fossil fuels and thus to reduce GHG emissions, and biogas production from energy crops and organic wastes for generating electricity became one of the major strategies (Herrmann and Rath, 2012), but may itself be afflicted by significant GHG and NH₃ emissions, in particular during open storage of AD (Meyer-Aurich et al., 2012; Claus et al., 2013). These emissions from AD storage have been investigated in the present thesis deploying a noninvasive remote sensing technique. Further attention was put on emissions from AD field application as fertilizer, where emissions are usually dominated by NH₃ volatilization (Amon et al., 2006). During various biochemical N transitions in soils N₂O is released to the atmosphere, and denitrification as the major N₂O source is largely promoted by organic fertilizers like AD or animal slurry (Saggar et al., 2013). These N₂O as well as N₂ emissions from organically fertilized soil have been investigated here in an incubation study involving an isotopomer approach for estimating the relative contribution of major N₂O source pathways as described earlier (Park et al., 2011; Toyoda et al., 2011). This isotopomer approach relies on precise knowledge about the isotope effects associated with the involved turnover processes (Ostrom and Ostrom, 2012); thus, in different experiments the isotopic fractionation factors during N₂O production and reduction via denitrification have been thoroughly investigated in the presented thesis. Finally, QCLAS as a novel and promising analytical technique for analyzing site-specific N₂O ¹⁵N signatures has been evaluated in a soil incubation study.

8.1 Emission measurements from open digestate lagoons by OP FTIR

Biogas production from energy crops and organic wastes for generating electricity expanded largely in several European countries during the recent years, (Herrmann and Rath, 2012), but may be afflicted with significant trace gas emissions, which are assumed to be particularly high when AD are stored in uncovered storage facilities (Meyer-Aurich et al., 2012; Claus et al., 2013). However, reliable data about these emissions is scarce, mainly because of methodological challenges. OP FTIR as a noninvasive remote sensing approach in combination with a micrometeorological transport model provides several advantages against other methods (Denmead, 2008) and has therefore been evaluated and deployed for emission measurements from open AD lagoons.

8.1.1 Validation of the OP FTIR methodology by trace gas release-recovery experiments

The OP FTIR approach was validated for its applicability in lagoon settings. During three trials, a tubing system was placed on a lagoon surface, and a trace gas (N₂O or NH₃, respectively) was released at a known rate in a regular pattern. The resulting increase in the trace gas concentrations was measured

downwind by OP FTIR, and the trace gas fluxes were determined using the bLS technique (Flesch et al., 1995; Flesch et al., 2004). A similar approach has recently been applied successfully by Ro et al. (2013). The determined gas emission rate (Q_{bLS}) and the actual gas release rate (Q) from the lagoon surface were compared, and revealed a good accuracy with Q_{bLS}/Q ratios between 0.89 and 1.23, over all three experiments with a Q_{bLS}/Q ratio of 1.13 (± 0.17).

It has been reported before that the bLS technique can achieve very good accuracy for estimating fluxes from ground level sources, averaging under ideal conditions to an inaccuracy of about 2% (Flesch et al., 2004; McBain and Desjardins, 2005), while in another study the inaccuracy was 9% (Gao et al., 2009). Thus, for routine emission measurements from agricultural fields under relatively undisturbed wind conditions, the bLS technique has already been shown to provide adequate flux estimations.

For situations with disturbed wind flow, which is likely to apply for emission measurements in lagoon settings, the bLS technique will give estimates of lower, but still acceptable accuracy, as it has been shown in studies with artificially wind disturbance (Flesch et al., 2005; McBain and Desjardins, 2005). During their lagoon experiments with synthetic trace gas emission sources for validating the bLS technique, Ro et al. (2013) achieved an accuracy between 0.81 and 0.93 (Q_{bLS}/Q). This accuracy is in a similar range compared to the present study. This suggests that for longer measurement periods well-founded assumptions about atmospheric conditions can also result in acceptable bLS estimates. Thus, routine measurements in lagoon settings are feasible when reasonable parameters are chosen without the need of experimental determination of ‘best fit’ settings.

8.1.2 Greenhouse gas and ammonia emissions from AD lagoons

The trace gas emissions from two open AD lagoons have been determined by OP FTIR in six trials lasting between one and seven days. Considerable trace gas emissions were measured from the two open digestate lagoons, which were dominated by CH_4 and NH_3 , and emissions were highest during the summer. N_2O emissions were only during the summer high enough for reliable quantification, while during winter only negligible N_2O emissions, if any, occurred.

The surface-related NH_3 emissions from the lagoons were similar to emissions found by Clemens et al. (2006), but about 10 times higher compared to Amon et al. (2006), both investigating emissions from fermented cattle slurry in pilot scale tanks. CH_4 emissions from the AD lagoons, however, were about two to four times higher compared to the aforementioned studies. Data on emissions from AD from energy crop digestion or co-digestion, however, is scarce (e.g. Liebetrau et al., 2013) and not detailed enough or afflicted with artificial conditions and do not allow direct comparison to our study, but still highlight the high emission potential.

Animal slurries often have similar physicochemical properties compared to AD and some studies were focused on emissions from slurry lagoons. NH_3 emissions in the present study were lower compared to (McGinn et al., 2008; Grant et al., 2013), CH_4 emissions were usually lower from animal slurry lagoons Sharpe et al. (2002) or in a similar range (Todd et al., 2011) compared to the present study, but also emissions up to ten times higher during midsummer emission peaks were reported (DeSutter and Ham, 2005). These studies highlight the high variability of possible NH_3 and CH_4 emissions.

N₂O emissions were only in one trial during midsummer high enough for quantification. During the other trials, the detected N₂O concentrations were only slightly above the atmospheric background concentration, especially during the winter, when almost no N₂O was detectable. During the trial with the highest N₂O emissions, these fluxes were in a similar range compared to previous findings (Amon et al., 2006; Clemens et al., 2006). In other studies it has been shown that N₂O released from stored animal slurries is primarily produced by biological processes within the surface crust (Sommer et al., 2000; Berg et al., 2006). In oxic zones of such crusts, ammonia oxidation (nitrification) will occur, while in anoxic zones nitrate and nitrite, the products of nitrification, can be denitrified, and thus also N₂O will be produced (Sommer et al., 2000).

The CO₂-equivalent weighted (CO₂-eq) trace gas emissions from both lagoons were high in relation to the GHG saving potential of the respective biogas plant. Highest CO₂-eq emissions were about 54% (energy crop co-fermented AD) and 297% (dairy slurry fermentation), respectively, compared to the CO₂ savings by replacing natural gas utilization (emissions during natural gas production not taken into account). This is of particular importance for the biogas plant predominantly operated with energy crops because these emissions considerably reduce the GHG balance of this biogas production chain. In contrast, biogas plants fed with cattle slurry only may, despite of clearly higher trace gas emissions from the lagoon per unit energy output, still reduce the overall CO₂-eq emissions, as they are to be compared to storage of undigested slurry (Marañón et al., 2011).

Previous studies on the climate balance of biogas energy (Meyer-Aurich et al., 2012; Claus et al., 2013) identified CH₄ emissions from open AD storage to be the factor adding the largest uncertainty to different biogas production scenarios, and concluded that GHG emissions from biogas production systems with open AD storage may release GHG emissions which are close to those from energy production from natural gas or even higher. However, these studies based their assumptions about CH₄ emissions during AD storage solely on the residual gas potential of AD determined in a survey on 61 biogas plants (FNR, 2009), but not on actual emission measurements. The present study strengthens these reports on high emission potential from AD storage with data of high accuracy obtained by an advanced remote sensing approach covering the whole emitting surface area of AD lagoons, and highlights that open storage facilities are likely the major contributor to the overall trace gas emissions of biogas energy. Although neither of these studies allows determining precise year-averaged emission factors due to the limited number of observations and involved biogas plants and the high variability of emissions as affected by different factors, they emphasize further systematic investigation of these emissions, as they counteract the GHG reduction as the principal motivation of biogas energy production. Consequently, the implementation of gastight covers on all AD storage facilities will help improving the GHG balance of biogas energy by reducing emissions and by increasing the use efficiency of substrates by capturing additional CH₄.

8.1.3 Effect of lagoon agitation and surface crust homogenization on trace gas emissions

Agitation of stored AD can strongly affect trace gas emissions from storage facilities, because naturally occurring surface crusts, which restrict emissions to the atmosphere, are destroyed. Here, the surface crust covering an AD lagoon was mechanically destroyed and homogenized twice prior to withdrawal of AD for land spreading. The NH₃ emissions during the 24 hours following these stirring events were four to seven times higher than during the undisturbed phase. This indicates that NH₃ emissions were

reduced efficiently by the surface crust by more than 80%. This is in agreement with previous studies where NH_3 emissions were reduced by 50 – 60% (Misselbrook et al., 2005; Smith et al., 2007), or even 80% (Sommer et al., 1993). AD from energy crop co-fermentation are characterized by large shares of plant fiber which can build a more effective surface crust than e.g. pig-slurry and the crust effect was high. During the following days the NH_3 emission clearly decreased because of a gradual regeneration of the surface crust, which causes depletion of NH_3 at the AD surface as reported before (Sommer et al., 1993). In contrast to NH_3 emissions, CH_4 fluxes peaked during and directly after the stirring events, but afterwards dropped to rates clearly below those of the undisturbed lagoon. As reported earlier, agitation stripes CH_4 from the liquid phase (Husted, 1993), but will also release CH_4 trapped by the surface crust. Furthermore, stirring may possibly cause a temporary reduction of methanogenesis due to aeration (Husted, 1993). These are probably the reasons for temporarily lower CH_4 fluxes during the days after agitation. In contrast to NH_3 , total CH_4 emissions seemed to be unaffected by homogenization, as the CH_4 emission rates averaged over several days before and after the stirring events were almost identical, i.e. the emission peaks during agitation were compensated by subsequent lower fluxes.

The frequency of such AD agitation events depends mainly on management practice, but the results presented here suggest to reduce such activities to a minimum to reduce NH_3 losses, as long as storage facilities are not equipped with gastight covers.

8.2 NH_3 emissions during AD land spreading during the winter season

Anaerobic digestates from biogas production are usually applied to agricultural land, similar to animal slurries, as organic fertilizers, to return nutrients into the agricultural production cycle. Thereby, NH_3 emissions can be particularly high (Quakernack et al., 2012; Chen et al., 2013), because of AD's usually high ammonium concentration and high pH value (Gutser et al., 2005; Tambone et al., 2009); however, previous studies only comprise emissions during the warmer growing season, while emissions occurring under colder winter conditions are still lacking.

In a field trial in late February the NH_3 concentrations after AD land spreading and a preceding application of pelleted urea were monitored continuously over six days by OP FTIR and the area integrated flux was determined using the bLS technique (Flesch et al., 1995; Flesch et al., 2004). This methodological approach has several advantages compared to other techniques, as it allows continuous measurements in much higher temporal compared to passive samplers, and is clearly less susceptible to spatial heterogeneity than chamber measurements, as large emission source areas can be covered (Denmead, 2008).

The relative NH_3 loss over the six day period was about 40% of the $\text{NH}_4^+\text{-N}$ contained in the applied AD, and the observed NH_3 volatilization may be attributed almost entirely to the AD application, because urea hydrolysis is very slow at low temperatures (Xu et al., 1993); however, AD may possibly contribute to faster hydrolysis of urea and promote NH_3 emissions in the further course due to its high pH value. This observed NH_3 emission was clearly higher compared to results of previous studies on NH_3 volatilization from AD land spreading during the growing season. In average, Quakernack et al. (2012) observed volatile NH_3 losses of 15% during their field trials, while Ni et al. (2012) reported even lower NH_3 emissions, ranging from 4 to 13%. However, NH_3 emissions after application of liquid animal slurries with similar physicochemical properties have often been reported to be clearly higher (e.g.

Misselbrook et al., 2000; up to 60% of ammoniacal N). NH₃ emissions after AD band spreading on arable land have been reported to be particularly high when the soil is covered by no or only low vegetation (Wulf et al., 2002), as it usually is the case during winter.

Several previous studies indicate that NH₃ volatilization is significantly affected by air temperature, especially during the initial 24 hours, and that the emission event may last longer under low air temperatures (Sommer et al., 1991; Huijsmans et al., 2003). Compared to these studies as well as to Quakernack et al. (2012), NH₃ volatilization in the present study lasted over a considerably longer phase. This may be attributed to the predominantly frozen soil by which infiltration of AD was clearly restricted, so most of applied AD remained on the soil surface. Due to the low temperature the AD on the soil surface remained moist or temporarily frozen during the whole measurement period but did not dry, and dissolved NH₄⁺ remained mobile. Therefore we conclude that the frozen soil hampering infiltration and the freeze-thaw cycles prolonged the emission phase and increased total NH₃ volatilization above amounts which would typically be emitted under the given environmental conditions. A similar observation was reported by Sommer et al. (1991) after surface application of cattle slurry on frozen soil. It has been shown earlier, that infiltration of slurry into the soil influences the NH₃ volatilization pattern (Sommer et al., 2004).

The observed NH₃ emissions were higher than expected under cold temperatures around the freezing point and point out that application of organic fertilizers on partly frozen soil poses a significant source of NH₃ emissions. Thus, AD land spreading appears non-advisable under frozen soil conditions with respect to ammonia volatilization.

8.3 N₂O and N₂ emissions from agricultural soil amended with AD and cattle slurry

While NH₃ emissions during and after AD land spreading are immediate short-term emissions, N₂O emissions after application of AD or other N fertilizers to soil can occur over longer periods, as they are intermediates or by-products of different biochemical N transformations (Butterbach-Bahl et al., 2013). Here, heterotrophic denitrification, the reduction of nitrate (NO₃⁻) and nitrite (NO₂⁻) via the gaseous intermediates NO and N₂O to N₂ (Wrage et al., 2001; Robertson and Groffman, 2007) is usually the main N₂O source (Saggar et al., 2013). Labile organic carbon (C) is a major driving factor for denitrification, because oxidized N species are used by bacterial denitrifiers as alternative electron acceptors when molecular oxygen (O₂) is limited (Robertson and Groffman, 2007). Therefore, organic fertilizers like AD and animal slurries have the potential to cause clearly higher N₂O emissions compared to mineral N fertilizers (Senbayram et al., 2009; Köster et al., 2011; Saggar et al., 2013).

In the present study a grassland soil was amended with AD (low C/N ratio) or with cattle slurry (CS; high C/N ratio) and incubated over 52 days in N₂-free atmosphere using an automated incubation system (Cárdenas et al., 2003), capable of online determination of N₂O, N₂, and CO₂ production. Here, the observed CO₂ production in organically amended soils was clearly higher compared to untreated soil, especially when CS was added due to its high C content. The cumulative N₂O production from AD treated soil was similar to untreated control soil, while emission with CS addition was clearly higher. This is in contrast to previous findings by Senbayram et al. (2009), who reported similar N₂O emissions from soil treated with AD compared to CS. This difference, however, may be attributed to different AD properties, for example the AD C/N ratio in the present study was considerably lower. Earlier studies on N₂O emissions from organically amended soils under comparable incubation conditions suggested

that most N₂O rather derived from denitrification, while nitrification contributed only minor amounts (Senbayram et al., 2009; Köster et al., 2011).

The emission of gaseous N products (i.e. N₂O and N₂) was highest with CS and lowest in the control treatment. Higher N₂O+N₂ release can clearly be attributed to the labile C fraction of the organic fertilizers, fostering microbial respiration and, thus, heterotrophic denitrification (e.g. Weier et al., 1993). This was confirmed by a positive correlation between the cumulative (N₂O+N₂)-N flux and the soil respiration rate as indicated by the CO₂-C flux ($R^2 = 0.82$). The overall N₂O/(N₂O+N₂) product ratio was considerably lower with the organic amendments compared to untreated soil, i.e. N₂O reduction to N₂ by denitrifiers was significantly promoted by labile carbon substrates in the organic fertilizers inducing high demand for electron acceptors, while soil nitrate concentration was low (Weier et al., 1993; Robertson and Groffman, 2007; Senbayram et al., 2012).

From these results it was concluded 1) that organic fertilizer application to soil even under conditions promoting denitrification does not necessarily increase the N₂O emissions, as N₂O reduction to N₂ can balance higher N₂O production; and 2) that anaerobic digestion of organic wastes and animal slurries may be an appropriate measure to reduce N₂O emissions by reducing their organic C content and thus denitrification.

So here, denitrification was assumed to be the major contributor to N₂O production. However, after application of ammonium based N fertilizers like AD, ammonium will be oxidized to nitrate (i.e. nitrified), whereat also significant amounts of N₂O may escape from the soil (Bateman and Baggs, 2005; Mørkved et al., 2007). For estimations about the relative contribution of the major N₂O source processes, the isotopomer ratios of emitted N₂O have been analyzed, as these isotopomer ratios and in particular the ¹⁵N site preference (SP) allow conclusions about the involved N₂O source pathways (Sutka et al., 2006; Sutka et al., 2008; Park et al., 2011; Toyoda et al., 2011). For this, the insights of further investigations of isotope signals associated with N₂O production and reduction via denitrification in soil as discussed below (sections 8.4 and 8.5) as well as from the literature (Ostrom et al., 2007; Jinuntuya-Nortman et al., 2008) have been applied. Based on these isotope fractionation factor ranges and the measured N₂O reduction, the isotope composition of N₂O unaffected by reduction was estimated. Isotope fractionation during N₂O reduction in soils is most probably characterized by a mixture of processes following open as well as closed isotope dynamics as discussed previously (Decock and Six, 2013). However, steady state conditions as presupposed for the applicability of open system models (Fry, 2006) were not given in the present study, but the high soil moisture conditions may favor N₂O accumulation in soil microsites prior to its reduction, which rather justifies the assumption of closed system isotope dynamics. Thus, the Rayleigh equation describing isotope dynamics in a closed system has been deployed (Mariotti et al., 1981; Fry, 2006). The resulting $\delta_{N_{2O-0}}$ signatures were then used to evaluate the contribution of nitrification and denitrification as the supposed major N₂O source pathways in a two source mixing model based on isotopic signature end-member ranges for SP and $\delta^{18}O$ values from the literature (Toyoda et al., 2005; Sutka et al., 2006; Sutka et al., 2008; Snider et al., 2012; Snider et al., 2013) as well as from the results presented here (sections 8.5). There was good agreement between the results based on SP and on $\delta^{18}O$ values, which indicates appropriate assumptions for the input parameters and thus realistic source estimates. The results confirmed that denitrification was the major N₂O source contributing between 82 - 92% of emitted N₂O in the untreated soil, while in the organically amended soils the relative N₂O contribution from denitrification was lower, being 65 - 79% with AD and 46 - 60% with CS, respectively, due to

higher nitrification in the latter ones. Other N₂O source pathways may have contributed only to minor extent, as there was a good fit between the estimates based on SP and $\delta^{18}\text{O}$ values. In an alternative two source scenario assuming N₂O production via bacterial and fungal denitrification fit of the SP and $\delta^{18}\text{O}$ based estimates was considerably lower and thus this scenario was rather unlikely. Remaining uncertainties afflicted with this approach derive mainly from uncertainties of the relevant fractionation factors and from N₂O production via other biological pathways, and not for all of those the isotopic signals have been investigated yet (Ostrom and Ostrom, 2012). Therefore, this approach does not yet allow to determine the exact contribution of individual N₂O sources, but still provides useful information on the major N₂O source pathways.

8.4 N₂O reduction via denitrification in different soils and associated isotope fractionation

Reduction of N₂O to N₂ via denitrification in soils reduces N₂O emissions to the atmosphere, but interaction of controlling factors is still not very well understood (Saggar et al., 2013), amongst others because direct determination of emitted N₂ is complicated by high atmospheric background N₂ levels (Groffman et al., 2006). N₂O reduction alters the intramolecular ¹⁵N distribution of N₂O by enriching ¹⁵N at the central position of the N₂O molecule, i.e. raises the SP (Ostrom et al., 2007; Jinuntuya-Nortman et al., 2008). This can bias conclusions about N₂O source processes based on SP data; however, a positive correlation between SP and $\delta^{18}\text{O}$ values has been reported to be indicative for N₂O significantly affected by N₂O reduction (Ostrom et al., 2007; Jinuntuya-Nortman et al., 2008; Well and Flessa, 2009a). This may help detecting the occurrence of significant N₂ production via denitrification in soils and might even allow estimating the relative proportion of N₂O being reduced (Park et al., 2011). However, isotope signals of N₂O reduction are not yet very well understood, and thus their applicability is still limited. Therefore, experiments were carried out incubating three contrasting, nitrate amended soils under anoxic conditions in N₂-free Helium atmosphere using an automated soil incubation system capable of dynamic incubations and online gas chromatographic analysis of N₂O, N₂, and CO₂ in the exhaust gas stream. Additional gas samples were collected at frequent intervals and the major N₂O isotopomer species were determined by IRMS.

In these experiments the N₂O and N₂ emissions differed clearly between the different soil types. Comparing the clay and the loam soil, both, N₂O as well as N₂ emissions were higher from nitrate treated clay, which also had the highest C content. However, when the loam and the sandy soil are compared, the N₂O production in the sandy soil was higher, but the N₂ flux was clearly lower. The N₂O/(N₂O+N₂) product ratio was similar for the clay and the loam soil, but comparing the loam soil and a sandy soil, it was clearly higher in the sandy soil. Over time, the N₂O/(N₂O+N₂) product ratio decreased in all soils, because gradual depletion of the added nitrate pool led increasingly to reduction of N₂O to N₂ (Weier et al., 1993).

N₂O reduction to N₂ affects the $\delta^{15}\text{N}^{\text{bulk}}$, $\delta^{18}\text{O}$, and SP values of residual N₂O as mentioned above. Thus, the N₂O $\delta^{18}\text{O}_0$ and SP₀ values, i.e. the isotopic signature of produced N₂O unaffected by reduction, have to be estimated before the isotopic N₂O composition may be used for N₂O source estimations. In this particular case, the $\delta^{15}\text{N}^{\text{bulk}}$ value is of low value, because the $\delta^{15}\text{N}$ value of the soil nitrate pool was not constant but rather affected by isotope fractionation during nitrate reduction; thus, the $\delta^{15}\text{N}_0$ value of produced N₂O will not be constant as well. In contrast, the N₂O $\delta^{18}\text{O}_0$ and SP₀ values may be assumed to be relatively constant.

For two of the three soils (loam soil and clay soil) the resulting $N_2O/(N_2O+N_2)$ product ratio covered a relatively wide range. Therefore, the net isotope effect η (NIE; according to Jinuntuya-Nortman et al., 2008) of the N_2O -to- N_2 reduction step as well as the N_2O $\delta^{18}O_0$ and SP_0 values could be determined by fitting the $N_2O/(N_2O+N_2)$ product ratio as well as the N_2O isotope values to the logarithmic Rayleigh equation (Mariotti et al., 1981). The application of this equation postulates a closed system in which no substrate (i.e. N_2O) is added (via production) nor removed and substrate is used up over time (Fry, 2006). In soils mostly a mixture of open and closed system isotope dynamics should occur. A simulation of isotope effects during N_2O reduction indicated that N_2O SP values only increase drastically when more than 80% of all substrate is consumed following closed system dynamics (Decock and Six, 2013). As this applies in the present study and the observed data can be described by a logarithmic function which is characteristic for closed systems, the experimental results in the present study were analyzed using the Rayleigh model. The η_{SP} values of the N_2O -to- N_2 reduction step of -6.1 ‰ (clay soil) and -8.2 ‰ (loam soil) were found, which is the range of several previous reports (Ostrom et al., 2007; Well and Flessa, 2009a), while also lower values were reported (Jinuntuya-Nortman et al., 2008).

However, only the N_2O SP_0 value of loamy soil (-3.9‰) matched with literature values of denitrification (Toyoda et al., 2005; Sutka et al., 2006), while in the clay soil the SP_0 value was clearly higher (+7.9‰), indicating additional contribution by other pathways than heterotrophic denitrification, possibly fungal denitrification (Sutka et al., 2008).

The $\eta_{\delta^{18}O}$ values for N_2O reduction were calculated as -8.6 and -3.4 ‰ for the loamy and the clay soil, respectively; for the clay soil, however, the R^2 of $\eta_{\delta^{18}O}$ was low. This indicates clearly lower O fractionation during N_2O reduction compared to previous studies (Ostrom et al., 2007; Yamagishi et al., 2007; Well and Flessa, 2009a). Furthermore, the $\delta^{18}O$ vs SP relationship in the present study was 0.69 and 0.93 in the two soils, while of 2.2 to 2.5 has been suggested to be indicative for N_2O reduction (Ostrom et al., 2007; Well and Flessa, 2009a). This discrepancy is probably caused by a fundamental difference in the experimental setup between the present study, in which N_2O was produced in the soil prior to reduction, and the aforementioned studies, in which N_2O was added to the head space of incubation flasks and may have affected isotope signatures not only by fractionation during reduction processes, but also during diffusion and passage of boundaries (e.g. into the liquid phase or into the bacterial cell). Fractionation during diffusion has been shown to affect N_2O $\delta^{18}O$ values much stronger than the SP (Well and Flessa, 2008), and, thus, will affect the $\delta^{18}O$ vs SP relationship. In the case of in situ produced N_2O in the present study, however, isotopically lighter N_2O will more rapidly escape from denitrifying micro-sites by diffusion which might to some extent favor accumulation and subsequent reduction of isotopically heavier N_2O . This effect is in opposite to enzymatic $\delta^{18}O$ and $\delta^{15}N$ effects as suggested earlier (Well and Flessa, 2009c) and might thus explain smaller apparent $\eta^{18}O$ values compared to literature results. In N_2O sampled in aquifers, the $\delta^{18}O$ vs SP relationship was found to be in the same range as the results presented here with values between 0.2 and 1.14 (Koba et al., 2009; Well et al., 2012), and those lower ratios were attributed to small isotope effect during N_2O diffusion in water (Well et al., 2012) which thus supports the hypothesis above.

8.5 Isotopic fractionation factors of N_2O production and reduction during denitrification

Isotopic fractionation factors associated with denitrification (i.e. N_2O production and reduction) have been further investigated deploying different experimental approaches, involving the C_2H_2 (acetylene)

inhibition technique, the use of waters with differing O isotope signature, and the ^{15}N labeling technique in soil incubation experiments. The isotopic fractionation factors of these (Chapter 6) as well as from the previous study (Chapter 5) were thoroughly studied using the Rayleigh equation (Mariotti et al., 1981; Fry, 2006) as well as a modelling approach using the Levenberg-Marquardt algorithm and Markov chain Monte Carlo simulations (Soetaert and Petzoldt, 2010).

Only a few previous studies determined isotope effects during N_2O production via denitrification in whole soil microbial communities (Mariotti et al., 1981; Menyailo and Hungate, 2006; Pérez et al., 2006; Snider et al., 2009; Well and Flessa, 2009b), and those results varied in a much wider range compared to the present study. Some indicated smaller isotope effects compared to the present study, possibly due to simultaneous occurrence of N_2O reduction when no C_2H_2 was applied (Snider et al., 2009; Snider et al., 2013), while in another study unconventional C_2H_2 inhibition was applied (Pérez et al., 2006), possibly contributing to their high isotope effects, which differed clearly from other studies (Menyailo and Hungate, 2006; Well and Flessa, 2009b). Thus, fractionation factors from studies without complete inhibition of N_2O reduction may not be directly comparable to the present study.

Significant O exchange during nitrate reduction was found, which had been shown already before (Snider et al., 2009). The O exchange with soil water was positively correlated with water saturation of the soil as shown in the first experiment, which was already proposed by Snider et al. (2013); however, O exchange could not be determined in the two other experiments, as there was no water with different O isotope signatures used, which is required to investigate O exchange (Snider et al., 2009).

The $\eta_1^{15}\text{N}$ of was quite similar in all three experiments and in the range from -55 to -38‰. However, larger fractionation was found in treatments with higher nitrate supply. The $\eta_1\text{SP}$ varied in the three experiments in a narrow range from -3 to +6‰. Such variations in $\eta_1\text{SP}$ should mostly depend on the microbial community of the soil (Schmidt et al., 2004; Ostrom and Ostrom, 2012) which may be associated with different soil types, soil properties or various experimental conditions. However, there was no indication of any significant trends.

The fractionation during N_2O production was also reflected in the isotopic signature of the residual nitrate in the soil ($\delta^{15}\text{N}_{\text{NO}_3}$) and was mostly consistent with the model estimations. Isotopic fractionation factors for $\delta^{18}\text{O}$ during nitrate reduction in aquifers have been found between -8‰ (Böttcher et al., 1990) and about -6‰ (Knöller et al., 2011). However, it has not yet been shown that these values are also valid for unsaturated soils. Moreover, it has recently been shown that $\delta^{18}\text{O}_{\text{NO}_3}$ values may be also affected by the O-exchange with water (Kool et al., 2011; Wunderlich et al., 2013) due to nitrite re-oxidation. The $\delta^{18}\text{O}_{\text{NO}_3}$ values observed in the experiments were rather unpredictable and in some cases higher, but in some cases lower than expected. Some of this variance was likely caused by O exchange with water, but still these results show that the isotopic fractionation during nitrate reduction may be very different and be positive as well as negative; thus, no consistent isotope effect can be determined. The direction and magnitude of this effect is most probably dependent on the soil microbial community, e.g. on the abundance of microbes capable of performing nitrite re-oxidation (Wunderlich et al., 2013).

As for N_2O production, also for N_2O reduction there are not many published studies investigating isotopic fractionation in whole soil with complex microbial communities (Menyailo and Hungate, 2006; Ostrom et al., 2007; Vieten et al., 2007; Jinuntuya-Nortman et al., 2008; Well and Flessa, 2009a). In general, these literature data are quite consistent for $\eta_2^{15}\text{N}$ and $\eta_2\text{SP}$ values, but indicate a very wide

range for $\eta_2^{18}\text{O}$. All of the experimental results of the present study confirm the range of $\eta_2\text{SP}$ values found in previous studies (Jinuntuya-Nortman et al., 2008; Well and Flessa, 2009a). In contrast, our values of $\eta_2^{15}\text{N}$ and $\eta_2^{18}\text{O}$ show very wide variations and are not always consistent with literature data, which applies in particular for the positive $\eta_2^{15}\text{N}$ and $\eta_2^{18}\text{O}$ values.

It is assumed that N_2O reduction occurs via two coexisting routes: (1) N_2O reduction immediately following its production, i.e. within the same denitrifying microsite or the same denitrifying cell prior to its potential escape; (2) produced N_2O escaped from the denitrifying microsite and re-enters a denitrifying cell where it is fully or partially reduced (Ostrom et al., 2007). These two routes may be associated with different η_2 values due to different combinations of enzymatic and diffusive isotope effects. This hypothesis may explain the variability in $\eta_2^{18}\text{O}$ and $\eta_2^{15}\text{N}$ by various contribution of diffusive effects, and is further supported in the present experiments by the consistent $\eta_2\text{SP}$, which is not significantly affected by diffusion, but also in previous studies (Ostrom et al., 2007; Jinuntuya-Nortman et al., 2008; Well and Flessa, 2009a).

Isotopic fractionation factors during N_2O production as well as N_2O reduction were determined assuming closed-system isotope dynamics. It is obvious that this assumption is justified for N_2O production from a nitrate pool which is gradually reduced. N_2O reduction, however, occurred simultaneously with N_2O production and thus appears as an open system, in which N_2O is produced and afterwards partially reduced. But the application of open-system equations for calculation of isotopic fractionation factors is only justified for 'steady-state' systems, i.e. when the substrate input and consumption rates are equal, because the equations for open-system calculations are derived from mass balance equations and adopt an assumption about balanced in and out fluxes (Fry, 2006). Such a simplification is not justified for the N_2O reduction process, because the product ratio during the experiment is not stable and consequently the N_2O substrate pool is not at 'steady-state' which is required for 'open-system' equations (Fry, 2006; Decock and Six, 2013). Furthermore, for physical reasons soils cannot act as perfectly open systems because there is always transient N_2O accumulation in pore space (Heincke and Kaupenjohann, 1999; Clough et al., 2005) due to inhibited diffusive efflux, which depends on the volume and geometry of water- and air-filled pores. Finally, results from experiments with simultaneous N_2O production and reduction where the reduction was directly measured, show the logarithmic correlation between the isotopic signature of N_2O and the fraction of residual substrate (Chapter 5; Decock and Six, 2013), while 'open-system' dynamics would express a linear correlation (Fry, 2003, 2006). Hence, this shows that the reduction process can be mathematically better described with 'closed-system' equations. While the reduction process can be described better with 'closed-system' equations, we cannot rule out that process dynamics consisted of a mix of open and closed system dynamics as proposed by (Decock and Six, 2013).

An important question is whether these fractionation factors apply also for natural conditions and if their robustness is sufficient for determining N_2O reduction and whole nitrogen loss due to denitrification. For such calculations, fractionation must be precisely predictable for a particular soil and ambient conditions. Despite relatively good understanding of $\eta_1^{15}\text{N}$ and $\eta_1\text{SP}$ during N_2O production, they cannot yet be robustly predicted for a particular soil without conducting laboratory experiments, because the range of variations is rather pronounced. Largest variation was found for $\eta_1^{18}\text{O}$, but this may possible to be estimated based on the presumed strict relation of oxygen isotope effect and soil WFPS. If this relation was universally applicable, this would enable us to predict the $\delta^{18}\text{O}$ of N_2O produced in the course of denitrification.

Proper determination of isotope effects during N₂O reduction is usually more complicated due to experimental difficulties. We showed that the experimental setup is a crucial factor for the measured isotope effects. The large variability of $\eta_2^{18\text{O}}$ and $\eta_2^{15\text{N}}$ is most probably due to the coexistence of diffusive and enzymatic fractionation, which may cause an opposite isotope effect. For N₂O reduction two different reduction routes may occur, which show very different interaction of diffusion and enzymatic fractionation, and consequently result in very different net isotope effects. Predicting the dominating reduction mechanism for natural conditions and corresponding fractionation factors for field studies is still impossible. Here we showed that the application of values obtained from N₂O addition experiments (Menyailo and Hungate, 2006; Ostrom et al., 2007; Jinuntuya-Nortman et al., 2008; Well and Flessa, 2009a) may be not representative for natural conditions, as it only allows to investigate one of two possible reduction pathways. However, the values obtained for $\eta_2\text{SP}$ are very consistent in the present as well as in previous experiments (Ostrom et al., 2007; Jinuntuya-Nortman et al., 2008; Well and Flessa, 2009a). Hence the range of -2 to -8‰ with a most probable estimate of -5‰ can be universally adopted, because the SP effect is only due to enzymatic processes and thus independent of differences in reduction routes.

8.6 Are new laser spectroscopic techniques an alternative to IRMS for isotopic N₂O analysis?

N₂O isotopomer analysis by IRMS has relatively low sample throughput, the instruments are not field deployable, and usually online or real-time measurements are not possible. New IR spectroscopic techniques may hold advantages in terms of these issues compared to IRMS. Therefore, a new experimental setup involving Quantum Cascade Laser Absorption Spectroscopy (QCLAS) capable of continuous site-specific ¹⁵N analysis of N₂O has been tested and compared to isotopic analysis of N₂O by IRMS as state-of-the-art technique for analyzing N₂O from incubated soil. The site specific isotopic composition ($\delta^{15\text{N}^\alpha}$ and $\delta^{15\text{N}^\beta}$) of N₂O emitted from the nitrate sucrose treated soil cores was analyzed online by QCLAS over three days at 1 Hz temporal resolution. Additionally, time-integrating gas samples were collected for comparative analysis by QCLAS and IRMS. To our knowledge this study constitutes the first example of a real-time analysis of N₂O isotopomers so far.

There was good agreement between the results of online N₂O site-specific ¹⁵N analysis and offline analysis on time-integrating gas samples by laser spectroscopy and IRMS. The results of both techniques exhibited an excellent correlation with $R^2 = 0.99$ and $p < 0.0001$. However, $\delta^{15\text{N}^{\text{bulk}}}$ values analyzed by QCLAS show a systematic offset of 1.2 ± 0.1 ‰ ($p < 0.0001$) as compared to samples analyzed by IRMS. The source of this disagreement has not yet been identified, and may be due to any one (or both) involved methods. As similar $\delta^{15\text{N}^{\text{bulk}}}$ values were obtained with both techniques for N₂O calibration gases, the discrepancy may be due to differences in the gas matrix (e.g. residual CO₂), transportation, or gas conditioning prior to analysis. For SP values the level of agreement was clearly lower ($R^2 = 0.76$; $p < 0.0001$). However, SP values from both techniques were not significantly different. Both may be explained to some extent by the considerably higher uncertainty of IRMS for SP (1 ‰, 2σ) as compared to $\delta^{15\text{N}^{\text{bulk}}}$ (0.4 ‰, 2σ), because SP includes the uncertainties of $\delta^{15\text{N}^\alpha}$ and $\delta^{15\text{N}^{\text{bulk}}}$ (Well et al., 2008). In contrast, the analytical precision (2σ) of the applied laser spectrometer at elevated N₂O mixing ratios (100 ppm) is higher, around 0.3 ‰ for both $\delta^{15\text{N}^{\text{bulk}}}$ and SP, for one minute average values.

This study demonstrated the performance of QCLAS in terms of precision and temporal resolution for measuring N₂O isotopomers and revealed an excellent agreement for N₂O $\delta^{15\text{N}^{\text{bulk}}}$ between QCLAS

results and IRMS analysis, while for the ^{15}N site preference the correlation suffered from the lower precision of IRMS for SP. These results confirm that laser spectroscopy is a feasible alternative technique to IRMS that will provide a large range of new process studies based on its capability for real-time N_2O isotopic analysis. Moreover, the higher precision of QCLAS compared to IRMS will enable more accurate analysis of isotope ratios of soil-derived N_2O which will improve the investigation of N_2O processes using the isotopomer approach.

Upcoming new laser spectrometers will provide additional capability for $\delta^{18}\text{O}$ analysis of N_2O , which will allow to investigate further processes. Furthermore, they will have improved sensitivity, reducing the required sample amount and need for preconcentration, as they are, for example, now equipped with continuous wave (cw) laser diodes instead of pulsed lasers as in the present study, allowing higher precisions (McManus et al., 2006), and first instruments are already deployed in field studies with the additional advantage of immediate data availability.

8.7 References

- Amon, B., Kryvoruchko, V., Amon, T., Zechmeister-Boltenstern, S., 2006. Methane, nitrous oxide and ammonia emissions during storage and after application of dairy cattle slurry and influence of slurry treatment. *Agriculture Ecosystems & Environment* 112, 153-162.
- Bateman, E.J., Baggs, E.M., 2005. Contributions of nitrification and denitrification to N_2O emissions from soils at different water-filled pore space. *Biology and Fertility of Soils* 41, 379-388.
- Berg, W., Brunsch, R., Pazsiczki, I., 2006. Greenhouse gas emissions from covered slurry compared with uncovered during storage. *Agriculture Ecosystems & Environment* 112, 129-134.
- Böttcher, J., Strebel, O., Voerkelius, S., Schmidt, H.L., 1990. Using Isotope Fractionation of Nitrate Nitrogen and Nitrate Oxygen for Evaluation of Microbial Denitrification in a Sandy Aquifer. *Journal of Hydrology* 114, 413-424.
- Butterbach-Bahl, K., Baggs, E.M., Dannenmann, M., Kiese, R., Zechmeister-Boltenstern, S., 2013. Nitrous oxide emissions from soils: how well do we understand the processes and their controls? *Philosophical Transactions of the Royal Society B-Biological Sciences* 368.
- Cárdenas, L.M., Hawkins, J.M.B., Chadwick, D., Scholefield, D., 2003. Biogenic gas emissions from soils measured using a new automated laboratory incubation system. *Soil Biology & Biochemistry* 35, 867-870.
- Chen, D.J., Jiang, L.N., Huang, H., Toyota, K., Dahlgren, R.A., Lu, J., 2013. Nitrogen dynamics of anaerobically digested slurry used to fertilize paddy fields. *Biology and Fertility of Soils* 49, 647-659.
- Claus, S., Taube, F., Wienforth, B., Svoboda, N., Sieling, K., Kage, H., Senbayram, M., Dittert, K., Gericke, D., Pacholski, A., Herrmann, A., 2013. Life-cycle assessment of biogas production under the environmental conditions of northern Germany: greenhouse gas balance. *Journal of Agricultural Science FirstView*, 1-10.
- Clemens, J., Trimborn, M., Weiland, P., Amon, B., 2006. Mitigation of greenhouse gas emissions by anaerobic digestion of cattle slurry. *Agriculture, Ecosystems & Environment* 112, 171-177.

- Clough, T.J., Sherlock, R.R., Rolston, D.E., 2005. A review of the movement and fate of N₂O in the subsoil. *Nutrient Cycling in Agroecosystems* 72, 3-11.
- Decock, C., Six, J., 2013. How reliable is the intramolecular distribution of ¹⁵N in N₂O to source partition N₂O emitted from soil? *Soil Biology and Biochemistry* 65, 114-127.
- Denmead, O.T., 2008. Approaches to measuring fluxes of methane and nitrous oxide between landscapes and the atmosphere. *Plant and Soil* 309, 5-24.
- DeSutter, T.M., Ham, J.M., 2005. Lagoon-biogas emissions and carbon balance estimates of a swine production facility. *Journal of Environmental Quality* 34, 198-206.
- Flesch, T.K., Wilson, J.D., Yee, E., 1995. Backward-time Lagrangian stochastic dispersion models and their application to estimate gaseous emissions. *Journal of Applied Meteorology* 34, 1320-1332.
- Flesch, T.K., Wilson, J.D., Harper, L.A., Crenna, B.P., Sharpe, R.R., 2004. Deducing ground-to-air emissions from observed trace gas concentrations: A field trial. *Journal of Applied Meteorology* 43, 487-502.
- Flesch, T.K., Wilson, J.D., Harper, L.A., 2005. Deducing ground-to-air emissions from observed trace gas concentrations: A field trial with wind disturbance. *Journal of Applied Meteorology* 44, 475-484.
- FNR, 2009. Biogas-Messprogramm II - 61 Biogasanlagen im Vergleich. Fachagentur Nachwachsende Rohstoffe e.V. (FNR), Gülzow, Germany. URL: http://www.fnr-server.de/ftp/pdf/literatur/pdf_385messdaten_biogasmessprogramm_ii.pdf; accessed: 01.09.2013.
- Fry, B., 2003. Steady state models of stable isotopic distributions. *Isotopes in Environmental and Health Studies* 39, 219-232.
- Fry, B., 2006. *Stable Isotope Ecology*. Springer Science+Business Media, LLC, New York, NY, USA, 316 pp.
- Gao, Z.L., Mauder, M., Desjardins, R.L., Flesch, T.K., van Haarlem, R.P., 2009. Assessment of the backward Lagrangian Stochastic dispersion technique for continuous measurements of CH₄ emissions. *Agricultural and Forest Meteorology* 149, 1516-1523.
- Grant, R.H., Boehm, M.T., Lawrence, A.F., Heber, A.J., 2013. Ammonia emissions from anaerobic treatment lagoons at sow and finishing farms in Oklahoma. *Agricultural and Forest Meteorology* 180, 203-210.
- Groffman, P.M., Altabet, M.A., Bohlke, J.K., Butterbach-Bahl, K., David, M.B., Firestone, M.K., Giblin, A.E., Kana, T.M., Nielsen, L.P., Voytek, M.A., 2006. Methods for measuring denitrification: Diverse approaches to a difficult problem. *Ecological Applications* 16, 2091-2122.
- Gutser, R., Ebertseder, T., Weber, A., Schraml, M., Schmidhalter, U., 2005. Short-term and residual availability of nitrogen after long-term application of organic fertilizers on arable land. *Journal of Plant Nutrition and Soil Science-Zeitschrift Fur Pflanzenernahrung Und Bodenkunde* 168, 439-446.
- Heincke, M., Kaupenjohann, M., 1999. Effects of soil solution on the dynamics of N₂O emissions: a review. *Nutrient Cycling in Agroecosystems* 55, 133-157.

- Herrmann, A., Rath, J., 2012. Biogas Production from Maize: Current State, Challenges, and Prospects. 1. Methane Yield Potential. *Bioenergy Research* 5, 1027-1042.
- Huijsmans, J.F.M., Hol, J.M.G., Vermeulen, G.D., 2003. Effect of application method, manure characteristics, weather and field conditions on ammonia volatilization from manure applied to arable land. *Atmospheric Environment* 37, 3669-3680.
- Husted, S., 1993. An open chamber technique for determination of methane emission from stored livestock manure. *Atmospheric Environment Part a-General Topics* 27, 1635-1642.
- Jinuntuya-Nortman, M., Sutka, R.L., Ostrom, P.H., Gandhi, H., Ostrom, N.E., 2008. Isotopologue fractionation during microbial reduction of N₂O within soil mesocosms as a function of water-filled pore space. *Soil Biology & Biochemistry* 40, 2273-2280.
- Knöller, K., Vogt, C., Haupt, M., Feisthauer, S., Richnow, H.H., 2011. Experimental investigation of nitrogen and oxygen isotope fractionation in nitrate and nitrite during denitrification. *Biogeochemistry* 103, 371-384.
- Koba, K., Osaka, K., Tobari, Y., Toyoda, S., Ohte, N., Katsuyama, M., Suzuki, N., Itoh, M., Yamagishi, H., Kawasaki, M., Kim, S.J., Yoshida, N., Nakajima, T., 2009. Biogeochemistry of nitrous oxide in groundwater in a forested ecosystem elucidated by nitrous oxide isotopomer measurements. *Geochimica et Cosmochimica Acta* 73, 3115-3133.
- Kool, D.M., Wrage, N., Oenema, O., Van Kessel, C., Van Groenigen, J.W., 2011. Oxygen exchange with water alters the oxygen isotopic signature of nitrate in soil ecosystems. *Soil Biology & Biochemistry* 43, 1180-1185.
- Köster, J.R., Cárdenas, L., Senbayram, M., Bol, R., Well, R., Butler, M., Mühling, K.H., Dittert, K., 2011. Rapid shift from denitrification to nitrification in soil after biogas residue application as indicated by nitrous oxide isotopomers. *Soil Biology & Biochemistry* 43, 1671-1677.
- Liebetrau, J., Reinelt, T., Clemens, J., Hafermann, C., Friehe, J., Weiland, P., 2013. Analysis of greenhouse gas emissions from 10 biogas plants within the agricultural sector. *Water Science and Technology* 67, 1370-1379.
- Marañón, E., Salter, A.M., Castrillón, L., Heaven, S., Fernández-Nava, Y., 2011. Reducing the environmental impact of methane emissions from dairy farms by anaerobic digestion of cattle waste. *Waste Management* 31, 1745-1751.
- Mariotti, A., Germon, J.C., Hubert, P., Kaiser, P., Letolle, R., Tardieux, A., Tardieux, P., 1981. Experimental determination of nitrogen kinetic isotope fractionation: Some principles; illustration for the denitrification and nitrification processes. *Plant and Soil* 62, 413-430.
- McBain, M.C., Desjardins, R.L., 2005. The evaluation of a backward Lagrangian stochastic (bLS) model to estimate greenhouse gas emissions from agricultural sources using a synthetic tracer source. *Agricultural and Forest Meteorology* 135, 61-72.
- McGinn, S.M., Coates, T., Flesch, T.K., Crenna, B., 2008. Ammonia emission from dairy cow manure stored in a lagoon over summer. *Canadian Journal of Soil Science* 88, 611-615.
- McManus, J.B., Nelson, D.D., Herndon, S.C., Shorter, J.H., Zahniser, M.S., Blaser, S., Hvozدارa, L., Muller, A., Giovannini, M., Faist, J., 2006. Comparison of cw and pulsed operation with a TE-

- cooled quantum cascade infrared laser for detection of nitric oxide at 1900 cm⁻¹). *Applied Physics B-Lasers and Optics* 85, 235-241.
- Menyailo, O.V., Hungate, B.A., 2006. Stable isotope discrimination during soil denitrification: Production and consumption of nitrous oxide. *Global Biogeochemical Cycles* 20. DOI: 10.1029/2005gb002527.
- Meyer-Aurich, A., Schattauer, A., Hellebrand, H.J., Klaus, H., Plochl, M., Berg, W., 2012. Impact of uncertainties on greenhouse gas mitigation potential of biogas production from agricultural resources. *Renewable Energy* 37, 277-284.
- Misselbrook, T.H., Van der Weerden, T.J., Pain, B.F., Jarvis, S.C., Chambers, B.J., Smith, K.A., Phillips, V.R., Demmers, T.G.M., 2000. Ammonia emission factors for UK agriculture. *Atmospheric Environment* 34, 871-880.
- Misselbrook, T.H., Brookman, S.K.E., Smith, K.A., Cumby, T., Williams, A.G., McCrory, D.F., 2005. Crusting of stored dairy slurry to abate ammonia emissions: Pilot-scale studies. *Journal of Environmental Quality* 34, 411-419.
- Mørkved, P.T., Dörsch, P., Bakken, L.R., 2007. The N₂O product ratio of nitrification and its dependence on long-term changes in soil pH. *Soil Biology & Biochemistry* 39, 2048-2057.
- Ni, K., Pacholski, A., Gericke, D., Kage, H., 2012. Analysis of ammonia losses after field application of biogas slurries by an empirical model. *Journal of Plant Nutrition and Soil Science* 175, 253-264.
- Ostrom, N.E., Pitt, A., Sutka, R., Ostrom, P.H., Grandy, A.S., Huizinga, K.M., Robertson, G.P., 2007. Isotopologue effects during N₂O reduction in soils and in pure cultures of denitrifiers. *Journal of Geophysical Research-Biogeosciences* 112. DOI: 10.1029/2006JG000287.
- Ostrom, N.E., Ostrom, P.H., 2012. The Isotopomers of Nitrous Oxide: Analytical Considerations and Application to Resolution of Microbial Production Pathways. In: Baskaran, M. (Ed.), *Handbook of Environmental Isotope Geochemistry*. Springer Berlin Heidelberg, Berlin, pp. 453-476.
- Park, S., Pérez, T., Boering, K.A., Trumbore, S.E., Gil, J., Marquina, S., Tyler, S.C., 2011. Can N₂O stable isotopes and isotopomers be useful tools to characterize sources and microbial pathways of N₂O production and consumption in tropical soils? *Global Biogeochemical Cycles* 25. DOI: 10.1029/2009gb003615.
- Pérez, T., Garcia-Montiel, D., Trumbore, S., Tyler, S., De Camargo, P., Moreira, M., Piccolo, M., Cerri, C., 2006. Nitrous oxide nitrification and denitrification ¹⁵N enrichment factors from Amazon forest soils. *Ecological Applications* 16, 2153-2167.
- Quakernack, R., Pacholski, A., Techow, A., Herrmann, A., Taube, F., Kage, H., 2012. Ammonia volatilization and yield response of energy crops after fertilization with biogas residues in a coastal marsh of Northern Germany. *Agriculture Ecosystems & Environment* 160, 66-74.
- Ro, K.S., Johnson, M.H., Stone, K.C., Hunt, P.G., Flesch, T., Todd, R.W., 2013. Measuring gas emissions from animal waste lagoons with an inverse-dispersion technique. *Atmospheric Environment* 66, 101-106.
- Robertson, G.P., Groffman, P.M., 2007. Nitrogen Transformations. In: Paul, E.A. (Ed.), *Soil Microbiology, Biochemistry, and Ecology*. Springer, New York, NY, USA, pp. 341 - 364.

- Saggar, S., Jha, N., Deslippe, J., Bolan, N.S., Luo, J., Giltrap, D.L., Kim, D.G., Zaman, M., Tillman, R.W., 2013. Denitrification and N₂O:N₂ production in temperate grasslands: Processes, measurements, modelling and mitigating negative impacts. *The Science of the total environment* 465.
- Schmidt, H.L., Werner, R.A., Yoshida, N., Well, R., 2004. Is the isotopic composition of nitrous oxide an indicator for its origin from nitrification or denitrification? A theoretical approach from referred data and microbiological and enzyme kinetic aspects. *Rapid Communications in Mass Spectrometry* 18, 2036-2040.
- Senbayram, M., Chen, R.R., Mühling, K.H., Dittert, K., 2009. Contribution of nitrification and denitrification to nitrous oxide emissions from soils after application of biogas waste and other fertilizers. *Rapid Communications in Mass Spectrometry* 23, 2489-2498.
- Senbayram, M., Chen, R., Budai, A., Bakken, L., Dittert, K., 2012. N₂O emission and the N₂O/(N₂O + N₂) product ratio of denitrification as controlled by available carbon substrates and nitrate concentrations. *Agriculture Ecosystems & Environment* 147, 4-12.
- Sharpe, R.R., Harper, L.A., Byers, F.M., 2002. Methane emissions from swine lagoons in Southeastern US. *Agriculture Ecosystems & Environment* 90, 17-24.
- Smith, K., Cumby, T., Lapworth, J., Misselbrook, T., Williams, A., 2007. Natural crusting of slurry storage as an abatement measure for ammonia emissions on dairy farms. *Biosystems Engineering* 97, 464-471.
- Snider, D.M., Schiff, S.L., Spoelstra, J., 2009. ¹⁵N/¹⁴N and ¹⁸O/¹⁶O stable isotope ratios of nitrous oxide produced during denitrification in temperate forest soils. *Geochimica et Cosmochimica Acta* 73, 877-888.
- Snider, D.M., Venkiteswaran, J.J., Schiff, S.L., Spoelstra, J., 2012. Deciphering the oxygen isotope composition of nitrous oxide produced by nitrification. *Global Change Biology* 18, 356-370.
- Snider, D.M., Venkiteswaran, J.J., Schiff, S.L., Spoelstra, J., 2013. A new mechanistic model of δ¹⁸O-N₂O formation by denitrification. *Geochimica et Cosmochimica Acta* 112, 102-115.
- Soetaert, K., Petzoldt, T., 2010. Inverse Modelling, Sensitivity and Monte Carlo Analysis in R Using Package FME. *Journal of Statistical Software* 33, 28.
- Sommer, S.G., Olesen, J.E., Christensen, B.T., 1991. Effects of temperature, wind speed and air humidity on ammonia volatilization from surface applied cattle slurry. *Journal of Agricultural Science* 117, 91-100.
- Sommer, S.G., Christensen, B.T., Nielsen, N.E., Schjorring, J.K., 1993. Ammonia volatilization during storage of cattle and pig slurry: effect of surface cover. *Journal of Agricultural Science* 121, 63-71.
- Sommer, S.G., Petersen, S.O., Sogaard, H.T., 2000. Greenhouse gas emission from stored livestock slurry. *Journal of Environmental Quality* 29, 744-751.
- Sommer, S.G., Hansen, M.N., Sogaard, H.T., 2004. Infiltration of slurry and ammonia volatilisation. *Biosystems Engineering* 88, 359-367.
- Stocker, T.F., Qin, D., Plattner, G.-K., Tignor, M., Allen, S.K., Boschung, J., Nauels, A., Xia, Y., Bex, V., Midgley, P.M., 2013. *Climate Change 2013: The Physical Science Basis. Contribution of Working*

- Group I to the Fifth Assessment Report of the Intergovernmental Panel on Climate Change
Cambridge University Press, Cambridge, United Kingdom and New York, NY, USA,
- Sutka, R.L., Ostrom, N.E., Ostrom, P.H., Breznak, J.A., Gandhi, H., Pitt, A.J., Li, F., 2006. Distinguishing nitrous oxide production from nitrification and denitrification on the basis of isotopomer abundances. *Applied and Environmental Microbiology* 72, 638-644.
- Sutka, R.L., Adams, G.C., Ostrom, N.E., Ostrom, P.H., 2008. Isotopologue fractionation during N₂O production by fungal denitrification. *Rapid Communications in Mass Spectrometry* 22, 3989-3996.
- Tambone, F., Genevini, P., D'Imporzano, G., Adani, F., 2009. Assessing amendment properties of digestate by studying the organic matter composition and the degree of biological stability during the anaerobic digestion of the organic fraction of MSW. *Bioresource Technology* 100, 3140-3142.
- Todd, R.W., Cole, N.A., Casey, K.D., Hagevoort, R., Auvermann, B.W., 2011. Methane emissions from southern High Plains dairy wastewater lagoons in the summer. *Animal Feed Science and Technology* 166-67, 575-580.
- Toyoda, S., Mutoke, H., Yamagishi, H., Yoshida, N., Tanji, Y., 2005. Fractionation of N₂O isotopomers during production by denitrifier. *Soil Biology & Biochemistry* 37, 1535-1545.
- Toyoda, S., Yano, M., Nishimura, S., Akiyama, H., Hayakawa, A., Koba, K., Sudo, S., Yagi, K., Makabe, A., Tobar, Y., Ogawa, N.O., Ohkouchi, N., Yamada, K., Yoshida, N., 2011. Characterization and production and consumption processes of N₂O emitted from temperate agricultural soils determined via isotopomer ratio analysis. *Global Biogeochemical Cycles* 25. DOI: 10.1029/2009gb003769.
- Vieten, B., Blunier, T., Neftel, A., Alewell, C., Conen, F., 2007. Fractionation factors for stable isotopes of N and O during N₂O reduction in soil depend on reaction rate constant. *Rapid Communications in Mass Spectrometry* 21, 846-850.
- Weier, K.L., Doran, J.W., Power, J.F., Walters, D.T., 1993. Denitrification and the dinitrogen/nitrous oxide ratio as affected by soil water, available carbon, and nitrate. *Soil Science Society of America Journal* 57, 66-72.
- Well, R., Flessa, H., 2008. Isotope fractionation factors of N₂O diffusion. *Rapid Communications in Mass Spectrometry* 22, 2621-2628.
- Well, R., Flessa, H., Xing, L., Ju, X.T., Römheld, V., 2008. Isotopologue ratios of N₂O emitted from microcosms with NH₄⁺ fertilized arable soils under conditions favoring nitrification. *Soil Biology & Biochemistry* 40, 2416-2426.
- Well, R., Flessa, H., 2009a. Isotopologue enrichment factors of N₂O reduction in soils. *Rapid Communications in Mass Spectrometry* 23, 2996-3002.
- Well, R., Flessa, H., 2009b. Isotopologue signatures of N₂O produced by denitrification in soils. *Journal of Geophysical Research-Biogeosciences* 114. DOI: 10.1029/2008JG000804.
- Well, R., Flessa, H., 2009c. On the control of isotopologue signatures of soil-emitted N₂O. In: Yoshida, N. (Ed.), *Proceedings of the 4th International Symposium on Isotopomers*. pp. 86-93.

- Well, R., Eschenbach, W., Flessa, H., von der Heide, C., Weymann, D., 2012. Are dual isotope and isotopomer ratios of N₂O useful indicators for N₂O turnover during denitrification in nitrate-contaminated aquifers? *Geochimica et Cosmochimica Acta* 90, 265-282.
- Wrage, N., Velthof, G.L., van Beusichem, M.L., Oenema, O., 2001. Role of nitrifier denitrification in the production of nitrous oxide. *Soil Biology & Biochemistry* 33, 1723-1732.
- Wulf, S., Maeting, M., Clemens, J., 2002. Application technique and slurry co-fermentation effects on ammonia, nitrous oxide, and methane emissions after spreading: I. Ammonia volatilization. *Journal of Environmental Quality* 31, 1789-1794.
- Wunderlich, A., Meckenstock, R.U., Einsiedl, F., 2013. A mixture of nitrite-oxidizing and denitrifying microorganisms affects the d¹⁸O of dissolved nitrate during anaerobic microbial denitrification depending on the d¹⁸O of ambient water. *Geochimica et Cosmochimica Acta* 119, 31-45.
- Xu, J.G., Heeraman, D.A., Wang, Y., 1993. Fertilizer and temperature effects on urea hydrolysis in undisturbed soil. *Biology and Fertility of Soils* 16, 63-65.
- Yamagishi, H., Westley, M.B., Popp, B.N., Toyoda, S., Yoshida, N., Watanabe, S., Koba, K., Yamanaka, Y., 2007. Role of nitrification and denitrification on the nitrous oxide cycle in the eastern tropical North Pacific and Gulf of California. *Journal of Geophysical Research* 112. DOI: 10.1029/2006JG000227.

Chapter 9

Summary

9 Summary

Biogas production from energy crops and organic residues for generating electricity is promoted in several European countries to reduce greenhouse gas (GHG) emissions from fossil fuels and thus to slow down global warming and climate change. However, significant GHG (in particular methane, CH₄, and nitrous oxide, N₂O) as well as ammonia (NH₃) emissions may occur from anaerobic digestates (AD), the residues of the biogas production process, during storage periods prior to land spreading as organic fertilizers, when these storage facilities are not covered. In the present study, Open-Path FTIR as a non-invasive remote sensing technique in combination with the micrometeorological bLS model was successfully evaluated upon its applicability at open AD lagoons, and emissions from two lagoons were determined in several trials. Emissions were found to be dominated by CH₄ and NH₃, reducing the GHG savings of biogas energy considerably.

During AD land spreading significant trace gas amounts can be emitted to the atmosphere, which are usually dominated by NH₃. During winter, these emissions are often considered to be low; however, in the present study it was shown that NH₃ emissions under cold temperature conditions can be significant, especially when the soil is frozen and AD infiltration is hampered.

AD applied to soil as organic fertilizer may increase N₂O emissions, which derive from biochemical N transformation processes. N₂O as well as N₂ emissions after AD and cattle slurry application to soil have been investigated in an incubation study, indicating lower N₂O and N₂ emissions via denitrification from AD treated soil due to its lower carbon content. N₂O source apportioning in such studies is crucial for improving process understanding and advancing mitigation strategies. The analysis of the different N₂O isotopomer species with particular focus on the intramolecular ¹⁵N distribution within the asymmetric N₂O molecules (the so-called 'site preference', SP) allows some insights into these source processes. Here, this approach confirmed denitrification as the predominating N₂O source.

The isotopic fractionation factors during N₂O production and reduction via denitrification are still an uncertainty factor for stable isotope approaches relying on isotope ratios at natural abundance level. Therefore, these fractionation factors have been further investigated using different soil incubation approaches in two studies. The observed isotope fractionation during these experiments was partly in agreement with previous studies; however, in some cases the results deviated from literature values, probably due to experimental artefacts in some of the previous studies.

N₂O Isotopomer analysis is commonly done by isotope-ratio mass spectrometry (IRMS), which has relatively low throughput and does not allow real-time analysis. Here, recently developed laser spectroscopic techniques capable of site-specific N₂O ¹⁵N analysis may provide significant advantages compared to IRMS. Therefore, an experimental setup involving a new QCL absorption spectrometer was tested for its applicability in soil studies. The SP values of soil-derived N₂O were successfully determined continuously over several days, and were in good agreement with IRMS analysis, presenting laser spectroscopy as a promising new analytical approach for analyzing N₂O in soil studies.

Chapter 10

Zusammenfassung

10 Zusammenfassung

Biogasproduktion aus Energiepflanzen und organischen Abfällen zur Stromerzeugung wird in verschiedenen europäischen Ländern gefördert, um Emissionen von Treibhausgasen (THGs) zu reduzieren, und somit die globale Erwärmung und den Klimawandel zu verlangsamen. Bei der Biogaserzeugung anfallende Gärreste werden als Wirtschaftsdünger auf landwirtschaftlichen Flächen ausgebracht. Jedoch können bei der Gärrestlagerung vor der Feldausbringung erhebliche THG- (v.a. Methan – CH_4 und Lachgas – N_2O) sowie Ammoniak-Emissionen (NH_3) auftreten, wenn die entsprechenden Lagerstätten nicht luftdicht abgedeckt sind. Das Ausmaß dieser Emissionen ist kaum bekannt, jedoch wichtig für die ökologische Bewertung von Biogas-Strom. Für Emissionsmessungen an offenen Gärrestlagunen wurde daher die Open-Path FTIR-Methodik in Kombination mit einem mikrometeorologischen Transportmodell als sensitives nicht-invasives Fernmessverfahren validiert. In sechs z.T. mehrtägigen Messkampagnen wurden die Spurengasemissionen aus zwei Gärrestlagunen ermittelt, welche von CH_4 und NH_3 dominiert wurden und deren Ausmaß die Klimabilanz von Biogas-Strom der untersuchten Anlagen deutlich verschlechterte.

Auch während der Feldausbringung von Gärresten können erhebliche NH_3 -Emissionen auftreten. Bei der Ausbringung im Winter werden diese Emissionen zumeist als gering eingeschätzt. Jedoch konnte hier gezeigt werden, dass auch bei kalter Witterung hohe NH_3 -Emissionen auftreten können, vor allem wenn bei gefrorenem Boden die Infiltration der Gärreste in den Boden eingeschränkt ist.

N_2O als besonders wirksames Treibhausgas wird vor allem durch biochemische Prozesse in Böden gebildet, wobei organische Düngung z.B. mit Gärresten die N_2O -Freisetzung beträchtlich erhöhen kann. In einem Bodeninkubationsversuch wurde die Produktion von N_2O als auch von molekularem N_2 nach Gärrest- und Gülledüngung untersucht. Dabei wurden geringere N_2O - und N_2 -Emissionen nach Gärrestbehandlung beobachtet, was auf den durch den Gärprozess reduzierten Kohlenstoffanteil der Gärreste zurückgeführt wurde. Die Abschätzung der N_2O -Beiträge verschiedener Bodenprozesse ist von großer Bedeutung für das Prozessverständnis und daher essentiell für die Entwicklung von N_2O -Minderungsstrategien. Die Bestimmung der intramolekularen ^{15}N -Verteilung im asymmetrischen N_2O -Molekül (die sogenannte ‚site preference‘, SP) ermöglicht gewisse Rückschlüsse über die involvierten Ursprungsprozesse und wies hier auf die überwiegende N_2O -Bildung durch Denitrifikation hin.

Die Isotopenfraktionierungsfaktoren während der N_2O -Produktion und -Reduktion durch Denitrifikation stellen noch einen Unsicherheitsfaktor bei der Nutzung natürlicher Isotopenverhältnisse dar. Daher wurden diese Fraktionierungsfaktoren mit Hilfe verschiedener Bodeninkubationstechniken näher untersucht. Die aus diesen Versuchen resultierenden Fraktionierungsfaktoren stimmen zum Teil gut mit Literaturwerten überein, in einigen Fällen jedoch weichen diese Werte deutlich voneinander ab, was wahrscheinlich in versuchsbedingten Unterschieden gegenüber den vorangegangenen Studien begründet liegt.

Die Bestimmung von N_2O -Isotopomerverhältnissen erfolgt i.d.R. durch Isotopenverhältnis-Massenspektrometrie (IRMS), die jedoch nur einen relativ geringen Probendurchsatz erlaubt und keine Echtzeit-Analysen ermöglicht. Daher wurde anhand eines Bodeninkubationsversuchs ein neuartiger Laser-spektroskopischer Messansatz zur positionsspezifischen ^{15}N -Analyse von N_2O getestet, mit welchem die N_2O SP-Werte in höchster zeitlicher Auflösung kontinuierlich über mehrere Tage bestimmt werden konnten. Die Ergebnisse stimmten gut mit IRMS-Vergleichsmessungen überein, wodurch sich der genutzte Laser-basierte Messansatz als vielversprechende Technik für N_2O -Isotopenanalysen in Bodenstudien herausstellte.

Chapter 11

Acknowledgements

11 Acknowledgements

At this point I would like to take the chance to thank my supervisors, colleagues, collaborators, friends, and family. Without their great support and help during all phases of my PhD work the present dissertation would not exist.

First of all, I thank my supervisor, Prof. Karl-Hermann Mühlhng, for the opportunity to work in this project and in his group. During this time, he always supported and motivated me in so many ways, and was always there when I needed advice. I am very grateful for the confidence and time he invested and for all the support during conception, preparation, and compilation of publications and this dissertation.

Klaus Dittert was the one who brought me in touch with scientific work during my B.Sc. and M.Sc. theses, and he supported me in many ways all the time during my PhD, even after his changeover to Uni Göttingen. In many discussions he contributed greatly with his ideas and experience to the realization and technical implementation of the new OP FTIR field measurements as well as to the incubation studies, but he also gave me motivation and support during manuscript preparations.

Andreas Pacholski largely helped with his knowledge and experience with ammonia emission measurements and micrometeorological techniques. He always kept his confidence about the FTIR project, despite of some unpromising indications in the initial phase, and contributed largely to succeeding in this project.

With Mehmet Senbayram I started working already during my M.Sc. thesis, and we continued collaborating successfully when he worked at YARA and later at Uni Göttingen. Due to his friendly and open nature it was always a great pleasure to work with him, and his highly motivated and efficient way of working was always an example to me.

Roland Bol and Laura Cárdenas gave me so much support especially during my stay at North Wyke Research as a master student, where Roland gave me the opportunity for my first publication, and Laura worked with me with her incubation system. But also during my PhD they gave me great support during follow up studies.

I thank Reinhard Well, Anette Giesemann, and Dominika Lewicka-Szczebak at the Thünen Institute. Without their cooperation and support all isotopomer work would not have been possible.

Deli Chen welcomed me during my stay in Melbourne and he, Tom Denmead, and David Griffith organized a great field trial at the Charlton feedlot and gave me first experiences with OP FTIR and a good idea of its potentials. They further supported me during the analysis of raw data and with useful advice during their visits at Kiel. Without their great support the FTIR project would probably not have been successful.

Jochim Mohn and Lukas Emmenegger at EMPA Dübendorf gave me the great opportunity during a COST STSM to work with their team on a small study using their extraordinary laser instrument. Here, also Béla Tuzson and Albert Manninen contributed greatly.

Antje Herrmann and Henning Kage were involved in several studies and contributed to their conception and realization.

Anne Putbrese did the project administration, but also supported me in many other ways and had always an ear for me. Especially during the long end phase she greatly motivated and urged me to finalize this dissertation.

Bärbel Biegler and Stefan Becker always gave me a hand during lab and fieldwork when needed. But also all other group members always supported me wherever possible. Many thanks for that!

Further support during measurements and field trials came from Kang, Achim, Robert, and Rüdiger Ströh.

But I also want to mention the great students who worked with me during field trials, especially Thomas, Claas, Nils-Ole, Tim, and Franziska.

Essential was also the support by Jan Albrecht, Hans-Johann Koll, and Rudolf Bonse, who permitted the measurements on their farms and were very helpful and cooperative.

I also thank my former and current PhD student colleagues Mareike, who helped me by proof reading this thesis, but also Caroline, Christina, Nicole, Dorothee, Christoph-Martin, Marcus, Sherif, Cheng, and Wang for their support and for contributing to a pleasant atmosphere.

With all my heart I thank my parents, my sister, and Isabel for their support in many ways, for their backup and confidence.

I am aware that I cannot explicitly give consideration to all the people here, who worked with me or gave me a helpful hand during this long time, but I want to give thanks to all of you.

My special thanks go to the German Federal Environmental Foundation (DBU) for supporting me during my PhD via a scholarship.

The FTIR project was supported by the Innovationsstiftung Schleswig-Holstein and by the Ministry of Energy, Education, and Traffic of Schleswig-Holstein and the European Regional Development Fund (ERDF) in the framework of the joint project 'Centre of Excellence of Biomass in Schleswig-Holstein'.

Chapter 12

Curriculum vitae

12 Curriculum vitae

Personal:

Name: Jan Reent Köster
Date of birth: 24.07.1979
Place of birth: Achim (Lower Saxony)
Nationality: german

Work:

Since 2013: ‘Experienced Researcher’ in the Marie Skłodowska-Curie ITN project *NORA* project at the Norwegian University of Life Sciences, Ås, Norway

Academic education:

02.07.2014: PhD defense at the Faculty of Agricultural and Nutritional Sciences, Kiel University
2009 – 2013: PhD student at the Institute of Plant Nutrition and Soil Science, Kiel University
2007 – 2009: M.Sc. course Agricultural Sciences, Kiel University;
degree: Master of Science
2003 – 2007: B.Sc. course Agricultural Sciences, Kiel University;
degree: Bachelor of Science

School, civilian service, and apprenticeship:

2000 – 2003: Apprenticeship for IT specialist, STN ATLAS Elektronik GmbH, Bremen;
degree: IT specialist (IHK)
1999 – 2000: Civilian service (Lebenshilfe Rotenburg-Verden gemeinnützige GmbH)
1992 – 1999: Domgymnasium Verden/Aller;
degree: general qualification for university entrance
1990 – 1992: Secondary school OS II Jahnschule Verden/Aller
1986 – 1990: Primary school Kirchlinteln-Bendingbostel

Kiel, June 2015